

**GREEN SYNTHESIS OF SILVER NANOPARTICLES USING
INVASIVE ALIEN PLANT SPECIES AND EVALUATION OF
THEIR ANTI-OXIDATIVE, ANTI-MICROBIAL AND ANTI-
CANCER ACTIVITIES**

**A THESIS SUBMITTED IN PARTIAL FULFILLMENT OF THE
REQUIREMENTS FOR THE DEGREE OF DOCTOR OF
PHILOSOPHY**

F. LALSANGPUII

MZU REGN NO: 1101 of 2011

Ph. D REGN NO: MZU/Ph.D./1273 of 04.09.2018



**DEPARTMENT OF BOTANY
SCHOOL OF LIFE SCIENCES
AUGUST 2024**

GREEN SYNTHESIS OF SILVER NANOPARTICLES USING INVASIVE ALIEN
PLANT SPECIES AND EVALUATION OF THEIR ANTI-OXIDATIVE, ANTI-
MICROBIAL AND ANTI-CANCER ACTIVITIES

BY

F. LALSANGPUII

MZU REGN NO: 1101 of 2011

Ph. D REGN NO: MZU/Ph.D./1273 of 04.09.2018

Name of supervisor: Prof. R. LALFAKZUALA

Joint supervisor: Dr. SAMUEL LALTHAZUALA ROKHUM

Submitted

In partial fulfillment of the requirement of the degree of Doctor of Philosophy in
Botany of Mizoram University, Aizawl

MIZORAM UNIVERSITY
(A Central University Established by an Act of Parliament of India)

R. Lalfakzuala Ph.D.
Professor



Department of Botany
School of Life Sciences
Tanhril-796004
Aizawl, Mizoram
Email: lalfaka@yahoo.com

CERTIFICATE

This is to certify that the thesis work entitled, **“Green Synthesis of Silver Nanoparticles Using Invasive Alien Plant Species and Evaluation of Their Anti-oxidative, Anti-microbial and Anti-Cancer Activities”**, submitted by F. Lalsangpuii (MZU/Ph.D./1273 of 04.09.2018) in partial fulfillment of the requirement of the degree of Doctor of Philosophy in Botany is a record of bonafide work carried out by her under my supervision and guidance.

(Prof. R. LALFAKZUALA)
Supervisor

(Dr. SAMUEL LALTHAZUALA ROKHUM)
Joint Supervisor

Associate Professor
Department of Chemistry
NIT SILCHAR, 788019

**DECLARATION
MIZORAM UNIVERSITY**

AUGUST 2024


I, **F. Lalsangpuii**, hereby declare that the subject matter of this thesis is the record of work done by me, that the contents of this thesis did not form basis of the award of any previous degree to me or to do the best of my knowledge to anybody else, and that the thesis has not been submitted by me for any research degree in any other University/Institute.

This is being submitted to the Mizoram University for the degree of Doctor of Philosophy in Botany.

(F. LALSANGPUII)
Candidate

(Prof. R. LALFAKZUALA)
Supervisor

(Prof. F. LALNUNMAWIA)
Head of Department


(Dr. SAMUEL LALTHAZUALA ROKHUM)
Joint Supervisor
Associate Professor
Department of Chemistry
NIT SILCHAR, 788019

ACKNOWLEDGMENT

First and foremost, I thanked Almighty God for granting me the strength, and wisdom to navigate this challenging yet rewarding path. His blessings and guidance have been my greatest source of inspiration and perseverance throughout this journey. Without His divine support, this achievement would not have been possible.

I would like to express my deepest gratitude to my supervisor, Prof. R. Lalfakzuala and joint supervisor, Dr. Samuel Lalthazuala Rokhum, for their invaluable guidance, and insightful feedback throughout the course of my Ph.D. journey. Your expertise, valuable suggestions, and encouragement have been crucial to my academic growth.

I am thankful to Prof. F. Lalnunmawia, Head of Department, for granting me permission to utilize the departmental facilities and laboratory equipment, which were vital in the successful completion of my research work.

I am grateful to the teaching faculty, Prof. Surya Kant Mehta, Dr. K. Sandhyarani Devi, Dr. J. Lalbiaknunga, Dr. Amit Kumar Mishra, and Prof. Awadhesh Kumar for their insightful comments and suggestions, which have significantly enhanced the quality of my research.

I am also appreciative of the technical assistance and administrative support provided by the non-teaching staff at the Botany Department, as well as the resources, facilities, and opportunities that SERB-DST and DBT-NECAB provided to me so as to conduct this research.

I extend my sincere appreciation to Dr. Zothansiam, Department of Zoology, Mizoram University, for his constant support and generosity. His assistance was crucial in enabling me to complete all of the cancer research included in this thesis.

My profound gratitude goes to, Prof. Nachimuthu Senthil Kumar, Department of Biotechnology, Mizoram University, and Dr. Amit Kumar Trivedi, Department of Zoology, Mizoram University, for their scholarly contributions that have enriched this thesis.

I acknowledge the funding support provided by University Grant Commission, Ministry of Tribal Affairs, Government of India, and Publishing grant provided by Mizoram University, which made this research possible.

The successful completion of my thesis would not have been possible without the priceless support provided by my labmates, namely Freddy MC. Vanlalmuana, PS. Lalbiaktluanga, Samuel Vanlalnghaka, Martin Lalnunthara, R. Zosangzuali, Esther Lalthazuali, Rachel Lalremruati, and Lalhminganga Chinzah.

I would also like to express my sincere gratitude to my fellow researchers and dear friends, Dr. Mary Zosangzuali, Dr. Annie Lalrawngbawli, F. Nghakliana, Joseph JVL Ruatpuia and Lalfakawma for their invaluable assistance, collaboration, and intellectual discourse, which have been profound sources of inspiration and determination.

A heartfelt thanks to my all friends whose moral support and encouragement have been a great source of motivation.

Last but not least, I would like to express my profound appreciation to my family for their prayers, unwavering support, and understanding throughout my academic endeavor. Their sacrifices and encouragement have laid the groundwork for my resilience. I dedicate this thesis to my loving mother, K. Laldingi, for her unconditional affection and unwavering faith in my abilities, and to my beloved father, F. Challawma (L), who has been my guiding light and inspiration throughout my life.

Thank you all for your invaluable contributions to this momentous milestone in my life.

F. LALSANGPUII

CONTENTS

Supervisor's certificate	<i>i</i>
Declaration certificate	<i>ii</i>
Acknowledgement	<i>iii-iv</i>
Table of contents	<i>v-vii</i>
Preface	<i>viii-ix</i>
List of figures	<i>x-xiv</i>
List of Tables	<i>xv</i>
Chapter 1: Introduction	1-7
Chapter 2: Review of Literature	8-32
Chapter 3: Synthesis and characterization of silver nanoparticles using <i>Mikania micrantha</i> and <i>Acmella ciliata</i> leaf extract	33-57
Introduction	33-36
Materials and methods	36-38
Results	38-42
Figures	43-52
Discussion	53-56
Conclusion	56-57
Chapter 4: Free radical scavenging activities of <i>Mikania micrantha</i> silver nanoparticles (MNP) and <i>Acmella ciliata</i> silver nanoparticles (ANP) (<i>in-vitro</i> and <i>ex-vivo</i>)	58-76
Introduction	58-61

Materials and methods	61-65
Results	65-67
Figures	68-73
Discussion	74-75
Conclusion	76
 Chapter 5: Antioxidant-mediated ameliorative of <i>Acmella ciliata</i> silver nanoparticles activity against doxorubicin-induced toxicity in Dalton's Lymphoma Ascites (DLA) bearing mice.	 77-92
 Introduction	 77-80
Materials and methods	80-83
Results	84-85
Tables & Figures	86-89
Discussion	90-91
Conclusion	91-92
 Chapter 6: Anti-microbial activity of <i>Mikania micrantha</i> and <i>Acmella ciliata</i> silver nanoparticles.	 93-122
 Introduction	 93-96
Materials and methods	96-100
Results	100-104
Tables & Figures	105-117
Discussion	118-122
Conclusion	122
 Chapter 7: Anti-cancer activity of <i>Mikania micrantha</i> and <i>Acmella ciliata</i> silver nanoparticles against type-II human lung adenocarcinoma (A549) cells	 123-158

Introduction	123-126
Materials and methods	126-132
Results	132-138
Figures	139-154
Discussion	155-158
Conclusion	158
 Consolidated Summary	 159-161
Animal ethnics approval	162
References	163-226
Abbreviations	227-230
Brief bio-data of the candidate	231
List of Publications	232
Conference/Seminar/workshop attended	233
Paper presented	234
Particular of the candidate	235

Preface

Silver nanoparticles (AgNPs) have emerged as a prominent nanomaterial in the biomedical and agriculture sectors owing to their unique physicochemical properties. In the realm of nanotechnology, it is imperative to establish reliable and environment-friendly approaches to the production of nanoparticles (NPs), as the conventional methods are expensive, harmful, and detrimental to the environment. To facilitate overcoming these issues, biological sources such as plants, bacteria, fungi, and biopolymers have been utilized to produce AgNPs, which can serve as both reducing and capping agents. This study focuses on the research on plant-assisted synthesis of AgNPs, an emerging area in nanotechnology, and their biological applications. Silver nanoparticles, usually with sizes less than 100 nm and consisting of 20–15,000 silver atoms, exhibit unique physical, chemical, and biological characteristics in comparison to their larger precursor materials. AgNPs have distinct physical and optical characteristics, along with tailored biochemical functionality achieved by controlling their size and shape. These features render them highly potential for various applications, including as antimicrobial agents, anticancer therapy, drug delivery carriers, anti-diabetic agents, wound healing, and biosensors. Although AgNPs have therapeutic benefits, it is crucial to prioritize gaining a deeper understanding of their mechanisms in order to expand their potential applications in nanomedicine, including diagnostics, therapeutics, and pharmaceuticals.

This thesis is broadly divided into seven chapters. Chapter 1 provides a general introduction, while chapter 2 focuses on reviewing the literature. Chapter 3 describes the synthesis and characterization of silver nanoparticles using *Mikania micrantha* and *Acmella ciliata* leaf extract. Chapter 4 provides a detailed account of the free radical scavenging activities of silver nanoparticles derived from *Mikania micrantha* and *Acmella ciliata* (*in vitro* and *ex vivo*). The chemical composition of the extract typically influences the antioxidant effects of silver nanoparticles, and these attributes generally enhance as the concentration of AgNPs increases. Chapter 5 describes the antioxidant-mediated ameliorative of *Acmella ciliata* silver nanoparticles activity against doxorubicin-induced toxicity in Dalton's Lymphoma Ascites (DLA) bearing

mice. This study found that biosynthesized AgNPs from *A. ciliata* leaf extract offers outstanding protections against cardiotoxicity and hepatotoxicity caused by DOX in DLA-bearing mice possibly by elevating the activities of antioxidants and reduction of lipid peroxidation. Chapter 6 gives an in-depth investigation of the antimicrobial activity exhibited by *Mikania micrantha* and *Acmella ciliata* silver nanoparticles. Our findings validate the concept that silver nanoparticles are appropriate for developing novel microbiocidal agents. Chapter 7 describes the cytotoxicity and anti-cancer activities of silver nanoparticles synthesized from *Mikania micrantha* and *Acmella ciliata* leaf extract against type-II human lung adenocarcinoma (A549) cells. Our study demonstrates the cytotoxic effects of AgNPs on human lung adenocarcinoma A549 cells by targeting the apoptotic pathway which is the preferred cell death pathway for any novel drug candidate.

LIST OF FIGURES

Figure No	Description	Page No
3.1	Visual identification of biosynthesized AgNPs as recorded at different time-interval: (a) Initial, (b) 2 h, and (c) 4 h.	43
3.2	UV-Vis absorption spectra of biosynthesized AgNPs using <i>M. micrantha</i> leaf extract at different time intervals.	43
3.3	FT-IR analysis of (a) biosynthesized AgNPs (b) <i>M. micrantha</i> leaf extract (MMAE), and (c) Silver nitrate.	44
3.4	(a-d) SEM micrographs of biosynthesized AgNPs. Elemental mapping of (e) silver, (f) oxygen, and (g) both elements for the inset region, and (h) EDS data of the area in the white box in (c) .	45
3.5	(a-d) TEM micrograph showing size of biosynthesized AgNPs Scale bars: (a) 10 nm, (b) 20 nm, (c) 50 nm, and (d) 100 nm. (e) Histogram of the TEM image (100 nm).	46
3.6	XRD pattern of biosynthesized AgNPs using <i>M. micrantha</i> leaf extract.	47
3.7	Visual identification of biosynthesized AgNPs as recorded at different time-interval: (a) Initial, (b) 2 h, and (c) 4 h.	48
3.8	UV-Vis absorption spectra of biosynthesized AgNPs using <i>A. ciliata</i> leaf extract at different time intervals.	48
3.9	FT-IR analysis of (a) Silver nitrate, (b) <i>Acmella ciliata</i> leaf extract (ACAE), and (c) biosynthesized AgNPs	49
3.10	(a-c) SEM micrographs of biosynthesized AgNPs. Elemental mapping of (d) oxygen, (e) silver, (f) chlorine, and (g) all three elements for the inset region, and (h) EDS data of the area in the white box in (c) .	50

3.11	(a-d) TEM micrograph showing size of biosynthesized AgNPs Scale bars: (a) 10 nm, (b) 20 nm, (c) 50 nm, and (d) 100 nm. (e) Histogram of the TEM image (100 nm).	51
3.12	XRD pattern of biosynthesized AgNPs using <i>A. ciliata</i> leaf extract.	52
4.1	Plots of log-doses of AgNPs, MMAE and ASA against (a) DPPH, (b) ABTS, and (c) O ₂ ^{•-} inhibition (%) for the calculation of IC ₅₀ .	68
4.2	IC ₅₀ (µg/ml) of AgNPs, MMAE and ASA for (a) DPPH, (b) ABTS, and (c) O ₂ ^{•-} .	69
4.3	Reducing power of AgNPs, MMAE and ASA at different concentrations.	70
4.4	(a) Anti-haemolytic, and (b) lipid peroxidation inhibitory activities of biosynthesized AgNPs.	70
4.5	Plots of log-doses of AgNPs, ACAE and ASA against (a) DPPH, (b) ABTS, and (c) O ₂ ^{•-} inhibition (%) for the calculation of IC ₅₀ .	71
4.6	IC ₅₀ (µg/ml) of AgNPs, ACAE and ASA for (a) DPPH, (b) ABTS, and (c) O ₂ ^{•-} .	72
4.7	Reducing power of AgNPs, ACAE and ASA at different concentrations.	73
4.8	(a) Anti-haemolytic, and (b) lipid peroxidation inhibitory activities of biosynthesized AgNPs.	73
5.1	Effects of biosynthesized AgNPs on (a) glutathione level (GSH) (b) glutathione-s-transferase activity (GST) and (c) superoxide dismutase activity (SOD) in the liver and heart of mice.	87-88
5.2	Effects of biosynthesized AgNPs on lipid peroxidation (LPO) expressed in malondialdehyde (MDA) in (a) liver, and (b) heart of DLA mice.	89

6.1	Antibacterial activity as determined by the decrease in zone of inhibition after treatment with different concentration of AgNPs (2.5, 5.0 and 10 µg/ml) and Ofloxacin (5.0 µg/ml) against (a) <i>E. coli</i> , (b) <i>P. aeruginosa</i> , (c) <i>B. subtilis</i> and (d) <i>S. aureus</i> .	105
6.2	Antibacterial activity of different concentration of AgNPs (2.5, 5.0 and 10 µg/ml) and Ofloxacin (5.0 µg/ml) against (a) <i>E. coli</i> , (b) <i>P. aeruginosa</i> , (c) <i>B. subtilis</i> and (d) <i>S. aureus</i> .	106
6.3	Determination of MIC for of different concentration of AgNPs against pathogenic bacteria.	107
6.4	Antibacterial activity as determined by the decrease in zone of inhibition after treatment with different concentration of AgNPs (2.5, 5.0 and 10 µg/ml) and Ofloxacin (5.0 µg/ml) against (a) <i>E. coli</i> , (b) <i>P. aeruginosa</i> , (c) <i>B. subtilis</i> and (d) <i>S. aureus</i> .	108
6.5	Antibacterial activity of different concentration of AgNPs (2.5, 5.0 and 10 µg/ml) and Ofloxacin (5.0 µg/ml) against (a) <i>E. coli</i> , (b) <i>P. aeruginosa</i> , (c) <i>B. subtilis</i> and (d) <i>S. aureus</i> .	109
6.6	Determination of MIC for of different concentration of AgNPs against pathogenic bacteria.	110
6.7	Microscopic view of rice pathogen (<i>Curvularia pseudobrachyspora</i>) showing conidia on the conidiophore.	111
6.8	Band showing PCR amplification using ITS region of fungal isolate.	111
6.9	Inhibition of the colony growth of <i>C. pseudobrachyspora</i> mediated by AgNPs.	112
6.10	Effect of AgNPs on the colony growth of <i>C. pseudobrachyspora</i> .	113
6.11	Effect of AgNPs on the biomass of <i>C. pseudobrachyspora</i> .	114

6.12	Inhibition of the colony growth of <i>C. pseudobrachyspora</i> mediated by AgNPs.	115
6.13	(b) Effect of AgNPs on the colony growth of <i>C. pseudobrachyspora</i> .	116
6.14	Effect of AgNPs on the biomass of <i>C. pseudobrachyspora</i> .	117
7.1	Plots of log-doses of various concentration of AgNPs in triplicate against inhibition (%) of A549 cells after 24 h treatment for the calculation of IC ₅₀ .	139
7.2	(a) Inhibition of colony formation of A549 cells mediated by AgNPs. (b) Effect of AgNPs on the reproductive viability of A549 cells, expressed as a surviving fraction (SF).	140
7.3	(a) Acridine orange/Ethidium bromide (AO/EtBr) dual staining of A549 cells after treatment with different doses of AgNPs for 24 h (b) Percentage of dead cells after treatment of A549 with biosynthesized AgNPs.	141
7.4	(a) Fluorescence images of Comets observed in control and A549 cells treated with different concentrations of AgNPs. (b - e) The extent of DNA damage expressed in terms of tail area, tail length, tail DNA and tail olive moment.	142-143
7.5	Effects of AgNPs on (a) glutathione (GSH) level; (b) glutathione-s-transferase (GST) activity; (c) superoxide dismutase (SOD) activity; and (d) lipid peroxidation (LPO) expressed in malondialdehyde (nmol/mg protein) in A549 cells after 24 h treatment.	144
7.6	Effects of AgNPs on mRNA expression levels of (a) <i>Bax</i> ; (b) <i>Bid</i> ; (c) <i>p53</i> ; (d) <i>Apaf-1</i> ; (e) <i>BCL-X_L</i> ; (f) <i>BCL-2</i> ; (g) <i>Survivin</i> and (h) <i>PARP</i> in A549 cells after 24 h treatment.	145-146
7.7	Effects of AgNPs on activities of (a) Caspase-3 and (b) Caspase-6 in A549 cells after 24 h treatment.	146

7.8	Plots of log-doses of various concentration of AgNPs in triplicate against inhibition (%) of A549 cells after 24 h treatment for the calculation of IC ₅₀ .	147
7.9	(a) Inhibition of colony formation of A549 cells mediated by AgNPs. (b) Effect of AgNPs on the reproductive viability of A549 cells, expressed as a surviving fraction (SF).	148
7.10	(a) Acridine orange/Ethidium bromide (AO/EtBr) dual staining of A549 cells after treatment with different doses of AgNPs for 24 h. (b) Percentage of dead cells after treatment of A549 with biosynthesized AgNPs.	149
7.11	(a) Fluorescence images of Comets observed in control and A549 cells treated with different concentrations of AgNPs. (b-e) The extent of DNA damage expressed in terms of tail area, tail length, tail DNA and tail olive moment.	150-151
7.12	Effects of AgNPs on mRNA expression levels of (a) <i>Bax</i> ; (b) <i>Bid</i> ; (c) <i>p53</i> ; (d) <i>Apaf-1</i> ; (e) <i>BCL- X_L</i> ; (f) <i>BCL-2</i> ; (g) <i>Survivin</i> and (h) <i>PARP</i> in A549 cells after 24 h treatment.	152
7.13	Effects of AgNPs on mRNA expression levels of (a) <i>Bax</i> ; (b) <i>Bid</i> ; (c) <i>p53</i> ; (d) <i>Apaf-1</i> ; (e) <i>BCL- X_L</i> ; (f) <i>BCL-2</i> ; (g) <i>Survivin</i> and (h) <i>PARP</i> in A549 cells after 24 h treatment.	153-154
7.14	Effects of AgNPs on activities of (a) Caspase-3 and (b) Caspase-6 in A549 cells after 24 h treatment.	154

LIST OF TABLES

Table No	Description	Page No
5.1	Effects of biosynthesized AgNPs on serum enzyme activities.	86
6.1	Determination of the Minimum Inhibitory Concentration (MIC) and Minimum Bactericidal concentration (MBC) values of different concentration of AgNPs against pathogenic bacteria.	107
6.2	Determination of Minimum Inhibitory Concentration (MIC) and Minimum Bactericidal concentration (MBC) values of different concentration of AgNPs against pathogenic bacteria.	110
7.1	Primer sequences used in the qRT-PCR analysis of A549 cells treated with AgNPs.	131

Chapter 1

Introduction

Nanotechnology has emerged as an interdisciplinary approach in biochemical applications, offering a broad scope of applications in fields including diagnostics, biomarkers, cell labelling, antimicrobial agents, drug delivery, and cancer therapy (Al-Sheddi *et al.*, 2018). The term "nanotechnology" refers to the use of nanoscale phenomena in the creation, characterization, fabrication, and implementation of materials and systems. Increased public funding for nanotechnology research and development over the past decade reveals that nanotechnology will lead to an unparalleled period of productivity and prosperity (Roco, 2003; Gonzalez *et al.*, 2013). The persistent application of nanotechnology in research and development to produce nanoscale items has the potential to profoundly impact human existence, economic circumstances, and societal dynamics (Malik *et al.*, 2023). Nanoparticles are considered the fundamental units of nanotechnology, and the development of a biological method for producing nanoparticles is emerging as a significant field within nanotechnology (Ankamwar *et al.*, 2005; Cataleya, 2006). Nanoparticles are small particles with dimensions ranging from 1–100 nm, possessing remarkable thermal conductivity, catalytic reactivity, non-linear optical performance, and chemical stability due to their high surface area to volume ratio (Joseph *et al.*, 2023). Certain parameters such as size, distribution, and shape determine the novel or enhanced features of the nanoparticles (Agarwal *et al.*, 2017). There are different types of nanoparticles, including carbon-based nanoparticles, metal nanoparticles, ceramic nanoparticles, polymeric nanoparticles, and several more (Khan *et al.*, 2019).

Noble metal nanoparticles have been garnering significant attention in recent years due to their potential applications in the fields of medicine, biology, material science, physics, and chemistry (Klębowski *et al.*, 2018). The intrinsic characteristics of a noble metal nanoparticle are now known to be determined by its dimensions, morphology, chemical composition, crystallinity, and structure, whether it is solid or hollow. Metal nanoparticles possess a substantial specific surface area and a significant proportion of surface atoms. AgNPs have attracted significant interest

among numerous noble metal nanoparticles due to their distinct characteristics, such as optimal electrical conductivity, chemical stability, catalytic capabilities, and antibacterial properties (Kumar *et al.*, 2004). Due to its high surface-to-volume ratio, silver at the nanoscale exhibits distinct properties compared to bulk particles composed of the same material (Ramamurthy *et al.*, 2013). Silver nanoparticles (AgNPs) are utilized in the advancement of cutting-edge technologies in the fields of electronics, material sciences, and medicine. In view of their extensive applications in numerous areas, scientists worldwide are currently conducting further studies on AgNPs (Husain *et al.*, 2023).

AgNPs can be synthesized through a vast array of methods, which are typically classified into two primary synthetic routes: the top-down and bottom-up approaches. Different methods, including biological, physical, chemical, photochemical, electrochemical, radiolytic, and sonolytic, may be employed to AgNPs. While the chemical synthesis technique allows for the rapid production of a large quantity of nanoparticles, it necessitates the use of capping agents to maintain the size stability of the nanoparticles. The chemicals utilized in the synthesis and stabilization of nanoparticles are hazardous and result in the production of environmentally unfriendly byproducts. The demand for environmentally friendly and non-toxic methods of synthesizing nanoparticles has led to an increasing interest in biological methods that do not involve the production of harmful chemicals. The physicochemical methods of synthesizing silver nanoparticles have several drawbacks, including the use of toxic chemicals, high temperature and pressure, and the formation of hazardous by-products. Therefore, it is imperative to explore safer alternative methods for synthesizing silver nanoparticles. Researchers have proposed using microorganisms and plant compounds in bio-inspired synthesis for silver nanoparticles as an excellent alternative to chemical methods, as it eliminates the need for toxic chemicals and high temperatures.

The biological approach, also known as the green synthesis process, is commonly categorized as a novel branch of nanotechnology called nanobiotechnology (Rajoriya *et al.*, 2017). The biosynthesis of AgNPs is primarily a bottom-up process that involves reduction and oxidation reactions. Due to the single-step nature of the process, compounds that possess both reducing and capping properties are currently

preferred (Mohanpuria *et al.*, 2008). Green synthesis involves utilizing biogenic materials such as plant extracts, biopolymers, and microbial sources (such as bacteria, fungi, algae, and yeast) to produce nanomaterials. Green chemistry focuses on developing biocompatible, non-toxic, and environmentally friendly techniques for producing AgNPs. Plant extracts, fungi, and bacteria are the three main sources that contribute to the biosynthesis of AgNPs. During the process of biological synthesis, the nanoparticles that are created are promptly enveloped by a protein molecule, forming a natural protective covering that effectively prevents the formation of clumps or clusters. The process of natural capping enhances the durability and stability of the produced nanoparticles. The utilization of plant extract for synthesizing nanoparticles has several advantages compared to microorganisms, including the simplicity of scaling up the process, reduced biohazard risks and environmentally friendly characteristics (Ahmed *et al.*, 2015). Furthermore, the use of plant extracts has garnered significant interest because of their ability to reduce the expense of isolating and cultivating microbes, thereby improving the cost-efficiency of synthesizing nanoparticles. Therefore, it is widely regarded as the most effective platform for the synthesis of nanoparticles, as it is devoid of toxic chemicals and offers natural capping agents to stabilize silver nanoparticles.

A silver metal ion solution and a reducing biological agent are the primary prerequisites for the green synthesis of AgNPs. In the majority of instances, the stabilizing and capping agents are provided by reducing agents or other constituents that are present in the cells, eliminating the requirement for external capping and stabilizing agents. The biological synthesis of AgNPs is facilitated by the abundance of organic compounds such as carbohydrates, fats, proteins, enzymes, coenzymes, phenols, flavonoids, terpenoids, alkaloids, and gums. These compounds have the ability to donate electrons, which leads to the reduction of Ag^+ ions to Ag^0 . The synthesis of noble AgNPs is a two-step process that begins with the reduction of Ag^+ ions to Ag^0 , followed by the agglomeration and stabilization of the oligomeric clusters of colloidal AgNPs (Iravani *et al.*, 2014). Reaction temperature, metal ion concentration, extract contents, reaction mixture pH, reaction duration, and agitation are the primary chemical and physical parameters that influence AgNPs production. Several physical and chemical factors, such as reaction temperature, pH of the reaction

mixture, reaction duration, metal ion concentration, extract composition, and reaction period, significantly influence the size, shape, and morphology of the AgNPs (Kora *et al.*, 2010).

Various analytical and spectroscopic methods are employed to determine the properties of nanoparticles, including their nature, size, shape, distribution, stability or aggregation state, morphology, elemental composition, and dispersity (monodisperse or polydisperse). The uniformity of these characteristics is crucial in numerous applications. The most frequently employed methods for characterizing nanoparticles are as follows: UV–visible spectrophotometry, Fourier transform infrared spectroscopy (FT-IR), Scanning electron microscopy (SEM), energy dispersive spectroscopy (EDS) transmission electron microscopy (TEM), and X-ray diffraction (XRD). UV-visible spectroscopy typically uses light wavelengths ranging from 300 to 800 nm to analyse metal nanoparticles with sizes ranging from 2 to 100 nm (Vijayaram *et al.*, 2024). FT-IR spectroscopy characterizes the surface chemistry of nanoparticles and other surface chemical residues and is useful for detecting organic functional groups (e.g., carbonyls, hydroxyls) adhered to the surface (Raj *et al.*, 2021). Scanning electron microscopy and transmission electron microscopy are employed to analyze the structure and shape of compounds from nanometers to micrometers (Malatesta, 2021). Transmission electron microscopy exhibits a resolution that is 1000 times higher than scanning electron microscopy (Brodusch *et al.*, 2021). Energy dispersive spectroscopy (EDS) is widely used to determine the elemental composition of metal nanoparticles (Mishra *et al.*, 2017). X-ray diffraction (XRD) is employed for the phase identification and characterization of the crystal structure of the nanoparticles (Holder and Schaak, 2019). X-rays penetrate the nanomaterial, and the resulting diffraction pattern is compared with known standards to acquire structural information.

Nanoparticles produced using green methods have important functions in the fields of medicine, clinical applications, and in vitro diagnostic applications (Jayalakshmi and Yogamoorthi, 2014; Arumugam *et al.*, 2015; Matussin *et al.*, 2020). AgNPs synthesized using green methods exhibit notable antibacterial (Gopinath *et al.*, 2014; Awwad *et al.*, 2015), antifungal (Mallmann *et al.*, 2015) and anti-parasitic activity (Velayutham *et al.*, 2013). AgNPs can induce cell wall damage, membrane damage, or generate free radicals, which in turn lead to oxidative, DNA, or electron

transport chain damage, ultimately leading to bacterial death (Chaloupka *et al.*, 2010; Gopinath *et al.*, 2014). AgNPs serve as viable substitutes for pesticides in the treatment and management of plant diseases, as well as efficient fertilizers that are environmentally friendly and enhance crop yield (Singh *et al.*, 2015). Moreover, green nanomaterials are extensively used in the remediation of surface water, groundwater, and wastewater that are polluted with hazardous metal ions, organic and inorganic solutes, and microorganisms (Roy *et al.*, 2021).

The imbalance between pro-oxidants and anti-oxidants within cells, caused by changes in lifestyle and environmental pollutants, results in an overproduction of free radicals in the body. Researchers have linked excessive free radicals to the oxidative degradation of dietary products and acknowledge their significant role in the onset of over 200 other pathophysiological conditions, such as atherosclerosis, cancer, inflammatory illnesses, diabetes, and aging (Coyle and Puttfarcken, 1993). An effective scavenger of these harmful free radicals could potentially be used as an intervention to treat diseases caused by free radicals. Several plant-derived products, including polyphenolic compounds such as flavonoids and tannins, are recognized for their antioxidant properties (Agati *et al.*, 2012). The antioxidant activity of phenolic compounds is attributed to their strong affinity for metal chelation. Phenolic compounds that contain hydroxyl and carboxyl groups have the potential to inactivate iron ions by chelating and suppressing the superoxide-driven Fenton reaction, which is considered to be the primary producer of reactive oxygen species (ROS). As a result, plants that contain a high concentration of phenolic compounds are among the most promising candidates for nanoparticle synthesis. Recent research has demonstrated that NPs exhibit free radical scavenging activity in both in vitro and in vivo systems (Ramamurthy *et al.*, 2013; Du *et al.*, 2013).

Silver nanoparticles are widely recognized as highly effective antimicrobial agents in the fields of biology and medicine. They possess a potent biocidal impact against a wide range of microbial species, thus rendering them valuable for decades in the prevention and treatment of different diseases, particularly infections. Silver nanoparticles are widely recognized as highly effective antimicrobial agents in the fields of biology and medicine. They possess a potent biocidal impact against a wide range of microbiological species, making them valuable for millennia in the

prevention and treatment of different illnesses, including infections (Atiyeh *et al.*, 2007). The substantial surface area of AgNPs enables them to establish a more direct connection with microorganisms, thereby ensuring that they exhibit effective antibacterial properties at lower concentrations. Once AgNPs are introduced into a pathogen, the particles release silver ions, which subsequently eliminate the pathogen. Several mechanisms have been suggested to elucidate the activity of silver ions or SNPs on bacteria, including: i) deactivation of the respiratory chain, ii) disruption of the cell membrane and release of cellular contents, iii) binding to functional groups of proteins, resulting in protein denaturation and cell death, iv) inhibition of DNA replication, and v) denaturation of enzymes responsible for transporting nutrients across the bacterial cell membrane (Kumar *et al.*, 2004). These properties render nano-silver an effective fatal agent against a wide range of bacteria, including antibiotic-resistant strains, both Gram-negative and Gram-positive (Mohanty *et al.*, 2012).

The proposed mechanism for anticancer activity of biogenic AgNPs is apoptosis caused by nanoparticles through caspase-dependent and mitochondrial dependent pathways (Arokiyaraj *et al.*, 2014). It has been proposed that biogenic AgNPs can enhance the efficacy of a specific anticancer drug by targeting it specifically to specific cancer cells (targeted drug delivery), resulting in a reduction in the dosage of the drug and a reduction in side effects due to their increased biocompatibility and higher efficiency. The combination of biogenic silver nanoparticles (AgNPs) with the cancer drug doxorubicin demonstrated a notably increased anticancer effect in the B16F10 cell line in comparison to the drug coupled with chemically produced nanoparticles. The morphology and dimensions of biogenic AgNPs are linked to the mechanism of anticancer activity through the generation of reactive oxygen species (ROS), which disrupts cellular homeostasis (Patra *et al.*, 2015). We anticipate that biogenic AgNPs may serve as a potential cancer therapeutic agent in the near future, considering the challenges and novelty they present. The demand for metal nanoparticles for a variety of applications is increasing at a rapid pace, necessitating their industrial production in stabilized formulations through green synthesis.

In this work, we have investigated the biosynthesis of AgNPs using leaves aqueous extract of invasive aliens plant species i.e *Mikania micrantha* and *Acmella*

ciliata. Invasive alien plant species (IAPs) are plants that are distributed outside their native region either through intentional or unintentional means and may cause harm to the environment. *Mikania micrantha* Kunth, commonly known as mile-a-minute, is a significant invasive weed that possesses therapeutic benefits. It also poses a serious threat to forests and crop plantations, negatively impacting the agriculture-based economy of a country. According to the previous report, *Mikania spp.* contain a variety of pharmacologically active compounds, such as flavonoids, sesquiterpenes, diterpenes, coumarins, sesquiterpene lactones, and phytosterols or terpenoids, which contribute to their medicinal properties and aid in the treatment of respiratory diseases, rheumatism, fever, and influenza (Nayak *et al.*, 2017). *Acmella ciliata* (HBK), also referred to as the 'toothache' plant, is a herb of significant therapeutic value that occurs extensively in tropical and subtropical regions (Jansen, 1985). The extracts of various species of *Acmella* plants have demonstrated multiple beneficial properties, including antimicrobial, antipyretic, local anaesthetic, insecticidal, antioxidant, aphrodisiac, and vasorelaxant properties. These properties were primarily attributed to the presence of various secondary metabolites, such as N-alkamides, phenolics, and flavonoids (Lagnika *et al.*, 2016; Kadir *et al.*, 1989; Abeysiri *et al.*, 2013; Rondanelli *et al.*, 2020; Sharma *et al.*, 2011; Wongsawatkul *et al.*, 2008). In this study, we present the biogenic synthesis of AgNPs that uses the aqueous extract of *Mikania micrantha* and *Acmella ciliata* to reduce Ag^+ ions. We also explored the antibacterial properties of silver nanoparticles produced using leaf extract, specifically targeting pathogenic bacteria. Furthermore, we assessed the antifungal activity of the nanoparticles against *Curvularia pseudobracyspora*, a rice pathogen. Additionally, we illustrated the cytotoxic and anti-cancer properties of AgNPs by using the Type II human lung adenocarcinoma cell line A549 as our model, which showed substantial anticancer activity.

Chapter 2

Review of Literature

Nanotechnology

Nanotechnology refers to the manipulation and control of structures, devices, and systems at the nanoscale scale, including their design, characterization, production, and application (Bayda *et al.*, 2019). Nanotechnology aims to develop nanostructures with enhanced functions based on atomic, molecular and supramolecular molecules and the term nanoparticle refers to particulate matter ranging in size from 1-100 nm (Limongi *et al.*, 2017). A nanoscale dimension has the advantage of having a significantly large surface area-to-volume ratio (Iravani, 2011).

The significant expansion of nanotechnology has created new opportunities in the field of materials science and engineering. This includes advancements in areas such as bio-nanotechnology, quantum dots, surface-enhanced Raman scattering, and applied microbiology (Medintz *et al.*, 2008). The advancements in the organization of nanoscale structures into predetermined superstructures guarantee that nanotechnology will have a crucial impact on numerous vital technologies. It is becoming increasingly significant in several fields, including mechanics, optics, biomedical sciences, chemical industry, electronics, space industries, drug-gene delivery, energy science, catalysis, optoelectronic devices, photoelectrochemical applications, and nonlinear optical devices (Malik *et al.*, 2023). Thus, controllably generated nanometer-scale germanium quantum dots (less than 10 nm) could create innovative optoelectronic device applications like light emitters and single electron transistors (Wang and Herron, 1991). The capacity to adjust the optical absorption and emission characteristics of quantum dots (nanoparticles made of semiconductors) by basic modifications in the size of the nanoparticles is especially appealing for the easy manipulation of material band gaps (Fendler and Meldrum, 1995) and the development of quantum dot lasers (Ledentsov *et al.*, 1996). Furthermore, developments in nanotechnology are resulting in a new class of magnetic resonance image contrast-enhancing agents, such as small particles of iron oxide and fullerenes that encapsulate Gd³⁺ ions. Investigating and manipulating materials at the atomic

and molecular levels, where characteristics differ significantly from those at higher scales, is the domain of nanoscience (Chanda and Mohanta, 2016). It is a multidisciplinary field that extends across the areas of physics, chemistry, biology, and medicine (Hojjat and Hojjat, 2016). In 1974, Professor Norio Taniguchi of Tokyo Science University provided the initial definition of nanotechnology as "the manipulation and alteration of materials at the atomic or molecular level through processes such as separation, consolidation, and deformation" (Bayda *et al.*, 2019). Nanotechnology is a scientific field that focuses on the creation, analysis, investigation, and utilization of nanoscale materials with the goal of advancing scientific knowledge (Shalaby *et al.*, 2015). The role of nanotechnology and nanostructured materials in science, research, the economy, and daily life is expanding as more products based on these materials are introduced to the market (Nisha *et al.*, 2015). The development of innovative biosynthetic devices and environmentally acceptable technologies for nanomaterial synthesis has led to the emergence of the discipline of nanobiotechnology, which is the junction of biotechnology and nanotechnology (Asha *et al.*, 2016).

Green nanotechnology

Green nanotechnology refers to the utilization of green chemical concepts in the creation of nanoscale products, the advancement of technologies for producing nanomaterials, and the application of such nanomaterials. The integration of green chemistry principles into nanotechnology has garnered significant interest and attention in the last decade (Mohammadlou *et al.*, 2016). Green chemistry is the process of designing, developing, and implementing chemical products and processes to reduce the use and generation of hazardous substances that have a detrimental effect on human health and the environment (Moosa *et al.*, 2015). Physical and chemical approaches can be used to synthesize AgNPs; however, they are either costly or involve the use of hazardous chemicals that are a threat to the environment (Gou *et al.*, 2015). The incorporation of non-toxic chemicals, ecologically friendly solvents, minimal energy usage, moderate operating conditions, and renewable resources are crucial factors that should be taken into account in a green synthesis strategy (Basu *et al.*, 2016).

Nanoparticles

Nanoparticles with dimensions ranging from 1 to 100 nm function as a connection between bulk materials and atomic or molecular structures (Khodashenas and Ghorbani, 2019). The prefix "nano" is derived from the Greek word "nanos," which means "dwarf" or "extremely small" (Karthika and Sevarkodiyone, 2015). Nanostructured materials, referred to as nanoparticles (NPs), exhibit distinctive and enhanced characteristics due to their increased ratio of surface area to volume. There are two main categories of nanoparticles (NPs): organic NPs and inorganic NPs. Inorganic NPs encompass noble metal NPs, such as silver and gold, as well as semiconductor NPs, such as titanium oxide and zinc oxide (Mathew *et al.*, 2016).

Metallic nanoparticles

Noble metal nanoparticles are widely recognized for their significant applications in the areas of electrical, magnetic, optoelectronics, and information storage (Gratzel, 2001; Dai and Bruening, 2002; Murray *et al.*, 2001). The intrinsic characteristics of a noble metal nanoparticle are now known to be determined by its size, shape, composition, crystallinity, and structure (whether it is solid or hollow) (Shiraishi and Toshima, 1999). The potential applications of metal and semiconductor nanoparticle synthesis have resulted in the development of novel technologies, leading to an extensive area of research. Metal nanoparticles possess a substantial specific surface area and a significant proportion of surface atoms. The distinctive physicochemical properties of nanoparticles, including as catalytic activity, optical properties, electronic properties, antimicrobial properties, and magnetic properties, have attracted the attention of scientists due to their innovative synthesis methods (Razavi *et al.*, 2015). The production of metal nanoparticles has become a prominent focus of study in modern material science over the last decade. Nano-crystalline silver particles have been extensively utilized in several domains such as high sensitivity biomolecular detection, diagnostics, antimicrobials, therapies, catalysis, and microelectronics.

Silver nanoparticles (NPs) are a prominent type of noble metal NPs that serve as highly effective substrates for surface enhanced Raman scattering to detect individual molecules. Additionally, they exhibit exceptional catalytic properties,

enabling them to accelerate various chemical reactions. Metal nanoparticles have attracted considerable attention from the scientific community for decades owing to their exceptional physicochemical characteristics, which often vary significantly from those of bulk material. Due to the fact that nearly all of the properties in the nanoscale regime are reliant on size and form, the synthesis of metal nanoparticles under control has grown in importance in the field of advanced materials in recent years. The cost and surface characteristics of as-prepared metal nanoparticles (NPs) will also be determined by the synthesis approach, therefore controlled synthesis of metal particles is highly desirable and has received a lot of attention (Lai *et al.*, 2017). The most intriguing and often utilized metals for the synthesis of nanoparticles (NPs) are gold (AuNPs) and silver nanoparticles (AgNPs), which have inherent peculiarities (Kesharwani *et al.*, 2009). AgNPs are among the most popular due to their distinctive physical, chemical, and biological characteristics in comparison to their counterparts, gold and platinum (Sharma *et al.*, 2009). Because of their exceptional qualities, such as excellent electrical and thermal conductivity, surface-enhanced Raman scattering, chemical stability, catalytic activity, and nonlinear optical behaviour, silver nanoparticles are particularly intriguing to be utilized in the polymer composites industries (Krutyakov *et al.*, 2008).

AgNPs are recognized as powerful antimicrobial agents that exhibit a wide range of effectiveness against bacteria (Ahmad *et al.*, 2015). They are extensively utilized in consumer products due to their optical features, which include a yellowish tint in water and a distinct absorbance peak at around 420 nm (Lai *et al.*, 2017). Researchers are interested in silver nanoparticles due to their wide range of applications in several fields, including integrated circuits, sensors, bio-labelling, filters, antimicrobial deodorant fibres, cell electrodes, and antimicrobials (Iravani, 2011). AgNPs possess distinct characteristics in the nanoscale system as a result of their facile production and ability to undergo chemical alterations. Electronics, material sciences, and medicine use AgNPs to advance their novel technologies. Due to their wide-ranging applications in numerous fields, scientists worldwide are doing further study on AgNPs (Husain *et al.*, 2023). In contemporary times, nanoparticles, particularly nano-silver, are commonly employed as an antibacterial agent in the realms of medicine and the environment.

Synthesis of Silver Nanoparticle

Silver nanoparticles (AgNPs) can be synthesized using a wide range of technologies, typically classified into two primary approaches: top-down and bottom-up procedures. Top-down approach: AgNPs are produced from their bulk materials by various processes and procedures, such as thermal breakdown, irradiation, laser ablation, and arc discharge, in the top-down (physical) approach. Bottom-up approach: AgNPs are produced using a bottom-up (chemical and biological) method, wherein their fundamental building elements react to produce AgNPs with the appropriate size and shape.

The eco-friendly methods in chemistry and chemical technologies developed out of concern for environmental problems. Hence, an ideal route for silver nanoparticle synthesis that provides a simple, cost-effective, eco-friendly method is required. Currently, there are several methods available to synthesize silver nanoparticles.

(i) Physical method: Various physical methods are commonly used to produce nanoparticles. These methods can be divided into two broad groups: (a) mechanical methods, such as high energy ball milling and melt mixing, and (b) vapor methods, such as physical vapor deposition, laser ablation, electric arc deposition, implantation of ions, and sputter deposition (Bindhu *et al.*, 2015; Giri *et al.*, 2007; Ayyub *et al.*, 2001; Okuyama and Lenggoro, 2003; Nieman *et al.*, 1991; Yoon *et al.*, 2003). The main limitations of these procedures include the incorporation of structural errors and surface pollution during synthesis, as well as their reliance on advanced instrumentation, resulting in elevated production costs.

(ii) Chemical method: Chemical processes can also synthesize nanoparticles. It consists of a range of methods that include coprecipitation, chemical reduction, electrochemical, microemulsion, pyrolysis, phytochemical, sonochemical, and microwave-assisted synthesis (Iravani *et al.*, 2014; Katsuki *et al.*, 2003). The chemical method necessitates the use of hazardous, flammable, and difficult-to-dispose reducing, capping, and stabilizing compounds. Furthermore, this technique exhibits very few material transformations and substantial energy demands, giving rise to environmental concern (Awwad *et al.*, 2015). The chemical methods present a variety of challenges, including the extensive use of hazardous substances, their lack of

environmental friendliness, the need for expensive chemicals that require high energy input, the requirement for advanced equipment, and the potential presence of toxic chemicals adsorbed on the surface, which can lead to unacceptable toxic effects on humans and adverse reactions in biomedical applications (Verma *et al.*, 2015). Organic and inorganic reducing agents, including sodium citrate, ascorbate, sodium borohydride, and Tollen's reagent, are generally used to reduce Ag⁺ ions in aqueous solutions (Yugandhar *et al.*, 2015).

(iii) Biological method: The latest advancements in green chemistry techniques for the production of silver nanoparticles have demonstrated their significant potential in a variety of biomedical applications. The production of silver nanoparticles utilizing various biological sources has consistently been a captivating endeavour for scientists, owing to its wide-ranging uses. Many researchers have used a variety of biological sources, including microbial sources (such as bacteria, fungi, and their culture media) and plant sources (extracts of leaves, roots, flowers, seeds, stalks, and fruits), to synthesize silver nanoparticles. Various biologically derived biomolecules, such as alkaloids, proteins, phenols, saponins, tannins, enzymes, and terpenoids, play a role in reducing and stabilizing nanoparticles, which are of therapeutic interest (Kulkarni and Muddapur, 2014).

Solvent system-based “green” synthesis

When it comes to the synthesis process, solvent systems are an essential component, regardless of whether the synthesis is considered "green" or not. Water is universally regarded as an optimal and appropriate solvent solution for synthesis activities. Sheldon asserts that the optimal choice for a solvent is none at all, and if a solvent is essential, water is the ideal solution (Shanker *et al.*, 2016). Water is the most cost-effective and widely available solvent on the planet. Since the emergence of nanoscience and nanotechnology, water has been utilized as a solvent for synthesizing diverse nanoparticles. As an illustration, we synthesized Au and Ag nanoparticles in an aqueous medium at ambient temperature using the bifunctional molecule gallic acid (Yoosaf *et al.*, 2007). A laser ablation method was used to produce gold nanoparticles in an aqueous solution. The synthesized gold nanoparticles partially oxidize due to the oxygen in the water, which ultimately increases their chemical reactivity and significantly affects their growth (Sylvestre *et al.*, 2004).

Characterization

Characterization is a crucial stage after the synthesis of nanoparticles, and there exist various physiochemical techniques for characterizing nanomaterials with the aim of comprehending their crystallinity, size, shape, hydrodynamic radii, charge, and surface functional groups. An in-depth analysis of nanomaterials through diverse analytical techniques enables us to comprehend their biological behaviour upon their introduction into the body. To evaluate the properties of nanomaterials, a range of analytical techniques are currently employed. These techniques include UV-visible spectroscopy for the purpose of detecting Surface Plasma Resonance (SPR) spectra, XRD for surface crystallinity, TEM for size comprehension, SEM for shape analysis, DLS for size and charge assessment, FT-IR for functional group detection, and XPS for elemental composition analysis.

UV Spectrometry analysis: UV-vis spectroscopy is defined as absorption spectroscopy within the UV-vis spectral region. Light wave lengths between 300 and 800 nm are commonly utilized to characterize various metal nanoparticles ranging in size from 2 to 100 nm (Mittal *et al.*, 2013). UV-vis spectroscopy is an important approach for assessing the synthesis and stability of AgNPs in a water-based system (Bar *et al.*, 2009). Biosynthesized silver nanoparticles from *mangosteen* leaf have a resolution of 1 nm between 300 and 700 nm, a scanning speed of 300 nm/min, and a maximum absorbance of 438 nm via a UV-visible absorption spectrophotometer. The synthesis of silver nanoparticles from a plant extract exhibits a peak absorbance at 430 nm, which progressively increases with the duration of the process. There is no indication of light absorption in the UV-visible spectra range of 400nm–800nm for the pure *Solanum torvum* plant extract. However, when the plant extract is subjected to AgNO₃ solutions, the highest level of light absorption is observed at 434 nm, which is attributed to the creation of nanoparticles. UV-vis spectral analysis confirmed the formation of stable silver nanoparticles in an aqueous colloidal solution containing *Jatropha curcas* seed extract. Distinctive absorption bands corresponding to surface plasmons are observed at a wavelength of 425 nm for silver nanoparticles produced using a concentration of 10^{−3}(M) AgNO₃ and a specific volume fraction ($f = 0.2$) of aqueous seed extract. The colour of the surface plasmon resonance band changed from

reddish yellow to deep red as the concentration of silver nitrate solution increased from 10^{-3} to 10^{-2} (M).

Fourier Transform Infra-Red Spectroscopy: FT-IR is a spectroscopic technique that analyses the molecular vibrations of chemical functional groups within specific absorbance areas ranging from 4000 to 400 cm^{-1} (Kassem *et al.*, 2023). FT-IR spectroscopy is used to determine the biomolecules that are potentially involved in reducing, capping, and stabilizing AgNPs, as well as to analyse the molecular environment of the capping agents on the nanoparticles (Chanda and Mohan, 2016). The silver nanoparticles are stabilized by the carboxylate ions peak at 1450 cm^{-1} (-COO-) in the FT-IR spectrum of the *S. torvum* leaf extract, which exhibits peaks at 1648 , 1535 , 1450 , and 1019 cm^{-1} . The utilization of seed extract from *Jatropha curcas* in the process of selected area electron diffraction (SAED) reveals that the produced silver nanoparticles possess a polycrystalline structure. The presence of three bands at 1744 , 1650 , 1550 , and 1454 cm^{-1} has been confirmed by FT-IR spectroscopy measurements. The intense absorption at 1744 cm^{-1} is attributed to the carbonyl stretching vibration of the acid groups present in the extract. Synthesized AgNPs with *A. spicifera* show intense FT-IR bands at 3351.28 , 2633.71 , 2083.50 , 1637.18 , 1082.87 , and 712.34 cm^{-1} . They represent the presence of alcohols and phenols (O-H), carboxylic acids and their derivatives (C=O), and chloroalkanes (CX), respectively (Kumar *et al.*, 2012). The FT-IR analysis of *Gliricidia sepium* indicate that the absorption peak at around 1020 cm^{-1} can be attributed to the absorption peaks of -CO-C- or -C-O-. The presence of a peak at approximately 1640 cm^{-1} signifies the presence of amide I bonds in proteins. The amide bonds originating from the proteins serve as the capping ligands for the nanoparticles (Rajesh *et al.*, 2009).

X ray diffraction analysis: X-ray diffraction (XRD) is an invaluable method for confirming the presence of AgNPs, determining their crystal structure, and assessing the size of the crystalline nanoparticles. XRD pattern for the plant-assisted synthesis of silver nanoparticles consists of photons with energy ranging from 100 electron volts (eV) to 100 kilo-electron volts (keV). Short-wavelength X-rays ranging from 1 - 120 keV were used for diffraction applications (Shi *et al.*, 2023). The XRD patterns of silver nanoparticles synthesized from *Jatropha curcas* seed extract show Bragg reflections with 2θ values of 38.03° , 46.18° , 63.43° , and 77.18° , corresponding

to lattice planes (1 1 1), (2 0 0), (2 2 0), and (3 1 1). These are indexed as the band for face-centered cubic structures of silver, and the XRD pattern demonstrates the crystalline nature of synthesized silver nanoparticles. Silver nanoparticles synthesized from papaya fruit extract show three strong peaks ranging from 10° to 80° , with an average particle size of 15nm (Banala *et al.*, 2015). The XRD patterns for silver nanoparticles generated using Neem leaf broth show a number of Bragg reflections that correspond to the (111), (200), (220), (311), and (222) sets of lattice planes (Ali *et al.*, 2023). Therefore, it is evident that the silver nanoparticles are produced through the reduction of Ag^+ ions, which possess a crystalline structure (Shankar *et al.*, 2004).

Scanning Electron Microscopy: SEM is a technique that produces an output image by employing electrons in place of light and characterize the size, shape, morphology and distribution of synthesized AgNPs (Zhang *et al.*, 2016). The purity and polydispersity of the resultant AgNPs are also indicated by the SEM micrographs (Mittal *et al.*, 2013). Scanning electron microscopy (SEM) confirmed the formation of spherical silver nanoparticles extracted from *Syzygium aromaticum*, with a size range of 20 nm to 149 nm. The silver nanoparticles synthesized by *A. paniculata* were found to be spherical in shape and were an average size of 35-55 nm with an interparticle distance. It is evident from the aggregation of the nanoparticles that they were in close proximity, but were stabilized by a capping agent (Panneerselvam *et al.*, 2011). The silver nanoparticles synthesized by the novel *Pseudomonas sp* exhibit peak sharpening, indicating that the particles are in the nanoscale range. The silver nanoparticles were spherical in shape and aggregated into a larger irregular structure that lacked a well-defined morphology (Mukunthan and Balaji, 2012).

High Resolution Transmission Electron Microscopy: TEM was employed to perform the structural characterisation and particle size analysis of silver nanoparticles. It allows for the observation of particle size at the nanoscale and enables accurate investigation of crystal structure with remarkable resolution. The size measurement of the biogenic Ag nanoparticles prepared by *Ulva lactuca* extract was determined to be 20–30 nm in diameter by HRTEM analysis (Hamouda *et al.*, 2023). Silver nanoparticles made from *Jatropha curcas* seed extract in aqueous colloidal solution exhibit red SPR band shift from 10^{-3} to 10^{-2} (M) and colour changes from reddish yellow to deep red based on increasing concentration of silver nitrate. The

HRTEM analysis reveals that the particles exhibit a spherical shape, with diameters ranging from 15 to 25 nm, along with bigger and irregularly shaped particles with diameters of 30-50 nm. The sizes of the particles at two different concentrations of AgNO₃ are consistent with the observed surface plasmon resonance (SPR) band, specifically at 425 and 452 nm, respectively.

Green synthesis of silver nanoparticles

Green synthesis involves utilizing biogenic components such as plant extracts, biopolymers, and microbial sources (such as bacteria, fungi, algae, and yeast) to produce nanomaterials. The focus of green chemistry is to develop environmentally acceptable ways for synthesizing AgNPs that are biocompatible and non-toxic (Arokiyaraj *et al.*, 2015). The development of sustainable production of silver nanoparticles (AgNPs) is becoming a significant field of nanotechnology. The development of green synthesis of AgNPs is a critical area of nanotechnology. The production of AgNPs through the use of biological entities such as microorganisms, plant extract, or plant biomass could serve as an environmentally benign alternative to chemical and physical methods (Phatak and Hendre, 2015). In the biological synthesis of AgNPs, living organisms synthesize compounds that serve as both reducing agents, which reduce Ag⁺ ions, and stabilizing agents, which prevent the aggregation of AgNPs. The advantages of green synthesis of AgNPs over traditional chemical procedures are as follows: (i) Green synthesis is a straightforward process that typically entails a single-pot reaction; (ii) it is scalable; (iii) the toxicity associated with hazardous chemicals is eliminated; (iv) green biological entities can be employed as reducing and capping agents; and (v) the process is cost-effective, requires minimal energy input or intervention, utilizes renewable resources, and is an environmentally friendly method that does not necessitate the use of high pressure, energy, temperature, or toxic chemicals (Ahmed and Ikram, 2015). Three primary steps are involved in the green synthesis of AgNPs, as per the perspectives of green chemistry (Keat *et al.*, 2015): (i) the selection of a biocompatible and non-toxic solvent medium, (ii) the selection of environmentally benign reducing agents, and (iii) the selection of a non-toxic capping and stabilizing agent to stabilize AgNPs, thereby preventing their aggregation. Capping agents have a vital and multifunctional role during the synthesis of AgNPs. Capping agents stabilize and functionalize AgNPs, allowing for control

over their size and shape, and providing surface protection that both inhibits aggregation and offers advantageous properties.

The advancement of environmentally friendly technologies for material synthesis and the development of effective green chemistry techniques that use natural reducing, capping, and stabilizing agents to prepare AgNPs with desired morphology and size have drawn increasing attention to the biosynthesis of AgNPs, an emerging highlight of the intersection of nanotechnology and biotechnology. The use of environmentally friendly materials like plant leaf extract to synthesize AgNPs without toxic chemicals for the synthesis protocol or particle surface offers several advantages for pharmaceutical and other biomedical applications (Gavarkar *et al.*, 2015). Compared to chemical and physical approaches, the synthesis of AgNPs using various components of medical plants, such as stem, root, leaf, flower, fruit, seed, and bark, is an innovative approach that supports environmentally friendly chemistry. In the biosynthesis method, plant extracts have been employed as reducing, capping, and stabilizing agents for the synthesis of AgNPs as a result of their reducing abilities (Krithiga and Briget, 2015). The primary mechanism explored for the green synthesis of AgNPs is the process of plant-assisted reduction, which is facilitated by the presence of phytochemicals in the extracts (Pandit, 2015). Plant material contains biomolecules such as alkaloids, flavonoids, terpenoids, amino acids, tannins, saponins, phenols, and carbohydrates, which can function as reducing, capping, and stabilizing agents (Priya *et al.*, 2016). The use of plants for synthesizing AgNPs is more favourable compared to other approaches, such as using micro-organisms, because it eliminates the need for complex and time-consuming processes involved in maintaining micro-organism cultures (Paul and Yadav, 2015). The production of AgNPs through microbe-mediated synthesis is not economically feasible due to the need for extremely aseptic conditions, multiple steps in maintaining cell culture, a longer incubation period for the intracellular reduction of Ag^+ ions, and additional purification steps.

The implementation of green synthesis methods is necessary to prevent the generation of undesirable or detrimental by-products by establishing dependable, sustainable, and environmentally friendly synthesis protocols. The utilization of optimal solvent systems and natural resources, such as organic systems, is

indispensable for accomplishing this goal. Plant extracts offer a straightforward and efficient way for synthesizing metal/metal oxide nanoparticles on a large scale, compared to the synthesis mediated by bacteria or fungus. Green synthesis techniques that utilize biological precursors are influenced by several reaction parameters, including solvent, temperature, pressure, and pH conditions (acidic, basic, or neutral). Due to the abundance of effective phytochemicals in a variety of plant extracts, particularly in leaves, such as ketones, aldehydes, flavones, amides, terpenoids, carboxylic acids, phenols, and ascorbic acids, plant biodiversity has been extensively considered in the synthesis of metal/metal oxide nanoparticles. These components have the ability to convert metal salts into metal nanoparticles (Doble and Kruthiventi, 2007). Numerous physical and chemical synthesis methods necessitate high radiation, highly toxic reductants, and stabilization agents, which can have devastating consequences for both marine life and humans. However, green synthesis of metallic nanoparticles is a one-pot or single-step eco-friendly bio-reduction process that starts with minimal resources and is cost-effective (Dahoumane *et al.*, 2017; El-Rafie *et al.*, 2013; Husen and Siddiqi, 2014; Khan *et al.*, 2015; Patel *et al.*, 2015; Siddiqi and Husen, 2016; Wadhwani *et al.*, 2016). Metallic nanoparticles have been synthesized using green synthesis to accommodate a variety of biological materials, including bacteria, fungi, algae, and plant extracts. Plant extracts offer a straightforward and efficient way for synthesizing metal/metal oxide nanoparticles on a large scale, compared to the synthesis mediated by bacteria or fungus.

Bacteria-based nanoparticles: Bacterial species are extensively employed in commercial biotechnological applications, including bioremediation, genetic engineering, and bioleaching, due to their capacity to decrease metal ions, and they are significant prospects for the creation of nanoparticles (Gericke and Pinches, 2006; Iravani *et al.*, 2014). Prokaryotic bacteria and actinomycetes are widely used to synthesize metal/metal oxide nanoparticles and other novel nanoparticles. The bacterial synthesis of nanoparticles has been employed as a result of the relative simplicity of modifying the bacteria (Thakkar *et al.*, 2010). Several bacterial strains have been widely used for producing bio-reduced silver nanoparticles with distinct size, shape, and morphological characteristics, such as *Bacillus amyloliquefaciens*, *Escherichia coli*, , *Bacillus cereus*, *Aeromonas sp.* *Phaeocystis antarctica*,

Pseudomonas proteolytica, , *Bacillus indicus*, *Arthrobacter gangotriensis*, *Bacillus cecembensis*, *Enterobacter cloacae*, *Lactobacillus casei*, *Corynebacterium sp.*, *Shewanella oneidensis* and *Geobacter spp.*

Fungi-based nanoparticles: The incorporation of fungi to synthesize metal or metal oxide nanoparticles is a highly efficient method for producing nanoparticles that are uniformly distributed and have distinct morphologies. The presence of a diverse array of intracellular enzymes renders them more effective biological agents for the production of metal and metal oxide nanoparticles (Chen *et al.*, 2009). Fungi with high competence are capable of producing greater quantities of nanoparticles in comparison to bacteria (Mohanpuria *et al.*, 2008). Furthermore, fungi have numerous advantages over other species because enzymes, proteins, and reducing compounds are present on cell surfaces (Narayanan and Sakthivel, 2011). Enzymatic reduction (reductase) within the fungal cell or in the cell wall is the most possible mechanism for the formation of the metallic nanoparticles. According to Kitching *et al.* (2015), the exposure of *Verticillium sp.* biomass to silver nitrate solution results in the production of AgNPs. It was also found that when *Trichoderma asperellum* was exposed to a solution of silver nitrate, it produced extracellular nanoparticles with sizes ranging from 13 to 18 nm (Alghuthaymi *et al.*, 2022). Fungi have the ability to release significant quantities of proteins, which subsequently leads to increased productivity of NPs. The manufacture of AgNPs is a two-step process involving the trapping of silver ions on the surface of fungal cells and the subsequent reduction of these ions by enzymes inherent in the fungal system.

Yeast-based nanoparticles: There are 1500 known species of yeast, which are single-celled microorganisms found in eukaryotic cells (Yurkov *et al.*, 2011). Several research groups have reported the successful production of nanoparticles/nanomaterials through yeast. A study has shown the production of silver and gold nanoparticles using a yeast strain that is resistant to silver and a broth made from *Saccharomyces cerevisiae*.

Algae-based nanoparticles: Several distinct types of algae have been reported to produce AgNPs by extracellular synthesis. *Chlorella vulgaris*, a type of single-celled green algae, is utilized to produce nanoparticles at ambient temperature. The marine algae *Chaetomorpha linum* (Kannan *et al.*, 2013), *Caulerpa resmosa* (Edison

et al., 2016), and *Sargassum polycystum* (Rudayni *et al.*, 2023) were also investigated for the synthesis of silver nanoparticles (AgNPs). According to Qing *et al.* (2022), the reduction of metal ions is caused by the presence of carboxyl groups in the aspartic and/or glutamine residues of the proteins, along with the presence of hydroxyl groups in the tyrosine residues.

Plants-based nanoparticles: Biosynthesis techniques utilizing plant extracts have garnered greater attention as straightforward, efficient, cost-effective, and viable methodologies, serving as a great substitute to conventional approaches for nanoparticle fabrication. Several plants can be used to decrease and stabilize metallic nanoparticles in a "one-pot" production method. Several researchers have utilized the green synthesis method to produce metal/metal oxide nanoparticles using plant leaf extracts in order to investigate their diverse applications. Plants possess biomolecules, such as carbohydrates, proteins, and coenzymes, that have remarkable potential to convert metal salts into nanoparticles. Plant extract-assisted synthesis was initially studied for the manufacture of gold and silver metal nanoparticles, similar to other biosynthesis techniques. A wide range of plants, such as neem (*Azadirachta indica*), oat (*Avena sativa*), alfalfa (*Medicago sativa*), tulsi (*Osimum sanctum*), lemon (*Citrus limon*), coriander (*Coriandrum sativum*), lemon grass (*Cymbopogon fexuosus*), mustard (*Brassica juncea*), and aloe vera (*Aloe barbadensis*), have been employed in the production of silver nanoparticles and gold nanoparticles. The primary focus of this line of research has been the ex-vivo synthesis of nanoparticles, while metallic nanoparticles can be produced in living plants (in-vivo) by reducing metal salt ions that are assimilated as soluble salts. Furthermore, the in-vivo synthesis of nanoparticles such as zinc, nickel, cobalt, and copper has been observed in sunflower (*Helianthus annuus*), alfalfa (*Medicago sativa*), and mustard (*Brassica juncea*) (Marchiol, 2012).

Plant leaf extract-based mechanism

Plant leaf extract is incorporated with metal precursor solutions under varying reaction conditions to facilitate the creation of nanoparticles (Mittal *et al.*, 2013). Plant extracts are utilized to biologically reduce metal ions, resulting in the formation of their nanoparticles. The production of silver nanoparticles can utilize plant extracts from leaves, flowers, seeds, barks, fruits, and roots as stabilizing and reducing agents

(Bar *et al.*, 2009; Marambio-Jones and Hoek, 2010; Velayutham *et al.*, 2005). The criteria that determine the circumstances of the plant leaf extract, such as the types and concentrations of phytochemicals, metal salts, pH, and temperature, are considered to regulate the yield and stability of nanoparticles as well as the rate of synthesis (Dwivedi and Gopal, 2010). Phytochemicals found in plant leaf extracts possess a remarkable ability to decrease metal ions in a significantly shorter amount of time when compared to bacteria and fungi, which require a longer incubation period (Jha *et al.*, 2009). Hence, plant leaf extracts are regarded as a remarkable and insignificant resource for the production of metal and metal oxide nanoparticles. In addition, plant leaf extract serves a dual purpose by functioning as both reducing and stabilizing agents throughout the process of synthesizing nanoparticles, therefore contributing in the formation of nanoparticles (Malik *et al.*, 2014).

Another crucial element in the creation of nanoparticles is the makeup of the plant leaf extract; for instance, various plants have variable amounts of phytochemicals in their extract (Li *et al.*, 2011; Mukunthan and Balaji, 2012). Flavones, terpenoids, sugars, ketones, aldehydes, carboxylic acids, and amides are the primary phytochemicals found in plants and are responsible for the bio-reduction of nanoparticles (Thatyana *et al.*, 2023). Flavonoids possess diverse functional groups that have an increased capacity to decrease metal ions. The release of the reactive hydrogen atom occurs as a result of tautomeric conversions in flavonoids, when the enol-form is changed into the keto-form. The reactive hydrogen atom is produced by tautomeric flavonoids that convert enol-form to keto-form by reducing metal ions into metal nanoparticles. The formation of biogenic silver nanoparticles in sweet basil (*Ocimum basilicum*) extracts is mainly mediated by the enol-to-keto transformation process (Ahmad *et al.*, 2010). Plant extracts contain sugars, such as glucose and fructose, which can contribute to the synthesis of metallic nanoparticles. Considering that fructose-mediated gold and silver nanoparticles are monodisperse, glucose can contribute to the creation of metallic nanoparticles with diverse sizes and shapes (Panigrahi *et al.*, 2004).

FT-IR analysis of nanoparticles generated using plant extracts confirmed that newly produced nanoparticles were consistently shown to be bound to proteins. Plant extracts consist of biomolecules such as carbohydrates and proteins, which function

as reducing agents to facilitate the synthesis of metallic nanoparticles (Iravani, 2011). Proteins possessing amino groups ($-\text{NH}_2$) that have been modified in plant extracts may assist in the process of reducing metal ions (Li *et al.*, 2007). According to FT-IR analysis, nanoparticle capping ligands are functional groups like $-\text{C}-\text{O}-\text{C}-$, $-\text{C}=\text{C}-$, $-\text{C}-\text{O}-$ and $-\text{C}=\text{O}$ (Mude *et al.*, 2009). According to Velmurugan *et al.* (2015), silver nanoparticles were also synthesized using peanut shell extract, and their features included an average diameter of 10–50 nm and a spherical and oval shape. Spherical silver nanoparticles with typical particle sizes ranging from 5 to 40 nm were synthesized using a leaf extract of *Ceratonia siliqua*. The leaf extract of *Ficus benghalensis* was used to synthesize spherical-shaped silver nanoparticles, which were stable and had an average size of 10–50 nm. Nakkala *et al.* (2014) studied the oxidation state, anti-cancer, and antibacterial effects of silver nanoparticles synthesized using *Acorus calamus* extract.

The synthesis of metal nanoparticles using plant extracts can be accomplished in a metal salt solution in a short period of time at room temperature, depending on the nature of the plant extract. The key elements influencing nanoparticle production are extract content, temperature, metal salt, pH, and contact duration (Mittal *et al.*, 2013). Plants are easily accessible and contain several active compounds that can reduce Ag ions, making them ideal for nanoparticle formation (Kharissova *et al.*, 2013). Terpenoids, polysaccharides, phenolics, alkaloids, flavones, amino acids, alcoholic compounds, enzymes, and proteins are among the active agents in plants that may contribute to the reduction of silver ions to silver nanoparticles (Sharma *et al.*, 2009; Bindhu and Umadevi, 2013). The rapid formation, non-pathogenic, and environmentally friendly reaction conditions of plant extracts in green synthesis, which occur in a single step using a very cost-effective technique, make them suitable candidates for synthesizing silver nanoparticles.

Free radical scavenging activity of silver nanoparticles

Oxidative stress is generated by reactive oxygen species (ROS), including superoxide, hydroxyl, peroxy nitrile, and singlet oxygen. This stress is accountable for the onset of various ailments, such as atherosclerosis, cancer, inflammation, aging, and neurodegenerative disorders. The antioxidant properties of a silver phyto-nanosystem render them beneficial in the treatment of a variety of diseases. Silver

nanoparticles synthesized with *Allium cepa* extract also exhibited substantial free radical scavenging activities against DPPH free radicals, which may be attributed to the presence of functional groups in *Allium cepa* (Jini and Sharmila, 2019). Consequently, researchers have found that silver phyto-nanoparticles synthesized using the extracts of the ornamental floral plants *Hyacinthus orientalis* and *Dianthus caryophyllus* (oriental hyacinth and garden clove) have a high level of antioxidant activity (Bunghez *et al.*, 2012). The ABTS (2,2-Azino-bis (3-ethylbenzthiazoline-6-sulfonic acid radical) and DPPH (1,1-diphenyl-2-picrylhydrazyl radical) assays are the most commonly employed and rapid methods for estimating antioxidant activity (Bedlovičová *et al.*, 2020).

The in vitro study proved the significant antioxidant properties of silver nanoparticles in an aqueous solution including a spice mixture made from garlic, ginger, and cayenne pepper (Otunola and Afolayan, 2018). The authors propose that various types of functional groups from the spice mixture, which were responsible for reducing and capping the AgNPs, could be attributed to the significant antioxidant activity of the nanoparticles. Plant extracts contain several kinds of biologically active compounds, such as polyphenols, enzymes, and alkaloids. These molecules have the ability to give hydrogen to free radicals, which in turn interrupts the free radical chain reaction (Wang *et al.*, 2016). Elemike *et al.* (2017) attribute the antioxidant properties of AgNPs to the presence of phenolic compounds, terpenoids, and flavonoids in plants, which allow the nanoparticles to act as singlet oxygen quenchers, hydrogen donors, and reducing agents. The primary adsorption of antioxidant compounds from the extract onto the surface of the nanoparticles may also be responsible for the higher antioxidant activity of AgNPs derived from *Lantana camara* leaves (Shriniwas *et al.*, 2017). Therefore, the presence of strong antioxidant phyto-nanoparticle activity may potentially be linked to the specific encapsulation of AgNPs, particularly for medicinal plants that have extracts rich in diverse antioxidant compounds such as polyphenols and flavonoids.

Silver Nanoparticles and Their Antimicrobial Application

Microorganisms, including bacteria, fungi, viruses, and parasites, have evolved the ability to inhibit and neutralize antimicrobial properties, which is referred to as antimicrobial resistance. There has been an increase in the number and range of

organisms that are resistant to antimicrobials, as reported by the World Health Organization (WHO). Furthermore, the utilization of sub-therapeutic antibiotic treatments in animal breeding to enhance animal growth and avoid infections might lead to the emergence of antibiotic-resistant microbes, which may be transmitted to human beings (Littier *et al.*, 2017). The prevalence of infections exhibiting multidrug resistance has experienced a rapid and significant rise in recent years, posing a significant challenge to the healthcare system (Roca *et al.*, 2015). A significant multitude of bacteria have been documented as being resistant to multiple drugs (MDR), resulting in substantial expenses for their management, including medication, personnel training, isolation supplies (Huebner *et al.*, 2016), and reduced productivity.

Nanomaterials have emerged as novel antimicrobials, revolutionizing the application of antibiotics in diverse domains. For instance, silver nanoparticles (AgNPs) are the most ancient nanomaterial employed for the aim of eliminating bacteria and inhibiting their growth. Nevertheless, for only a few decades, these have been generated via biogenic or bio-based methods. The synthesis of AgNPs using biological, biogenic, or bio-based processes offers four advantages: (1) enhanced biocompatibility, achieved by generating AgNPs in water and capped with biomolecules such as proteins, sugars, or metabolites; (2) decreased toxicity, due to the use of plant-based compounds as reducing agents, which are harmless; (3) ease of production, achieved by extracting fungi, bacteria, or plants and adding silver nitrate; and (4) low cost (Thakkar *et al.*, 2010). Although there are some beneficial characteristics, the fact that biogenic synthesis methods lack the ability to control the shape and size of the nanoparticles remains a challenge.

Mechanisms of Antibacterial Action

The existing research mostly supports three methods by which AgNPs demonstrate their antibacterial activity, either in combination or individually (Marambio-Jones and Hoek, 2010; Qing *et al.*, 2018; Dakal *et al.*, 2016). The first hypothesis states that AgNPs can penetrate the outer membrane and accumulate in the inner membrane, where their adhesion to the cell destabilizes and damages it, enhancing membrane permeability and causing cellular leakage and death (Seong and Lee, 2017; Ivask *et al.*, 2014). Additionally, studies have shown that AgNPs may interact with sulfur-containing proteins in bacteria's cell walls, potentially rupturing

the cell wall through structural damage. The second approach suggests that nanoparticles have the capacity to disrupt and penetrate the cell membrane, causing changes in its structure and permeability. Further, these nanoparticles can enter the cell and interact with sulfur or phosphorus groups found in intracellular components like DNA and proteins, thereby modifying their structure and functions. They may also disrupt the respiratory chain in the inner layer of the membrane by interacting with enzyme thiol groups, generating free radicals and reactive oxygen species, damaging intracellular machinery, and initiating the apoptotic pathway. Another proposed mechanism that operates simultaneously with the other two involves the liberation of silver ions from the nanoparticles. These ions, due to their size and charge, have the ability to interact with cellular components, causing changes in metabolic pathways, membranes, and the DNA (Ivask *et al.*, 2014; Agnihotri *et al.*, 2013).

Factors Affecting Antibacterial Activity of AgNPs

The variability in antibacterial activity of nanoparticles, based on their properties, enables their alteration and production to achieve specific goals in nanoparticle synthesis. This allows for the development of an antimicrobial agent with optimized properties. The dimensions of the nanoparticles affect the extent of contact and interaction between the nanoparticle and its environment, while the electric charge and surface composition regulate the stability of the nanoparticles (Sharma and Zboril, 2017). The antibacterial activity of 5, 15, and 55 nm AgNPs was tested against *Actinomyces comitans*, *E. coli*, *Fusobacterium nucleatum*, *Sanguis mitis*, and *Streptococcus mutans*. The 5 nm nanoparticles proved more effective against microbes, with MIC values between 25 and 50 µg/ml, except for the *E. coli* strain, which had a MIC value of 6 µg/ml. The aerobic nature of *E. coli* explains the significant disparity in MICs between it and the other microorganisms studied. It suggests that this effect may be caused by the oxidation of AgNPs in aqueous medium when exposed to air, which lowers their antibacterial ability (Lu *et al.*, 2013). The rate at which silver ions are released from nanoparticles is influenced by their size and surface properties. This suggests that smaller nanoparticles may play a significant role in the antibacterial action of nanoparticles, as they have been found to disintegrate rapidly in various types of media and release silver ions in the process (Raza *et al.*,

2016; Ivask *et al.*, 2014; Le Ouay and Stellacci, 2015). The antibacterial ability is influenced by these characteristics in relation to the processes by which AgNPs interact with microorganisms. The features that improve antimicrobial efficacy are those that facilitate interactions between nanoparticles and bacterial cells, as well as their ability to penetrate into the cells.

Silver Nanoparticles in Plant Disease Management

Nanoparticles are extensively studied for their diverse applications in biology and the environment, thus becoming a crucial aspect of nanotechnology. Due to their exceptional catalytic activity, conductivity, chemical stability and antibacterial potential, they have demonstrated significant economic value. Phytopathogenic microorganisms as well as plant pests are natural plant enemies that reduce agricultural yield by 20–40% worldwide (Savary *et al.*, 2012). Chemical pesticides are an effective means of quickly eliminating pathogenic microbes, but their misuse and long-term presence in soils unintentionally lower soil fertility and disturb the native micro- and macro-biota of the soil (Shahid *et al.*, 2018). A significant number of microbes that are beneficial to plants are either eradicated or their natural ecosystem is compromised. This necessitates the development of alternative plant disease control strategies, and nanotechnology has made significant strides in medicine, such as alternative antimicrobials (Rani *et al.*, 2022; Kaur *et al.*, 2022; Janani *et al.*, 2022), and pharmacology, particularly drug delivery.

Silver nanoparticles (AgNPs) can be utilized to manage plant diseases as part of their application. Several research have been conducted to investigate the use of AgNPs with the goal of controlling phytopathogenic fungus (Jo *et al.*, 2015). AgNPs have emerged as an improved technique for replacing synthetic fungicides. There is an immense demand for the most recent anti-fungal drugs due to the emergence of resistance in disease-causing fungi (Nyilasi *et al.*, 2010). Globally, antifungal resistance has occurred due to consistently pesticide use, which alters the fungus population and promotes resistant variants (Guilger *et al.*, 2017; Auyeung *et al.*, 2017). The AgNPs have shown antifungal activity against *Candida albicans* and *C. tropicalis* (Mallmann *et al.*, 2015), as well as *F. oxysporum* (Gopinath and Velusamy, 2013). Because of their improved permeability and retention effects, AgNPs are highly appealing and intriguing for various antifungal applications. In recent years, there has

been an increased emphasis on developing secure management strategies that prioritize the resolution of synthetic fungicide vulnerabilities and reduce the risk to humans and animals. AgNPs possess numerous antifungal mechanisms, including plasma-membrane interactions and linkages to DNA phosphate groups (Matsumura *et al.*, 2003). These mechanisms lead to proton dispersion and cell mortality, degradation of the electron transportation chain, and disruption of membrane proton motive force and phosphate groups (Feng *et al.*, 2000). Additionally, AgNPs contribute to sulfhydryl protein and enzyme group degradation. Silver nanoparticles (AgNPs) have the potential to benefit the agricultural industry by effectively targeting and controlling pathogens, thereby reducing the occurrence of plant diseases in a controlled and specific manner. Overall, the utilization of AgNPs in agriculture has considerable promise for enhancing agricultural output (Latif *et al.*, 2017). The sustainable use of biologically synthesized AgNPs has been the subject of numerous efforts by nanotechnologists and microbiologists worldwide to improve conventional agriculture. Technological advancements in AgNPs synthesis and characterization methods have improved the precision and advancement in controlling their size, shape, and yield.

Silver Nanoparticles and their anti-cancer applications

Cancer arises from genetic mutations that initiate a cascade of molecular events, ultimately resulting in tumor development. According to Hollstein *et al.* (2017), a malignant condition is characterized by the rapid division of cells without any regulation and the subsequent invasion of normally functioning cells and tissues. Cancer is one of the major risk factors of morbidities and mortalities all over the world. Either internal or external factors can generally cause cancer. External factors include chemical exposure, radiation, and viruses. Frequent exposure to toxic metals and ionizing radiation puts workers at heightened risk of developing cancer (Manzoor *et al.*, 2016). Hormones, mutations, and immune conditions are internal factors that may act sequentially to initiate or promote the process of carcinogenesis (Anand *et al.*, 2008). Most cancer treatments whether they be radiation therapy, chemotherapy, surgery, immunotherapy, cancer vaccines, photodynamic therapy, stem cell transformation, or any combination of these are associated with serious adverse effects. The use of chemotherapeutic agents can result in various toxicities, including

non-specificity, limited bioavailability, toxicity, rapid clearance, and restriction of metastasis (Patra *et al.*, 2014; Lim *et al.*, 2011; Mukherjee and Patra, 2016). 5-fluorouracil, a frequently utilized chemotherapeutic agent, is known to cause cardiotoxicity, myelotoxicity, and vasoconstriction (Macdonald, 1999). Avilés *et al.* (1993) linked doxorubicin, a cancer prophylactic medication, to renal toxicity, cardiotoxicity, and myelotoxicity. These facts motivate us to explore innovative methods and develop promising compounds for effective cancer treatment with minimal side effects.

Nanotechnology-cancer interaction

There is a growing demand for more affordable and cost-effective therapeutic agents made from natural resources, such as plants, as an alternative to conventional cancer therapy approaches (Patra *et al.*, 2014; Khan *et al.*, 2015; Singh *et al.*, 2016; Kumar and Yadav, 2009). Medicinal plants not only offer new chemical compounds through bioprospecting but also novel cancer therapy strategies, including the green production of silver nanoparticles (AgNPs). Nanotechnology has the potential to be utilized at the molecular level to regulate matter. Recent developments in nanotechnology have created new opportunities for the delivery, treatment, and diagnosis of drugs (Klefenz, 2004). Metal nanoparticles possess unique characteristics, resulting from their specific size and high surface area-to-volume ratio, that make them very suitable for various biological uses (Caswell *et al.*, 2003; Bhatte *et al.*, 2012). Fungi and bacteria can be employed to synthesize nanoparticles, but the plant-based synthesis platform is eco-friendly and effective since it doesn't require expensive, toxic, or harmful chemical compounds in growing conditions. Employing plants for this purpose can mitigate certain biosafety concerns associated with the use of fungi and bacteria in green synthesis (Kumar and Yadav, 2009). Research on medicinal plants and nanotechnology has resulted in a significant increase in the number of cancer treatments that are now possible, which is economically beneficial for patients (Shinwari *et al.*, 2006; Shinwari and Khan, 2003). These nanoparticles can dodge immune reactions and pass impermeable membranes, thus rendering them useful for cancer treatment (Oberdörster *et al.*, 2005). Metal nanoparticles have been observed with enormous interest for developing alternative theranostic strategies of cancer treatment (Munger *et al.*, 2014; Patra and Barui, 2013). Prior studies have

successfully demonstrated the use of labelled nanocrystals for monitoring and detecting tumors, as well as targeted therapy delivery using chemotherapeutic medicines (Alivisatos, 2004; Gao *et al.*, 2004).

Mechanism of anti-cancer activity of AgNPs

The proposed mechanism for anticancer activity of biogenic AgNPs is apoptosis caused by nanoparticles through caspase-dependent and mitochondrial dependent pathways (Arokiyaraj *et al.*, 2014). It has been proposed that biogenic AgNPs can enhance the efficacy of a specific anticancer drug by targeting it specifically to specific cancer cells (targeted drug delivery), resulting in a reduction in the dosage of the drug and a reduction in side effects due to their increased biocompatibility and higher efficiency. The morphology and dimensions of biogenic AgNPs are linked to the mechanism of anticancer activity through the generation of reactive oxygen species (ROS), which disrupts cellular homeostasis.

It was found that increasing cancer cell population in the sub-G1 phase stimulates caspase-3, which induces apoptosis (Mao *et al.*, 2004). The death of malignant cells treated with biogenic AgNPs may be attributed to the elevation of sub-G1-phase cancerous cells, which is highly correlated with apoptosis induction, as per scientific reports. Several studies have found that treating cancer cells with biogenic AgNPs results in the production of reactive oxygen species (ROS), which causes cellular damage (Zhang *et al.*, 2013; Minai *et al.*, 2013; Franco-Molina *et al.*, 2010). The transmembrane potential of mitochondria and respiration uncoupling are also associated with an increase in superoxide radical generation (Hass and Barnstable, 2021). Current research clearly suggests that biogenic AgNPs stimulate the production of reactive oxygen species (ROS), which ultimately induces apoptosis and cell death. The study conducted by Mukherjee *et al.* (2014) demonstrated the increase in p53 protein levels using western blotting analysis in the lysate of B16 cells that were treated with biosynthesized silver nanoparticles. Silver ions released by AgNPs cause caspase-3 activation and oxidative stress (Gurunathan *et al.*, 2013). Further, it was proposed that the acidic nature of the tumor was responsible for the release of phytoconstituents from biogenic AgNPs, hence increasing the potential anticancer effects of colloidal biogenic AgNPs (Mukherjee *et al.*, 2014).

Colloidal biogenic AgNPs synthesized using green techniques have potential applications in cancer therapy and diagnosis, including biosensing, bioimaging, and MRI imaging applications (Smith *et al.*, 2013; Boisselier and Astruc, 2009; Daniel and Astruc, 2004). Historical evidence demonstrates the extensive utilization of silver as a powerful therapeutic substance, with nano-silver serving as a therapeutic agent for over a century (Nowack *et al.*, 2011; Alexander, 2009). In the past decade, numerous researchers have experimentally demonstrated the nontoxic status of AgNPs in vitro, a status that differs considerably from in vivo environments (Stensberg *et al.*, 2011; Homan *et al.*, 2012; Hackenberg *et al.*, 2011). The implications of this study can be utilized to achieve future potential therapeutic benefits against aggressive-type malignancies, as AgNPs possess a unique ability to target tumor tissues.

Invasive alien plant species

People or human activities can purposefully or unintentionally introduce alien plants, also known as exotic, introduced, foreign, non-indigenous, or non-native plants, from one location to another. A naturalized species refers to an alien plant that has successfully established itself in a new ecosystem and is able to reproduce independently within its own plant community. When naturalized aliens spread so widely that they disrupt native biota or jeopardize important agricultural, human, or environmental resources, we refer to them as "invasive". The world's flora and fauna are being homogenized by the worldwide spread and rapid growth of invasive species, which has been reported as a primary cause of global declines in biodiversity (Rai and Singh, 2020). According to Drake *et al.* (1989), bio-invasion is a type of biological pollution, a significant contributor to global change, and one of the main causes of species extinction. Typical invasive species exhibit the following characteristics: they are "pioneer species" in a variety of landscapes; they are tolerant of a wide range of soil and weather conditions; they are versatile in distribution; they produce extensive amounts of seed that disperse easily; they grow aggressive root systems; they have a short generation time; they have high dispersal rates; they have long flowering and fruiting periods; they have a broad native range; and they are abundant in their native ecosystem. Initial findings from intriguing research indicate that invasive species tend to possess relatively small numbers of DNA within their cell nuclei. It's obvious that the cells in these plants possess the ability to undergo rapid division and multiplication,

resulting in accelerated growth compared to species with higher cellular DNA content. As a result, these plants have a competitive advantage in disturbed environments.

The alien plant is under cultivation for several economic goals, including food production, fodder, lumber, and ornamental use. Invasive alien plants have adaptable behavior and can be found in a variety of habitats, including woods, crop areas, waste lands, plantations, gardens, and roadway sides. *Mikania micrantha*, *Prosopis juliflora*, *Salvinia molesta* and *Cabomba caroliniana* are well-known examples of invasive species. Furthermore, the following are invasive alien weeds: *Chromolaena odorata*, *Lantana camara*, *Opuntia dillenii*, *Mimosa pudica*, *Lippia geminata*, *Eichhornia crassipe* and *Jaropha gossipifolia* (Mandal, 2011). The most prominent invasive foreign plants in India are *Eupatorium odoratum* and *Lantana camara*, which are among the most problematic invasive species in the world. The Calcutta Botanical Garden brought these invasive plants to India from the Neotropics a century ago (Soumya and Sajeew, 2020).

In contrast to chemical control, which is frequently highly effective as a short-term remedy, mechanical control is particularly target-specific and labour-intensive. Due to its environmentally benign character and restrictions on pesticide use in conservation areas, classical biological control is extremely economical, long-lasting, self-sustaining, ecologically safe, and suitable for use in these regions. Implementing initiatives to control invasive species provides a rational and sustainable answer, however, no such projects have been earnestly undertaken in India. In an effort to maintain the endeavour to regulate the culture of alien species in the country, a series of strategic national plans and guidelines have been established for the import of alien organisms (Pyšek *et al.*, 2020). The initial stage in managing invasive alien species (IAS) is the establishment of a national strategy.

Chapter 3

Synthesis and characterization of silver nanoparticles using *Mikania micrantha* and *Acmella ciliata* leaf extract

1. Introduction

The study of phenomena and material manipulation at the atomic and molecular levels, where properties differ noticeably from those at higher scales, is known as nanoscience (Bayda *et al.*, 2019). Green nanoscience encompasses the utilization of green chemical principles in the creation of nanoscale products, the advancement of technologies for producing nanomaterials, and the application of these nanomaterials. According to the Oxford English Dictionary (OED), the prefix nano comes from the Greek word nanos, which means "dwarf" or "extremely small." Nanostructured materials, referred to as nanoparticles (NPs), exhibit distinctive and enhanced characteristics due to their increased surface area relative to their volume (Khan *et al.*, 2019). NPs are broadly classified into two categories: organic NPs and inorganic NPs, which include noble metal NPs (such as silver and gold) and semiconductor NPs (such as titanium oxide and zinc oxide).

The synthesis of nanoparticles can be achieved by a wide range of methods, typically classified into two primary approaches: top-down and bottom-up. NPs are produced from their bulk materials by various processes and procedures, such as thermal breakdown, irradiation, laser ablation, and arc discharge, in the top-down (physical) approach. AgNPs are produced using a bottom-up (chemical and biological) method, wherein their fundamental building elements react to produce AgNPs with the appropriate size and shape. Due to the diverse array of uses provided by nanoparticles in various scientific and technological domains, multiple techniques have been developed for their synthesis. Nanoparticles can be generated through chemical, physical, and biological processes. Chemical processes have several disadvantages, such as the utilization of toxic solvents and surfactants, higher costs, the production of dangerous by-products, and increased energy consumption, all of which pose significant threats to human health and the environment (Badmus *et al.*, 2021). Compared to chemical and physical approaches, green nanoparticle synthesis

offers advantages such as cost-effectiveness, environmental friendliness, ease of scaling up for large-scale synthesis, and a lack of need for hazardous chemicals and high temperatures (Osman *et al.*, 2024). Metal nanoparticles possess distinctive physio-chemical properties that render them highly suitable for a wide range of biological applications. AgNPs have garnered significant interest among other noble metal nanoparticles due to their distinct characteristics, such as favourable electrical conductivity, chemical stability, catalytic, and antimicrobial properties (Xu *et al.*, 2020). Due to its high surface-to-volume ratio, silver at the nanoscale exhibits distinct properties compared to bulk particles composed of the same material (Altammar, 2023).

Green synthesis methods leverage the extensive bioresources that are naturally present, including plants, bacteria, fungi, yeast, and enzymes. Researchers have proposed the use of microorganisms and plant compounds in biological synthesis for silver nanoparticles as a valuable alternative to chemical methods, as it avoids the use of toxic chemicals and high temperatures. The utilization of plant extracts in nanoparticle synthesis is gaining significant attention due to its dual role as reducing agents and stabilizing agents (Mittal *et al.*, 2013). The approaches to producing nanoparticles using plant extracts are easily scalable, safe for human therapeutic use and potentially more cost-effective compared to the more expensive methods relying on microbial activities (Vijayaraghavan and Ashokkumar, 2017). Plant extracts are more advantageous than other biological processes because they eliminate the complex process of cell culturing and maintenance and can be scaled up for large-scale nanoparticle synthesis (Adeyemi *et al.*, 2022). The source of the plant extract can influence the characteristics of nanoparticles due to variations in the concentration and combinations of organic reducing agents found in different extracts (Antunes *et al.*, 2023).

The fundamental mechanism for the reduction of silver ions in a biological system is postulated to begin with the immobilization of silver ions on the protein surface in the extract through electrostatic interactions, also known as a recognition process. Proteins cause the reduction of silver ions, resulting in alterations to their secondary structure and the creation of silver nuclei. These silver nuclei then increase in size by the reduction of silver ions and their aggregation at the nuclei (Chung *et al.*,

2016). Despite the lack of full elucidation of the precise mechanisms behind the synthesis of nanoparticles (NPs) in plants, there may be some correlation with the concept of phytoremediation in plants (Masarovičová and Král'ová, 2012).

Given the intricate nature of research on green synthesis, it is important to consider the following points when synthesizing AgNPs: (i) Chemical composition of the plant extract: The reduction of Ag^+ to Ag^0 is mostly attributed to the oxidation of several biomolecules, including flavonoids, ketones, aldehydes, tannins, carboxylic acids, phenolic compounds, and plant proteins. Furthermore, the stability and size of the generated AgNPs are contingent upon the biomolecules that serve as capping agents (Vijilvani *et al.*, 2020). (ii) Concentration of the plant extract: The morphology and dimensions of the produced AgNPs are dependent on the concentration of plant extract used. An increase in the extract concentration results in the production of a significant quantity of nanoparticles up to a specific level (López-Miranda *et al.*, 2016). (iii) Concentration of AgNO_3 : As the concentration of AgNO_3 increased, the number of AgNPs also increased proportionally, leading to the complete consumption of the AgNO_3 salt and the subsequent reduction of all Ag^+ to Ag^0 . By increasing the intensity of UV-Vis spectroscopy, we can readily monitor this process (Sangaonkar and Pawar, 2018). (iv) pH: The pH level can alter the electrical charges of biomolecules present in the plant extract, which can potentially impact their ability to cap and stabilize nanoparticles and hence affect their growth. An increase in pH generally leads to an increase in the rate of formation and promotes a more uniform distribution of the size of nanoparticles (Gavade *et al.*, 2015). (v) Reaction temperature: Typically, a high temperature is necessary to fully reduce AgNO_3 to AgNPs via a chemical method. However, considering economic and green chemistry factors, conducting the reaction at room temperature is the most favourable option (Farooq *et al.*, 2019). (vi) Reaction time: A red shift in the UV-Vis spectrometer data indicates that the size of the NPs is increasing over time. As a result, it is critical to continuously monitor the reaction in order to obtain stable, small-sized NPs (Ratan *et al.*, 2020).

Various analytical and spectroscopic methods are employed to determine the properties of nanoparticles, including their nature, size, shape, distribution, stability or aggregation state, morphology, elemental composition, and dispersity (monodisperse

or polydisperse). The uniformity of these characteristics is crucial in numerous applications. The most frequently employed methods for characterizing nanoparticles are as follows: UV-visible spectrophotometry, Fourier transform infrared spectroscopy (FT-IR), Scanning electron microscopy (SEM), energy dispersive spectroscopy (EDS), transmission electron microscopy (TEM), and X-ray diffraction (XRD). UV-visible spectroscopy typically uses light wavelengths ranging from 300 to 800 nm to analyse metal nanoparticles with sizes ranging from 2 to 100 nm (Vijayaram *et al.*, 2024). FT-IR spectroscopy characterizes the surface chemistry of nanoparticles and other surface chemical residues and is useful for detecting organic functional groups (e.g., carbonyls, hydroxyls) adhered to the surface (Raj *et al.*, 2021). Scanning electron microscopy and transmission electron microscopy are employed to analyze the structure and shape of compounds from nanometers to micrometers (Malatesta, 2021). Transmission electron microscopy exhibits a resolution that is 1000 times higher than scanning electron microscopy (Brodusch *et al.*, 2021). Energy dispersive spectroscopy (EDS) is widely used to determine the elemental composition of metal nanoparticles (Mishra *et al.*, 2017). X-ray diffraction (XRD) is employed for the phase identification and characterization of the crystal structure of the nanoparticles (Holder and Schaak, 2019). X-rays penetrate the nanomaterial, and the resulting diffraction pattern is compared with known standards to acquire structural information.

2. Materials and methods

2.1 Chemicals and reagents

Silver nitrate (AgNO_3) and sodium hydroxide (NaOH) were purchased from Merck Chemicals.

2.2 Preparation of plant extract

Fresh leaves of *Mikania micrantha* and *Acmella ciliata* were collected from Mizoram University campus, Tanhril, Aizawl, Mizoram. The plants were identified and authenticated by the Mizoram University Herbarium, Department of Botany, as *Mikania micrantha* (L.) and *Acmella ciliata* (Kunth) with accession numbers MZUH000963 and MZUH000964, respectively. The leaves were washed, dried, and

minced. 25 g of pulverised leaves of *M. micrantha* and *A. ciliata* were boiled separately in 100 ml of distilled water for 1 h. The liquid extract was then centrifuged and filtered using Whatman No.1 filter paper. After filtration, the extract was stored at 4°C until further processed for the synthesis of AgNPs.

2.3 Preparation of 1 mM silver nitrate solution

For the preparation of 1 mM silver nitrate (AgNO_3), 17 mg of AgNO_3 was dissolved in 100 ml of double distilled water. The solution was stored in an amber bottle to avoid light-induced oxidation of silver.

2.4 Synthesis of *Mikania micrantha* silver nanoparticles (MNP)

For reduction of silver ions, *M. micrantha* leaf extract (10 ml) was mixed with 90 ml of 1 mM AgNO_3 solution and the pH of the mixture was maintained at 7.0. The reaction mixture changed from light yellowish to reddish brown due to excitation of surface plasmon resonance with continuous stirring at room temperature, indicating the synthesis of AgNPs. The biosynthesized AgNPs were centrifuged at 15,000 rpm for 5 min and redispersed in deionized water to eliminate any uncoordinated biological molecules. UV-Vis spectral analysis was further performed to confirm the formation of AgNPs from the reduction of Ag^+ from AgNO_3 .

2.5 Synthesis of *Acmella ciliata* silver nanoparticles (ANP)

A. ciliata leaf extract (10 ml) was mixed with 90 ml of 1 mM AgNO_3 solution and the pH of the mixture was maintained at 7.0. After stirring at 3 h at room temperature, the reaction mixture changed to reddish brown from light yellowish, indicating the synthesis of AgNPs. The biosynthesized AgNPs were centrifuged at 15,000 rpm for 5 min and redispersed in deionized water to eliminate any uncoordinated biological molecules. Further, the formation of AgNPs by the reduction of Ag^+ from AgNO_3 was ascertained by UV-Vis spectral analysis.

2.6 Characterization of silver nanoparticles (MNP and ANP)

The bio-reduction of Ag^+ ions in solutions was monitored by measuring the UV-vis spectrum (Shimadzu UV-1900I UV-Vis Spectrophotometer) at 300-600 nm.

FT-IR (Fourier transform infrared spectroscopy) spectrum analysis (Perkin-Elmer Spectrum Two with Universal ATR Software 10; Spectrum 10.5.2.636) was performed to analyse the possible functional groups involved in the synthesis of AgNPs. The crystalline nature of metallic AgNPs was determined by X-ray diffraction analysis (X-ray diffractometer D8 ADVANCE ECO BRUKER) in the range of 10–80° at 2 θ angles with a Cu K α radiation (λ = 1.54060 Å, 40 kV, 30 mA) monochromatic filter. The morphology of biosynthesized AgNPs was investigated by Transmission Electron Microscopy (TEM) (JEM-2100 Plus Electron Microscope, JEOL Ltd) and Scanning Electron Microscopy (JSM-IT800 Schottky Field Emission; JEOL Ltd).

3. Results

3.1 Characterization of *Mikania micrantha* silver nanoparticles (MNP)

3.1.1 Visual confirmation and UV-Visible spectra analysis

The preliminary detection of the formation of AgNPs was done by visual observation as the reaction mixture changed from a light-yellow to a reddish-dark-brown colour (Figure 3.1). The absorption spectra of biosynthesized AgNPs formed in the reaction mixture was recorded using UV-Vis analysis at different time intervals. The SPR of the nanoparticles produced a peak centered at 459 nm, confirming the reduction of AgNO₃ into AgNPs at room temperature (Figure 3.2). The intensity of the SPR peak increased with reaction time indicating the increasing yield of AgNPs.

3.1.2 FT-IR Spectrum

FT-IR spectrum analysis was used to investigate the possible functional groups involved in the synthesis of AgNPs (Figure 3.3). Strong stretching vibrations of the hydroxyl and amino groups of alcohols and phenolic compounds are indicated by the intense bands observed in the FT-IR spectrum of AgNPs at 3,175 cm⁻¹. The single-bonded C-H alkane and -CH₃-sym stretching vibrations were responsible for the absorption peak detected at 2,910 cm⁻¹ and 1521 cm⁻¹, respectively. The stretching of carbonyl groups (C=O) is responsible for the high peak at 1,627 cm⁻¹, indicating the presence of compounds such as terpenoids and flavonoids. A prominent peak was observed in the infrared spectra of *M. micrantha* leaf extract at 1632 cm⁻¹ which

corresponds to the C=O stretching or amide 1 bending, indicating the reduction of silver ions to silver nanoparticles. The peak at $1,029\text{ cm}^{-1}$ corresponds to C-O stretching from alcohol, carboxylic acid, ester, and ether assigned by protein and metabolite functional groups covering the AgNPs. The peak at 516 cm^{-1} corresponds to C-Cl, C-Br stretching vibrations to alkyl halides. Comparison of the FT-IR spectra of the plant extract and AgNPs revealed a shift in the absorption peak of the hydroxyl and carbonyl groups.

3.1.3 SEM and EDS analysis

Scanning electron microscopy (SEM) micrographs confirmed the formation of uniformly spherical nanoparticles at different magnification images [Figure 3.4(a-c)]. The chemical composition of the silver nanoparticles that have been synthesized using *M. micrantha* leaf extract is revealed by energy dispersive spectroscopy (EDS) [Figure 3.4(d,h)]. The biosynthesized AgNPs exhibit optical absorption peak of the surface plasmon resonance at around 3 keV showing strong signal for silver and oxygen, which could be attributed to biomolecules attached to the surface of the silver nanoparticles [Figure 3.4(d-h)].

3.1.4 TEM analysis

Transmission electron microscope (TEM) is used to determine the morphology, individual size, and precise shape of AgNPs at various angles. The TEM images [Figure 3.5(a-d)] showed that the biosynthesized AgNPs exhibit poly-dispersed spherical morphology and are predominantly spherical and oval in shape. The average size of the AgNPs is 23.9 nm, with particle sizes ranging from 10 to 40 nm [Figure 3.5(e)]. A very slight thin layer on the surface of the AgNPs was clearly visible in the TEM images, which may be related to the organic compounds from the extract possibly acting as capping and stabilizing agents of AgNPs.

3.1.5 X-ray Diffraction analysis

X-ray diffraction was employed to analyse the crystallinity nature of the biosynthesized AgNPs. Significant diffraction peaks were detected at 2θ values of 38.42° , 44.71° , 64.92° and 77.75° corresponding to the (111), (200), (220) and (311)

planes of pure silver based on the face-centered cubic structure (JCPDS file No. 04-0783). Thus, the XRD pattern showed that the biosynthesized AgNPs are composed of pure crystalline silver. The sharp peaks confirm cubic crystalline nature of AgNPs synthesized by *M. micrantha* leaf extract (Figure 3.6). The broadening of Bragg's peaks was used as confirmation for the synthesis of silver nanoparticles. Several unidentified peaks were attributed to the phytochemical compounds found in the *M. micrantha* leaf extract.

3.2 Characterization of *Acmella ciliata* silver nanoparticles (ANP)

3.2.1 Visual identification and UV-Visible spectra analysis

Prior to UV-Vis spectral analysis, the formation of AgNPs was identified through visual observation of the change in colour from pale yellowish-brown to a reddish-dark brown colour after 30 min of stirring the mixture (Figure 3.7). This colour change was due to the reduction of Ag^+ to Ag^0 (metallic silver) by the bioactive ingredient of the *A. ciliata* leaf extract and the excitation of surface plasmon resonance (SPR) with the AgNPs. UV-Vis absorbance of the reaction mixture was then recorded at different time intervals. The steady rise in intensity of SPR suggested a gradual increase in the yield of AgNPs with the increase in time. The SPR of the nanoparticles produced a peak centered at 430 nm, indicating the reduction of AgNO_3 into AgNPs (Figure 3.8).

3.2.2 FT-IR Spectrum

FT-IR spectroscopy was used to investigate the presence of bioactive compounds of *A. ciliata* leaf extract in the synthesized AgNPs which may act as an efficient capping agent and stabilization factors. In the FT-IR spectrum of *A. ciliata* leaf extract and its biosynthesized AgNPs (Figure 3.9), the FT-IR peak observed at $3,193\text{ cm}^{-1}$ corresponds to strong stretching vibrations of hydroxyl and amino groups of alcohols and phenolic compounds. The peak at $2,937\text{ cm}^{-1}$ and 1549 cm^{-1} can be assigned to the C–H-asym. stretching vibration and $-\text{CH}_3$ -sym. stretching vibration respectively, which indicates the presence of aromatic and carbonyl groups of the protein and metabolites present in the *A. ciliata* leaf extract. The strong peak at $1,650$

cm^{-1} can be assigned to the stretching of carbonyl groups ($\text{C}=\text{O}$) which indicates the presence of compounds like flavonoids and terpenoids. The peak at $1,066\text{ cm}^{-1}$ was due to $\text{C}-\text{O}$ stretching vibration whereas the peak at 545 cm^{-1} corresponds to $\text{C}-\text{Cl}$ stretching in the alkyl group. The IR spectrum of *A. ciliata* leaf extract exhibited a strong peak at 1635 cm^{-1} which corresponds to the $\text{C}-\text{O}$ of amide I proteins stretching mode. This peak shifted to 1650 cm^{-1} in the IR spectrum of AgNPs suggesting the possible involvement of the aforementioned groups in AgNPs synthesis by binding the proteins to Ag^+ through free amine groups or carboxylate ions.

3.2.3 SEM and EDS analysis

SEM analysis confirmed the spherical shape of AgNPs at different magnification images [Figure 3.10(a-c)]. The occurrence of the elemental silver was indicated by the EDS analysis [Figure 3.10(c,h)], which confirmed the reduction of silver ions to silver elements in the reaction mixture. The EDS spectrum also illustrated the presence of strong metallic Ag signals and confirmed the elemental constituents of silver (82.2 %), chlorine (15.05 %) and oxygen (2.68 %) (Figure 10d-h).

3.2.4 TEM analysis

TEM analysis elucidates the shape and size of the biosynthesized AgNPs. The TEM images [Figure 3.11(a-d)] showed that the biosynthesized AgNPs are poly-disperse and are predominantly spherical and oval in shape with particle sizes ranging from 10 to 35 nm [Figure 3.11(e)]. Figure 3.11(b) showed the biomolecular coating on the surface layer of AgNPs, which is responsible to enhanced stability of AgNPs

3.2.5 X-ray Diffraction analysis

X-ray diffraction pattern of the biosynthesized AgNPs is shown in Figure 3.12. At 2θ , values of 27.81° , 32.16° , 38.12° , 44.3° , 46.21° , 54.83° , 57.39° , 64.42° and 77.45° , a number of Bragg reflection is observed corresponding to (210), (122), (111), (200), (231), (142), (241), (220) and (311) planes of pure silver based on the face-centered cubic structure (JCPDS file No. 04-0783) indicating the formation of AgNPs. From XRD results, it is observed that the AgNPs synthesized by *A. ciliata* leaf extract are

face-centered cubic (fcc) and crystalline in nature. Full width at half-maximum (FWHM) data was used with Scherrer's formula to determine mean particle size. Scherrer's equation is given as $d = 0.9\lambda/\beta \cos \theta$, where d is the mean diameter of nanoparticles, λ is the wavelength of the X-ray radiation source, and β is the angular FWHM of the XRD peak at the diffraction angle θ . The crystalline size of the biosynthesized AgNPs as estimated from the FWHM of the peak (111) using Scherrer's formula was found to be 6.702 nm.

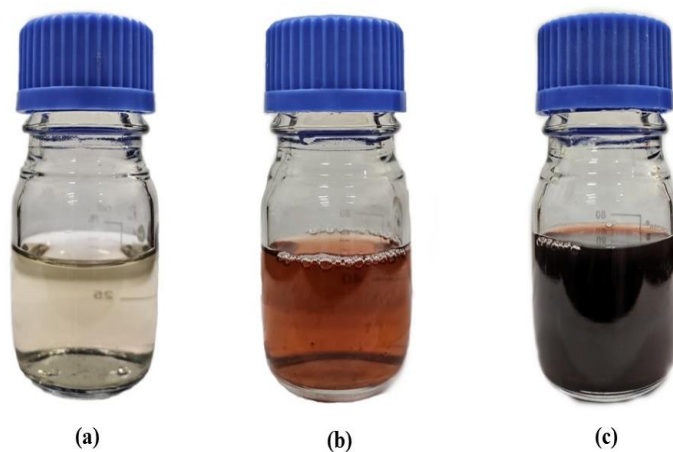


Figure 3.1: Visual identification of biosynthesized AgNPs as recorded at different time-interval: (a) Initial, (b) 2 h, and (c) 4 h. The formation of reddish-brown colour revealed the formation of AgNPs in the reaction mixture.

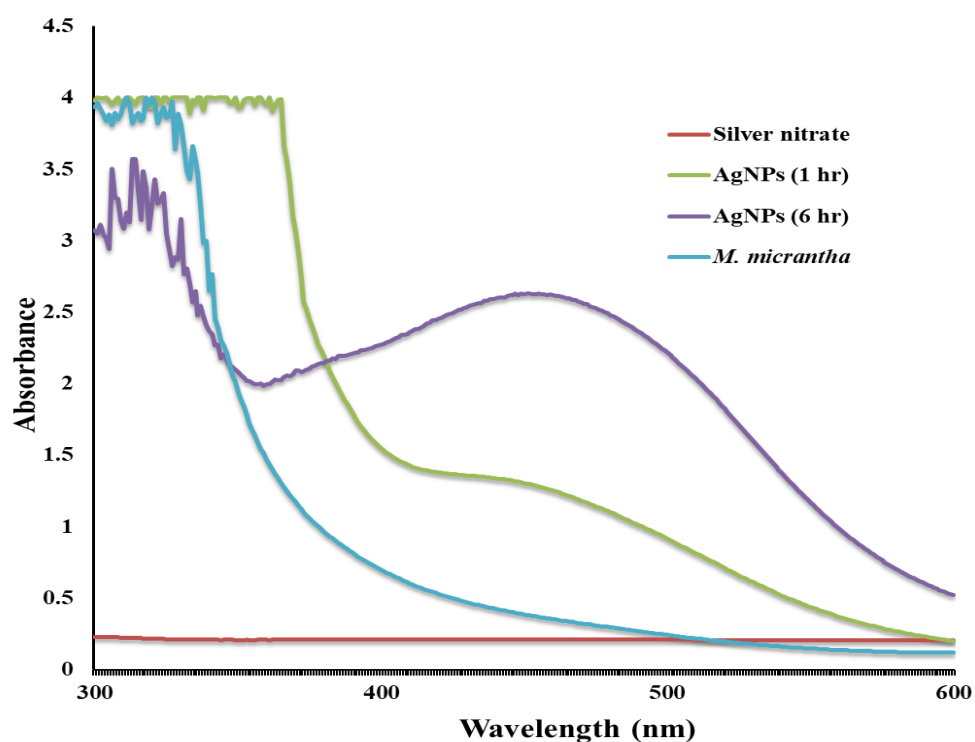


Figure 3.2: UV-Vis absorption spectra of biosynthesized AgNPs using *M. micrantha* leaf extract at different time intervals.

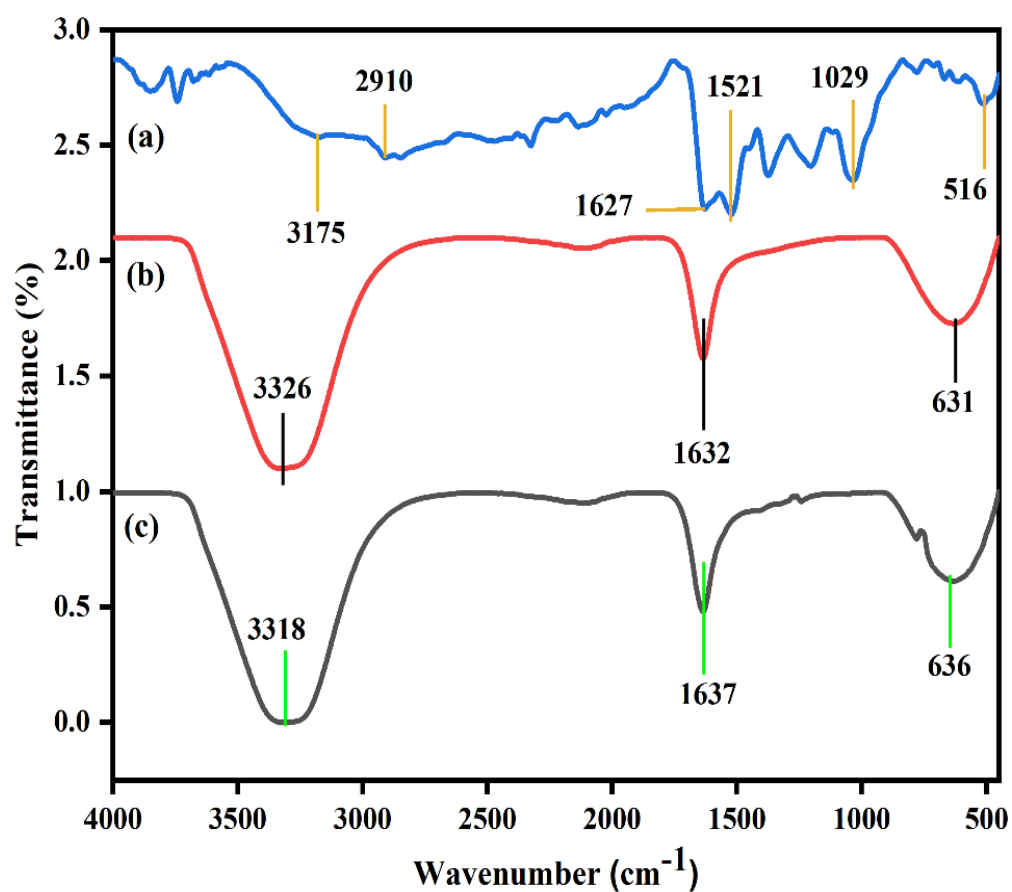


Figure 3.3: FT-IR analysis of (a) biosynthesized AgNPs (b) *M. micrantha* leaf extract (MMAE), and (c) Silver nitrate.

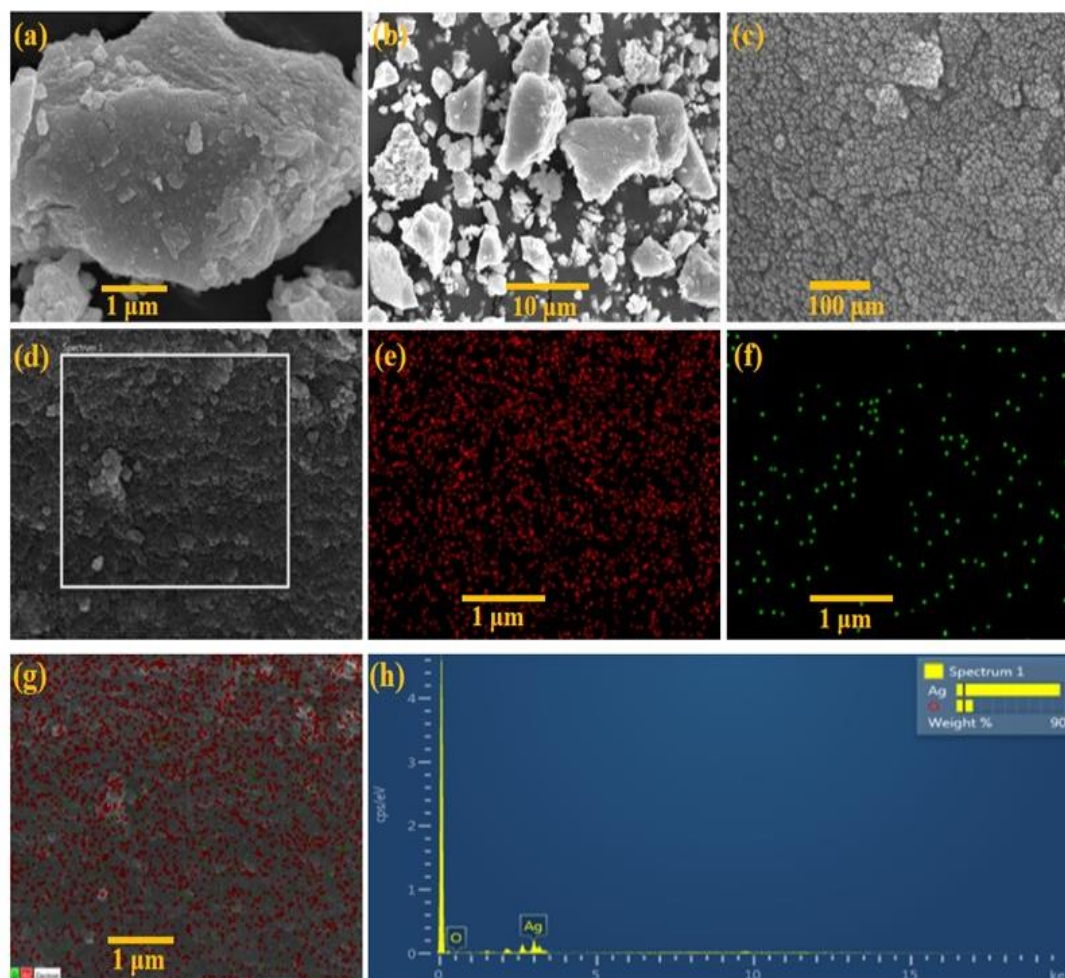


Figure 3.4: (a-d) SEM micrographs of biosynthesized AgNPs. Elemental mapping of (e) silver, (f) oxygen, and (g) both elements for the inset region, and (h) EDS data of the area in the white box in (c). Scale bars: (a) 1 μm (b) 10 μm (c) 100 μm , and (e-g and inset) 1 μm .

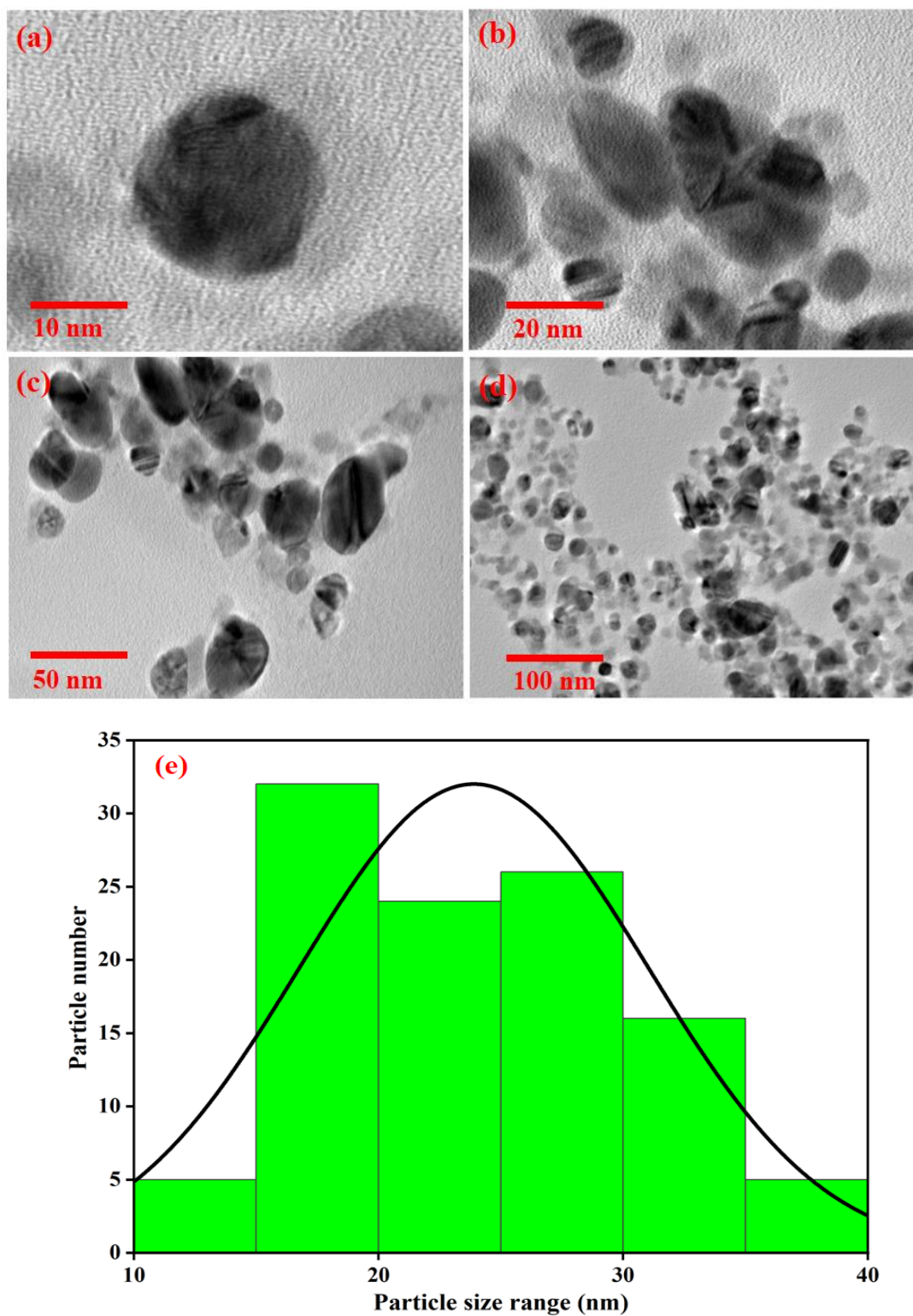


Figure 3.5: (a-d) TEM micrograph showing size of biosynthesized AgNPs Scale bars: (a) 10 nm, (b) 20 nm, (c) 50 nm, and (d) 100 nm. (e) Histogram of the TEM image (100 nm).

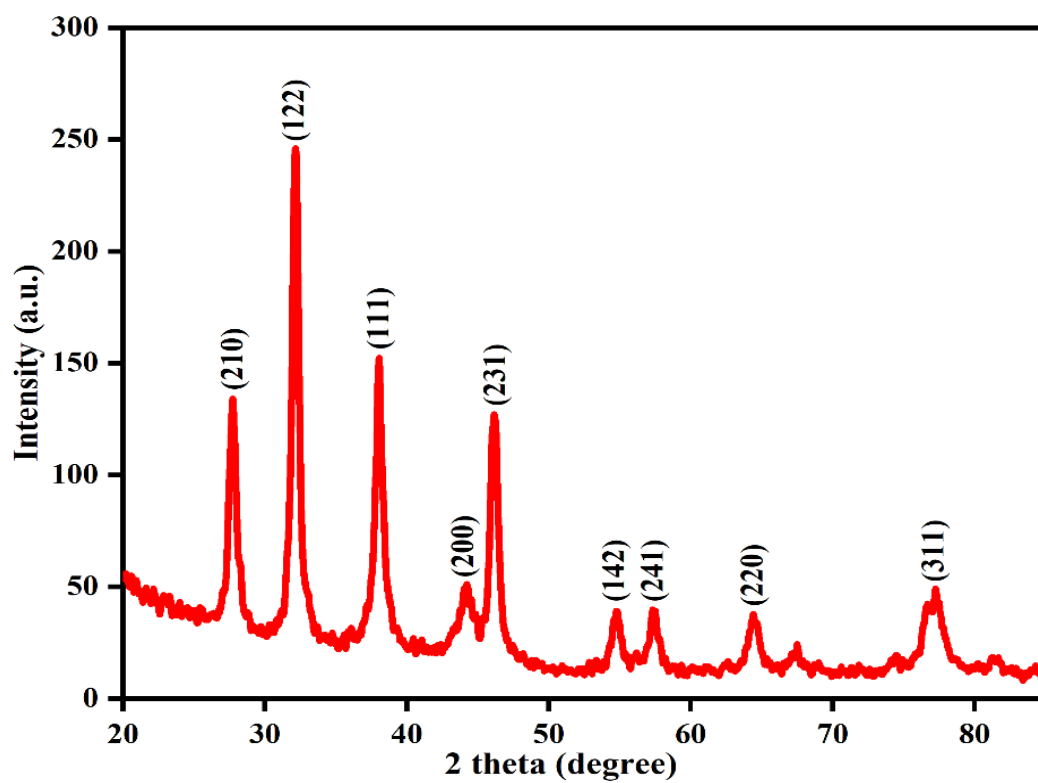


Figure 3.6: XRD pattern of biosynthesized AgNPs using *M. micrantha* leaf extract.

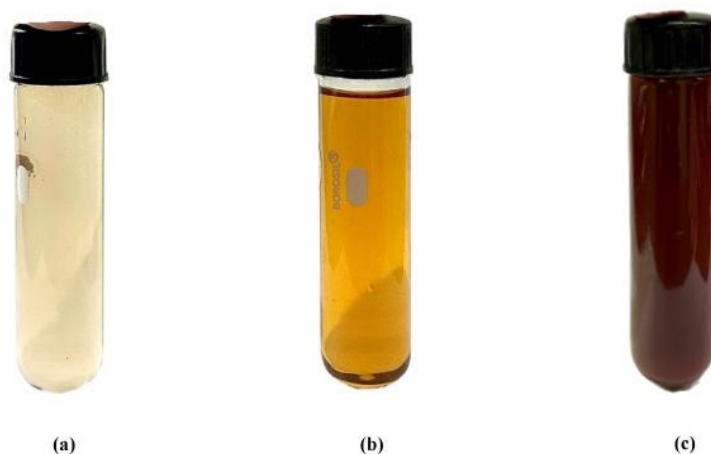


Figure 3.7: Visual identification of biosynthesized AgNPs as recorded at different time-interval: (a) Initial, (b) 2 h, and (c) 4 h. The formation of reddish-brown colour revealed the formation of AgNPs in the reaction mixture.

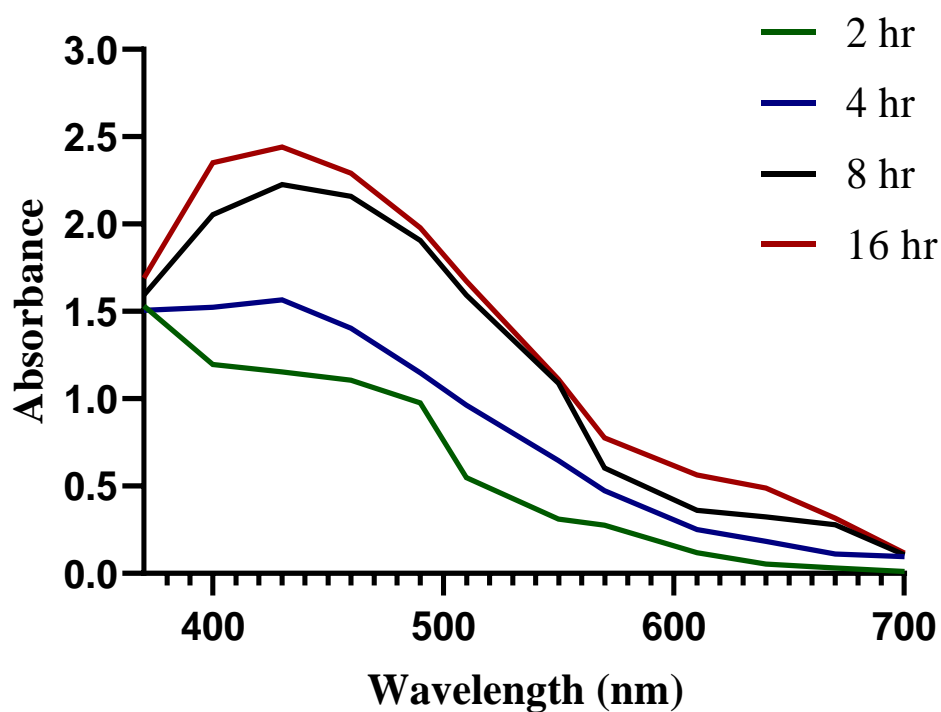


Figure 3.8: UV-Vis absorption spectra of biosynthesized AgNPs using *A. ciliata* leaf extract at different time intervals.

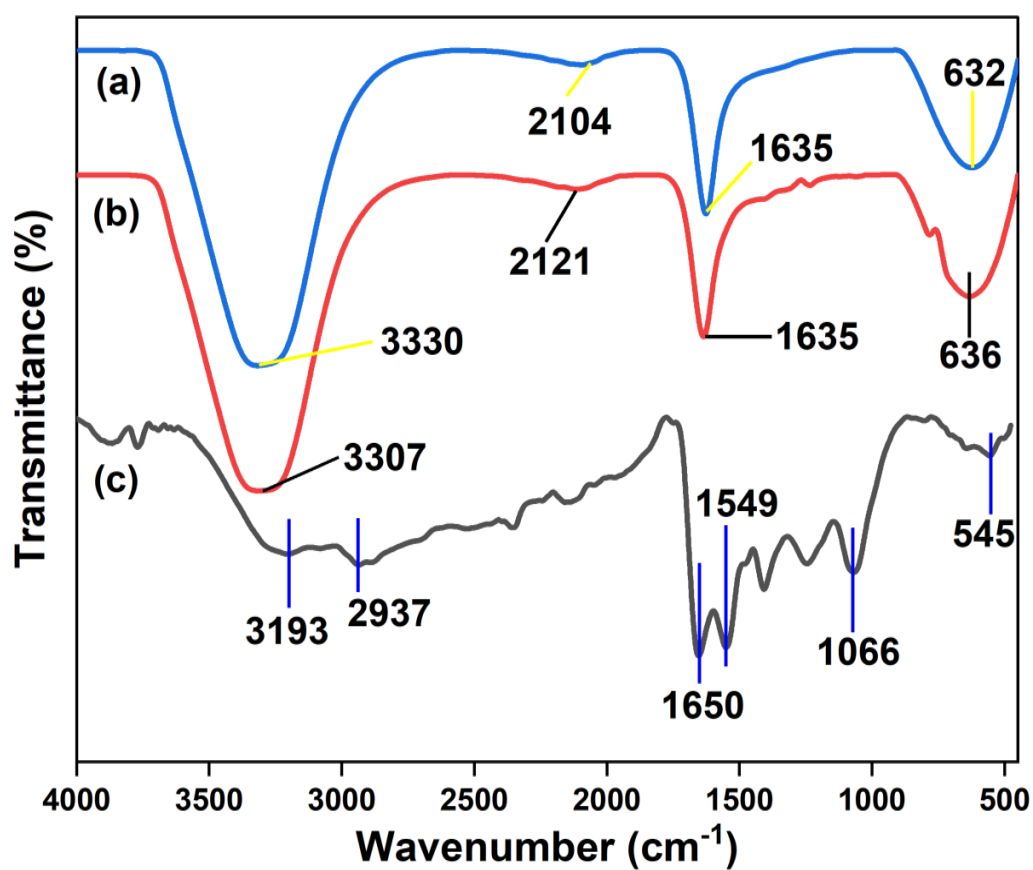


Figure 3.9: FT-IR analysis of (a) Silver nitrate, (b) *Acmella ciliata* leaf extract (ACAE), and (c) biosynthesized AgNPs.

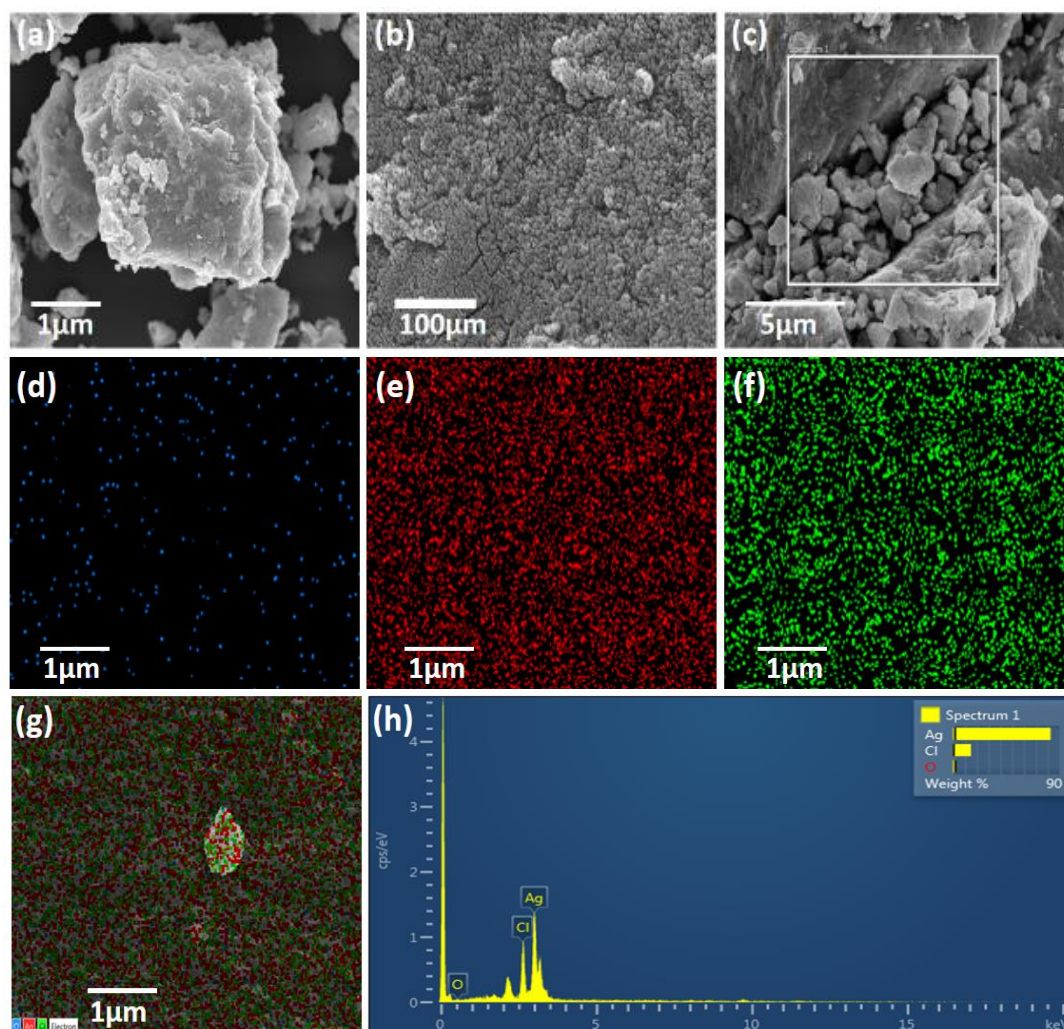


Figure 3.10: (a-c) SEM micrographs of biosynthesized AgNPs. Elemental mapping of (d) oxygen, (e) silver, (f) chlorine, and (g) all three elements for the inset region, and (h) EDS data of the area in the white box in (c). Scale bars: (a) 1 μm, (b) 100 μm, (c) 5 μm, and (d-g and inset) 1 μm.

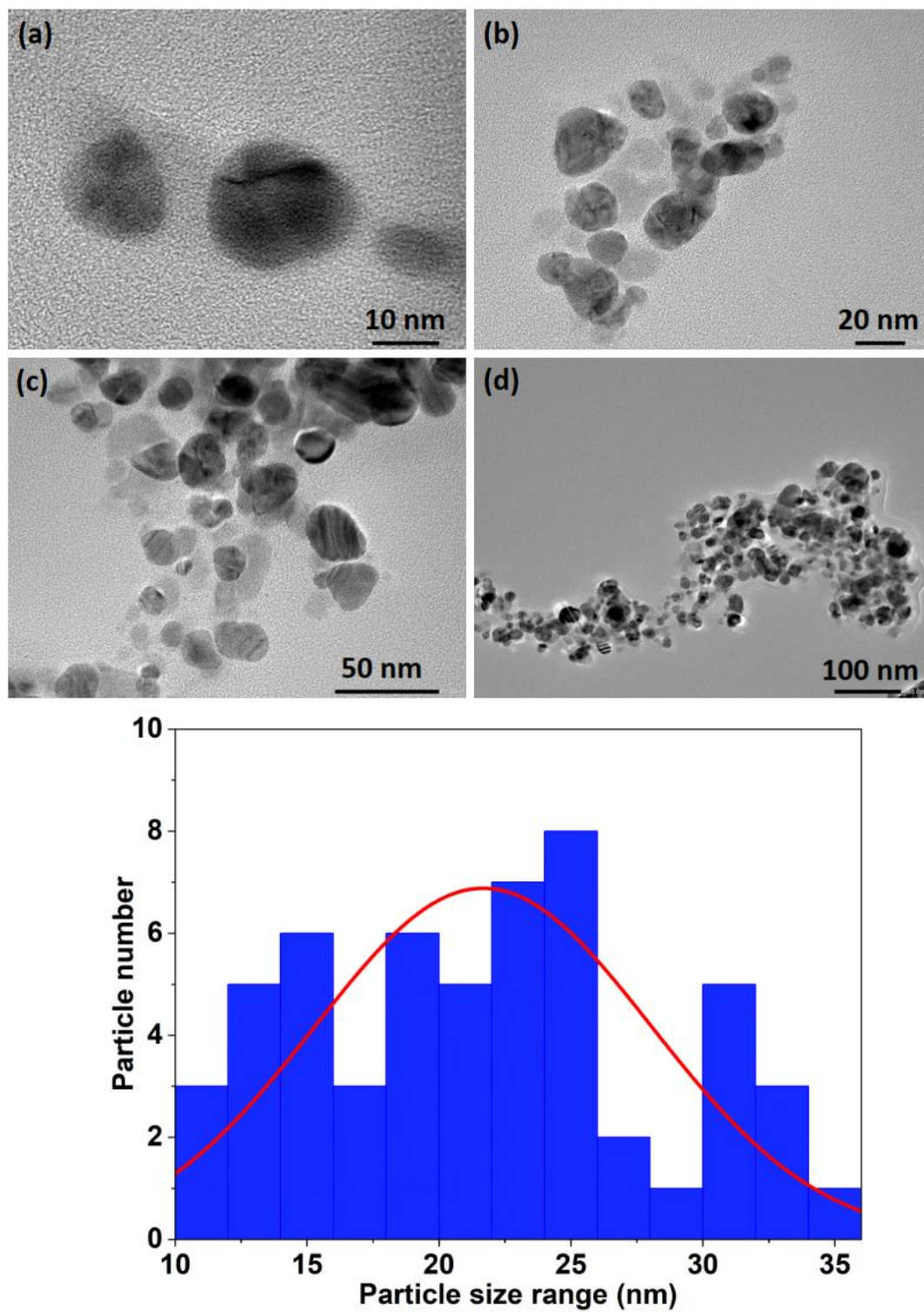


Figure 3.11: (a-d) TEM micrograph showing size of biosynthesized AgNPs Scale bars: (a) 10 nm, (b) 20 nm, (c) 50 nm, and (d) 100 nm. (e) Histogram of the TEM image (100 nm).

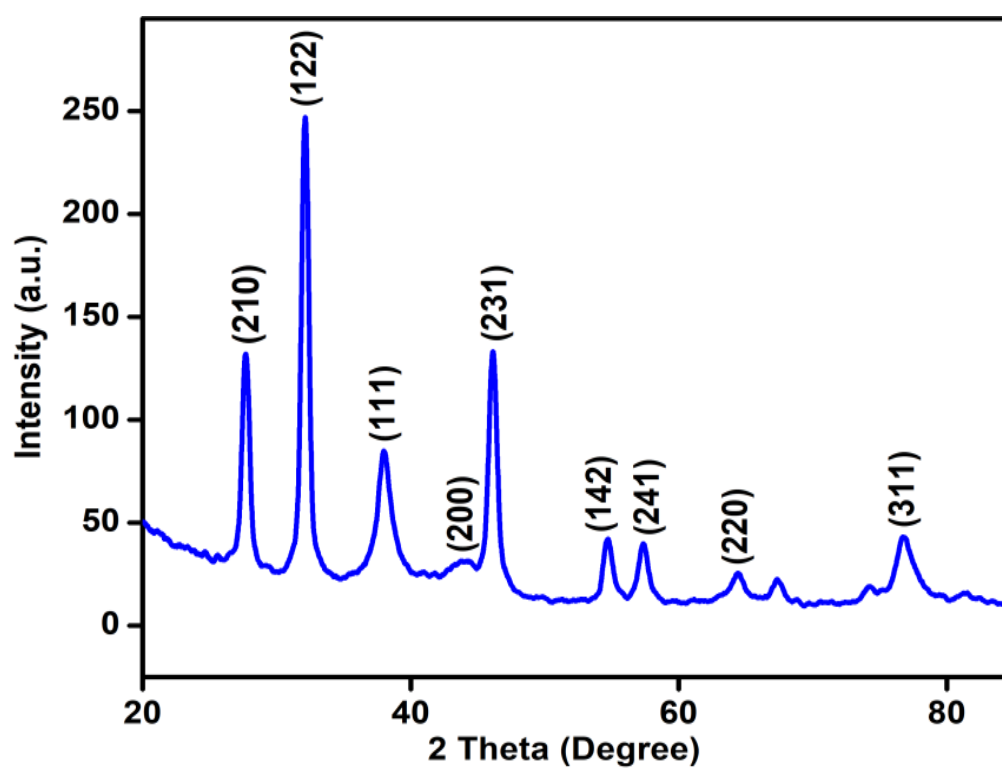


Figure 3.12: XRD pattern of biosynthesized AgNPs using *A. ciliata* leaf extract.

4. Discussion

This study proposes a green synthesis of silver nanoparticles using leaf extracts from commonly available invasive alien plants (*Mikania micrantha* and *Acmella ciliata*), as well as their characterization. A multitude of analytical and spectroscopic methods are employed to determine the properties of nanoparticles, including their nature, size, shape, distribution, stability or aggregation state, morphology, elemental composition, and dispersity (whether they are mono-disperse or poly-disperse) (Lin *et al.*, 2014; Mourdikoudis *et al.*, 2018).

The primary and essential technique to elucidate the generation of silver nanoparticles during the initial synthesis stage is UV-visible spectroscopy. The characteristics of AgNPs, such as their shape, size, and distribution, are highly influenced by surface plasmon resonance. The smaller silver nanoparticles, which are spherical in shape, exhibit absorption at wavelengths close to 400 nm and have narrow peaks. In contrast, larger silver nanoparticles exhibit a redshift, indicating they absorb at longer wavelengths and display broader peaks. The appearance of secondary peaks at higher wavelengths, accompanied by a decrease in intensity and broadening of the peaks, indicate the stability of AgNPs and particle aggregation (Paramelle *et al.*, 2014). Furthermore, broadening peaks provides information about the dispersion of AgNPs (Meva *et al.*, 2019). Specifically, the colour of the solution during synthesis is also a characteristic of its size and shape, and the distinctive colour of the solution allows for the perception and monitoring of the progress of the synthesis reaction (Im *et al.*, 2005). This colour change was due to the excitation of surface plasmon resonance (SPR) of the silver nanoparticles. Electrostatic interactions between metal complexes and organic functional groups, such as polyphenols, flavonoids, terpenoids, amino acids, reducing sugars and alkaloid of the leaves extract are involved for the formation and stabilization of silver nanoparticles (Widatalla *et al.*, 2022). Nevertheless, UV-vis spectroscopy alone does not provide a comprehensive understanding of the produced AgNPs.

FT-IR spectroscopy was employed to determine the primary functional groups and their potential role in the production and stabilization of silver nanoparticles. In order to analyse the presence of chemical residue on the surface of AgNPs, Fourier

transform infrared spectroscopy (FT-IR) examines the interaction between infrared electromagnetic radiation and the bonding in molecules, specifically the stretching and bending vibrations that occur in the range of 4000-400 cm^{-1} region (Zhang *et al.*, 2016). The single-bonded C-H alkane and -CH₃-sym stretching vibrations were responsible for the absorption peak detected at 2,910 cm^{-1} and 1521 cm^{-1} , respectively. This suggests the existence of aromatic and carbonyl groups in the protein and metabolites found in the *M. micrantha* leaf extract (Shahzadi *et al.*, 2022). The stretching of carbonyl groups (C=O) is responsible for the high peak at 1,627 cm^{-1} , indicating the presence of compounds such as terpenoids and flavonoids (Biswas *et al.*, 2018). The peak at 1,029 cm^{-1} corresponds to C-O stretching from alcohol, carboxylic acid, ester, and ether assigned by protein and metabolite functional groups covering the AgNPs (Bhakya *et al.*, 2016). The peak at 516 cm^{-1} corresponds to C-Cl, C-Br stretching vibrations to alkyl halides (Ahmed and Ikram, 2015). The peak at 2,937 cm^{-1} and 1549 cm^{-1} can be assigned to the C-H-asym. stretching vibration and -CH₃-sym. stretching vibration respectively, which indicates the presence of aromatic and carbonyl groups of the protein and metabolites present in the *A. ciliata* leaf extract which is probably involved in the reduction of Ag⁺ to Ag⁰ (Kalyanasundaram *et al.*, 2012). The strong peak at 1,650 cm^{-1} can be assigned to the stretching of carbonyl groups (C=O) which indicates the presence of compounds like flavonoids and terpenoids (Huang *et al.*, 2007) that are responsible for the efficient capping and stabilization of biosynthesized AgNPs. Comparison of the FT-IR spectra of the plant extract and AgNPs revealed a shift in the absorption peak of the hydroxyl and carbonyl groups, suggesting that these biomolecules act on both the bio-reduction and stabilization of AgNPs synthesized using leaf extract. The reduction, capping, and stability of AgNPs are attributed to the involvement of amide (-CO-NH₂), carbonyl (-CO), and hydroxyl (-OH) functional groups, as demonstrated by the FT-IR spectral analysis (Das *et al.*, 2019; Hamouda *et al.*, 2019; Zahed *et al.*, 2018). Biological components have the ability to interact with metal salts through functional groups and facilitate their reduction into nanoparticles (Singh *et al.*, 2018).

The XRD pattern analysis validated the crystalline structure of the silver nanoparticles. Due to the distinct X-ray diffraction (XRD) pattern exhibited by each crystalline material, it serves as a reliable identification tool and allows for the

determination of its crystallinity (Rai *et al.*, 2013). The four diffraction peaks observed at 2θ values of 38.15, 44.30, 64.53, and 76.96 can be attributed to the reflection planes (111), (200), (220), and (311) of the face-centered cubic structure of silver. Aside from the Bragg peaks that are indicative of silver nanocrystals, there were also peaks at 27.89, 32.24, 46.26, and 54.79. The presence of organic compounds in the extract is responsible for the reduction of silver ions and the stability of the generated nanoparticles, leading to the formation of these peaks (Almatroudi, 2020). The XRD pattern observed aligns with previous findings (Meena *et al.*, 2020).

Scanning electron microscopy (SEM) has been utilized to analyse the surface structure, dimensions, clustering, and dispersion of nanoparticles using electron beams as imaging probes. This instrument offers high-resolution images at the nanoscale scale, illustrating the role of biomatrix in encapsulating AgNPs and measuring the size of nanoparticles (Fissan *et al.*, 2014). The interactions between hydrogen bonds and electrostatic interactions among the bioorganic capping molecules attached to the AgNPs produced the SEM image of the silver nanoparticles. Nevertheless, it necessitates a dry and conductive sample, and the size measurements from SEM are occasionally less precise than those from TEM as a result of Van der Waals concentrations of small entities (Theivasanthi and Alagar, 2011). The SEM analysis reveals that the plant extract synthesizes high-density AgNPs that are usually spherical and have a uniform distribution. The nanoparticles exhibited no direct contact, even when aggregated, suggesting that the nanoparticles were stabilized by a capping agent (Priya *et al.*, 2011).

The elemental composition, relative abundance, and impurities of nanoparticles are characterized by energy-dispersive spectroscopy (EDS), based on X-ray interaction with the sample. The detection of emission peaks at 3 keV indicates the existence of silver crystallites confirming the formation of silver nanoparticles, while the absence of any additional peaks confirms the purity of the AgNPs (Radhakrishnan *et al.*, 2018). Metallic silver nanocrystals typically exhibit an optical absorption peak at 3 keV as a result of their surface plasmon resonance (Ibrahim, 2015). The emission energy at 3 keV is a clear indication of the reduction of silver ions to the elemental silver (Ag^0) (Parveen *et al.*, 2016). The strong sharp signal observed for silver is a clear indication of the absorption of the crystalline nature of biosynthesized AgNPs

(Muthukrishnan *et al.*, 2015). However, the presence of other peaks, such as carbon and oxygen, suggests the potential interaction of metabolites with AgNPs on the surface or the oxidation of AgNPs.

Transmission electron microscopy (TEM) is a technique that uses a beam of electrons to interact with ultrathin samples and provides highly accurate and detailed imaging information about the size, shape, morphology, state of aggregation, and distribution of nanoparticles at a nano-meter resolution. This technique is considered to be the most precise and high-resolution method for studying nanoparticles (Borchert *et al.*, 2005; Williams and Carter, 1996). Additionally, it is beneficial to visualize the function of capping agents and the encapsulation of metabolites by AgNPs. TEM studies have confirmed the formation of nanocrystalline silver particles, which mostly exhibit a spherical shape and tend to form small aggregates (Dawadi *et al.*, 2021). The TEM images revealed a fine bioactive component coating the small particle aggregates, acting as a capping organic agent. This may also account for the fact that the nanoparticles exhibited a highly effective dispersion within the bio-reduced aqueous solution, even at the macroscopic level (Kouvaris *et al.*, 2012).

There is a noticeable disparity in the size of spherical AgNPs within the same sample when examined using different techniques, highlighting the inconsistencies arising from the various instrumental methods. Nevertheless, each characterization technique in the synthesis of AgNPs is significant in that it offers a comprehensive understanding of the properties, which then serves as the foundation for the applications. The data and results acquired from these characterization techniques are complementary in nature, as they validate each other and provide distinct perspectives on the results, which are crucial for scientific research.

5. Conclusion

A sustainable and economical method for producing silver nanoparticles has been proposed using invasive alien plants. The synthesis reaction of AgNPs appeared to reach completion within an hour, and it was determined that room temperature facilitated the formation of smaller particles. Furthermore, the initial concentration of silver nitrate significantly influenced the size distribution of AgNPs. The biosynthesized AgNPs were characterized by UV-vis spectroscopy, FT-IR, SEM, EDS,

TEM, and XRD. Our study shows that *Mikania micrantha* and *Acmella ciliata* leaf extract is capable for the green and eco-friendly synthesis of silver nanoparticles which provides simple, cost effective and efficient methodology. The formation of AgNPs was confirmed by a UV-Vis spectrum that revealed an absorption band at 459 nm (MNP) and 430 nm (ANP). A shift in the absorption bands in FT-IR confirmed the bioactive molecules of leaf extract that acted as a reducing and capping agent. The crystalline nature is evident from sharp peaks in the XRD spectrum. The presence of elemental silver was indicated by EDS. SEM and TEM studies validated the spherical shape and size of AgNPs, respectively. Further research into AgNPs synthesized using extracts from *M. micrantha* and *A. ciliata* leaves could bring a promising application in the fields in agriculture and medicine.

Chapter 4

Free radical scavenging activities of *Mikania micrantha* silver nanoparticles and *Acmella ciliata* silver nanoparticles (*in-vitro* and *ex-vivo*)

1. Introduction

Nanoparticles (NPs) display novel and enhanced physicochemical characteristics, which are determined by their size, morphology, distribution, and their attachment to other organic/biological substances, in contrast to their larger counterparts at the macro scale (Joudeh and Linke, 2022). Silver nanoparticles (AgNPs) exhibit remarkable biochemical and catalytic activity, which can be attributed to their considerably large surface area in comparison to other particles with comparable chemical structures (Kumar *et al.*, 2020). Biological catalysts (enzymes) are necessary for the reduction of Ag^+ ions, and several plant extracts can be used to produce AgNPs with antioxidant characteristics. Research findings suggest that biomolecules such as proteins, polyphenols, and flavonoids are involved in both the reduction of ions to nanoscale size and the capping of nanoparticles. Plants are considered an extremely promising system for nanoparticle synthesis because of their remarkable ability to yield a wide variety of bioactive secondary compounds with significant reduction potential. Plants are less susceptible to metal toxicity compared to bacteria and algae, making them a viable alternative for the production of silver nanoparticles (Pandey *et al.*, 2013). Plant-derived polyphenols are widely recognized as the broad category of natural antioxidants, possessing exceptional potential as pharmaceuticals, nutraceuticals, and food supplements. The ability of plant extracts to produce nanoparticles with enhanced properties can be linked to the strong reducing properties of these secondary metabolites (Kharissova *et al.*, 2013).

ROS, or reactive oxygen species, are ions or molecules that possess unpaired electrons (Li *et al.*, 2016). Several enzymes, including cytochrome P450, xanthine oxidase, and NAD(P)H oxidase, produce radical superoxide by reducing molecular oxygen by one electron within the cell. In addition to these enzymes, a variety of

external sources, including ionizing radiation, fossil burning furnaces, pollutants from automobiles, cigarette smoke, various drugs, and specific types of other chemical compounds, also contribute to the generation of ROS. Reactive oxygen species (ROS) such as hydroxyl, superoxide, peroxylnitrile, and singlet oxygen generate oxidative stress, leading to the growth of various diseases such as inflammation, atherosclerosis, aging, cancer, and neurodegenerative disorders (Jomova *et al.*, 2023). Oxidative stress is a condition that arises when there is an imbalance between the protective mechanisms of cells against oxidation and the presence of oxidants. Oxidative stress can arise due to three main factors: (i) an elevated rate of reactive oxygen species (ROS) generation; (ii) insufficiencies in low-molecular-weight antioxidants; and (iii) the deactivation of enzymes with antioxidant properties. An increased and/or extended condition of oxidative stress can cause severe damage to the cell and potentially lead to its death (Brown and Borutaite, 2001). The existence of oxidants causes molecular-level oxidative changes in the biological system (unsaturated bonds in lipids, proteins, DNA, etc.), which damage the system and ultimately accelerate cellular death (Azeez *et al.*, 2017). This situation, known as oxidative stress, occurs when there is an excessive production or accumulation of reactive compounds and the body's defense mechanisms are unable to cope with them. A balance between oxidants and antioxidants (AOs) within the cell is essential for cell function, growth, regulation, and adaptation as ROS plays a significant role in cell survival, cell mortality, inflammation, cell signalling and differentiation (Bardaweel *et al.*, 2018).

Antioxidants are substances, whether natural or synthetic, that have the potential to prevent or delay the damage to cells caused by oxidants (e.g., free radicals, reactive oxygen species, and other unstable molecules) (Apak *et al.*, 2016). For a substance to be classified as an antioxidant, it must exhibit activity at low concentrations, have a sufficiently high quantity to neutralize the specific molecule, react with oxygen or nitrogen free radicals, and produce a final reaction product that is less toxic than the removed radical. Antioxidants may function through a wide range of mechanisms, including the scavenging of radicals, the sequestration of transition metal ions, the decomposition of hydrogen peroxide or hydroperoxides, the quenching of active pro-oxidants, the enhancement of endogenous antioxidant defense, and the repair of the resulting cellular damage. Hence, antioxidants are occasionally

categorized as either primary or chain-breaking antioxidants or as secondary or preventative antioxidants (Flieger *et al.*, 2021). Cells possess antioxidant enzymes, including catalase, superoxide dismutase (SOD), glutathione (GSH) and GSH-related enzymes, lipoic acid, N-acetyl-L-cysteine, thioredoxin, ubiquinones and vitamin E, which help eliminate excessive reactive oxygen species (ROS). Oxidative stress (OS) occurs when there is an imbalance between the creation of reactive oxygen species (ROS) and their breakdown by the antioxidant defense mechanism in the cell (Kovacic *et al.*, 2005). Elevated levels of ROS are accountable for numerous detrimental consequences, including DNA and mitochondrial damage, protein and lipid oxidation, initiation of apoptosis, acceleration of aging, and promotion of carcinogenesis (Panyal *et al.*, 2008).

The efficacy of the silver phyto-nanosystem for the treatment of disease is attributed to its antioxidant properties. The synthesis of silver nanoparticles in involved the use of several phenolic compounds, such as flavonoids (quercetin, rutin, and hesperidin), benzoic acids (gallic acid, protocatechuic acid, salicylic acid, and benzoic acid), and cinnamic acids (caffeic acid, ferulic acid, p-coumaric acid, and trans-cinnamic acid) (Bhutto *et al.*, 2018). The antioxidant abilities of phenolic compounds with varying structures were assessed. The hydroxylation of the aromatic ring significantly influenced the production of silver nanoparticles. The higher degree of hydroxylation in the chemical structures of phenolic compounds demonstrated the increased radical scavenging capacity and greater tendency to reduce Ag^+ to AgNPs (Docea *et al.*, 2020). Silver can occur in two states of oxidation (Ag^+ and Ag^{2+}) depending on the conditions of the reaction, which accounts for the mechanism of silver nanoparticles' antioxidant activity. The AgNPs that are generated may be capable of neutralizing free radicals by providing or accepting electrons (Shanmugasundaram *et al.*, 2013). Generally, the chemical composition of the extract determines the antioxidant activities of silver nanoparticles, which enhance as the concentration of AgNPs increases. The nanoparticles demonstrate high scavenging activity when the extract is abundant in phenolic compounds and flavonoids.

The DPPH (1,1-diphenyl-2-picrylhydrazyl radical) and ABTS (2,2-Azino-bis (3-ethylbenzthiazoline-6-sulfonic acid radical) assays are the most popular and efficient methods used to estimate antioxidant activity (Bedlovicová *et al.*, 2020). The

free radical chain reaction can be disrupted by the donation of hydrogen to free radicals by a variety of biologically active substances in plant extracts, such as enzymes, polyphenols, and alkaloids. Elemike *et al.* (2017) attribute the antioxidant properties of AgNPs to the presence of phenolic compounds, and flavonoids and terpenoids in plants, which allow the nanoparticles to act as singlet oxygen quenchers, hydrogen donors, and reducing agents. Consequently, the specific capping of AgNPs for medicinal plants, whose extracts contain a diversity of antioxidant compounds (polyphenols, flavonoids, etc.), may also be associated with elevated levels of antioxidant activity of silver nanoparticles (Chang *et al.*, 2001). The antioxidant activity of the nanoparticles is mostly determined by the reducing substances that are bound or capped to the surface of the nanoparticles. Thus, this study aimed to investigate the potential of AgNPs using the aqueous leaf extract of *M. micrantha* and *A. ciliata* for free radical scavenging action, anti-haemolytic and lipid peroxidation inhibition.

2. Materials and methods

2.1 Chemicals and reagents

1,1-diphenyl 2-picrylhydrazyl (DPPH) radicals and thiobarbituric acid were obtained from Sigma Aldrich Inc (Louis, Germany). 2,2'-azino-bis- (3-ethylbenzothiazoline-6-sulfonic acid) (ABTS), , nicotinamide adenine dinucleotide, gallic acid, 2-deoxyribose, phenazine methosulfate, sodium nitrite, nitro blue tetrazolium (NBT), potassium persulfate, Quercetin dihydrate, ferric chloride, disodium hydrogen phosphate and hydrogen peroxide (H_2O_2) were obtained from HiMedia Laboratories Pvt., Ltd. (Mumbai, India). Potassium ferricyanide was purchased from Loba Chemie Pvt., Ltd. (Mumbai, India). Folin–Ciocalteu's reagent, ascorbic acid (ASA), trichloroacetic acid (TCA), ferrous sulfate, sodium carbonate, and sodium hydroxide were purchased from SD fine–Chem Ltd. (Mumbai, India). Aluminum chloride, Ethylenediaminetetraacetic acid and sodium dihydrogen phosphate were obtained from Merck Specialities Pvt., Ltd. (Mumbai, India.).

2.2 Determination of free radical scavenging activity (*in vitro*)

2.2.1 DPPH radical scavenging activity

DPPH radical scavenging activity of the biosynthesized AgNPs was assessed using the standard protocol (Leong and Shui, 2002) with minor modifications. Briefly, 1 ml of methanolic solution of DPPH (0.1 M) was added to different concentration of AgNPs (0.5 ml, 1-10 µg/ml) and incubated in dark for 30 min. The optical density of the solution was measured at 523 nm using UV-Visible spectrophotometer (SW 3.5.1.0. Biospectrometer, Eppendorf India Ltd., Chennai). The antioxidant activity of AgNPs was expressed as IC₅₀, the concentration (µg/ml) of AgNPs that inhibits the formation of DPPH radicals by 50%. Each test was performed in triplicate and the scavenging activity of AgNPs was compared with the standard ascorbic acid (ASA) and aqueous leaf extract. Based on the percentage of DPPH radicals scavenged, the scavenging activity was then estimated using the formula:

$$\text{Scavenging (\%)} = \frac{A_{\text{blank}} - A_{\text{sample}}}{A_{\text{blank}}} \times 100$$

Where A_{blank} is the absorbance of the control (solution containing all the reagents except AgNPs) and A_{sample} is the absorbance of the solution containing AgNPs.

2.2.2 ABTS radical scavenging activity

The ABTS radical scavenging activity of AgNPs was determined according to the standard method described earlier (Re *et al.*, 1999). Briefly, a stock solution containing 5 ml each of 7 mM ABTS and 2.4 mM potassium persulfate was prepared and incubated for 12 h at room temperature in the dark to yield a dark-colored solution that contains ABTS^{•+} radicals. A fresh working solution was prepared by diluting the stock solution with 50% methanol having an initial absorbance of 0.70 (±0.02) at 745 nm before each assay. ABTS^{•+} radicals scavenging activity was then determined by mixing AgNPs (5-35 µg/ml) with ABTS working solution in a ratio of 1:10. The decrease in absorbance was measured immediately at 745 nm. Each test was performed in triplicate and the scavenging activity of AgNPs was compared with the standard

ascorbic acid (ASA) and aqueous leaf extract. The scavenging activity was then calculated using the formula:

$$\text{Scavenging (\%)} = \frac{A_{\text{blank}} - A_{\text{sample}}}{A_{\text{blank}}} \times 100$$

Where A_{blank} is the absorbance of the control (solution containing all the reagents except AgNPs) and A_{sample} is the absorbance of the solution containing AgNPs.

2.2.3 Superoxide radical scavenging activity

Superoxide scavenging activity of AgNPs was determined by the Nitroblue tetrazolium (NBT) reduction method (Khan *et al.*, 2012) with minor modifications. Briefly, the reaction mixture containing 1 mM NBT (dissolved in 100 mM phosphate buffer), 1 mM NADH (dissolved in 100 mM phosphate buffer) and 0.1 ml of different concentration (1-25 $\mu\text{g/ml}$) of AgNPs was prepared. Following the addition of 60 μM PMS (dissolved in 100 mM phosphate buffer) the samples were then incubated for 15 min under visible light and the absorbance was read at 530 nm. The superoxide radical scavenging activity was then calculated using the following formula:

$$\text{Scavenging (\%)} = \frac{1 - A_e}{A_o} \times 100$$

Where A_o is absorbance without sample and A_e is absorbance with the sample.

2.2.4 Reducing power

The reducing power of AgNPs was estimated using the method describe earlier (Oyaizu, 1986) with minor modifications. Briefly, a solution containing 0.1% potassium ferricyanide and 0.2 M phosphate buffer (pH-6.6) in a ratio 1:1 was mixed with different concentration (10 - 100 $\mu\text{g/ml}$) of AgNPs. Following the addition of 10% TCA, the mixture was incubated for 20 min at 50 $^{\circ}\text{C}$ and then centrifuged at 3000 rpm for 10 min. The supernatant was taken and equal volume of distilled H_2O was added followed by addition of 1% ferric chloride solution. The absorbance of the mixture was measured at 700 nm. The increase in absorbance indicated increasing reducing power of AgNPs.

2.3 *Ex vivo* antioxidant assay

The inbred Swiss albino mice colony is being maintained under controlled conditions of temperature ($22^{\circ}\text{C} \pm 5^{\circ}\text{C}$) and 12 h light-dark cycles (Frontier Euro Digital Timer, Taiwan) at the Animal Care Facility of the Department of Zoology, Mizoram University, Aizawl, India. The animals were fed with commercially available food pellets and water *ad libitum*. The animal care and handling were carried out according to the guidelines issued by World Health Organization, Geneva, Switzerland.

2.3.1 *Anti-haemolytic activity*

The inhibitory effect of AgNPs against mice erythrocyte haemolysis was measured (Zhao *et al.*, 2014) to determine its antioxidative potential. All experimental procedure involving animal care and handling was carried out in accordance with the guidelines of American Veterinary Medical Association (AVMA) for the Euthanasia of Animals (2020) and approved by the Mizoram University Institutional Animal Ethical Committee (MZU/IAEC/2022-23/03). Blood was collected from healthy adult Swiss albino mice by heart puncture in a heparinized tube. Erythrocyte haemolysis was induced with hydrogen peroxide (H_2O_2) that serves as free radical initiator. A reaction mixture containing 5 % (v/v) suspension of RBC in PBS, 0.2 ml of different concentration (0.1-0.5 mg/ml) of AgNPs and 1 mol/L H_2O_2 was prepared. The mixture was incubated at 37°C for 3 h with constant gentle agitation. Following dilution with PBS, the solution was centrifuged at 2000 rpm for 10 min, the absorbance of the supernatant was measured at 540 nm. The inhibition rate of erythrocyte haemolysis was then calculated.

$$\text{Inhibition rate (\%)} = [1 - (A_1 - A_2)A_0] \times 100$$

Where, A_0 is the absorbance of the control, A_1 is the absorbance of the solution containing AgNPs and A_2 is the absorbance without RBC.

2.3.2 Inhibition of lipid peroxidation

Lipid peroxidation inhibitory action of AgNPs was measured according to the standard method (Gill *et al.*, 2015) using mice liver. The liver homogenate (1 % w/v) prepared in PBS was centrifuged at 3000 rpm at 4 °C for 10 min and the supernatant (0.5 ml) was mixed with different concentrations (0.05-0.2 mg/ml) of AgNPs. Following the addition of 25 mmol/L FeCl₂ and H₂O₂, the solution was incubated at 37 °C for 1 h and absorbance was measured at 535 nm. The rate of inhibition of lipid peroxidation was calculated using the formula:

$$\text{Inhibition rate (\%)} = 1 - \left(A_1 - \frac{A_2}{A_0} \right) \times 100$$

Where, A₀ is the absorbance of the control, A₁ is the absorbance of the solution containing AgNPs and A₂ is the absorbance without liver homogenate.

2.4 Statistical analysis

Data are expressed as mean ± standard error of the mean. One-way ANOVA followed by Tukey's test was performed to test significant variations in free radical scavenging activities using SPSS ver.16.0 software (SPSS Inc, Chicago, IL, USA). The IC₅₀ was also calculated using GraphPad Prism software ver. 6.0. A 'p' value of less than 0.05 was considered statistically significant.

3. Results

3.1 *In vitro* antioxidant assays of *Mikania micrantha* silver nanoparticles (MNP)

The antioxidative potential of AgNPs was determined by *in vitro* antioxidant assays using DPPH, ABTS^{•+} and O₂^{•-}. The free radical scavenging activities of AgNPs increased in a concentration-dependent manner. To determine the IC₅₀, the log-doses of AgNPs, *M. micrantha* aqueous extract (MMAE), and ascorbic acid (ASA) were plotted against the inhibition (%) of DPPH, ABTS^{•+}, and O₂^{•-} radicals (Figure 4.1). The scavenging activities of AgNPs against DPPH (IC₅₀: 4.90 ± 0.31 µg/ml), ABTS^{•+} (IC₅₀: 16.27 ± 0.62 µg/ml) and O₂^{•-} (IC₅₀: 13.33 ± 0.38 µg/ml) were found to be significantly higher than MMAE (IC₅₀: 991.86 ± 11.30 µg/ml for DPPH; 1256.67 ±

9.53 $\mu\text{g/ml}$ for $\text{ABTS}^{\bullet+}$; $2713.67 \pm 89.99 \mu\text{g/ml}$ for $\text{O}_2^{\bullet-}$). Despite non-significant variations, AgNPs outperformed standard ASA in DPPH and $\text{ABTS}^{\bullet+}$ scavenging. Similarly, no significant variation ($p > 0.001$) was found between AgNPs and the standard ascorbic acid in $\text{O}_2^{\bullet-}$ scavenging activities (Figure 4.2). The ability of AgNPs to convert ferric (Fe^{3+}) into ferrous (Fe^{2+}) was used to determine their reducing power and the reducing activity of AgNPs increased in a dose-dependent manner. The total reducing power of AgNPs at 100 $\mu\text{g/ml}$ (0.39 ± 0.004) was found to be significantly ($p < 0.001$) higher than MMAE (0.15 ± 0.006) and standard ascorbic acid (0.29 ± 0.01) (Figure 4.3). This study showed that the high ferric-reducing power of AgNPs is a crucial indicator of its potential antioxidant activity.

3.2 *Ex vivo* antioxidant assay of *Mikania micrantha* silver nanoparticles (MNP)

The concentration of AgNPs determines the potential of their anti-haemolytic activity and ability to inhibit lipid peroxidation (Figure 4.4). At a concentration of 0.5 mg/ml, the inhibitory activity of AgNPs against mice erythrocyte haemolysis was 61.7% indicating the potent anti-haemolytic activity of biosynthesized AgNPs. The highest inhibitory effect of AgNPs against lipid peroxidation in mice liver homogenate was recorded at 0.2 mg/ml with an inhibition rate of 79.9 %.

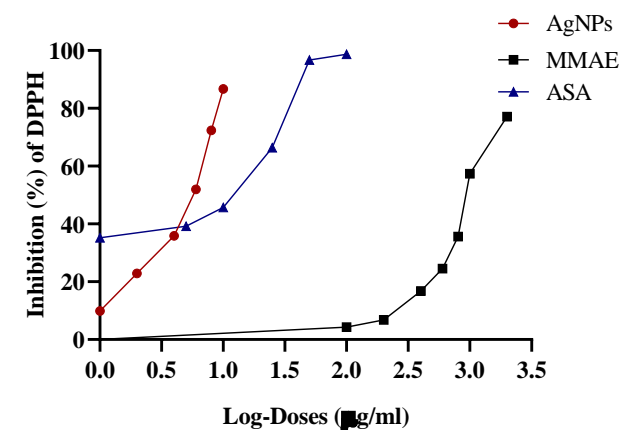
3.3 *In vitro* antioxidant assays of *Acmella ciliata* silver nanoparticles (ANP)

In vitro antioxidant assays using DPPH, $\text{ABTS}^{\bullet+}$ and $\text{O}_2^{\bullet-}$ revealed the antioxidative potential of AgNPs. The free radical scavenging activities of AgNPs increased in a concentration-dependent manner. Log-doses of AgNPs, ACAE and ASA were plotted against inhibition (%) of DPPH, $\text{ABTS}^{\bullet+}$ and $\text{O}_2^{\bullet-}$ radicals for the calculation of IC_{50} [Figure 4.5(a-c)]. The scavenging activities of AgNPs against DPPH (IC_{50} : $3.85 \pm 0.04 \mu\text{g/ml}$), $\text{ABTS}^{\bullet+}$ (IC_{50} : $14.62 \pm 0.10 \mu\text{g/ml}$) and $\text{O}_2^{\bullet-}$ (IC_{50} : $16.13 \pm 0.11 \mu\text{g/ml}$) were found to be significantly higher than ACAE (IC_{50} : $474.0 \pm 8.80 \mu\text{g/ml}$ for DPPH; $1409.33 \pm 17.8 \mu\text{g/mL}$ for $\text{ABTS}^{\bullet+}$; $6156.33 \pm 15.23 \mu\text{g/ml}$ for $\text{O}_2^{\bullet-}$). Despite the non-significant variations, AgNPs showed better scavenging activities against DPPH and $\text{ABTS}^{\bullet+}$ when compared to the standard ASA. Similarly, no significant variation ($p > 0.001$) was found between AgNPs and the standard

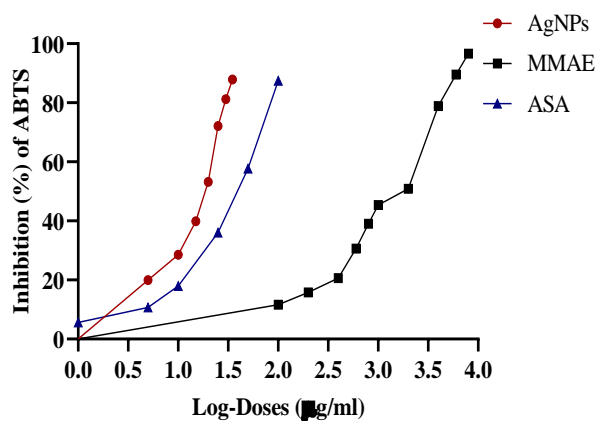
ascorbic acid in O_2^{\bullet} scavenging activities [Figure 4.6(a-c)]. The reducing power of AgNPs was assessed by measuring their ability to transform ferric (Fe^{3+}) into ferrous (Fe^{2+}). The reducing activity of AgNPs also increased in a dose-dependent manner. The total reducing power of AgNPs at 100 μ g/ml ($0.40 \pm .005$) was found to be significantly higher than ACAE ($0.17 \pm .003$) and standard ascorbic acid (0.29 ± 0.01) (Figure 4.7).

3.4 *Ex vivo* antioxidant assay *Acmella ciliata* silver nanoparticles (ANP)

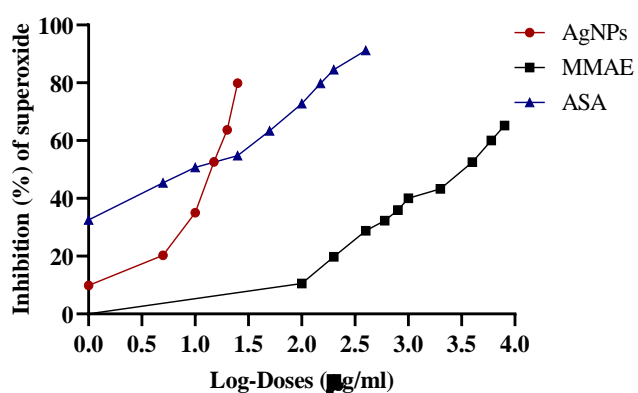
Lipid peroxidation in liver cells of mice and haemolysis was induced using H_2O_2 and the inhibitory potential of AgNPs was studied. Both the anti-haemolytic activity and lipid peroxidation inhibitory effect of AgNPs occurs in a concentration-dependent manner [Figure 4.8(a,b)]. Inhibitory activity of AgNPs against mice erythrocyte haemolysis at the dose of 0.5 mg/ml was 64.07 % indicating the potent anti-haemolytic activity of biosynthesized AgNPs. The highest inhibitory effect of AgNPs against lipid peroxidation in mice liver homogenate was recorded at 0.2 mg/ml with an inhibition rate of 84.2 %.



(a)



(b)



(c)

Figure 4.1: Plots of log-doses of AgNPs, MMAE and ASA against (a) DPPH, (b) ABTS, and (c) $O_2^{\bullet-}$ inhibition (%) for the calculation of IC_{50} . AgNPs: biosynthesized AgNPs using *M. micrantha* leaf extract; MMAE: *M. micrantha* leaf extract; ASA: Ascorbic acid (standard).

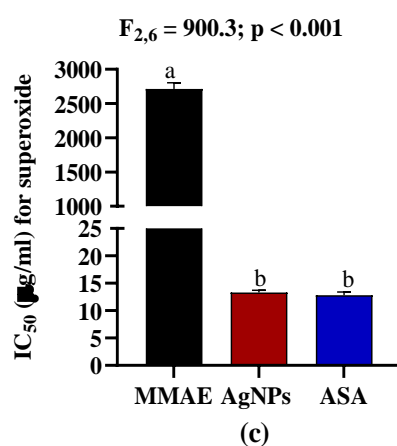
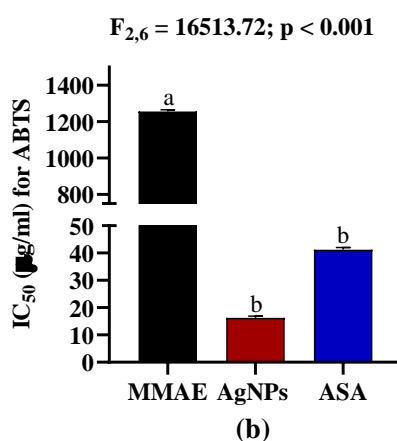
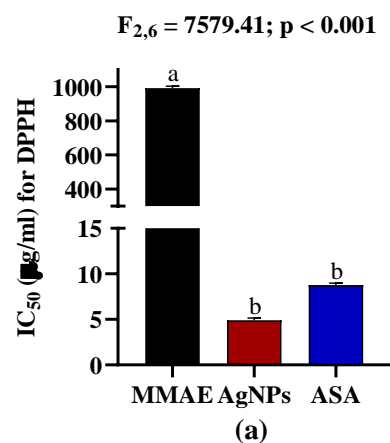


Figure 4.2: IC₅₀ (µg/ml) of AgNPs, MMAE and ASA for (a) DPPH, (b) ABTS, and (c) O₂^{•-}. AgNPs: biosynthesized AgNPs using *M. micrantha* leaf extract; MMAE: *M. micrantha* leaf extract; ASA: Ascorbic acid (standard). Values are expressed as Mean ± SEM, n=3. Different letters indicate significant variation.

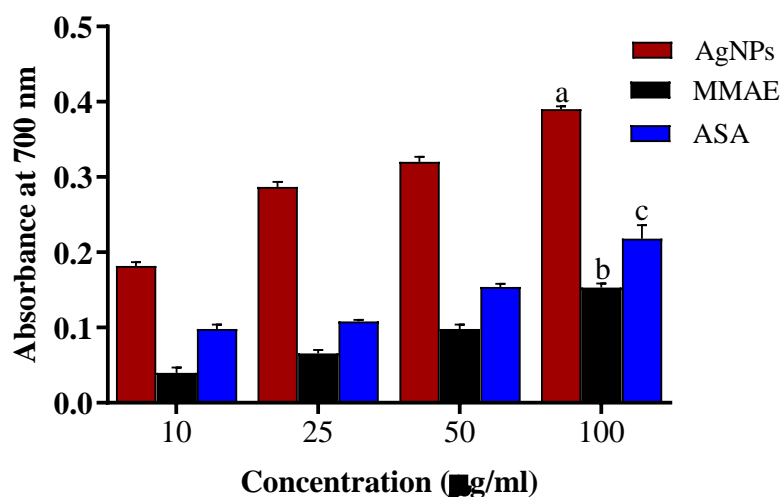


Figure 4.3: Reducing power of AgNPs, MMAE and ASA at different concentrations. AgNPs: biosynthesized AgNPs using *M. micrantha* leaf extract; MMAE: *M. micrantha* leaf extract; ASA: Ascorbic acid (standard). Values are expressed as Mean \pm SEM, n=3. Different letters indicate significant variation.

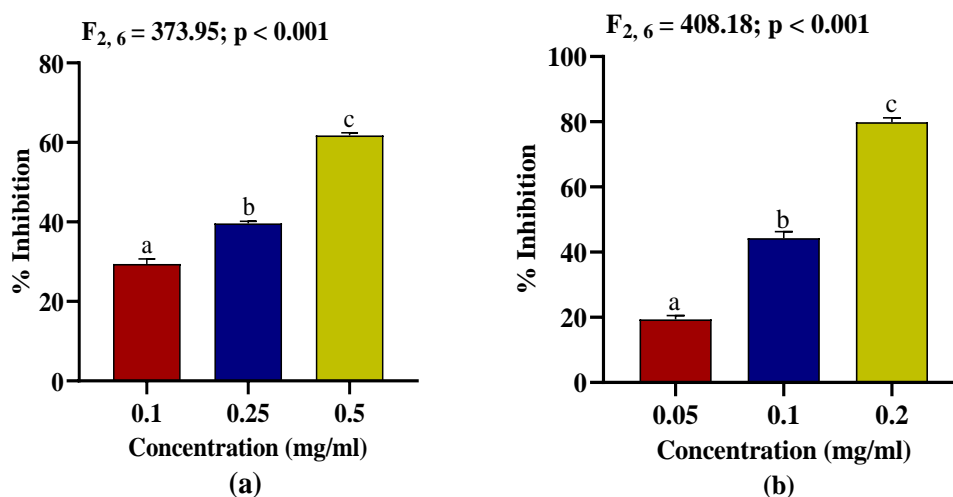


Figure 4.4: (a) Anti-haemolytic, and (b) lipid peroxidation inhibitory activities of biosynthesized AgNPs. Values are expressed as Mean \pm SEM, n=3. Different letters indicate significant variation.

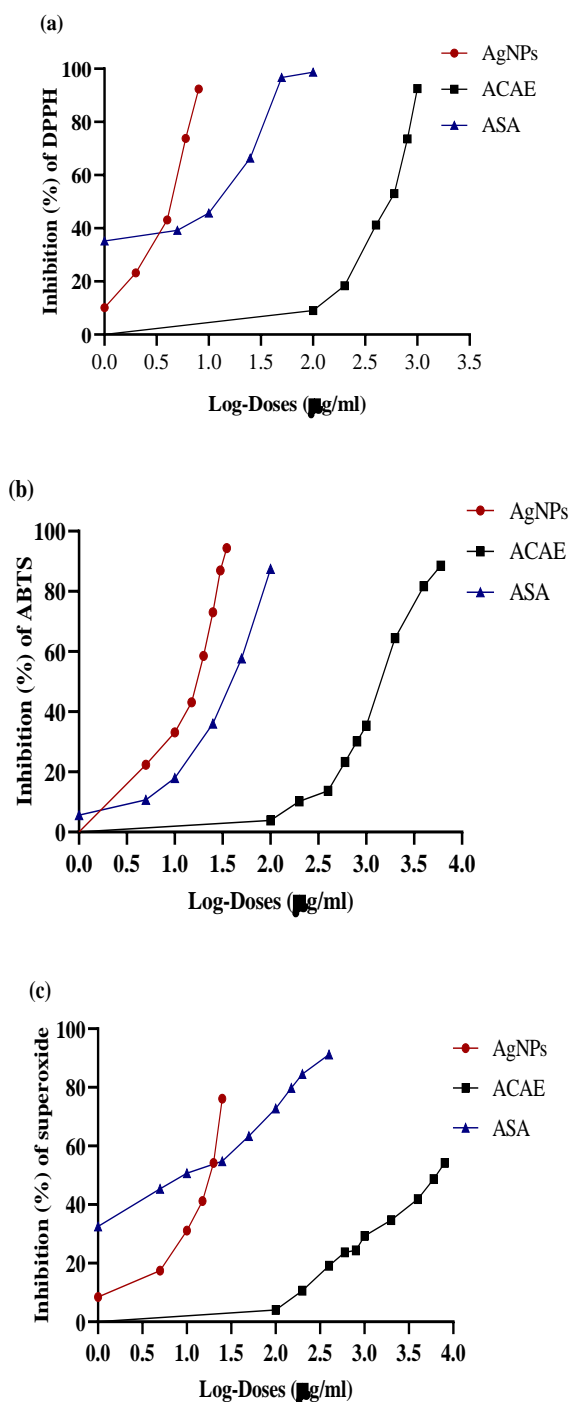


Figure 4.5: Plots of log-doses of AgNPs, ACAE and ASA against (a) DPPH, (b) ABTS, and (c) $\text{O}_2^{\bullet-}$ inhibition (%) for the calculation of IC_{50} . AgNPs: biosynthesized AgNPs using *A. ciliata* leaf extract; ACAE: *A. ciliata* leaf extract; ASA.

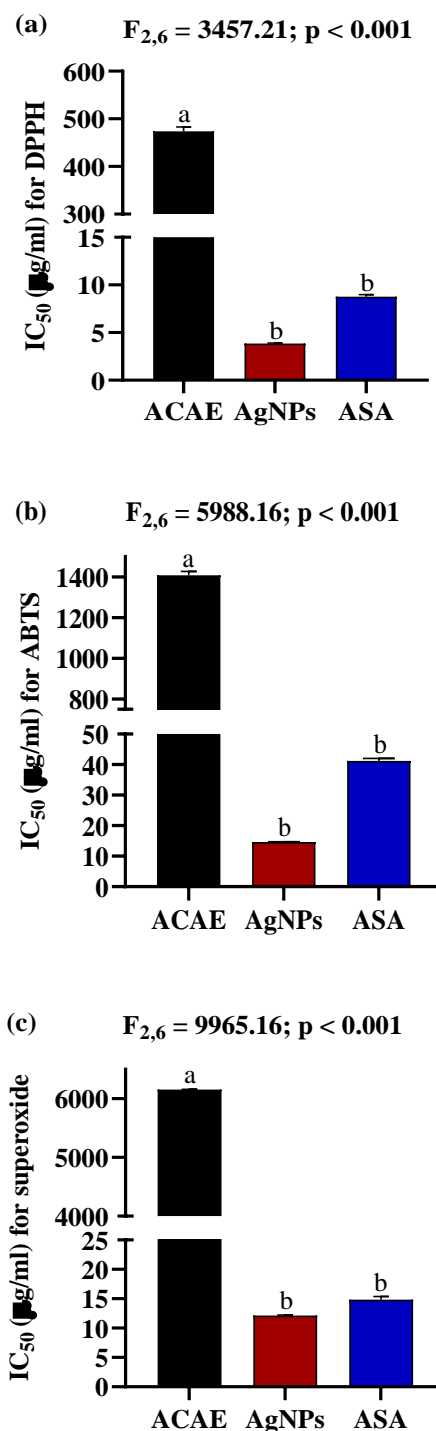


Figure 4.6: IC₅₀ (µg/ml) of AgNPs, ACAE and ASA for (a) DPPH, (b) ABTS, and (c) O₂[•]. AgNPs: biosynthesized AgNPs using *A. ciliata* leaf extract; ACAE: *A. ciliata* leaf extract; ASA: Ascorbic acid (standard). Values are expressed as Mean ± SEM, n=3. Different letters indicate significant variation.

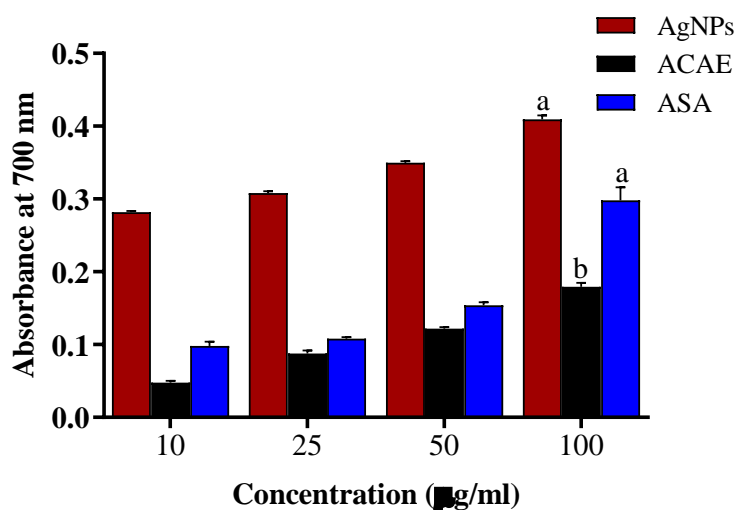


Figure 4.7: Reducing power of AgNPs, ACAE and ASA at different concentrations. AgNPs: biosynthesized AgNPs using *A. ciliata* leaf extract; ACAE: *A. ciliata* leaf extract; ASA: Ascorbic acid (standard). Values are expressed as Mean \pm SEM, n=3. Different letters indicate significant variation.

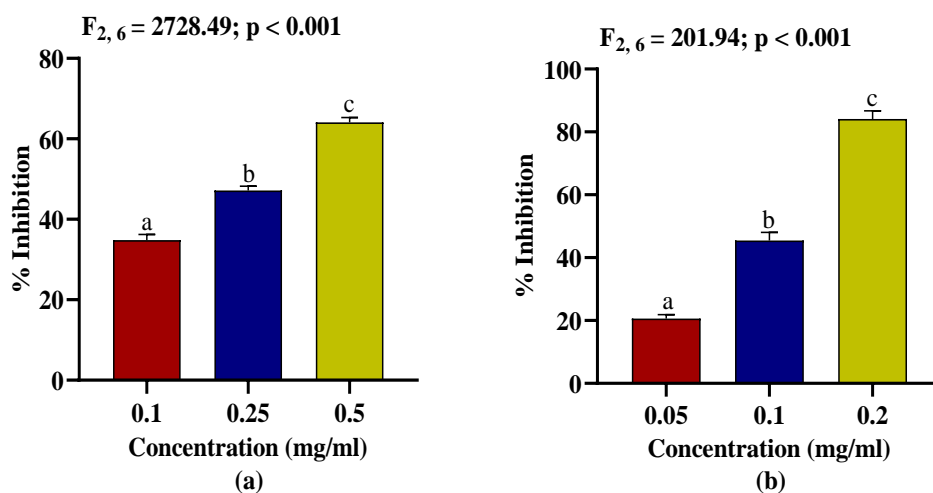


Figure 4.8: (a) Anti-haemolytic, and (b) lipid peroxidation inhibitory activities of biosynthesized AgNPs. Values are expressed as Mean \pm SEM, n=3. Different letters indicate significant variation.

4. Discussion

Despite the crucial roles of ROS in modulating many physiological activities of the body, excessive generation of ROS can impair the antioxidant defence mechanisms of the body resulting in a condition called 'oxidative stress'. Use of plants and plant-derived products as a source of natural antioxidants has been practised as a standard way for maintaining oxidative balance due to their high phytochemical contents, which are often harmless. Due to their ability to effectively scavenge free radicals, gold, silver, and selenium nanoparticles have been found to significantly reduce oxidative stress (Bhakya *et al.*, 2016; Sood *et al.*, 2018). The ability of AgNPs to efficiently convert the purple radical DPPH into the non-radical yellow DPPH-H and $\text{ABTS}^{+\bullet}$ to ABTS in the current study are also an indication of their strong antioxidant activities. The green synthesis of AgNPs depends mainly on the keto-enol conversion of polyphenolic compounds, which possess significant antioxidant and radical-scavenging properties (Abdel-Aziz *et al.*, 2014). Antioxidant activities of silver nanoparticles are based on the chemical composition of the extract and tend to improve as AgNPs concentration increases. The invasive plants, *M. micrantha* and *A. ciliata* are rich in structurally diverse phenolic compounds with potential health benefits for humans (Dong *et al.*, 2017; Rahim *et al.*, 2021). The nanoparticles of an extract rich in phenolic compounds and flavonoids have a greater potential for radical scavenging (Bedlovicova *et al.*, 2020). The main factor contributing to the antioxidant properties of plants and plant-derived compounds is the presence of phenolic compounds, which have hydroxyl groups and conjugated ring structures enabling them to catalyze the scavenging of free radicals involved in oxidative processes via hydrogenation (Kumar and Goel, 2019). Furthermore, the induction of lipid peroxidation by a highly reactive superoxide anion radical, a by-product of inefficient oxygen metabolism, can result in tissue damage (Aruoma and Halliwell, 1987). Stronger reactive oxygen species (ROS), including hydroxyl radicals, can be created when the superoxide ($\text{O}_2^{\bullet-}$) radical decomposes. As a result, scavenging of $\text{O}_2^{\bullet-}$ will prevent the chain of ROS formation, thereby preventing oxidative damage to the cells. The bioactive compounds of *M. micrantha* and *A. ciliata* leaf extract that attached to the spherical form nanoparticles are responsible for the free radical scavenging

abilities of biosynthesized AgNPs against DPPH, ABTS $^{•+}$ and $O_2^{•-}$ via transferring of a single electron and hydrogen atom (Vaiserman *et al.*, 2020). The simultaneous action of phenolic compounds as antioxidant agents and silver ions as a catalyst may be the reason of the greater scavenging activities of biosynthesized AgNPs compared to the plant leaf extract. The reducing power of AgNPs was assessed by assessing the oxidation of Fe^{3+} to Fe^{2+} . The reducing power of AgNPs, which occurs in a dose-dependent manner, may significantly indicate their potential antioxidant activity. The function of antioxidants has been attributed to multiple mechanisms, including the prevention of chain initiation, binding of transition metal ion catalysts, breakdown of peroxides, mitigation of continued hydrogen abstraction, reductive ability, and radical scavenging (Fahn and Cohen, 1992).

One of the main targets of free radicals is the cellular membrane, and haemolysis occurs as a result of membrane damage brought on by the chain reaction of free radicals on erythrocytes (Ebrahimzadeh *et al.*, 2009). Damage to membranes can result from the peroxidation of lipid moieties by the actions of free radicals, such as polyunsaturated fatty acids (Klaunig *et al.*, 1998). In this study, H_2O_2 was used to induce haemolysis and lipid peroxidation in mice liver cells, and the inhibitory effect of AgNPs was examined. The present study indicated the protective actions of biosynthesized AgNPs against haemolysis and lipid peroxidation. The bioactive components of the plant are responsible for nanoparticle formation and impart biological properties such as anti-haemolytic activity (Badmus *et al.*, 2022). It has been observed that some phenolic compounds partitioned cell membranes, preventing free radical transport and decreasing the kinetics of free radical interactions (Singh *et al.*, 2008). Moreover, flavonoids have been shown to bind to the membrane of erythrocytes, which increased their integrity against lyses and inhibited lipid peroxidation (Chaudhuri *et al.*, 2007). Based on our findings, biosynthesized AgNPs may interact with the lipids of the erythrocyte membrane and have a protective effect against haemolysis because of their distinctive physio-chemical characteristics and high surface area to volume ratio.

5. Conclusion

The standard approach for synthesizing AgNPs is a biological technique, mostly employing plant extracts to reduce silver ions and create stable Ag⁰ nanoparticles. Due to the prevalent use of plant extracts in synthesizing nanoparticles, the antioxidant activity of AgNPs is frequently compared to that of the plant extract. However, nanoparticles consistently demonstrate more significant results than the plant extract itself. The chemical composition of the extract typically influences the antioxidant effects of silver nanoparticles, and these attributes generally enhance as the concentration of AgNPs increases. When the extract is abundant in flavonoids and phenolic compounds, the nanoparticles demonstrate significant scavenging activity. Therefore, biogenic synthesis offers numerous opportunities to investigate novel green precursor strategies.

Chapter 5

Antioxidant-mediated ameliorative of *Acmella ciliata* silver nanoparticles activity against doxorubicin-induced toxicity in Dalton's Lymphoma Ascites (DLA) bearing mice

1. Introduction

The utilization of biological methods in the synthesis of nanoparticles has been found to be advantageous in the production of metal nanoparticles. Biomolecules such as amino acids, proteins, NAD(P)⁺ reductases, dehydrogenases and various secondary metabolites present in the plant extract reduced silver ions in the synthesis of AgNPs (Xu *et al.*, 2020). In the synthesis of AgNPs, plant extract acts as both a reducing and stabilizing agent that protects from agglomeration and affects the morphology of nanoparticles by preventing their uncontrolled growth (Saranyadevi *et al.*, 2014). The biosynthesis of AgNPs mediated by phytochemicals found in the plant extract can operate as efficient antioxidants or free radical scavengers by reducing ROS generation and protecting various biomolecules (Allafchian *et al.*, 2016).

Doxorubicin (DOX) is an indispensable anthracycline antibiotic that displays a broad spectrum of anti-cancer activity and has been clinically used to treat various malignant neoplasms (Carvalho *et al.*, 2009). DOX is administered to patients with solid tumors and haematological malignancies, such as breast, bile duct, prostate, uterus, ovary, oesophagus, stomach, and liver tumors. It is also used to treat childhood solid tumors, osteosarcomas, soft tissue sarcomas, Kaposi's sarcoma, acute myeloblastic and lymphoblastic leukemia, and Wilms Tumor (Danesi *et al.*, 2002, Borchmann *et al.*, 1997; Breslow *et al.*, 2004). The anticancer activity of DOX has been linked to its tendency to intercalate into the DNA helix and/or form covalent bonds with proteins involved in DNA replication and transcription, as demonstrated by numerous investigations (Box *et al.*, 2007). These interactions cause the suppression of DNA, RNA, and protein production, ultimately resulting in the death of the cell (Cutts *et al.*, 1996). DOX has been demonstrated to enter cancer cells through simple diffusion and bind to the proteasome in the cytoplasm with a high

degree of affinity. Following its binding to the 20S proteasomal subunit, DOX forms a DOX proteasome complex, which is then aided by nuclear localization signals and requires ATP to translocate into the nucleus through nuclear pores. Ultimately, DOX separates from the proteasome and attaches to DNA because it has a greater attraction to DNA compared to the proteasome. The therapeutic application of DOX was quickly hindered by significant obstacles, including the emergence of resistance in cancer cells and toxicity in normal tissues.

Despite having an effective therapeutic role, DOX administration has been constrained due to cumulative dose-dependent effects that led to organ toxicity such as cardiotoxicity, hepatotoxicity and nephrotoxicity, which subsequently reduces its clinical utility (Shivakumar *et al.*, 2012). Although the mechanisms involved in the onset of DOX-induced organ toxicity remain obscure, numerous studies have revealed it to be multifactorial, among which the induction of oxidative stress due to the generation of free radicals seems to be the key player. Free radicals are atoms, molecules or ions with unpaired electrons which are biologically derived from oxygen, nitrogen and sulphur molecules. When present in low to moderate concentrations, free radicals such as superoxide ($O_2^{\cdot-}$), hydroxyl radicals (OH^{\cdot}), and singlet oxygen (1O_2) are essential in regulating various physiological functions of the body (Halliwell and Gutteridge, 2015). However, owing to their unpaired electron, they are extremely reactive with other cellular molecules and can hamper the body's antioxidant defence systems thereby leading to oxidative stress (Stadtman, 1992). DOX promotes oxidative stress by the formation of a semiquinone derivative via an NADPH-dependent reduction reaction. The redox cycling of semiquinone to quinone in the presence of oxygen generates superoxide radicals ($O_2^{\cdot-}$). The superoxide radical produces several free radicals through a subsequent chain reaction, including hydrogen peroxide (H_2O_2) and hydroxyl ions ($^{\cdot}OH$) (Bachur *et al.*, 1979). In addition, DOX generates free radicals *via* an iron ion-dependant non-enzymatic mechanism thereby resulting in lipid peroxidation, DNA/RNA damage, inhibition of autophagy, disturbance of calcium homeostasis and the subsequent activation of inflammatory response and apoptosis (Elberry *et al.*, 2010).

Even though cells are equipped with a strong endogenous antioxidant system to counter balance the increasing levels of ROS to prevent oxidative stress, it has been

reported that DOX can suppress the endogenous antioxidant system such as glutathione and catalase thereby promoting the accumulation of free radicals and subsequently causing redox imbalance (Sangomla *et al.*, 2018). It is known that mitochondrial DNA (mt-DNA) reacts with DOX to form adducts that impair the normal function of mitochondria, protein expression, and lipid oxidation (Eder *et al.*, 2006). The oxidation of particular thiol residues in mitochondrial proteins is a crucial factor in regulating the activation of the permeability transition pore (PTP) (Constantini *et al.*, 1996). Considering the pro-oxidant properties of DOX, it is reasonable to predict a correlation between the toxicity of DOX and the induction of PTP. DOX treatment leads to an elevation in the quantity of oxidized thiol residues in proteins of the PTP complex (Oliveira *et al.*, 2006). Researchers also reported a decline in the level of vitamin E and glutathione (GSH), two important cellular antioxidants, which results in reduced protection against ROS generated during DOX redox cycling (Cardoso *et al.*, 2008)

DOX-induced apoptosis is a prevalent mechanism in cancer cells, and it is believed that toxicity in healthy cells may also arise from this effect, albeit through alternative pathways. DOX-administered animals exhibited elevated levels of Bax, a protein that promotes apoptosis, and decreased levels of Bcl2, a protein that inhibits apoptosis (Tsang *et al.*, 2003). DOX, like a multitude of genotoxic agents, induces the binding of p53 to DNA through the activation of nuclear factor-kB (NF-kB) and p53 promotes apoptotic cell death via caspase cascade activation (Ashikawa *et al.*, 2004). Multiple efforts have been undertaken to reduce the adverse effects of DOX, including the use of compounds with antioxidant and/or anti-apoptotic properties, the creation of effective delivery systems, and the development of DOX alternatives. Thus, one strategy to combat DOX-induced organ toxicity is an exogenous supply of antioxidants.

In this study, we explored the ability of biosynthesized AgNPs using *Acmella ciliata* leaf extract to provide protective actions against DOX-induced toxicity. *A. ciliata*, commonly known as the toothache plant, is a member of the Asteraceae family. This herb has been traditionally used for the treatment of various illnesses such as toothache, throat and gum infections, stomatitis, articular rheumatism, tuberculosis and leucorrhoea by different communities (Dubey *et al.*, 2013). Different parts of *A.*

ciliata have been shown to contain different bioactive groups including phenolics, alkyl amide, glycosides, coumarins, triterpenoids and pyroglutamate with potent anaesthetic, antipyretic, analgesic, antifungal, antimalarial, aphrodisiac, vasorelaxant and immunomodulatory properties (Paulraj *et al.*, 2013; Rahim *et al.*, 2021). Since increased ROS levels are frequently associated with DOX-induced toxicity, an approach to achieving redox homeostasis may represent an effective tactic to improve the therapeutic efficacy of doxorubicin. Thus, this study investigated the protective effects of biosynthesized AgNPs using *A. ciliata* leaf extract against DOX-induced cardiotoxicity and hepatotoxicity in Dalton's Lymphoma Ascites (DLA) bearing mice.

2. Materials and methods

2.1 Chemicals and reagents

Nicotinamide adenine dinucleotide (NADH), nitro-blue tetrazolium (NBT), disodium hydrogen phosphate, n-butyl alcohol, 2-thiobarbituric acid (TBA), phenazine methosulfate (PMS), glutathione reduced, potassium persulfate, gallic acid, quercetin dihydrate, sodium nitrite, methanol and cumene hydroperoxide were obtained from HiMedia Laboratories Pvt., Ltd. (Mumbai, India). Glacial acetic acid, aluminium chloride and 5, 5'-dithio-2-nitrobenzoic acid (DTNB) were obtained from Merck Specialities Pvt., Ltd. (Mumbai, India). 1-chloro-2,4-dinitrobenzene (CDNB), cupric sulfate, Trichloroacetic acid (TCA), Folin-ciocalteu's reagent, sodium hydroxide and ascorbic acid were obtained from SD finechem Ltd. (Mumbai, India). Doxorubicin (Getwell Oncology Pvt., Ltd., Haryana, India) was purchased from a local pharmacy.

2.2 Animals and tumor model

All experimental procedure involving animal care and handling was carried out in accordance with the guidance for caring and using of Laboratory Animals (National Institutes of Health, USA) and approved by the Mizoram University Institutional Animal Ethical Committee (MZU/IAEC/2022-23/03). The adult Swiss albino mice weighing 25-30 g were selected and maintained under controlled temperature ($25^{\circ}\text{C} \pm 2^{\circ}\text{C}$) and photoperiod of 12/12 h light/dark cycles (Frontier Euro Digital Timer, Taiwan) at the Animal Care Facility, Department of Zoology, Mizoram University,

India. All animals were provided sawdust as bedding and had access to standard food pellets and water *ad libitum*. Dalton's Lymphoma Ascites (DLA) tumor has been maintained in 10-12 weeks old mice by serial intraperitoneal (i.p) transplantation of 1×10^6 viable tumor cells per animal (in 0.25 ml Phosphate-buffered saline (PBS), pH 7.4) under aseptic condition.

2.3 Experiment Design

All animals, except the control group, were injected (i.p) with DLA cells on day 0. The AgNPs treatment was carried out for 7 consecutive days. Animals were randomly divided into seven groups consisting of six individuals each ($n = 6$) as follows:

Group I (Control group): Mice were injected (i.p) with 0.5 ml of normal saline on day 1.

Group II (DLA group): Mice were injected (i.p) with 0.5 ml of normal saline on day 1 followed by 0.5 ml of distilled water (vehicle) by oral gavage daily.

Group III (DOX group): Mice were injected (i.p) with doxorubicin (20 mg/kg b.wt) on day 1 followed by 0.5 ml of distilled water by oral gavage daily.

Group IV, V, VI (DOX + AgNPs groups): Mice were injected (i.p) with doxorubicin (20 mg/kg b.wt) on day 1 followed by different dosage of AgNPs (25, 50 and 100 mg/kg b.wt) by oral gavage daily.

Group VII (AgNPs group): Mice were injected (i.p) with 0.5 ml of normal saline on day 1 followed by of AgNPs (50 mg/kg b.wt) by oral gavage daily.

2.4 Preparation of tissue homogenates for biochemical assays

After 7 days of treatment, the animals were sacrificed and the liver and heart were immediately excised. 5% (w/v) tissue homogenate was prepared with ice-cold buffer (5 mM EDTA, 150 mM NaCl, pH 7.4). The homogenates were centrifuged at 13,000 rpm for 30 min at 4°C and the supernatants were stored at -80°C in aliquots until used for biochemical assays.

2.5 Estimations of serum Aspartate amino-transferase (AST), Alanine amino-transferase (ALT) and Lactate dehydrogenase (LDH)

Blood was collected by heart puncture using a heparin-coated syringe and centrifuged at 2,000 rpm for 15 min at 4°C. The serum was assayed for AST (EC 2.6.1.1), ALT (EC 2.6.1.2) and LDH (EC 1.1.1.27) according to the manufacturer's instruction (Transasia Bio-Medicals Ltd, Mumbai, India).

2.6 Biochemical assays

The protein content of the liver and heart was determined using the standard method (Lowry *et al.*, 1951).

2.6.1 Glutathione (GSH)

Glutathione (GSH) levels were estimated using the method described earlier (Moron *et al.*, 1979). Briefly, 80 µl of 5% tissue homogenate was incubated with a mixture of 20 µl of DTNB (10 mM) and 900 µl of sodium phosphate buffer (0.2 M) for 2 min at room temperature. The absorbance was taken at 412 nm against blank. A mixture devoid of tissue lysates served as blank. The concentration of GSH was calculated from the standard graph and expressed as µmol/mg protein.

2.6.2 Glutathione-s-transferase (GST)

The activity of glutathione-s-transferase (GST) was determined using the standard method (Beutler, 1984). Briefly, 50 µl of CDNB (5 mM) was mixed with 850 µl of phosphate buffer (0.1 M; pH 6.5) and incubated at 37°C for 10 min. To the reaction mixture, 50 µl each of GSH (20 mM) and tissue homogenate were added. A mixture devoid of tissue lysates served as blank. The absorbance was recorded at 1 min interval for 6 min at 340 nm. GST activity was measured as:

$$GST\ Activity = \frac{OD\ of\ test - OD\ of\ blank}{9.6 \times volume\ of\ test\ sample} \times 1000$$

where, 9.6 is the molar extinction coefficient for GST.

GST activity was expressed as Unit/mg protein.

2.6.3 Superoxide dismutase (SOD)

The activity of SOD was estimated by the NBT reduction method (Fried, 1975) with minor modifications. Briefly, 100 μ l each of tissue homogenate and PMS (186 μ M) were mixed with 300 μ l of NBT (3 mM) and 200 μ l of NADH (780 μ M). After incubation of the mixture at 30°C for 90 sec, 1 ml of acetic acid and 4 ml of n-butanol were added to stop the reaction. A mixture devoid of tissue lysates served as blank. The absorbance was measured at 560 nm and the enzyme activity was expressed in the unit (1 unit = 50% inhibition of NBT reduction)/mg protein.

$$\% \text{ inhibition} = \frac{OD \text{ of blank} - OD \text{ of sample}}{OD \text{ of blank}} \times 1000$$

2.6.4 Lipid peroxidation (LPO) assay

LPO was measured by the standard method (Buege and Aust, 1978). Briefly, the tissue homogenate was added to a mixture of 0.8% TBA, 10% TCA and 0.25 N HCl in a 1:2 ratio. After boiling the mixture for 10 min, it was cooled immediately at room temperature and centrifuged at 12,000 rpm for 10 min. The absorbance of the supernatant was recorded at 535 nm against blank. A mixture devoid of tissue lysates served as blank. The concentration of MDA was calculated using the extinction coefficient of $1.56 \times 10^6 \text{ M}^{-1}\text{cm}^{-1}$ and expressed as nmol/mg protein.

2.3 Statistical analysis

Data are expressed as mean \pm standard error of the mean. One-way ANOVA followed by Tukey's test was performed to test significant variations in antioxidants status, lipid peroxidation, and serum enzyme activities of treatment groups using SPSS ver.16.0 software (SPSS Inc, Chicago, IL, USA). The IC_{50} was also calculated using GraphPad Prism software ver. 6.0. A 'p' value of less than 0.05 was considered statistically significant.

3. Results

3.1 Serum enzyme assays

The protective effect of AgNPs against DOX-induced toxicity was assessed by determining the serum enzyme activities in different experimental groups (Table 5.1). Administration of DLA mice with 20 mg/kg b.wt of DOX led to a significant ($p < 0.001$) increase in ALT, AST and LDH when compared to the normal control group as well as untreated DLA mice. Co-administration of DLA mice with DOX (20 mg/kg b.wt) and AgNPs (50 mg/kg b.wt) result in a significant decrease ($p < 0.001$) in serum enzyme activities when compared to DLA mice receiving DOX only indicating the protective effects of AgNPs against DOX-induced cardio- and hepatotoxicity.

3.2 Effects of AgNPs in antioxidant status and lipid peroxidation (LPO)

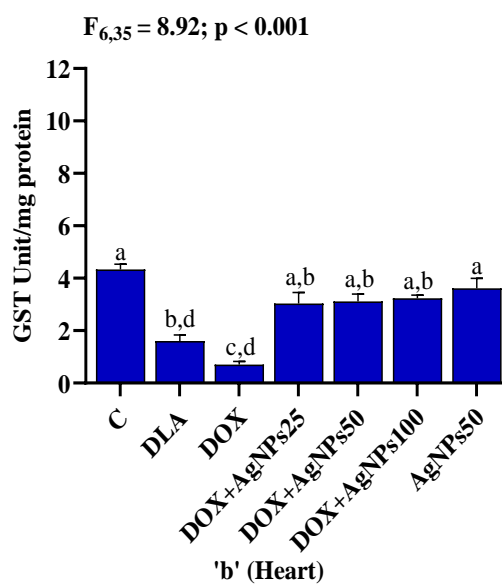
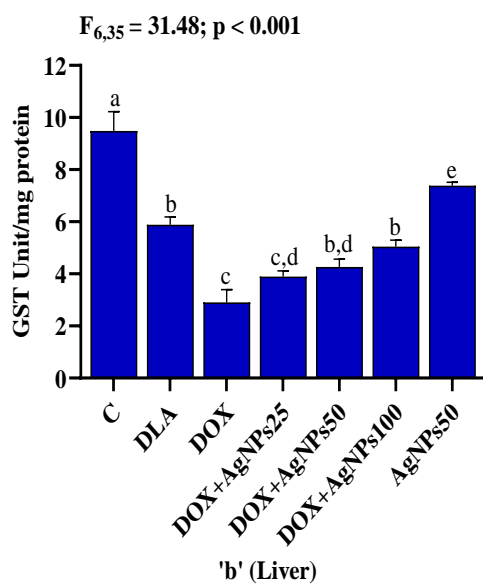
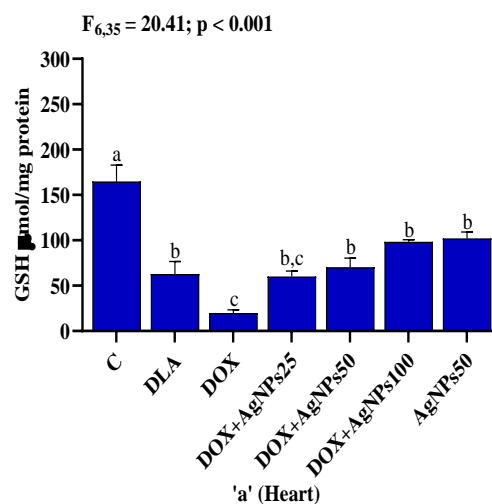
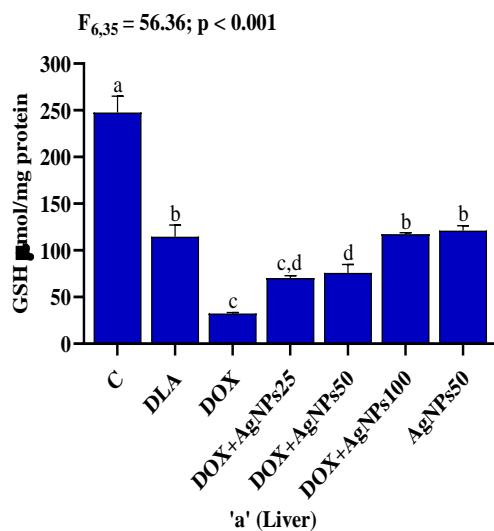
DLA mice treated with DOX (20 mg/kg b.wt) showed significantly reduced GSH contents (Liver: 3.56 folds; Heart: 3.26 folds), and the activities of GST (Liver: 2.0 folds; Heart: 2.28 folds) and SOD (Liver: 3.0 folds; Heart: 3.25 folds) in liver and heart when compared to the untreated DLA mice (Figure 5.1). Co-administration of AgNPs for 7 consecutive days to DOX-treated DLA mice resulted in a significant increase in GSH content, and activities of GST and SOD in both the liver and heart of mice. The protective effects of AgNPs against DOX-induced hepato- and cardiotoxicity occurred in a dose-dependent manner. DLA mice treated with AgNPs alone (50 mg/kg b.wt) did not induce any significant change in the GSH contents when compared to untreated DLA mice. However, treatment of DLA mice with AgNPs alone led to a significant increase in GST and SOD activities as compared to untreated DLA mice, and the increased antioxidant status was comparable to that of the normal control group (Figure 5.1).

Administration of DOX to DLA mice resulted in significant ($p < 0.001$) increase in the MDA levels (Liver: 1.83 folds; Heart: 3.91 folds) in the liver and heart when compared to untreated DLA mice. Co-administration of different doses of AgNPs for 7 consecutive days to DOX-treated DLA mice led to the significant reduction of MDA level (Figure 5.2). DOX-treated DLA mice that received a higher dose (100 mg/kg

bw.t) of AgNPs showed similar MDA levels when compared with the normal control mice. Furthermore, no significant variation ($p>0.05$) was observed in the level of MDA between DLA mice treated with AgNPs alone (50 mg/kg bw.t) and the normal control group.

Table 5.1. Effects of biosynthesized AgNPs on serum enzyme activities. Normal control: Healthy mice without any treatment; DLA control: Dalton's Lymphoma Ascites (DLA) bearing mice without treatment; DLA+DOX: DLA bearing mice treated with doxorubicin (20 mg/kg b.wt); DLA+DOX+AgNPs₅₀: DLA mice treated with 20 mg/kg of doxorubicin followed by *Acmella ciliata* silver nanoparticles at the dose of 50mg/kg b.wt. Values are expressed as Mean \pm SEM, n=3. Different letters indicate significant variation.

GROUPS	ALT (U/L)	AST (U/L)	LDH (U/L)
Normal Control	13.56 \pm 0.40 ^a	97.13 \pm 2.10 ^a	427.66 \pm 2.20 ^a
DLA Control	18.63 \pm 0.38 ^b	111.33 \pm 3.71 ^b	580.00 \pm 5.77 ^b
DLA+DOX	36.00 \pm 2.12 ^c	159.27 \pm 2.24 ^c	1010.68 \pm 8.80 ^c
DLA+DOX+AgNPs ₅₀	17.46 \pm 0.83 ^{a, b}	128.40 \pm 3.18 ^d	502.15 \pm 5.57 ^d



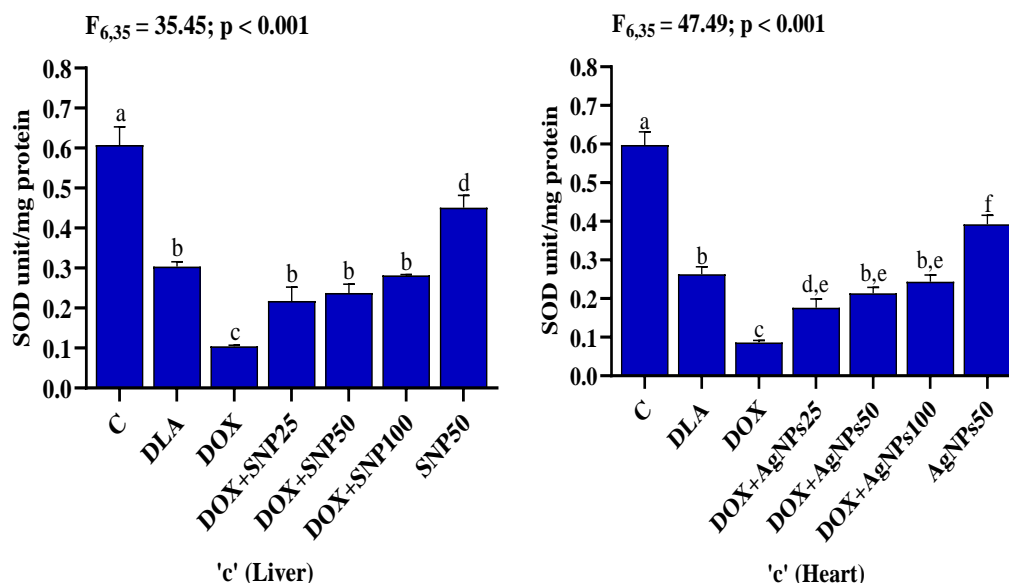


Figure 5.1: Effects of biosynthesized AgNPs on (a) glutathione level (GSH) ($\mu\text{mol}/\text{mg}$ protein), (b) glutathione-s-transferase activity (GST) (Unit/mg protein), and (c) superoxide dismutase activity (SOD) (Unit/mg protein) in the liver and heart of mice. C: normal control; DLA: Dalton's Lymphoma Ascites bearing mice without any treatment; DOX: DLA mice treated with 20 mg/kg of doxorubicin; DOX+AgNPs25, DOX+AgNPs50, DOX+AgNPs100: DLA mice treated with 20 mg/kg of doxorubicin followed by biosynthesized AgNPs at the dose of 25, 50, 100 mg/kg, respectively. AgNPs50: DLA mice treated with biosynthesized AgNPs (50 mg/kg). Means not sharing the same letter are significantly different.

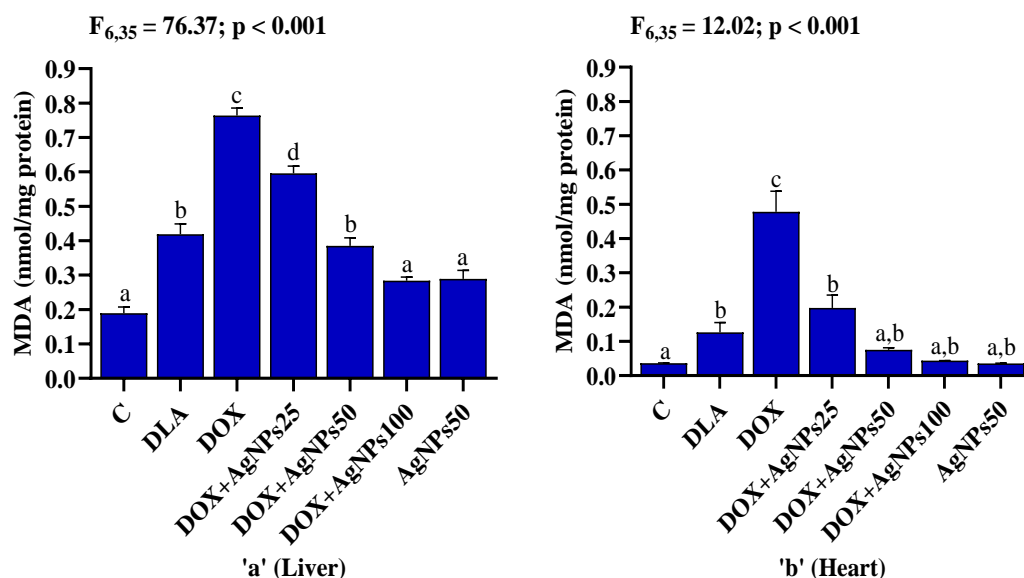


Figure 5.2: Effects of biosynthesized AgNPs on lipid peroxidation (LPO) expressed in malondialdehyde (MDA) (nmol/mg protein) in (a) liver, and (b) heart of DLA mice. C: normal control; DLA: Dalton's Lymphoma Ascites bearing mice without any treatment; DOX: DLA mice treated with 20 mg/kg of doxorubicin; DOX+AgNPs25, DOX+AgNPs50, DOX+AgNPs100: DLA mice treated with 20 mg/kg of doxorubicin followed by biosynthesized AgNPs at the dose of 25, 50, 100 mg/kg, respectively. AgNPs50: DLA mice treated with biosynthesized AgNPs (50 mg/kg). Means not sharing the same letter are significantly different.

4. Discussion

The broad applicability of doxorubicin in cancer therapy is constrained by the adverse effects associated with the drug. Researchers have developed several approaches to counteract the detrimental impacts of doxorubicin. The generation of reactive oxygen species (ROS) through DOX has been documented to contribute to the development of serious cardiac issues, such as cardiomyopathy and congestive heart failure (Takemura and Fujiwara, 2007; Ewer and Ewer, 2010). DOX usage has been linked to higher levels of serum toxicity markers including alanine transaminase (ALT), aspartate transaminase (AST), and lactate dehydrogenase (LDH) (Ahmed *et al.*, 2019). Due to cellular enzyme leakage, damaged liver cells exhibit increased membrane permeability and altered cell transport function, which raise serum levels of AST and ALT (Mohan *et al.*, 2010). The activity of ALT in DLA mice co-administered with DOX and AgNPs reversed to nearly normal mice exhibiting the protective effect of AgNPs against DOX- induced toxicity.

The long-term use of DOX for cancer treatment has been constrained due to the toxic side effects of the drug that results in organ toxicity. Uses of antioxidants of natural origin have become promising strategies to combat their toxic effects. The deleterious effect of DOX on different organs has been elucidated based on different components, with oxidative stress being considered the most important factor. The oxidative stress caused by a disruption in the antioxidant system can be measured by determining the levels and activities of antioxidants such as glutathione (GSH), glutathione-s-transferase (GST) and superoxide dismutase (SOD). In the present study, we investigated the chemo-preventive functions of biosynthesized AgNPs using *A. ciliata* leaf extract against DOX-induced organ damage in DLA-bearing mice. The antioxidant status was determined in the liver and heart of DLA mice to elucidate the antioxidative potential of AgNPs. Decreased GSH levels following DOX treatment in DLA bearing mice could be due to excessive utilization of GSH in the liver and heart for scavenging of DOX metabolites. The majority of toxicant covalent binding to hepatic protein has been reported to occur only after GSH depletion (Uetrecht, 2010). Improved antioxidant status in DOX-treated DLA-bearing mice after administration of AgNPs may occur due to maintenance of GSH through neutralization of free

radicals by the combined action of bioactive constituents of *A. ciliata* leaf extract along with the silver ions. The preventive effects of numerous naturally occurring antioxidants against DOX-induced organ toxicity have been reported earlier (Lalmuansangi *et al.*, 2022). Phenolic compounds such as oleuropein, sesamol, anthocyanins, curcumin, gingerol and hydro-xytyrosol have been used to reduce DOX-induced toxicity (Della Torre *et al.*, 1999; Ojha *et al.*, 2016). Similarly, flavonoids, a type of naturally occurring phenolic compounds, such as chrysin, naringenin, kaempferol, avicularin, isorhamnetin, chrysoeriol, hesperidin, apigenin and baicalein have been reported to possessed protective effects against DOX-induced hepatotoxicity, nephrotoxicity, and cardiotoxicity by increasing antioxidant enzymes (Ojha *et al.*, 2016; Rashid *et al.*, 2013).

Malondialdehyde (MDA), which is formed during the breakdown of polyunsaturated fatty acids, is a useful index for determining the extent of lipid peroxidation. The most frequently cited evidence to support the involvement of free radical reactions in toxicity is the detection and measurement of lipid peroxidation (Gaschler & Stockwell, 2017). The increased levels of lipid peroxidation in DOX-treated DLA-bearing mice could be attributed to DOX-induced superoxide anion overproduction and a decrease in detoxifying hydroperoxide. Treatment with biosynthesized AgNPs protects against DOX-induced cellular lipid peroxidation, possibly by inhibiting lipid peroxidation chain reactions in the cytoplasm.

5. Conclusion

Acemella ciliata contains a wide range of bioactive compounds, such as phenolics, alkyl amides, glycosides, coumarins, triterpenoids, and pyroglutamate with potent anaesthetic, antipyretic, analgesic, antifungal, antimalarial, aphrodisiac, vasorelaxant, and immunomodulatory activities. This leads us to the synthesis of silver nanoparticles using *A. ciliata* leaf extract. The capping of oxidised phenolic compounds and carboxyl protein was responsible for the stability of biosynthesized AgNPs, as confirmed by an FT-IR study. Despite having an effective therapeutic role against various malignant neoplasms, DOX-induced toxic side effects in cancer treatment are well documented. This study found that biosynthesized AgNPs from *A. ciliata* leaf extract offers outstanding protections against cardiotoxicity and

hepatotoxicity caused by DOX in DLA-bearing mice possibly by elevating the activities of antioxidants and reduction of lipid peroxidation. Co-administration of biosynthesized AgNPs also reduces the DOX-induced increase in the activities of various serum enzyme markers, confirming its antioxidant potential. Our study also demonstrated that AgNPs synthesized from *A. ciliata* leaf extract had a great clinical potential for prospective use as anticancer agents by increasing antioxidant levels. However, more research into the precise mechanism of action of biosynthesized AgNPs in protecting against DOX-induced toxicity is needed. Overall, our findings support the use of biosynthesized AgNPs as an effective agent against DOX-mediated toxicity and provide a viable option for increasing doxorubicin's therapeutic efficacy.

Chapter 6

Anti-microbial activity of *Mikania micrantha* and *Acmella ciliata* silver nanoparticles

1. Introduction

The research and development of nanoparticles for diverse biological and environmental applications has emerged as a crucial aspect of nanotechnology. Because of their outstanding physicochemical characteristics, silver nanoparticles are extensively studied and utilized in a wide range of applications (Silva *et al.*, 2017). Silver, in all of its various forms, has been traditionally employed as an antibacterial agent either on its own or in conjunction with other technologies. Researchers have conducted extensive research on this metal to utilize its ability to inhibit bacterial growth in various applications, such as burn and ulcer treatments, food packaging, home appliances, and industrial applications (Miller *et al.*, 2010; Castellano *et al.*, 2007; Kim *et al.*, 2008; Kampmann *et al.*, 2008). With the advent of nanotechnology, the investigation of the antibacterial properties of AgNPs was an obvious progression, considering the existing knowledge and evidence regarding antibacterial properties of silver. AgNPs are nanomaterials with diameters between 1 and 100 nm that have a higher capacity and surface area than silver in its bulk form. The incorporation of AgNPs is particularly beneficial in the medical and healthcare sectors because of the remarkable antimicrobial activity of Ag at the nanoscale (Ge *et al.*, 2014). The efficacy of AgNPs as antibiotics is due to their diverse modes of action, which simultaneously target several structures in microorganisms, allowing them to effectively eliminate a variety of bacterial strains (Cheng *et al.*, 2016).

Antibiotics, one of the greatest discoveries in medical science, have prevented millions of people from diseases caused by pathogenic microorganisms (Luepke *et al.*, 2017). On the other hand, antibiotics pose a paradoxical challenge for human health. Antimicrobial resistance refers to the tendency of microorganisms, such as bacteria, fungi, viruses, and parasites, to develop mechanisms that can resist and render ineffective antimicrobial compounds. According to the World Health Organisation (WHO), the intensive use and misapplication of antimicrobials are the primary causes

of the emergence of drug-resistant pathogens. Additionally, the administration of low doses of antibiotics in animal breeding to avoid infections and enhance animal growth might lead to the development of resistant microbes, which may potentially spread to humans (Littier *et al.*, 2017). Antimicrobial resistance has become a major concern for the successful diagnosis and treatment of infectious diseases due to the emergence and spread of drug-resistant pathogens that have acquired new resistance mechanisms (Tang and Zheng, 2018). Microorganisms employ various mechanisms to develop antibiotic resistance, such as reducing uptake and increasing efflux pumps, acquiring and expressing drug-resistant genes, modifying antimicrobial targets, altering antimicrobial drugs through drug-degrading enzymes, producing competitive inhibitors, forming biofilms, and the emergence of persister cells (Blecher *et al.*, 2011). Ultimately, these mechanisms result in a reduction in the accumulation of antibiotics in bacterial cells, which in turn lowers the therapeutic level of the drug. Consequently, a higher and repeated dose of the drug will be necessary, which can have detrimental effects on both humans and animals. Therefore, the emergence of multidrug resistance (MDR) in pathogens has facilitated the development of innovative antibacterial pharmaceuticals.

The expanding application and extensive research on nanomaterials have provided new perspectives into the development of novel antibacterial materials and nanocomposites to combat the current epidemic of multidrug-resistant bacteria (MDRB). The assessment of the antibacterial potential of AgNPs is an appropriate approach considering the knowledge and facts that exist about the antibacterial activity of silver. AgNPs have the potential to serve as antibiotics due to their diverse action mechanisms, which attack multiple microorganism structures simultaneously and provide them with the ability to kill distinct types of bacteria (Bruna *et al.*, 2021). They exhibit their antimicrobial action through three primary pathways:

(i) Degradation of the cell membrane and cell wall- The primary function of bacterial cell walls and membranes is to provide protection against various detrimental stresses and enable the transportation of diverse beneficial nutrients (Madigan *et al.*, 1997). It has been proposed that AgNPs bind to the bacterial cell wall through an ionic bond, thereby generating a high proton motive force that disrupts the action of enzymes that contain thiol groups (Sereemasapun *et al.*, 2008). The disintegration of the cell wall and

permeability of the membrane result in the release of several components of the bacterial cell to the surroundings, including nucleic acid, proteins, enzymes, metabolites, and sources of energy (Ravichandran *et al.*, 2018; Yuan *et al.*, 2018). This antibacterial mechanism is based on the attachment of AgNPs to bacterial cell walls and their subsequent breakdown (Ansari *et al.*, 2015).

(ii) Intracellular penetration and damage caused by AgNPs- AgNPs bind to proteins and DNA in bacterial cells, causing conformational changes that alter cell function by converting them into other, less stable states (Hsueh *et al.*, 2015). According to, AgNPs with a large surface area contact and enter bacterial cells, releasing Ag ions that interact with phosphorous and sulfur compounds such as DNA, inhibiting replication and causing cell death (Jyoti *et al.*, 2016).

(iii) Oxidative stress in treated bacterial cells- Oxidative stress typically arises from the administration of antimicrobial agents to the bacterial cell. One method for inhibiting resistant bacteria growth is to stimulate the production of reactive oxidative species (ROS) within these microbes. A recent study indicates that the incorporation of AgNPs into resistant microbes leads to an increase in reactive oxygen species (ROS), which in turn inhibits the growth of bacteria. Wypij *et al.* (2021) concluded that AgNPs generate reactive oxygen species (ROS) that harm the cell membrane, proteins, and DNA of both *E. coli* and *S. aureus* bacteria.

The action of the nanoparticles may be significantly influenced by their size, shape, and encapsulating molecules when they bind to the cell wall and membrane and are internalized. Smaller nanoparticle sizes also lead to an improved bactericidal impact, which is attributed to a higher surface area in contact with the bacteria, facilitating membrane breakage and internalization. The release rate of silver ions from the nanoparticles is influenced by both the size and surface properties, which is worth mentioning. The stability of the nanoparticles is determined by the charge and surface composition, while the contact area and interaction with the medium are influenced by the size of nanoparticles (Sharma and Zboril, 2017). Accordingly, studies have shown that smaller nanoparticles have a higher dissolution rate in different media, releasing silver ions in the process, which may be a significant factor in the antibacterial action of nanoparticles (Ivask *et al.*, 2014). Furthermore, the utilization of AgNPs in conjunction with antibiotics, as well as the functionalization

or conjugation of AgNPs with other molecules, has been suggested as a viable method to achieve potent bactericidal effects without developing bacterial resistance (Brown, *et al.*, 2012). Silver nanoparticles (NPs) thus constitute a feasible alternative to antibiotics for treating many diseases, specifically those caused by multidrug-resistant bacteria.

The application of AgNPs as a substitute for synthetic fungicides has emerged as a novel technique with improved effectiveness. There have been global instances of antifungal resistance, which promotes the generation of resistant variants due to repeated applications of agrochemicals that also impact the fungus population. As a result of improved permeability and retention effects, AgNPs appear to be highly appealing for a multitude of antifungal applications. AgNPs possess numerous antifungal mechanisms, including plasma-membrane interactions and linkages to DNA phosphate groups (Matsumura *et al.*, 2003). These mechanisms contribute to proton dispersion and cell mortality, degradation of the electron transportation chain, and disruption of membrane proton motive force and phosphate groups (Feng *et al.*, 2000). This study demonstrates that silver nanoparticles (AgNPs) produced using extracts from *Mikania micrantha* and *Acmella ciliata* leaves have the potential to effectively suppress the growth of pathogens and control plant diseases.

2. Materials and methods

2.1 Chemicals and reagents

Sterile disc, Antibiotics disc, Nutrient broth, Nutrient agar, Nutrient broth, Mueller–Hinton agar for bacteria culture, potato dextrose agar for fungal cultures, barium chloride, sodium chloride, H₂SO₄, ethanol, sodium hypochlorite, Phenol:Chloroform:Isoamyl alcohol mixture, were obtained from HiMedia chemical, India. Carbendazim (commercial fungicide) was purchased from a local market. PCR master mix was purchased from Takara Bio, USA.

2.2 Anti-bacterial study

All the bacteria strains were cultured in Mueller Hinton broth (MHB)) at 37°C for 24 h. The pure culture of *E. coli* (ATCC 11220), *P. aeruginosa* (ATCC 9027), *B.*

subtiles (ATCC 11774) and *S. aureus* (ATCC 6538P) for antibacterial studies have been acquired from the American Type Culture Collection (Rockville, MD, United States).

2.2.1 Disc diffusion method

Antibacterial activity of the biosynthesized AgNPs was determined using Kirby-Bauer disc diffusion method (Hudzicki, 2009). Gram-negative bacteria (*E. coli* ATCC 11220, *P. aeruginosa* ATCC 9027) and Gram-positive bacteria (*B. subtilis* ATCC 11774, *S. aureus* ATCC 6538P) were selected for the test microorganisms. The inoculums were prepared from 24 h old pure agar culture adjusted to 0.5 McFarland Standard (1.5×10^8 cfu/ml). Microorganisms suspended in normal saline were inoculated into Mueller Hinton Agar (MHA) petri-plates with a sterilized cotton swab. The sterile discs were separately impregnated with double distilled water (negative control), plants leaf extracts, AgNO₃, AgNPs, and ofloxacin (positive control) and then air-dried in a sterile condition. After drying, the treated discs were placed on the agar plates and incubated at 37 °C for 24 h in an incubator. The diameter of the zone of inhibition was measured using inhibition scale (Himedia). Three replicates were performed for each pathogen and the mean diameter value was expressed in

$$W = \frac{(T - D)}{2}$$

Where:

W - Diameter of clear zone of inhibition

T - Total diameter of including disc and clear zone

2.2.2 Minimum Inhibitory Concentration (MIC)

AgNPs were evaluated for anti-bacterial activity by MIC at different concentration using the standard method (Elshikh *et al.*, 2016). All the wells were filled with 100µl of sterilized media from 1-11 and 200 µl in 12th of the plate using a multichannel pipette. 100 µl of silver nanoparticles (80 µg/ml) were filled in the first well and serially diluted two folds up to the 10th well. 11th well was used as growth control (broth + inoculum only). 100µl of the inoculum was added to all the wells

except at the 12th row (acts as a blank control for sterility). The plate was incubated overnight at 37 °C for 24 h in an incubator. 50µl of resazurin (0.015 %) was added to all wells and further incubated for 2–4 h for the observation of colour change. On completion of the incubation, columns with no colour change (blue resazurin colour remained unchanged) were scored as above the MIC value.

2.2.3 Minimum Bactericidal concentration (MBC)

The minimum killing time was performed from the result of minimum inhibitory concentration (MIC). 100µl from each row of MIC were spread on fresh media plates with the help of a spreader. Incubation temperature was adjusted depending on the type of pathogen. A clear plate without any colonies was indicative of the Minimum Bactericidal concentration. The MBC value was determined when there was no colony growth from the directly plated contents of the wells.

2.3 Anti-fungal study

2.3.1 Sample collection

Fungal infected rice samples were collected from the paddy field of Zotlang, Champhai district, Mizoram. The plant samples showing the symptoms of rice blast were kept in plastic bags and stored at 4 °C for further studies.

2.3.2 Isolation of pathogen

The infected leaves were cut into small pieces with a sterile scalpel and sterilized with 70% ethanol and 1% sodium hypochlorite for 30 seconds and 1 min, respectively. Then, the infected leaves were washed three times with sterile water for 30 seconds, and placed on sterile filter paper. The sample was then placed aseptically on a sterile petri-plate containing Potato Dextrose Agar (PDA) medium amended with streptomycin and incubated at 25 ± 2°C for 4-6 days. The pure culture was utilized for subsequent tests.

2.3.3 Morphological identification

A slide was prepared using cotton blue lacto-phenol for the identification of the fungus specimen after five days of incubation. Using a needle, a tiny strain of the colony was isolated and observed under a microscope. Identification of the specimen was performed based on the features of the spores, colony appearance, and mycelium shape, size, and structure (Ellis, 1965; Gilman, 1957).

2.3.4 Molecular Identification of fungal isolates

The genomic DNA isolation was performed using the phenol/chloroform/isoamyl method. The fungal isolates were subjected to amplification of the nuclear ribosomal DNA internal transcribed spacer (ITS) using the forward primer, ITS1-F (5'-CTTGGTCATTTAGAGGAAGTAA-3') and the reverse primer, ITS4 (5'-CTTGGTCATTTAGAGGAAGTAA-3') (White *et al.*, 1990). The reaction was conducted in a 50µl mixture including 5µl of 10X PCR buffer, 1.5µl of primers (ITS1 and ITS4), 0.2µl of 25mM dNTPs, 0.4µl of 3U/µl Taq polymerase, 1.5µl of template DNA, and 41.8µl of millipore water in a thermal cycler. The PCR products were then sent to a commercial sequencing lab (Bioscience), for DNA sequencing. The ITS sequences were compared with sequences in GenBank using the Basic Local Alignment Search Tool to determine the closest matched sequence from the database. Nucleotide sequences have been submitted and assigned GenBank Accession numbers.

2.3.5 Inhibition of colony growth

Assessment of the antifungal activity of AgNPs was performed using the poisoned food technique as described by Adjou *et al.* (2012). Silver nanoparticles were dissolved in sterile water as a stock solution. Silver nanoparticles were dissolved in sterile water as a stock solution. 1ml of various concentrations of AgNPs (50, 25, and 12.5 µg/ml) and Carbendazim (200 µg/ml) were added to each plate containing 20 ml of Potato Dextrose Agar (PDA). The treated plates were then allowed to solidify. The plates without silver nanoparticles were maintained as control. A fungal block with a diameter of 5 mm, taken from a freshly grown culture, was placed in the middle of

each Petridish, which contained varying concentrations of silver nanoparticles. The plates were then incubated at a temperature of 25 ± 2 °C for a period of 4-6 days. Experiments were carried out in triplicate for both the control and treatment groups.

2.3.6 Estimation of fungal Biomass

The biomass of fungal culture was determined using the standard method (Sunder Rao and Sinha, 1963). Different concentrations of AgNPs (50, 25, and 12.5 µg/ml) or Carbendazim (200 µg/ml) were added to each conical flask containing 20 ml of medium. The medium without any treatment served as the control, and the experiments were performed in triplicate. The conical flasks were inoculated with a pure fungal block with a diameter of 5 mm under sterilized conditions. The tested culture was incubated at 25 ± 2 °C for 4-6 days. Following incubation, the inoculated flasks were filtered using Whatman filter paper No 1. The initial weight of the filter papers was measured using an electronic balance. The entire residue (filter paper) is thoroughly rinsed with distilled water to eliminate any remaining debris adhering to the media and then dried in an oven to obtain the final weight. The microbial biomass was measured by using formula:

$$\text{Dry weight of the fungal pathogen} = W2 - W1$$

Where,

W1 - Initial weight of filter paper

W2 = Final weight of filter paper

3. Results

3.1 Anti-bacterial activity of *Mikania micrantha* silver nanoparticles

3.1.1 Disc diffusion method

The antimicrobial activity of biosynthesized silver nanoparticles was assessed using the disc diffusion method against both gram-positive and gram-negative bacteria. Silver nanoparticles showed significant antibacterial activity as indicated by the formation of inhibition zone. AgNPs prepared from *M. micrantha* extract shows prominent inhibition for *E. coli*, *P. aeruginosa*, *B. subtilis* and *S. aureus* (Figure 6.1).

AgNPs at the dose of 10 µg/ml possessed the highest antibacterial activity against *E. coli* (21.9 mm) followed by *P. aeruginosa* (20.84 mm), *B. subtilis* (18.36 mm) and *S. aureus* (16.82 mm). Our findings also demonstrated that, in comparison to gram-negative bacteria (*E. coli*, *P. aeruginosa*), gram-positive bacteria (*B. subtilis* and *S. aureus*) displayed a reduced zone of inhibition. The antibacterial activity of AgNPs at the dose of 10 µg/ml was found to be comparable with the standard antibiotics (Ofloxacin, 30 µg/ml) (Figure 6.2).

3.1.2 Minimum Inhibitory Concentration (MIC) and Minimum Bactericidal concentration (MBC)

MIC was defined as the lowest concentration of the antibacterial agent to inhibit the growth of bacteria by serial dilution. AgNPs doses of 80 µg/ml to 0.156 µg/ml were tested on pathogenic bacteria, including *E. coli*, *P. aeruginosa*, *B. subtilis*, and *S. aureus* (Figure 6.3). The lowest minimum inhibitory concentration (MIC) was against *E. coli* (2.5 µg/ml), followed by *P. aeruginosa* (5.0 µg/ml), *B. subtilis* (5.0 µg/ml), and *S. aureus* (5.0 µg/ml). A lower minimum inhibitory concentration (MIC) for tested bacterial strains indicates higher inhibition activity. MBC was calculated by subculturing MIC dilutions on sterile MH agar plates and observing drug concentrations where no apparent growth emerged on the agar plates. The MBC for *E. coli* was determined to be 5.0 µg/ml, whereas for *P. aeruginosa*, *B. subtilis*, and *S. aureus*, it was found to be 10 µg/ml (Table 6.1). These values are consistent with the MIC results, which indicated that *E. coli* was the most susceptible. Furthermore, the results show that the MBC was 2-fold higher than the MIC.

3.2 Anti-bacterial activity of *Acmella ciliata* silver nanoparticles

3.2.1 Disc diffusion method

The antimicrobial activity of biosynthesized silver nanoparticles was assessed using the disc diffusion method against both gram-positive and gram-negative bacteria. Silver nanoparticles showed significant antibacterial activity as indicated by the formation of inhibition zone. AgNPs prepared from *M. micrantha* extract shows prominent inhibition for *E. coli*, *P. aeruginosa*, *B. subtilis* and *S. aureus* (Figure 6.4).

AgNPs exhibited the most potent antibacterial activity against *E. coli* (21.9 mm), *P. aeruginosa* (20.84 mm), *B. subtilis* (18.36 mm), and *S. aureus* (16.82 mm) at a concentration of 10 µg/ml. AgNPs exhibited the most potent antibacterial activity against *P. aeruginosa* (23.79 mm), *E. coli* (23.39 mm), *B. subtilis* (20.96 mm), and *S. aureus* (20.04 mm) at a concentration of 10 µg/ml. AgNPs exhibited comparable antibacterial activity to conventional antibiotics (Ofloxacin, 30 µg/ml) at a concentration of 10 µg/ml. In addition, our results indicated that gram-positive bacteria (*B. subtilis* and *S. aureus*) exhibited a diminished zone of inhibition in comparison to gram-negative bacteria (*E. coli* and *P. aeruginosa*) (Figure 6.5).

3.2.2 Minimum Inhibitory Concentration (MIC) and Minimum Bactericidal concentration (MBC)

The MIC value was determined as the minimum concentration of the drug that inhibited growth in bacteria in comparison to the control. Various pathogenic bacteria, such as *E. coli*, *P. aeruginosa*, *B. subtilis*, and *S. aureus*, were subjected to different concentrations of AgNPs, varying from 80 µg/ml to 0.156 µg/ml (Figure 6.6). The minimum inhibitory concentration (MIC) was lowest against *E. coli* (1.25 µg/ml), followed by *P. aeruginosa* (2.5 µg/ml), *B. subtilis* (2.5 µg/ml), and *S. aureus* (5.0 µg/ml). MBC was calculated by subculturing MIC dilutions on sterile MH agar plates and observing drug concentrations where no apparent growth emerged on the agar plates. The MBC value was 2-fold higher than the MIC. The MBC for *E. coli* was determined to be 2.5 µg/ml, whereas for *P. aeruginosa*, *B. subtilis*, and *S. aureus*, it was found to be 5.0 µg/ml and 10 µg/ml, respectively (Table 6.2). These values are consistent with the MIC results, which indicated that *E. coli* was the most susceptible.

3.3 Morphological and molecular identification of fungal isolate

Morphological characterization was achieved by observing fungus colonies and conidia and molecular characterization by DNA extraction and amplification with sequence-specific primers. The leaf spots are fusiform or elliptical, initially brown-red, and subsequently brown with a light brown in the middle. Colonies of fungal isolate cultured on PDA attain a diameter of 70–80 mm in 7 days, with sparse aerial mycelium and fimbriate margins. The surface is characterized by pale mouse gray

zones and alternate grey olivaceous to olivaceous zones. The hyphae are transparent to light brown, with branches divided into segments (septate). Microscopical image of a fungal isolate illustrating conidia on the conidiophore (Figure 6.7). Conidiophores emerge individually or in clusters, with divisions, straight or bending, occasionally forming an attachment at the upper section. The cell walls of the conidiophores are thicker than those of the vegetative hyphae.

Molecular characteristics, such as gene sequences, can be employed to facilitate the reliable identification of *Curvularia* species and related species, in addition to the classic approach of morphological characterization. The ITS sequences exhibited a high percentage of similarity with the GenBank database, with a 98.23% similarity based on BLAST search. ITS sequences of the isolates were deposited into Genbank and the GenBank accession number for the nucleotide sequences is PP874630.

3.4 Antifungal Activity of *Mikania micrantha* silver nanoparticles against rice pathogen, *Curvularia pseudobrachyspora*.

3.4.1 Inhibition of Colony Growth

Silver nanoparticles showed a significant inhibitory effect on colony growth, as illustrated in Figure 6.8. The diameter of *C. pseudobrachyspora*, without any treatment of silver nanoparticles determined using the cross method, was 88.6 mm (Figure 6.9). At a concentration of 50 µg/ml, the silver nanoparticles exhibited their smallest diameter, measuring 15.35 mm. As the concentration of silver nanoparticles increased, the diameter gradually decreased (Figure 6.10).

3.4.2 Estimation of fungal Biomass

Biomass of *C. pseudobrachyspora* treated with different concentrations of AgNPs (50, 25, and 12.5 µg/ml) and control group was determined by measuring the initial and final weight of the filter paper. Our observation revealed that the control group exhibited the greatest biomass, while minimal growth was found in the group treated with 50 µg/ml of AgNPs (Figure 6.11). The growth of fungal mycelia was also significantly affected by the 25 µg/ml

AgNPs treatment, which was followed by the 12.5 µg/ml treatment. The addition of progressively larger quantities of AgNPs reduced mycelia growth to a greater extent, revealing a consistent trend of biomass decrease.

3.5 Antifungal Activity of *Acmella ciliata* silver nanoparticles against rice pathogen, *Curvularia pseudobrachyspora*

3.5.1 Inhibition of Colony Growth

Fungal growth was assessed by measured colony area on PDA in treated and control groups. The biosynthesized silver nanoparticles exhibit a notable inhibitory effect on the growth of *C. pseudobrachyspora* colonies, as shown in the Figure 6.12. The fungal growth diameter, without any treatment of AgNPs, was 88.6 mm where at the highest concentration, exhibited their smallest diameter, measuring 12.21 mm. The diameter of fungal growth gradually decreased in a concentration dependent manner (Figure 6.13).

3.5.2 Estimation of fungal Biomass

The effect of AgNPs on *C. pseudobrachyspora* was assessed by measuring the dry weight of fungal mycelia cultured in liquid broth containing varying concentrations of AgNPs (50, 25, and 12.5 µg/ml) along with a control group. Our observation showed that the control group had the highest biomass, while the group treated with 50 µg/ml AgNPs showed little or no growth (Figure 6.14). The 25 µg/ml treatment of AgNPs had considerable effects on the proliferation of fungal mycelia, which was then followed by the 12.5 µg/ml treatment. The gradual increase in AgNPs resulted in an increasingly significant inhibition of mycelia growth, indicating a consistent pattern of biomass reduction.

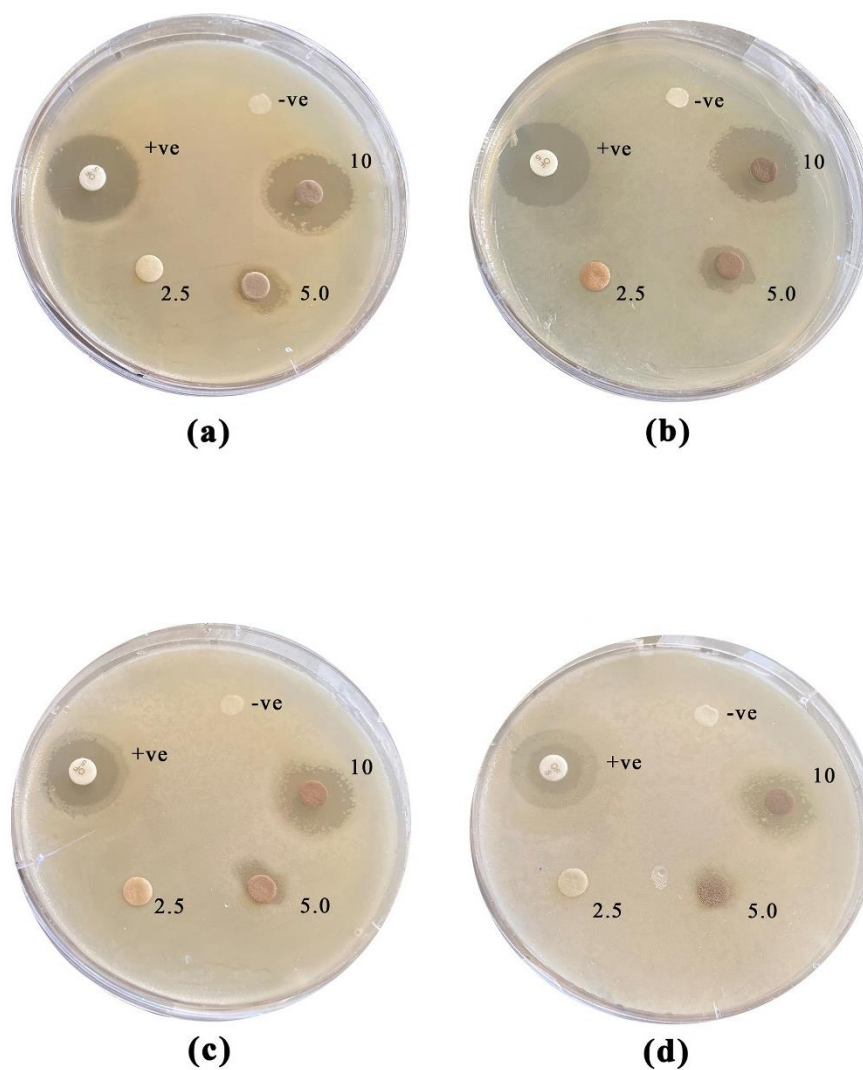


Figure 6.1: Antibacterial activity as determined by the decrease in zone of inhibition after treatment with different concentration of AgNPs (2.5, 5.0 and 10 µg/ml) using *M. micrantha* leaf extract and Ofloxacin (30 µg/ml) against (a) *E. coli*, (b) *P. aeruginosa*, (c) *B. subtilis* and (d) *S. aureus*.

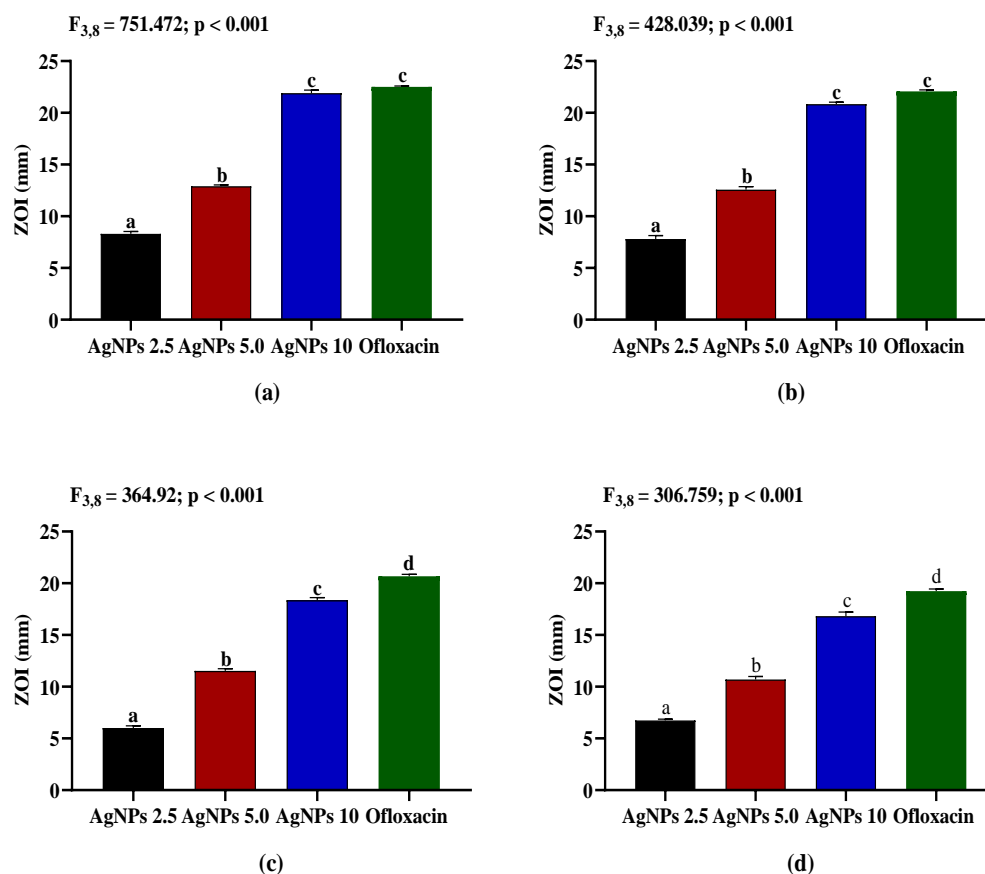


Figure 6.2: Antibacterial activity of different concentration of AgNPs (2.5, 5.0 and 10 µg/ml) using *M. micrantha* leaf extract and Ofloxacin (30 µg/ml) against (a) *E. coli*, (b) *P. aeruginosa*, (c) *B. subtilis* and (d) *S. aureus*.

Table 6.1. Determination of the Minimum Inhibitory Concentration (MIC) and Minimum Bactericidal concentration (MBC) values of different concentration of AgNPs against pathogenic bacteria. All values are expressed in $\mu\text{g/ml}$. Different letters indicate significant variation.

Bacteria	MIC	MBC
<i>B. subtilis</i>	5.0 ± 0.05^a	10 ± 0.02^a
<i>S. aureus</i>	5.0 ± 0.03^a	10 ± 0.07^a
<i>E. coli</i>	2.5 ± 0.03^b	5.0 ± 0.04^b
<i>P. aeruginosa</i>	5.0 ± 0.01^a	10 ± 0.04^a

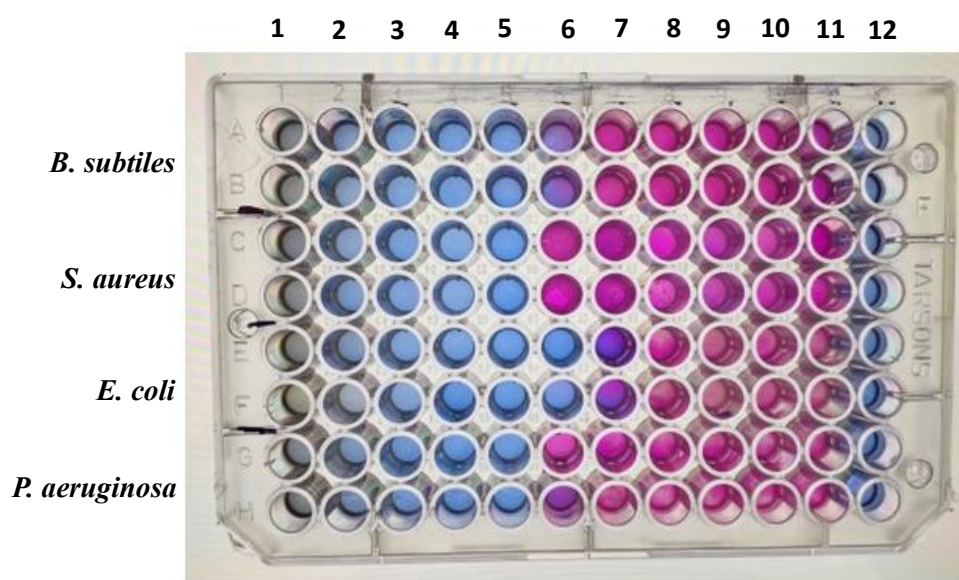


Figure 6.3: Determination of MIC for of different concentration of AgNPs using *M. micrantha* leaf extract against pathogenic bacteria. Column 12 confirms no contamination occurred while preparing the plate. Column 11, a negative control shows a change of resazurin natural colour (blue/purple) to the reduced form (pink). The highest concentration incorporated into the plate is $80 \mu\text{g/ml}$ and the lowest achieved through double serial dilution is $0.156 \mu\text{g/ml}$.

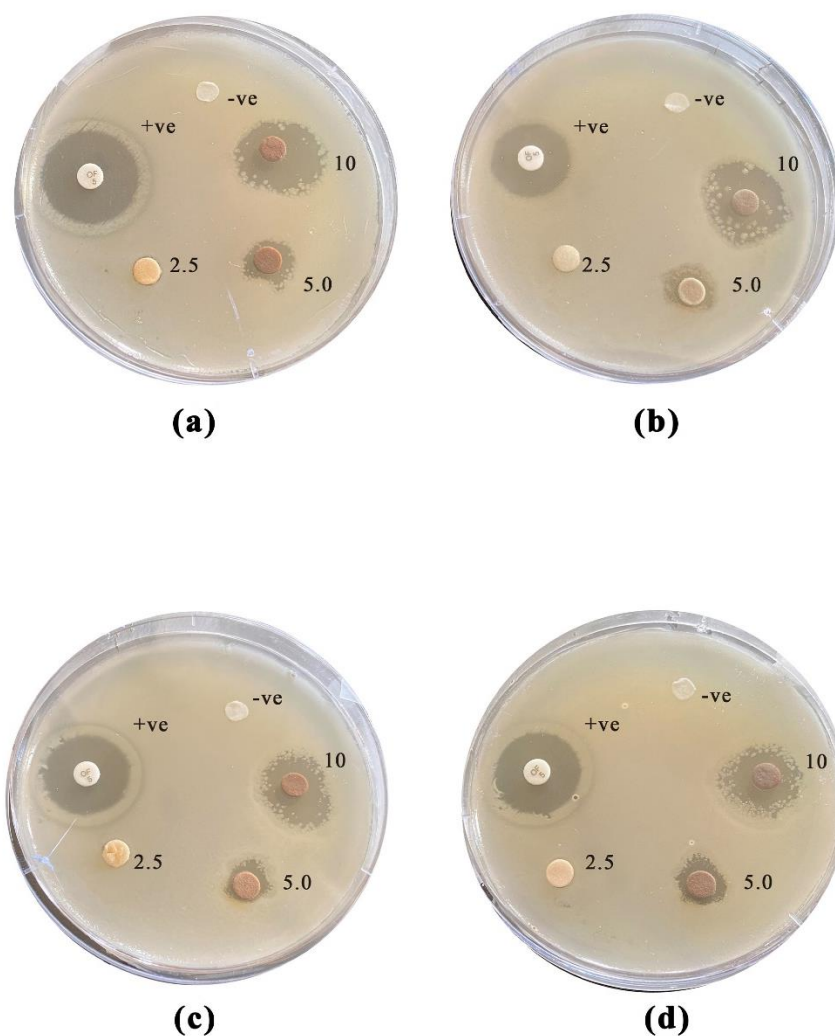


Figure 6.4: Antibacterial activity as determined by the decrease in zone of inhibition after treatment with different concentration of AgNPs (2.5, 5.0 and 10 µg/ml) using *A. ciliata* leaf extract and Ofloxacin (30 µg/ml) against (a) *E. coli*, (b) *P. aeruginosa*, (c) *B. subtilis* and (d) *S. aureus*.

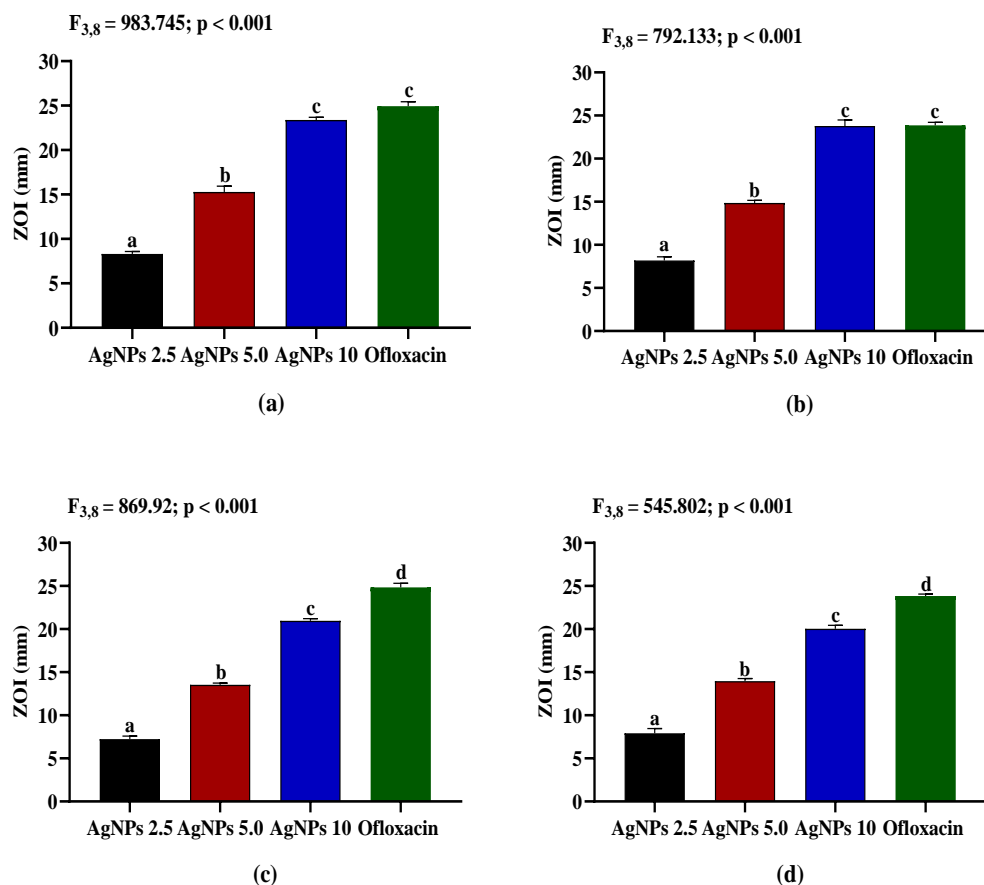


Figure 6.5: Antibacterial activity of different concentration of AgNPs (2.5, 5.0 and 10 µg/ml) using *A. ciliata* leaf extract and Ofloxacin (30 µg/ml) against (a) *E. coli*, (b) *P. aeruginosa*, (c) *B. subtilis* and (d) *S. aureus*.

Table 6.2. Determination of Minimum Inhibitory Concentration (MIC) and Minimum Bactericidal concentration (MBC) values of different concentration of AgNPs against pathogenic bacteria. All values are expressed in $\mu\text{g/ml}$. Different letters indicate significant variation.

Bacteria	MIC	MBC
<i>B. subtilis</i>	2.5 ± 0.08^a	5 ± 0.03^a
<i>S. aureus</i>	5.0 ± 0.01^b	10 ± 0.05^b
<i>E. coli</i>	1.25 ± 0.08^c	2.5 ± 0.01^c
<i>P. aeruginosa</i>	2.5 ± 0.03^a	5 ± 0.02^a

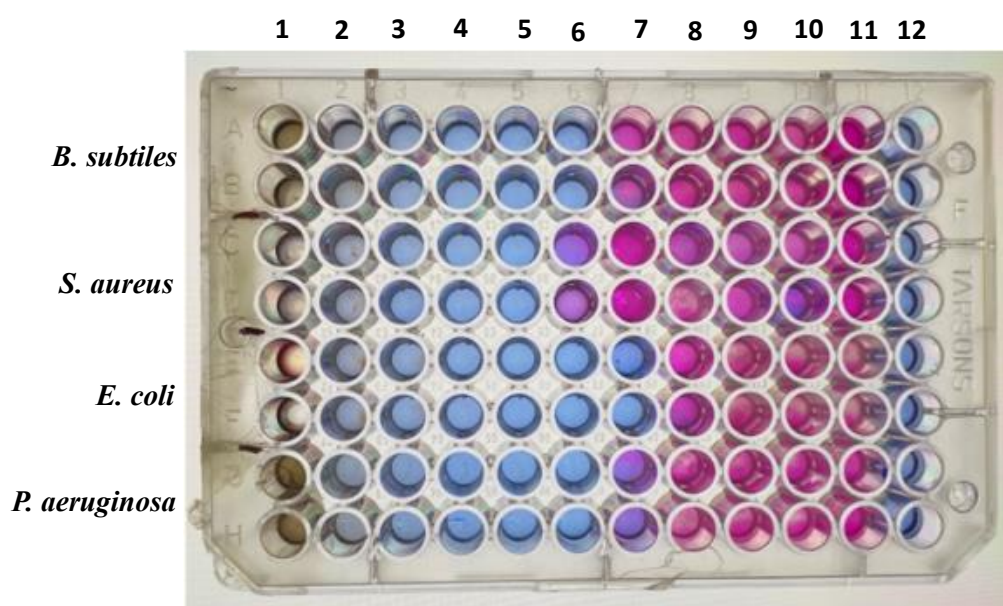


Figure 6.6: Determination of MIC for of different concentration of AgNPs using *A. ciliata* leaf extract against pathogenic bacteria. Column 12 confirms no contamination occurred while preparing the plate. Column 11, a negative control shows a change of resazurin natural colour (blue/purple) to the reduced form (pink). The highest concentration incorporated into the plate is $80 \mu\text{g/ml}$ and the lowest achieved through double serial dilution is $0.156 \mu\text{g/ml}$.

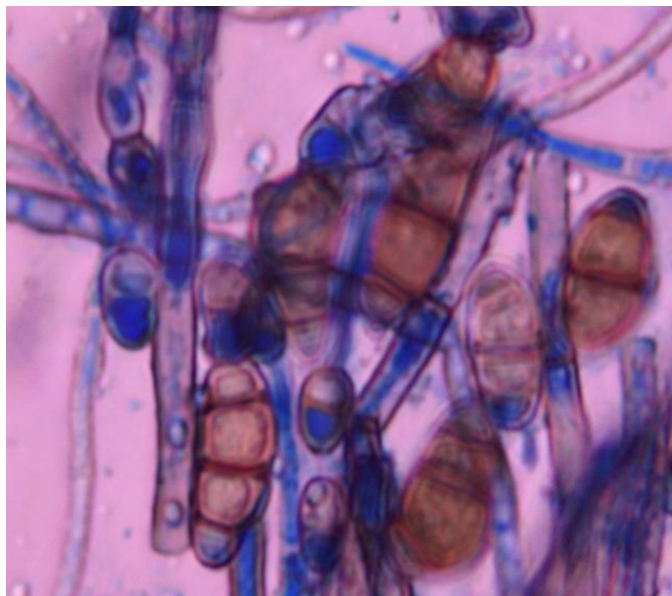


Figure 6.7: Microscopic view of rice pathogen (*Curvularia pseudobrachyspora*) showing conidia on the conidiophore

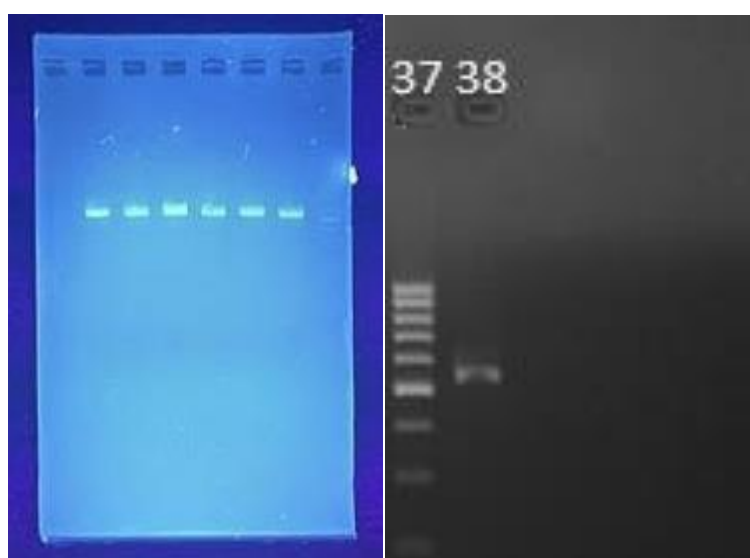


Figure 6.8: Band showing PCR amplification using ITS region of fungal isolate (*Curvularia pseudobrachyspora*).

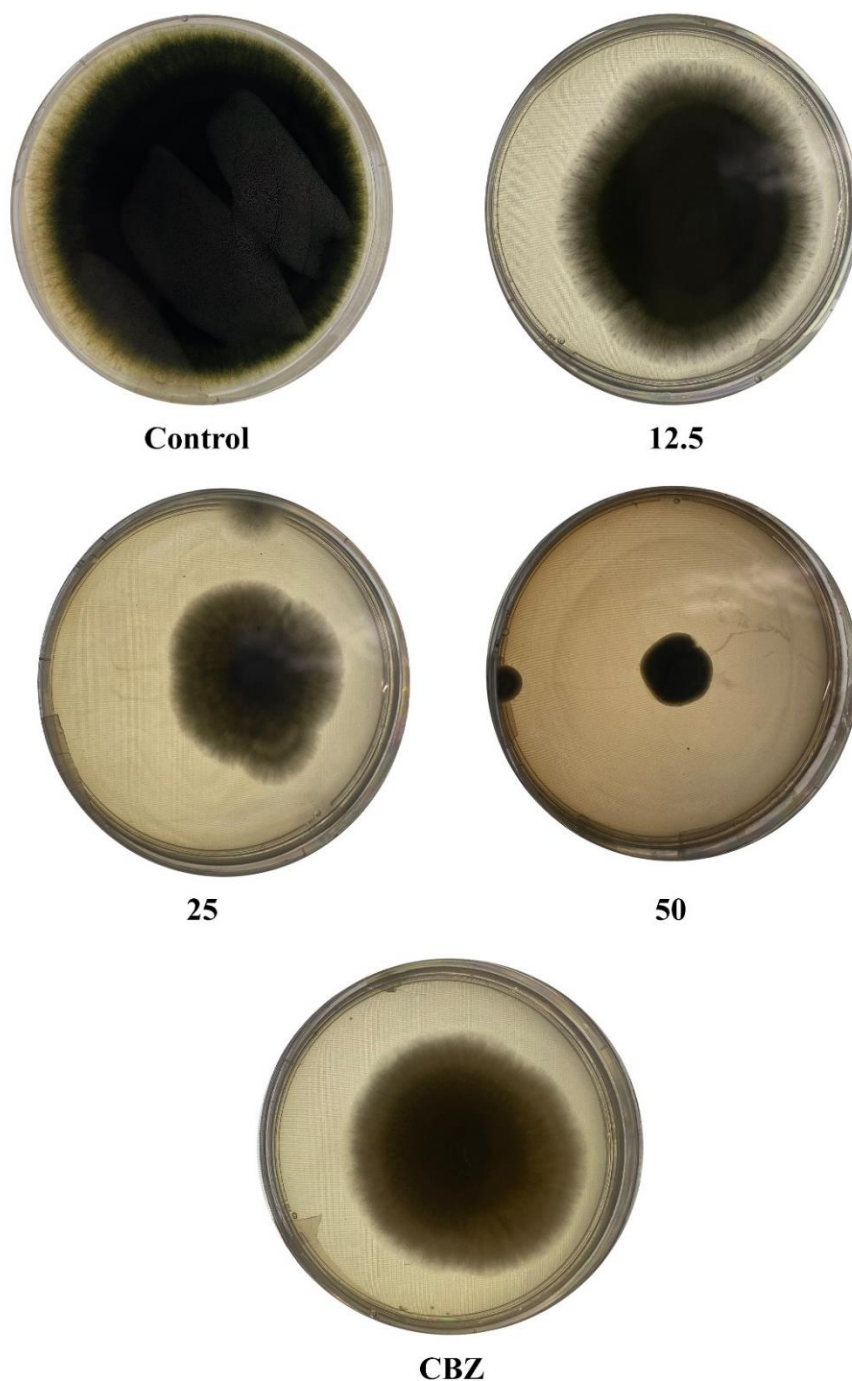


Figure 6.9: Inhibition of the colony growth of *C. pseudobrachyspora* mediated by AgNPs using *M. micrantha* leaf extract. Control: fungal culture without treatment; AgNPs 12.5, AgNPs 25 and AgNPs 50: fungal culture treated with 12.5, 25 and 50 $\mu\text{g/ml}$ of AgNPs respectively; CBZ: fungal culture treated with 200 $\mu\text{g/ml}$ of Carbendazim (positive control).

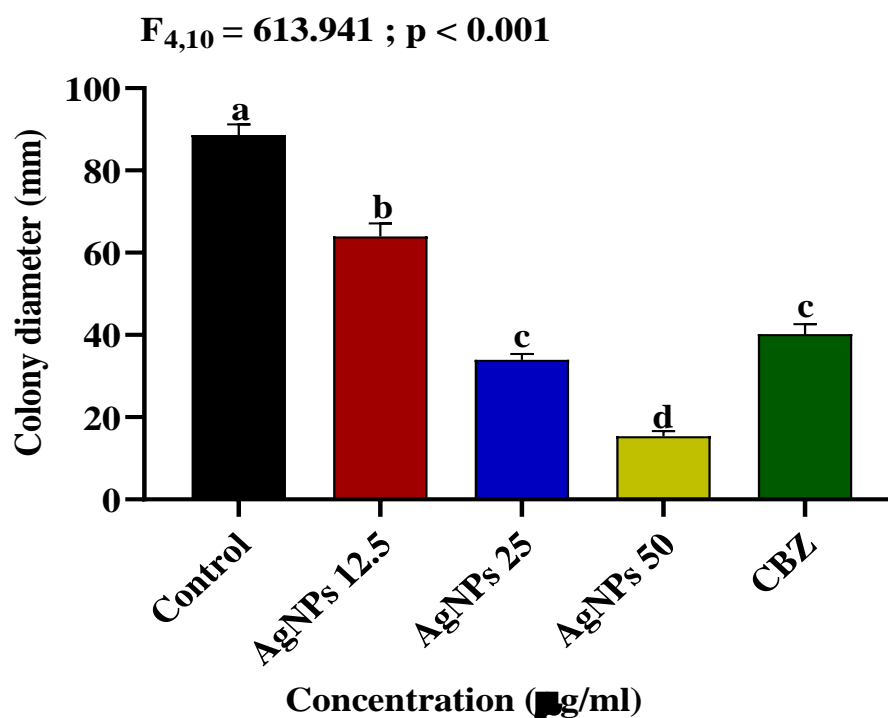


Figure 6.10: Effect of AgNPs on the colony growth of *C. pseudobrachyspora*. Control: fungal culture without treatment; AgNPs 12.5, AgNPs 25 and AgNPs 50: fungal culture treated with 12.5, 25 and 50 µg/ml of AgNPs respectively; CBZ: fungal culture treated with 200 µg/ml of Carbendazim (positive control). Values are expressed as Mean ± SEM. Different letters indicate significant variation.

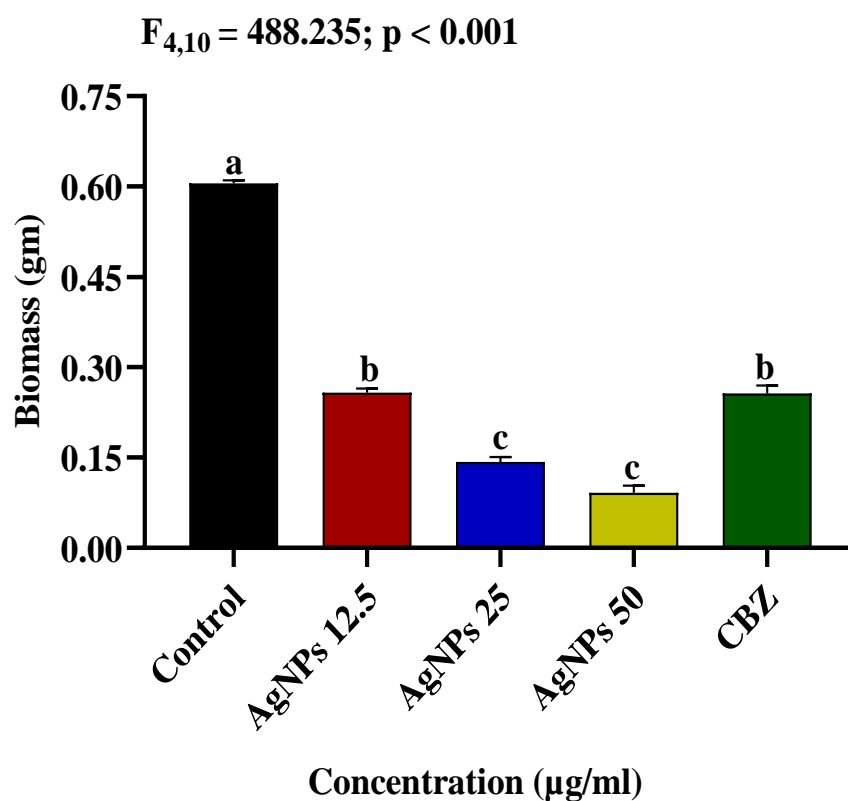


Figure 6.11: Effect of AgNPs on the biomass of *C. pseudobrachyspora*. Control: fungal culture without treatment; AgNPs 12.5, AgNPs 25 and AgNPs 50: fungal culture treated with 12.5, 25 and 50 $\mu\text{g/ml}$ of AgNPs respectively; CBZ: fungal culture treated with 200 $\mu\text{g/ml}$ of Carbendazim (positive control). Values are expressed as Mean \pm SEM. Different letters indicate significant variation.

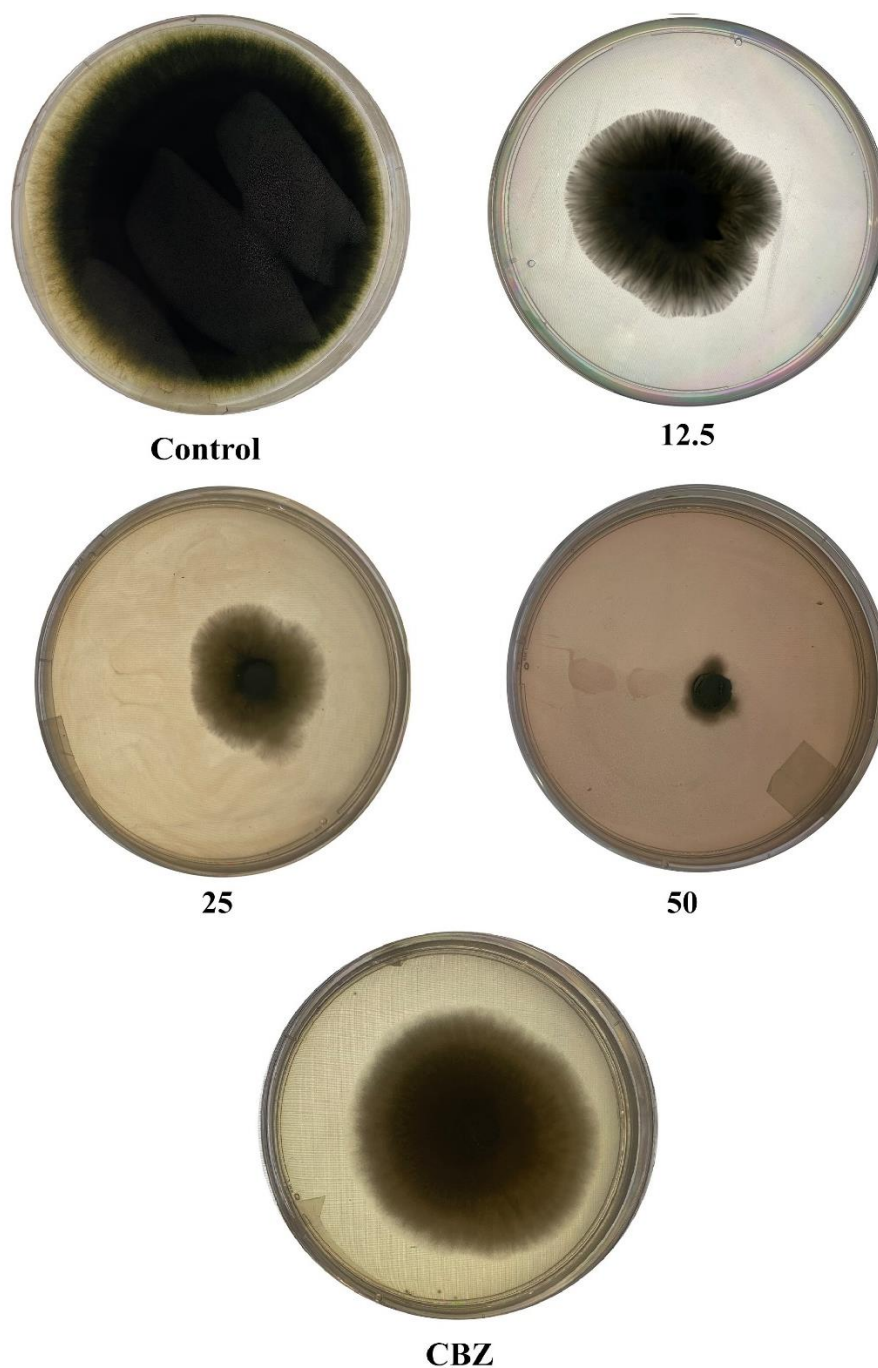


Figure 6.12: Inhibition of the colony growth of *C. pseudobrachyspora* mediated by AgNPs using *A. ciliata* leaf extract. Control: fungal culture without treatment; AgNPs 12.5, AgNPs 25 and AgNPs 50: fungal culture treated with 12.5, 25 and 50 $\mu\text{g/ml}$ of AgNPs respectively; CBZ: fungal culture treated with 200 $\mu\text{g/ml}$ of Carbendazim (positive control).

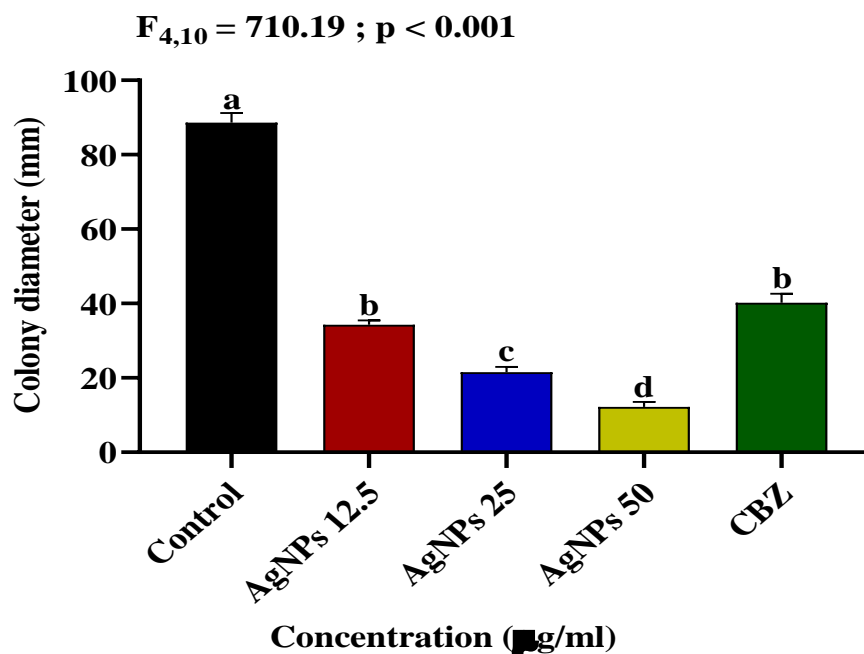


Figure 6.13: Effect of AgNPs on the colony growth of *C. pseudobrachyspora*. Control: fungal culture without treatment; AgNPs 12.5, AgNPs 25 and AgNPs 50: fungal culture treated with 12.5, 25 and 50 µg/ml of AgNPs respectively; CBZ: fungal culture treated with 200 µg/ml of Carbendazim (positive control). Values are expressed as Mean \pm SEM. Different letters indicate significant variation.

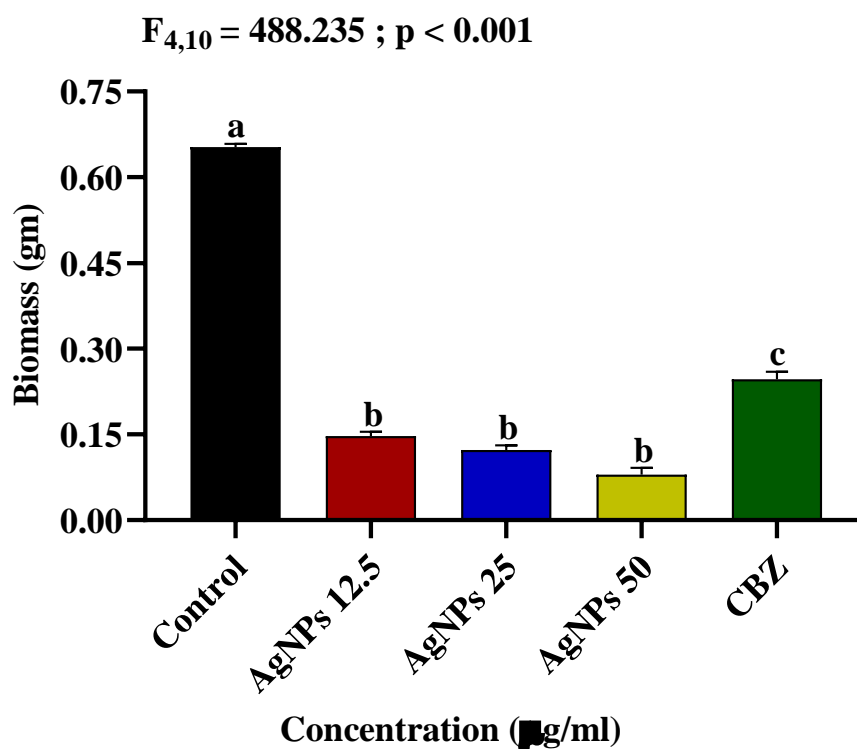


Figure 6.14: Effect of AgNPs on the biomass of *C. pseudobrachyspora*. Control: fungal culture without treatment; AgNPs 12.5, AgNPs 25 and AgNPs 50: fungal culture treated with 12.5, 25 and 50 $\mu\text{g/ml}$ of AgNPs respectively; CBZ: fungal culture treated with 200 $\mu\text{g/ml}$ of fungicide (positive control). Values are expressed as Mean \pm SEM. Different letters indicate significant variation.

4. Discussion

The most effective metallic nanoparticles against bacteria and other pathogens have been reported to be AgNPs, in addition to being extremely biocompatible and simple to use in medical applications. The disc diffusion method demonstrated the antibacterial activity of silver nanoparticles by forming an inhibitory zone. According to our results, *Mikania micrantha* silver nanoparticles (MNP) demonstrated the highest antibacterial efficacy against *E. coli* (21.9 mm), followed by *P. aeruginosa* (20.84 mm), *B. subtilis* (18.36 mm), and *S. aureus* (16.82 mm) when administered at a concentration of 10 µg/ml. On the other hand, *Acmella ciliata* silver nanoparticles (ANP) exhibited the most effective antibacterial activity against *P. aeruginosa* (23.79 mm), *E. coli* (23.39 mm), *B. subtilis* (20.96 mm), and *S. aureus* (20.04 mm) at the same concentration of 10 µg/ml. The antibacterial activity of MNP and ANP at a concentration of 10 µg/ml was comparable to that of standard antibiotics (Ofloxacin, 30 µg/ml). Therefore, AgNPs could be proposed as an alternative to antibiotics since numerous mechanisms of action would need to be targeted for the bacterium to become resistant to AgNPs (Bruna *et al.*, 2021). This finding is consistent with previous studies that demonstrated the presence of an inhibitory zone caused by AgNPs against pathogenic microorganisms (Awwad *et al.*, 2013; Bar *et al.*, 2009). Our study indicated that AgNPs offer an excellent alternative for creating novel bactericidal agents for infection treatments since antibiotic-resistant pathogens are a worldwide concern. Multidrug-resistant strains are created as a result of adaptive resistance driven by the formation of biofilm and quorum sensing systems during bacterial development (de Brito *et al.*, 2022). Chronic disease status and high morbidity and mortality are caused by the infection and dissemination of resistant microorganisms. Previous study suggest that AgNPs may adhere to the surface of the cell membrane, interfering with its permeability, osmoregulation, electron transport and respiration processes due to their high surface area-to-volume ratio and unique physical and chemical properties providing better contact with cell wall of microorganisms (Ronavari *et al.*, 2021). It has also been reported that AgNPs display their antibacterial activities by adhering to or penetrating bacterial cell walls and then altering cellular communication by dephosphorylating potential critical peptide

substrates on tyrosine residues (More *et al.*, 2023). The fact that gram-positive bacteria's cell wall is made up of multiple, hard layers of peptidoglycan, which prevents AgNPs from penetrating the cell wall, could be the reason for the present study's substantially better efficacy of biosynthesized AgNPs against gram-negative bacteria ((Dong *et al.*, 2017). Although, it might be assumed that leaf extract of *M. micrantha* and *A. ciliata* possesses antibacterial properties, the plant extract alone exhibited no antibacterial activity due to its extraction medium and lower concentration during the experiment.

In this study, we successfully produced nanoparticles with an average size ranging from 5 to 40 nm, which exhibited significant antibacterial activity. MNP exhibited the lowest minimum inhibitory concentration (MIC) against *E. coli* (2.5 µg/ml), followed by *P. aeruginosa* (5.0 µg/ml), *B. subtilis* (5.0 µg/ml), and *S. aureus* (5.0 µg/ml). Similarly, ANP showed the lowest MIC against *E. coli* (1.25 µg/ml), followed by *P. aeruginosa* (2.5 µg/ml), *B. subtilis* (2.5 µg/ml), and *S. aureus* (5.0 µg/ml). A decreased MIC for the studied bacterial strains suggests an increased level of inhibition activity. Additionally, we determined the minimum bactericidal concentration (MBC) by culturing diluted samples of the MIC on sterile agar plates and identifying the AgNPs concentrations at which no apparent growth occurred. The results showed that the MBC of MNP and ANP was 2-fold higher than the MIC. The incorporation of AgNPs inhibits the growth of pathogenic bacteria by damaging their cell membrane and causing leakage of cytoplasm, ultimately resulting in bacterial death. The existing research primarily supports three pathways that AgNPs exhibit their antibacterial effect through, either jointly or independently (Marambio-Jones and Hoek, 2010; Qing *et al.*, 2018; Dakal *et al.*, 2016). The first theory states that AgNPs can penetrate the outer membrane and accumulate in the inner membrane, where their adhesion to the cell destabilizes and damages it, enhancing membrane permeability and causing cellular leakage and death (Seong *et al.*, 2017). The second mechanism suggests that nanoparticles have the ability to disrupt and penetrate the cell membrane, causing changes in its structure and permeability. Additionally, these nanoparticles can enter the cell and interact with sulfur or phosphorus groups found in intracellular components like DNA and proteins, thereby modifying their structure and functions (Krishnamoorthy *et al.*, 2012). The discharge of silver

ions from the nanoparticles is the third mechanism that occurs in conjunction with the other two. These ions, which are able to interact with cellular components due to their size and charge, can alter metabolic pathways, membranes, and, in some instances, genetic material (Quinteros *et al.*, 2016; Agnihotri *et al.*, 2013). Smaller nanoparticles possess a greater surface area, which is the most critical characteristic that influences antimicrobial activity. Consequently, they are capable of generating a greater bactericidal effect and a higher interaction area than larger particles (Raza *et al.*, 2016). Research has demonstrated that decreasing the size of nanoparticles improves their efficacy in eradicating bacteria. This is because smaller nanoparticles can easily adhere to the cell membrane, causing damage and increasing membrane permeability, ultimately leading to cell death (Li *et al.* 2013; Yacaman *et al.*, 2001). Furthermore, apart from size, shape was also found to influence the antibacterial efficacy of silver nanoparticles. Helmlinger *et al.* (2018) conducted comprehensive studies on the impact of shape on antibacterial activity and synthesized five distinct types of AgNPs that exhibited exceptional uniformity in both shape and size. The underlying cause of this shape-dependent antibacterial activity is closely linked to the specific surface area and rate of dissolution. Consequently, the antibacterial activity of variously shaped AgNPs is primarily attributed to the formation of Ag^+ ions on the surface, which is consistent with the size-dependent antibacterial activity.

Observing fungus colonies and conidia provided morphological characterization, while DNA extraction and amplification using sequence-specific primers provided molecular characterisation. The occurrence of leaf spot symptoms in rice is widespread in rice-growing regions worldwide (Dela Paz *et al.*, 2006). The symptoms varied in size, ranging from minor to severe lesions, which resulted in chlorotic and necrotic damage to the leaves. The morphological characteristics indicate that conidiophores can emerge either singly or in groups, showing divisions and occasionally creating a connection at the upper part, resembling the typical features of *Curvularia pseudobrachyspora* as described by Wang *et al.* (2018). The ITS sequences showed a significant degree of similarity to the GenBank database, with a 98.23% similarity as determined by a BLAST search.

The utilization of nanoparticles, particularly metal nanoparticles, in combating phytopathogens is a recently emerged area of research. Incorporating these

compounds into plant disease management could reduce long-term dependence on chemical pesticides and address issues such as environmental contamination, pesticide residue, and fungicide resistance. According to Ivask *et al.* (2014), the size, morphology, dispersity, and purity of silver nanoparticles may directly correlate with their antimicrobial activity. The biosynthesized MNP and ANP demonstrate a significant inhibitory effect on the growth of *C. pseudobrachyspora* colonies, which occur in a dose-dependent manner. When compared to the untreated control (88.6 mm), the fungal growth diameters of MNP and ANP at the highest concentration were 15.35 mm and 12.21 mm, respectively, revealing a notable antifungal effect against *C. pseudobrachyspora*. AgNPs at the concentration of 50 µg/ml significantly inhibited the growth of *C. pseudobrachyspora* colonies, as evidenced by the decreased biomass and colony growth when compared to the fungicide carbendazim (200 µg/ml). Our findings suggested that the spherical AgNPs exhibited potent antifungal activity in comparison to commercially available antifungal agents, as reported by various authors (Matras *et al.*, 2022; Mussin and Giusiano, 2022; Hashem *et al.*, 2022).

The antifungal activity is likely strongly associated with its reduced size and altered shape, resulting in an increased surface area that enhances its antifungal action. Nasrollahi *et al.* (2011) indicate that one potential mechanism of action of AgNPs against fungi involves the penetration of NPs into the cell membrane and subsequent impact on the respiratory chain, leading to cell death. In addition, NPs engage with fungal proteins, resulting in protein inactivation and direct contact with DNA. As a result, the contact mechanism leads to mutation and prevents DNA replication (Mikhailova, 2021). Further, the small dimensions of NPs facilitate their penetration into the cell wall, leading to their accumulation in the cell membrane and subsequent cell lysis. NPs can penetrate fungal spores via cell membranes, creating an electron-light zone with DNA molecules and NPs inside the cell (Sandhu *et al.*, 2024). Following this, nanoparticles disrupt the respiration process and ultimately halt cell division, resulting in cell death (Malathi *et al.*, 2014). As a result, we urge the effective use of these nanoparticles in many biomedical applications, as well as industrial and therapeutic purposes, due to their stable nature and antimicrobial properties. In this regard, the synthesized metal nanoparticles can be utilized as a potent fungicide in the agriculture sector to manage phytopathogenic fungi in plants. Furthermore, more

research should concentrate on the parameters that affect their antifungal activity, including surface charge, aggregation behaviour, ultraviolet rays, and high temperature.

5. Conclusion

AgNPs are known for their remarkable antibacterial properties, and they currently serve as an exceptional antimicrobial agent. They address numerous criteria that are considered necessary for the efficacy of new antimicrobial technologies, including antimicrobial performance, rapid action, and low cytotoxicity. Additionally, nanoparticles can be modified to achieve selectivity and delivery to specific targets. Assessing the action of AgNPs in biological environments, as well as their interactions with other substances, will provide critical insights for the development of advanced technologies and nanomaterials capable of effectively preventing infections or selectively eradicating pathogenic bacteria. Size and coating factors influence the toxicity of AgNPs, and modifying their characteristics through functionalization can potentially mitigate or eliminate the cytotoxic effects associated with AgNPs exposure. Additionally, this functionalization can enhance the antibacterial activity and specificity of AgNPs.

Agricultural nanotechnology research and development is a very promising field, with active exploration of the potential of nanoparticles for the production of highly efficient products. Our findings validate the concept that silver nanoparticles are appropriate for developing novel fungicidal agents. The following study aims to investigate the broader use of AgNPs for managing *C. pseudobrachyspora* in agricultural settings, as well as assess the effectiveness of AgNPs against various diseases that pose a threat to rice cultivation. The utilization of plant extracts for the synthesis of AgNPs has numerous benefits, including environmental sustainability, compatibility with living organisms, and economic efficiency. Based on these distinctive characteristics, it may be inferred that AgNPs will play a crucial role in numerous nanotechnology processes.

Chapter 7

Anti-cancer activity of *Mikania micrantha* and *Acmella ciliata* silver nanoparticles against type-II human lung adenocarcinoma (A549) cells

1. Introduction

Green-mediated synthesis of nanoparticles has earned a promising role in the area of nanotechnology due to their biomedical applications in various fields such as diagnostics, biomarkers, cell labelling, antimicrobial agents, drug delivery, and cancer therapy (Al-Sheddi *et al.*, 2018). The intrinsic nature of nanoparticles and their unique physicochemical properties such as increased surface-volume ratios, the ability to absorb or carry other compounds and their efficiency of cell penetration make them ideal for many biological applications when compared to bulk materials (Fageria *et al.*, 2017). Silver nanoparticles (AgNPs) have garnered significant attention among a variety of nanomaterials due to their exceptional therapeutic potential, which includes anti-inflammatory, antimicrobial, and anticancer properties, as well as their chemical stability and conductivity (Austin *et al.*, 2014). Due to phytochemical components of plants that serve as a reducing and coating agent of nanoparticles as well as their eco-friendliness, affordability, and accessibility, plant extracts have gained significant interest among biomaterials as a nanomedicine. The diverse phytoconstituents in plants provide significant benefits, such as antibacterial, anticancer, and antioxidant properties; thus, plant-based green synthesis platforms are recommended as one of the ideal techniques for synthesizing metal nanoparticles (Chang *et al.*, 2021).

The uncontrolled growth and dissemination of abnormal cells are the hallmarks of cancer, a multifactorial disease that is the result of an intricate combination of genetic, environmental, internal, and external factors (Siegel *et al.*, 2015). It has been treated with a diverse array of treatments, such as radiation, immunotherapy, surgery, chemotherapy, hormone therapy, and targeted therapy. Although there have been significant research breakthroughs, the scientific community still faces a major challenge in combating cancer. Cancer has emerged as a highly alarming disease, with

a continuously increasing mortality rate on a global scale. An estimated 14 million more cases of cancer will occur by 2035, significantly impacting the global economy and society (Pilleron *et al.*, 2019). Treatment using cytotoxic medications, either alone or in conjunction with radiation, is a conventional approach that has not been highly effective in eradicating the disease. Tumor cells evade the impact of chemotherapy by acquiring an inherent or acquired susceptibility to the drugs. In addition, there is a significant psychological impact associated with the development of post-chemotherapy side effects, which can be extremely harmful to the patient and, in some cases, even fatal, leading to increased mortality rates (Holohan *et al.*, 2013).

Lung cancer contributes to the highest incidence of cancer-related deaths among various types of cancer (Schabath and Cote, 2019). Despite several advances in treatment regimes, controlling lung cancer mortality has become increasingly challenging. Lack of early detection, non-specific systemic drug distribution, lipophilic chemistry and high first-pass metabolism of existing chemotherapeutic drugs contribute to the limitations of cancer treatment thereby resulting in poor prognosis (Ioele *et al.*, 2022). Current therapeutic drugs are also associated with the development of resistance and undesirable side effects (Talib *et al.*, 2021). Therefore, there is a pressing requirement for the creation of more sophisticated, cutting-edge, and economical therapies that can effectively eradicate cancerous cells. Nanoparticles provide an intriguing substitute for traditional chemotherapy drugs. Because of their unique physical-chemical characteristics, AgNPs are getting more attention for cancer research, demonstrating inherent antiproliferative activity (Ahmed *et al.*, 2019). Nanoparticles possess a distinct capability to selectively target tumor tissues by exploiting the leaky blood vessels in these tissues, a phenomenon known as the increased permeability and retention (EPR) effect (Prabhakar *et al.*, 2013). This can augment the anticancer properties of the NPs if they possess inherent cytotoxicity or are employed as carriers for drug delivery. Anti-cancer research of AgNPs is still in its infancy, and the current findings are limited and ambiguous.

The introduction of nanoscale materials to cancer care has garnered substantial interest over the past ten years and recently, clinical studies using metal nanoparticle-based therapeutics have been established to treat cancer (Gavas *et al.*, 2021). It has been demonstrated in numerous in vitro and in vivo research studies that AgNPs have

the potential to inhibit the growth and viability of cancer cells through multiple pathways (Loutfy *et al.*, 2015). AgNPs can trigger apoptosis and necrosis by disrupting the ultrastructure of cancer cells and promoting the generation of reactive oxygen species (ROS) and DNA damage (Muhamad *et al.*, 2022). AgNPs can also induce apoptosis by modulating critical signaling pathways, including the hypoxia-inducible factor (HIF) pathway, and up- or down-regulating the expression of critical genes, such as p53 (Yuan *et al.*, 2018). Following exposure to AgNPs, numerous cancer cells undergo apoptosis and sub-G1 arrest (Yin *et al.*, 2022). In addition, AgNPs may reduce distant metastasis by inhibiting tumor cell migration and angiogenesis (Kitimu *et al.*, 2022). Therefore, Nanoparticles are potential platforms for therapeutically relevant drug development due to the cancer-specific targeting, the resulting reduced side-effects, and the enormous anti-cancer characteristics (Kovács *et al.*, 2022).

In the recent years, a wide range of scientific studies have documented the medicinal properties of *Mikania micrantha* and *Acmella ciliata* such as antibacterial, anti-inflammatory, anticancer, antidiabetic, antioxidant, anti-stress, its cytotoxic effects and wound-healing actions (Sheam *et al.*, 2020; Sharma *et al.*, 2022). Plant extracts have been shown to contain several groups of active compounds, including terpenoids, flavonoids, coumarins, diterpenes, sesquiterpene lactones, and sesquiterpenes which may be linked to their medicinal properties (Nayak *et al.*, 2017; Silveira *et al.*, 2016). Interestingly, the anticancer effects of plant extracts have been shown earlier using cancer cell lines and animal models. Aqueous extract of *M. micrantha* and *A. ciliata* inhibited cancer cell proliferation, cell cycle arrest, induction of apoptosis and inhibition of tumor growth (Dou *et al.*, 2014; Singh *et al.*, 2020). Although medicinal plant extracts show activities against pathogenic conditions and alteration of cellular functions, their activities are often augmented in green metallic nanoparticle form. With this view, we hypothesized that *M. micrantha* and *A. ciliata* activities may be enhanced by silver nanoparticles. Thus, aqueous leaf extracts of *M. micrantha* and *A. ciliata* were used as a bio-reducing agent of Ag^+ to Ag for the synthesis of silver nanoparticles. Using Type II human lung adenocarcinoma cell line A549 as our model, we tested the anticancer effects of biosynthesized AgNPs. With cancer being a global health issue affecting millions of lives, it is the need of the hour

to hunt for cancer treatment with high efficacy and less side effect and the green synthesized AgNPs may pose as an attractive agent.

2. Materials and methods

2.1 Chemicals and reagents

Eagle's Minimal Essential Medium (MEM), Trypsin-EDTA, fetal bovine serum (FBS), bovine serum albumin (BSA), 3-(4,5-dimethylthiazole-2-yl)-2, 5-diphenyl tetrazolium bromide (MTT), sodium bicarbonate, glutathione (GSH) reduced, Folin-ciocalteu's reagent, nicotinamide adenosine dinucleotide (NADH), nitroblue tetrazolium (NBT), n-butanol, thiobarbituric acid (TBA), potassium chloride (KCl), 5, 5' dithio 2-nitrobenzoic acid (DTNB), sodium chloride (NaCl), phenazine methosulphate (PMS), ethidium bromide, dimethyl sulfoxide (DMSO), 1-chloro-2,4 dinitrobenzene (CDNB) and Triton X-100 were purchased from HiMedia Laboratories Pvt. Ltd. (Mumbai, India). Ethylenediamine tetra-acetic acid (EDTA), L-Glutamine, agarose (low gelling temperature), phenol red, trichloroacetic acid (TCA), silver nitrate, Trizma base and Trizma hydrochloride were purchased from Sigma Chemical Co., Bangalore, India. Fluorouracil (5FU) was obtained from GLS Pharma Ltd. (Hyderabad, India). The remaining chemicals were purchased from Merck Specialities Pvt.

2.2 Cell lines and Culture.

Type II human lung adenocarcinoma cell line (A549 cells) was procured from the National Centre for Cell Sciences (NCCS), Pune, India. The cells were maintained in MEM supplemented with 10% FBS and 1% L-Glutamine in a humidified incubator with 5% CO₂ at 37° C (Eppendorf, Hamburg, Germany).

2.3 Cytotoxicity assay

The cytotoxicity of AgNPs was estimated by a 3-(4,5-dimethylthiazol-2-yl)-2,5 diphenyltetrazolium bromide (MTT) reduction assay (Mosmann, 1983). Briefly, 100 µl of MEM containing 1×10^4 cells were seeded into 96 well plates (Himedia Laboratories Pvt. Ltd., Mumbai, India). The cells were treated with different

concentrations of AgNPs (1-20 µg/ml) for 24 h, along with a control sample, after being allowed to adhere for 24 h at 37 °C and 5% CO₂. Drug-containing media were discarded and cells were rinsed in FBS-free media after the completion of treatments. Then, each well received 10 µl of MTT (5 mg/ml) and was incubated for a further 2 h at 37 °C in a CO₂ incubator. Following this, 100 µl of DMSO was used to dissolve the insoluble purple formazan crystals. After 30 min of incubation, the absorbance of the solution was measured at 560 nm using a microplate reader (Spectramax m2e, Molecular Devices). For each treatment, three independent experiments with three replicates were conducted. Cytotoxicity was expressed as inhibition (%) which was calculated by the formula given below:

$$\% \text{ Inhibition} = \frac{\text{Control} - \text{Treatment}}{\text{Control}} \times 100$$

2.4 Clonogenic Assay

The clonogenic assay was performed to determine the effect of AgNPs on the reproductive viability of A549 cells (Franken *et al.*, 2006). 200 cells were seeded into individual petri-dishes with 5 ml of media. Cells were treated with different concentrations of AgNPs (1.0, 2.5 and 5.0 µg/ml) or 5FU at the dose of 100 µg/ml (positive control) after being allowed to adhere for 24 h. Following a sterile 1X PBS wash, cells were cultured for an additional 11 days in a fresh medium. Colonies having more than 50 cells were counted using an inverted microscope after being stained with 1% crystal violet in methanol (w/v) for 30 min at room temperature. Plating efficiency (PE) and surviving fraction (SF) of A549 cells were calculated by the following formula:

$$PE = \frac{\text{Number of colonies} \times 100}{\text{Number of cells seeded}}$$

$$SF = \frac{\text{Number of colonies counted}}{\text{Number of cell seeded} \times \text{Mean plating efficiency (PE)}}$$

2.5 Cell morphology analysis by fluorescent staining (Apoptotic assay)

Acridine orange/Ethidium bromide (AO/EtBr) staining was performed to assess the ability of AgNPs to induce apoptosis. After 1×10^5 A549 cells were seeded in six-well plates containing 5 ml of media, cells were allowed to adhere overnight and treatment was given for 24 h with different concentrations of AgNPs (1-5 $\mu\text{g/ml}$) along with 5FU as positive control (100 $\mu\text{g/ml}$). Untreated controls were also maintained in the culture medium alone. Cells were washed with sterile 1X PBS following treatments and then detached with 1X trypsin EDTA. The pelleted cells were resuspended in 100 μl of FBS-free media. Acridine orange (100 $\mu\text{g/ml}$) and ethidium bromide (100 $\mu\text{g/ml}$) were added to a 25 μl cell solution and stained for 2 min in a ratio of 1:1. The morphology of apoptotic cells was then observed on a slide using a fluorescence microscope (Thermo Fisher Scientific, EVOS^R Fluorescence Imaging, AMEP-4615). The cationic dye acridine orange is a fluorescent nucleic acid that permeates both living and dead cells, intercalating in double-stranded DNA to turn the nucleus green. Only dead cells with compromised cytoplasmic membrane integrity may absorb ethidium bromide, which causes the nuclei to become yellowish-orange in color. For this reason, ethidium bromide-incorporated apoptotic cells show condensed and fragmented orange chromatin, in contrast to living cells, which have green nuclei. Conversely, necrotic cells have a structurally normal orange nucleus (Kasibhatla *et al.*, 2006). The apoptotic index of at least 300 cells was evaluated as follows:

$$\text{Apoptotic index (\%)} = \frac{\text{Number of apoptotic cell scored}}{\text{Total number of cells counted}} \times 100$$

2.6 Assessment of genotoxicity of AgNPs using Comet assay

The alkaline single cell gel electrophoresis (Comet assay) was carried out using standard method (Singh *et al.*, 1988) with minor modifications. Briefly, 1×10^5 A549 cells treated with different concentrations of AgNPs or 5FU for 24 h along with the untreated control were suspended in 0.5 % low-melting point agarose (75 μl) prepared in 1X PBS and spread onto a frosted slide precoated with 1% normal-melting point agarose. Slides were immersed for 2 h in freshly prepared lysing solution (2.5 M NaCl,

100 mM Na₂EDTA, 10 mM Trizma base, 1% Triton X-100 and 10% DMSO, pH 10). Following lysis, slides were placed in a horizontal electrophoresis tank containing freshly prepared alkaline electrophoresis buffer (300 mM NaOH, 1 mM Na₂EDTA, pH13) for 20 min to allow unwinding of DNA. Electrophoresis was then carried out for 30 min at 24 V and 300 mA and the slides were then neutralized by washing with neutralization buffer (0.4 M Tris-HCl, pH 7.5) for 5 min. Slides were washed with distilled water after neutralization and then stained with ethidium bromide (EtBr) solution (2 µg/ml) for 5 min. Each slide was prepared in triplicate and 100 randomly selected cells from each slide were examined using a fluorescence microscope (Thermo Fisher Scientific, EVOS^R Fluorescence Imaging, AMEP-4615) with a magnification of 200x. The images captured were analysed with Image J software.

2.7 Antioxidant assays

2.5×10⁶ cells were seeded in a T-25 flask with 5 ml of medium for the assessment of antioxidant enzyme activities and the level of lipid peroxidation. After 24 h of AgNPs or 5FU treatments, the drug-containing medium was discarded and the cells were harvested after being washed in sterile 1XPBS. The cells were pelleted, sonicated (PCI Analytics Pvt. Ltd., Mumbai, India), and a 5% homogenate was prepared in cold sterile PBS (pH-7.4) for biochemical assays. Total protein contents were determined using the standard protocol (Lowry *et al.*, 1951) using bovine serum albumin as standard.

Glutathione (GSH) levels were assessed using the standard method (Moron *et al.*, 1979). Briefly, the cell homogenate (80 µl) was incubated with 0.02M sodium phosphate buffer (900 µl) and 10 mM DTNB (20 µl) for 2 min at room temperature. A mixture devoid of tissue lysates served as blank. The absorbance of the sample was taken against blank at 412 nm in a UV-visible spectrophotometer (SW 3.5.1.0. Biospectrometer, Eppendorf India Ltd., Chennai). GSH concentration was calculated from the standard graph and expressed in µmol/mg protein.

Glutathione-s-transferase (GST) was measured using the standard method (Beutler, 1984). Briefly, 5 mM CDNB (50 µl) was mixed with 0.1M phosphate buffer (850 µl, pH 6.5) and incubated at 37 °C for 10 min. Then, 50 µl each of 20 mM GSH

and cell homogenate was added to the mixture. A mixture devoid of tissue lysates served as blank. The absorbance was measured at 1 min interval for 5 min at 340 nm. GST activity was expressed as Unit/mg protein. GST activity was measured as:

$$GST\ Activity = \frac{OD\ of\ test - OD\ of\ blank}{9.6 \times volume\ of\ test\ sample} \times 1000$$

where, 9.6 is the molar extinction coefficient for GST.

The activity of superoxide dismutase activity was estimated by the NBT reduction method (Fried, 1975). Briefly, cell homogenate (100 μ l) and 186 μ M PMS (100 μ l) was mixed with 3 mM NBT (300 μ l) and 780 μ M NADH (200 μ l). The mixture was incubated at 30 °C for 90 sec and the reaction was stopped by adding 1 ml of acetic acid and 4 ml of n-butanol. A mixture devoid of tissue lysates served as blank. The absorbance was measured at 560 nm and the enzyme activity was expressed in unit (1unit = 50% inhibition of NBT reduction)/mg protein.

$$\% inhibition = \frac{OD\ of\ blank - OD\ of\ sample}{OD\ of\ blank} \times 1000$$

Lipid peroxidation (LPO) assay: Lipid peroxidation (LPO) was estimated using standard method (Buege and Aust, 1978). Briefly, 10% TCA, 0.8% TBA and 0.02 N HCl were mixed with cell homogenate in 1:2 ratio. After boiling for 10 min, the mixture was cooled immediately and centrifuged at 12000 rpm for 10 min. The absorbance of supernatant was taken at 535 nm against blank. A mixture devoid of tissue lysates served as blank. The MDA concentration of the sample was calculated using the extinction coefficient of $1.56 \times 10^6\ M^{-1}cm^{-1}$

2.8 qRT-PCR analysis of pro-apoptotic and anti-apoptotic gene expression

Briefly, 3×10^6 A549 cells were seeded in T-25 flask with 5 ml media. After an overnight adherence, cells were treated with 2.5 μ g/ml AgNPs or 5FU for 24 h along with a control sample. Cells were washed and harvested following treatments. Total RNA was extracted from the pelleted cells using Tri reagent (BR Biochem, Life Science Pvt. Ltd, R1022). Extracted RNA was quantified using Nanodrop Spectrophotometer (Eppendorf Biophotometer Plus, Hamburg, Germany) and an RQ1

DNase kit (Promega, M198A, Madison, WI, USA) was used to remove the genomic contamination. 3 µg of total RNA was used to synthesize cDNA with a first-strand cDNA synthesis kit (Thermo scientific, K1621; Lithuania, Europe). Gene-specific primers were designed using Primer 3, Boston, MA, USA. qPCR was performed using Quant-Studio 5 (ThermoFisher Scientific, Foster City, CA, USA). 1 µl of cDNA, 1 µl of gene-specific forward and reverse primers, 1 µl of nuclease-free water (ThermoFisher Scientific, A19938, Bangalore, India) and 3 µl of PowerUp™ SYBR™ Green Master Mix (Thermo Fisher Scientific, A25742, Lithuania, Europe) constitute a 7 µl PCR reaction volume for each gene. The cycling condition of qPCR was 1 cycle at 95 °C (20 s), 35 cycles at 95 °C (01 s), 60 °C (20 s), and 95 °C (01 s), additional melt curve plot step included 1 cycle of 60 °C (20 s) and 1 cycle of 95 °C (01 s). Melting curves were subsequently generated to confirm a single uniform peak. For the purpose of determining the relative expression levels of specific target genes, the GAPDH gene was selected as a reference gene. Each sample was run in duplicate along with non-template and negative RT controls. The relative expression of genes was determined using the $\Delta\Delta C_t$ method (Livak and Schmittgen, 2001).

Table 7.1. Primer sequences and their product size used in the qRT-PCR analysis of A549 cells treated with AgNPs.

Gene	Forward Primer	Reverse Primer
<i>P53</i>	GTTCCGAGAGCTGAATGAG	TCTGAGTCAGGCCCTTCTGT
<i>Bax</i>	TCCCCCGAGAGGTCTTTT	CGGCCCCAGTTGAAGTTG
<i>Bid</i>	CCTTGCTCCGTGATGTCTTC	GTAGGTGCGTAGGTTCTGGT
<i>Apaf-1</i>	AAGGTGGAGTACCACAGAG	TCCATGTATGGTGACCCATCC
<i>Bcl-2</i>	GGATGCCTTTGTGGAAGTGT	AGCCTGCAGCTTTGTTTCAT
<i>Bcl-xl</i>	GGCCACTTACCTGAATGAC	AAGAGTGAGCCCAGCAGAAC
<i>Survivin</i>	AGAACTGGCCCTTCTTGGAG	CTTTTATGTTCTCTATGGTC
<i>PARP</i>	CCAGATGCTTGTCTTCCTGG	AGTGACAGCAGGGTTGGCATA
<i>GAPDH</i>	GAGTCAACGGATTTGGTCT	GACAAGCTTCCCGTTCTCAG

2.9 Caspase-3/6 activity assay

A quantitative enzymatic activity assay for caspase 3 and caspase 6 was performed in accordance with the manufacturer's protocols (BioVision Incorporated, USA). Briefly, 2×10^6 A549 cells were treated with 2.5 $\mu\text{g/ml}$ AgNPs or 5FU for 24 h in T-25 flask with 5 ml of medium along with the untreated control. Following treatment, cells were washed and lysed in 50 μl of chilled lysis solution, followed by a 10 min incubation on ice. The cell lysates were centrifuged at $15,000 \times g$ for 1 min at 4 °C, and the supernatant was collected. The total amount of protein was estimated using the Bradford assay (Bradford, 1976). The assay was performed in a total volume of 100 μl in 96-well plates. 150 μg of protein from each sample was assayed for caspase-3/6 activity against their specific colorimetric substrate DEVD-*p*NA for caspase-3, and VEID-*p*NA for caspase-6. The mixture was incubated for another 2 h at 37 °C and the absorbance of free *p*-nitroanilide (*p*NA) produced via cleavage from their specific substrates by activated caspase-3 and caspase- 6 was measured at 405 nm using a microplate reader

2.10 Statistical analysis

All data were expressed as mean \pm standard error of the mean. One-way ANOVA followed by Tukey's test was performed to test significant variations between control and treatment groups. SPSS ver.16.0 software (SPSS Inc, Chicago, Illinois, USA) and Graph Pad Prism ver. 6.0 were used for statistical and graphical analyses. A *p*-value of less than 0.05 was considered statistically significant.

3. Results

3.1 Anticancer activity of *Mikania micrantha* silver nanoparticles

3.1.1 The antiproliferative and cytotoxic effects of AgNPs in A549 cells

A549 cells were treated for 24 h with different concentrations of AgNPs to determine their cytotoxicity and the amount of cell death induced by AgNPs was assessed by the MTT assay. Treatment of cells with AgNPs showed a dose dependent increase in cytotoxicity. The inhibition (%) of A549 cells by AgNPs was plotted against log doses for the calculation of IC_{50} (Figure 7.1). The cytotoxic effect of

AgNPs (IC_{50} : 2.8 ± 0.02 $\mu\text{g/ml}$) at 24 h treatment was found to be significantly higher than the *M. macrantha* extract alone as well as AgNO_3 , where the IC_{50} could not be determined even at the dose of 200 $\mu\text{g/ml}$. The cytotoxicity of AgNPs was assessed in normal fibroblast cells (L929), and the IC_{50} of the synthesized AgNPs could not be determined even at a concentration of 50 $\mu\text{g/ml}$, suggesting the safety of the synthesized AgNPs in a normal cell line.

3.1.2 The inhibitory effect of AgNPs on the clonogenicity of A549 cells

Cancer cells are able to regulate their growth and spread by forming colonies, which they utilise as a means of communicating and assembling themselves into a tumor. Compared to the untreated control, our results reveal that AgNPs treatment significantly decreased the clonogenicity of A549 cells in a dose-dependent manner [Figure 7.2(a)]. Colony-forming ability was considerably suppressed in A549 cells treated with AgNPs at concentrations of 1.0, 2.5 and 5.0 $\mu\text{g/ml}$ with 24.21, 3.35, and 0.17 surviving fraction, respectively [Figure 7.2(b)]. The colony inhibitory effect of AgNPs at a concentration of 5.0 $\mu\text{g/ml}$ was comparable to that of the standard drug 5FU, showing the efficacy of AgNPs in reducing the formation of colonies in cancer cells.

3.1.3 Morphological evidence of apoptosis induced by AgNPs

The apoptotic morphology was identified and quantified using acridine orange/ethidium bromide (AO/EtBr) dual staining to ascertain whether apoptosis is the mechanism underlying AgNPs-induced suppression of A549 cell growth. A549 cells treated with various concentrations of AgNPs for 24 h revealed a dose-dependent increase in apoptotic cells. Fluorescence microscopic images of the AgNPs treated cells [Figure 7.3(a)] showed morphological alterations such as nuclear condensation and nuclear fragmentation which are the distinct characteristics of apoptotic cells. Treatment with AgNPs at 1.0, 2.5, and 5.0 $\mu\text{g/ml}$ resulted in a progressive increase in the apoptotic index (%), with the percentage of dead cells being 34.4%, 68.5%, and 91.2%, respectively. The apoptotic index of A549 cells treated with 5.0 $\mu\text{g/ml}$ of AgNPs was found to be significantly higher than that of the standard drug 5FU [Figure 7.3(b)].

3.1.4 Induction of DNA strand breaks by AgNPs

DNA damage and activation of apoptosis in response to anti-cancer drugs is a crucial component of anticancer therapy. The alkaline Comet assay was performed to evaluate DNA damage in A549 cells after treatment with different concentrations of AgNPs. Our findings revealed that AgNPs treatment led to significant DNA damage in A549 cells, as indicated by the increased tail area, tail length, tail DNA, and tail olive moment in AgNPs-treated groups when compared to untreated control group [Figure 7.4(a-e)]. Moreover, the levels of DNA damage induced by AgNPs were found to be significantly higher when compared with the damage induced by the standard drug 5FU [Figure 7.4(b-e)].

3.1.5 Antioxidants/Oxidant Status

The level and activities of antioxidants and oxidants in A549 cells were measured after treatment with AgNPs. The treatment of cancer cells with AgNPs decreases the levels and activities of antioxidant in a dose-dependent manner when compared to untreated cells [Figure 7.5(a-c)]. The reducing action of AgNPs (5 µg/ml) on the antioxidants activities was found to be significantly better than the standard 5FU (100 µg/ml). In order to determine whether AgNPs treatment affects intracellular oxidant levels, the level of lipid peroxidation (LPO) as an oxidative stress biomarker was measured. Consistent with the decreased antioxidant enzyme activities, oxidative stress levels increased significantly after AgNPs treatment of cancer cells. The increase in LPO was found to be dose dependent up to 5µg/ml in response to AgNPs treatment [Figure 7.5(d)].

3.1.6 Effect of AgNPs on the relative expression of pro-apoptotic and anti-apoptotic genes

The relative mRNA expression levels of both pro-apoptotic (Bax, Bid, p53, and Apaf-1) and anti-apoptotic (BCL-X_L, BCL-2, Survivin, and PARP) genes were assessed using qRT-PCR techniques. Treatment of A549 cells with AgNPs (2.5 µg/ml) for 24 h induced up-regulation of pro-apoptotic genes such as *Bax*, *Bid*, *p53*, and *Apaf-1* by 3.5, 13.4, 4.4, and 5.2 folds, respectively, in comparison to the untreated control [Figure 7.6(a-d)]. Moreover, anti-apoptotic genes including *BCL-X_L*, *BCL-2*, and *PARP*

were downregulated by 4.5, 9.6, and 4.5-fold relative to the untreated group [Figure 7.6(e,f,h)].

3.1.7 Activation of caspase-3/6 by AgNPs on A549 cells

Caspase-3/6 plays a crucial role in the activation of apoptosis in cancer cells, and the effect of AgNPs on apoptosis in A549 cells was evaluated by assessing caspase-3/6 activity. Treatment of A549 cells with 2.5 µg/ml AgNPs resulted in a 2.4- and 2.9-fold increase in the activities of caspase-3 and caspase-6, respectively, compared to the untreated control (Figure 7.7). The activity of caspase-3 was significantly higher in the AgNPs treated group than the standard drug 5FU.

3.2 Anticancer activity of *Acmella ciliata* silver nanoparticles

3.2.1 The antiproliferative and cytotoxic effects of AgNPs in A549 cells

The MTT assay was performed to evaluate the cytotoxicity and rate of cell mortality induced by AgNPs in A549 cells that were treated with varying concentrations of AgNPs synthesized using aqueous leaf extract of *A. ciliata* for 24 hours. Treatment of cells with AgNPs resulted in a dose-dependent increase in cytotoxicity. The percentage of inhibition of A549 cells by AgNPs was plotted against log doses to determine the IC₅₀ (Figure 7.8). The cytotoxic effect of AgNPs (IC₅₀: 2.46 ± 134 µg/ml) was significantly higher than that of the *A. ciliata* extract alone and AgNO₃, even at a dose of 200 µg/ml, during a 24 h treatment. A549 cells were treated for 24 h with different concentrations of AgNPs to determine their cytotoxicity and the amount of cell death induced by AgNPs was assessed by the MTT assay. Treatment of cells with AgNPs showed a dose dependent increase in cytotoxicity. The inhibition (%) of A549 cells by AgNPs was plotted against log doses for the calculation of IC₅₀ (Figure 7.8). The cytotoxic effect of AgNPs (IC₅₀: 2.46 ± 134 µg/ml) at 24 h treatment was found to be significantly higher than the *A. ciliata* extract alone as well as AgNO₃, where the IC₅₀ could not be determined even at the dose of 200 µg/ml. The cytotoxicity of AgNPs was evaluated in normal fibroblast cells (L929), and the IC₅₀ of the synthesized AgNPs could not be established even at the concentration of 50 µg/ml, indicating the safety of the synthesized AgNPs in a normal cell line.

3.2.2 The inhibitory effect of AgNPs on the clonogenicity of A549 cells

Cancer cells are able to regulate their growth and spread by forming colonies, which they utilise as a means of communicating and assembling themselves into a tumor. Compared to the untreated control, our results reveal that AgNPs treatment significantly decreased the clonogenicity of A549 cells in a dose-dependent manner [Figure 7.9(a)]. Colony-forming ability was considerably suppressed in A549 cells treated with AgNPs at concentrations of 1.0, 2.5 and 5.0 $\mu\text{g/ml}$ with 21.92, 2.83, and 0.09 surviving fraction, respectively [Figure 7.9(b)]. The colony inhibitory effect of AgNPs at a concentration of 5.0 $\mu\text{g/ml}$ was significantly higher than the standard drug 5FU, showing the efficacy of AgNPs in reducing the formation of colonies in cancer cells.

3.2.3 Morphological evidence of apoptosis induced by AgNPs

The apoptotic morphology was identified and quantified using acridine orange/ethidium bromide (AO/EtBr) dual staining to ascertain whether apoptosis is the mechanism underlying AgNPs-induced suppression of A549 cell growth. A549 cells treated with various concentrations of AgNPs for 24 h revealed a dose-dependent increase in apoptotic cells. Fluorescence microscopic images of the AgNPs treated cells [Figure 7.10(a)] showed morphological alterations such as nuclear condensation and nuclear fragmentation which are the distinct characteristics of apoptotic cells. Treatment with AgNPs at 1.0, 2.5, and 5.0 $\mu\text{g/ml}$ resulted in a progressive increase in the apoptotic index (%), with the percentage of dead cells being 28.11%, 54.21%, and 84.05%, respectively. The apoptotic index of A549 cells treated with 5.0 $\mu\text{g/ml}$ of AgNPs was found to be significantly higher than that of the standard drug 5FU [Figure 7.10(b)].

3.2.4 Induction of DNA strand breaks by AgNPs

DNA damage and activation of apoptosis in response to anti-cancer drugs is a crucial component of anticancer therapy. The alkaline Comet assay was performed to evaluate DNA damage in A549 cells after treatment with different concentrations of AgNPs. Our findings revealed that AgNPs treatment led to significant DNA damage

in A549 cells, as indicated by the increased tail area, tail length, tail DNA, and tail olive moment in AgNPs-treated groups when compared to untreated control group [Figure 7.11(a-e)]. Moreover, the levels of DNA damage induced by AgNPs were found to be significantly higher when compared with the damage induced by the standard drug 5FU [Figure 7.11(b-e)].

3.2.5 Antioxidants/Oxidant Status

The level and activities of antioxidants and oxidants in A549 cells were measured after treatment with AgNPs. The treatment of cancer cells with AgNPs decreases the levels and activities of antioxidant in a dose-dependent manner when compared to untreated cells [Figure 7.12(a-c)]. The reducing action of AgNPs (5 $\mu\text{g/ml}$) on the antioxidants activities was found to be significantly better than the standard 5FU (100 $\mu\text{g/ml}$). In order to determine whether AgNPs treatment affects intracellular oxidant levels, the level of lipid peroxidation (LPO) as an oxidative stress biomarker was measured. Consistent with the decreased antioxidant enzyme activities, oxidative stress levels increased significantly after AgNPs treatment of cancer cells. The increase in LPO was found to be dose dependent up to 5 $\mu\text{g/ml}$ in response to AgNPs treatment [Figure 7.12(d)].

3.2.6 Effect of AgNPs on the relative expression of pro-apoptotic and anti-apoptotic genes

The relative mRNA expression levels of both pro-apoptotic (*Bax*, *Bid*, *p53*, and *Apaf-1*) and anti-apoptotic (*Bcl-X_L*, *Bcl-2*, *Survivin*, and *PARP*) genes were assessed using qRT-PCR techniques. Treatment of A549 cells with AgNPs (2.5 $\mu\text{g/ml}$) for 24 h induced up-regulation of pro-apoptotic genes such as *Bax*, *Bid*, *p53*, and *Apaf-1* by 4.5, 14.8, 4.9, and 3.6 folds, respectively, in comparison to the untreated control [Figure 13(a-d)]. Moreover, anti-apoptotic genes including *Bcl-X_L*, *Bcl-2*, *Survivin*, and *PARP* were downregulated by 5.7, 4.5, 1.06 and 4.6-fold relative to the untreated group [Figure 7.13(e,f,h)].

3.2.7 Activation of caspase-3/6 by AgNPs on A549 cells

Caspase-3/6 plays a crucial role in the activation of apoptosis in cancer cells, and the effect of AgNPs on apoptosis in A549 cells was evaluated by assessing caspase-3/6 activity. Treatment of A549 cells with 2.5 µg/ml AgNPs resulted in a 2.6- and 3.0-fold increase in the activities of caspase-3 and caspase-6, respectively, compared to the untreated control (Figure 14). The activity of caspase-3 was significantly higher in the AgNPs treated group than the standard drug 5FU.

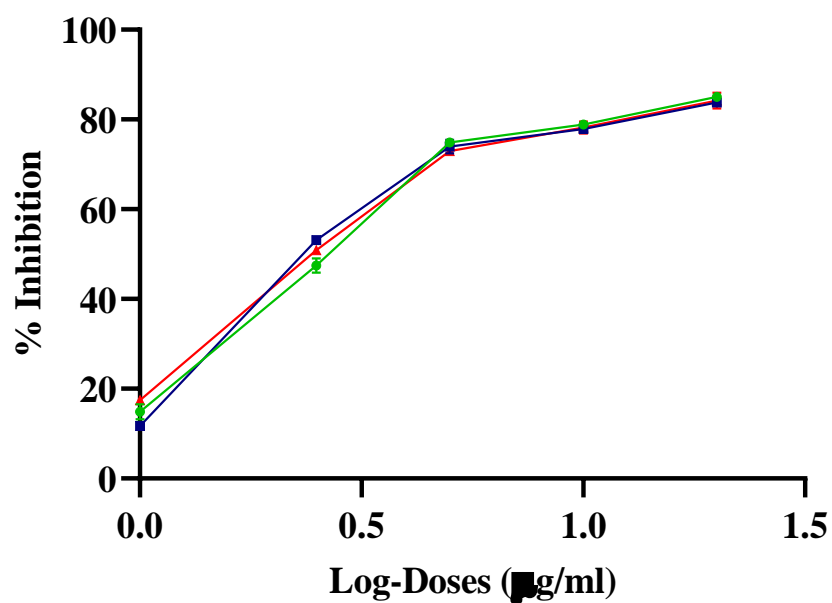


Figure 7.1: Plots of log-doses of various concentration of AgNPs synthesized using *M.Micrantha* in triplicate against inhibition (%) of A549 cells after 24 h treatment for the calculation of IC_{50} .

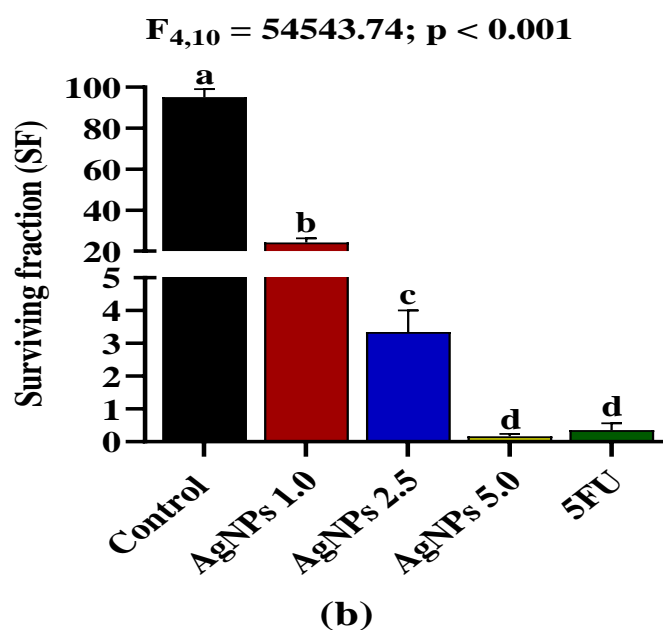
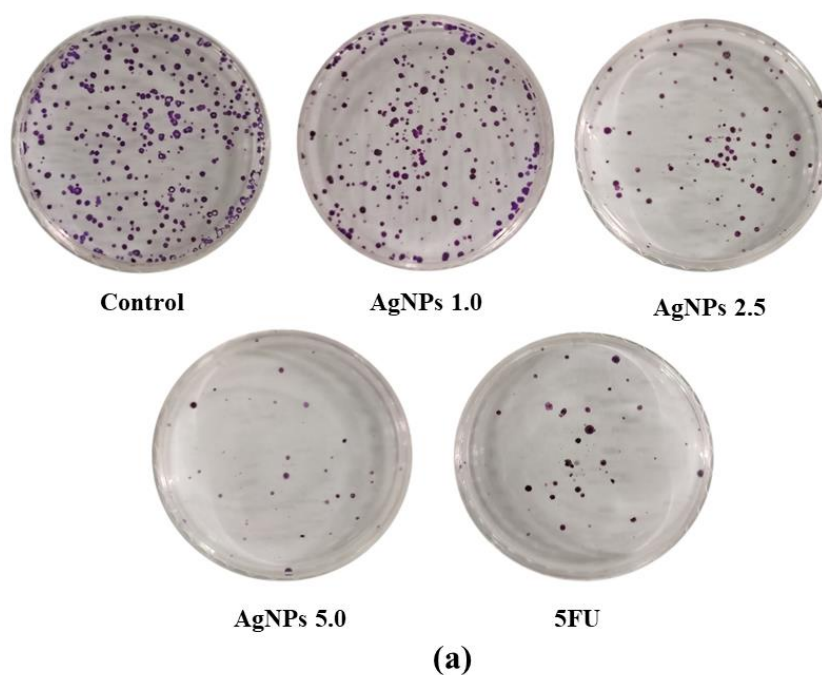


Figure 7.2: (a) Inhibition of colony formation of A549 cells mediated by AgNPs. (b) Effect of AgNPs on the reproductive viability of A549 cells, expressed as a surviving fraction (SF) Control: A549 cells without treatment; AgNPs 1.0, AgNPs 2.5 and AgNPs 5.0: A549 cells treated with 1.0, 2.5 and 5.0 $\mu\text{g/ml}$ of AgNPs respectively; 5FU: A549 cells treated with 100 $\mu\text{g/ml}$ of 5FU (positive control). Values are expressed as Mean \pm SEM. Different letters indicate significant variation.

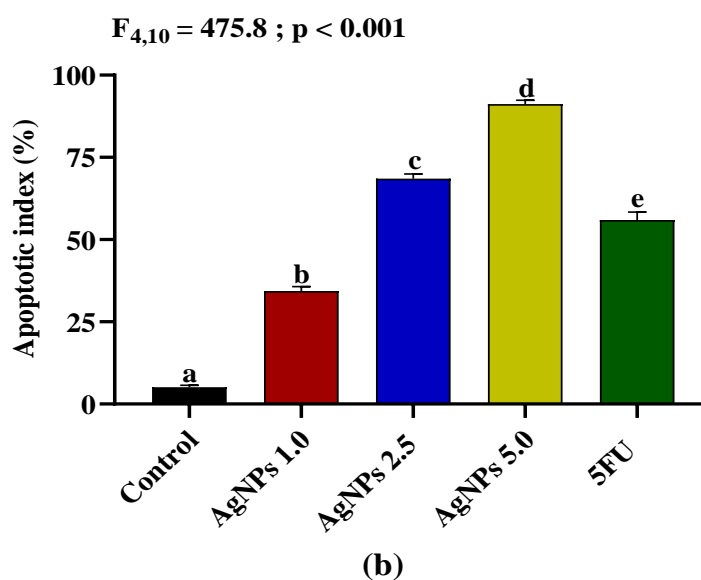
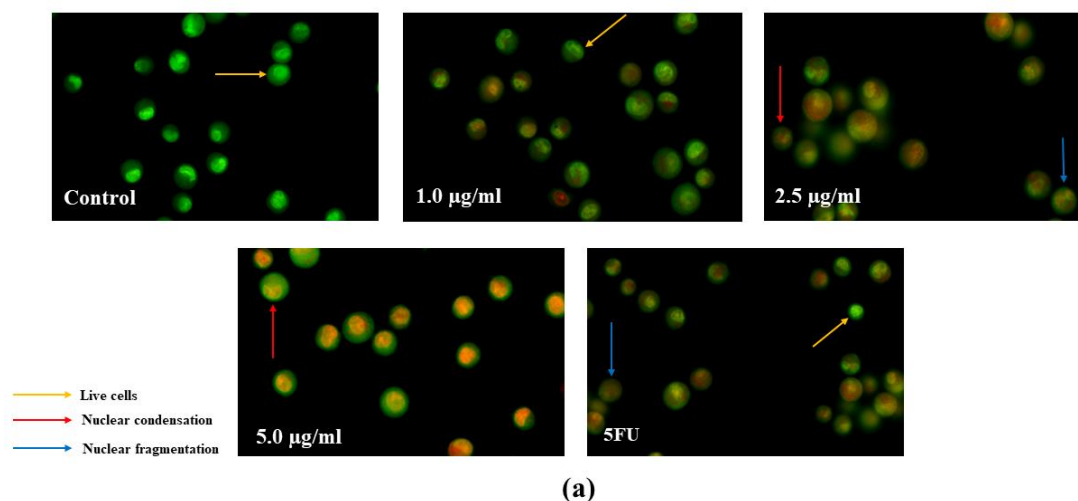
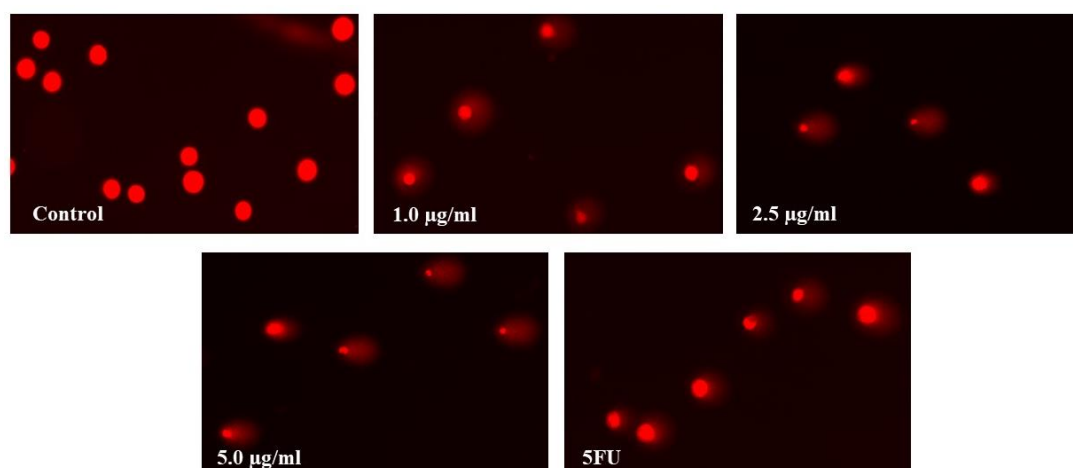
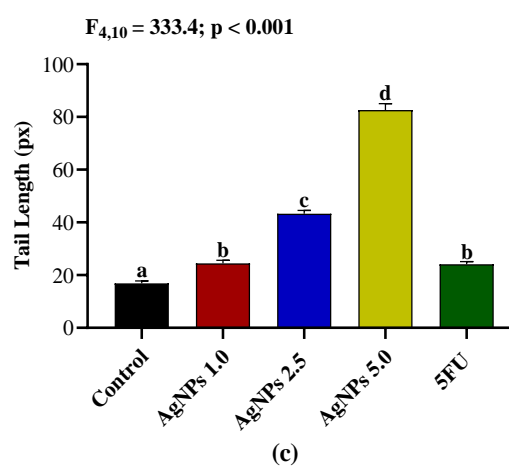
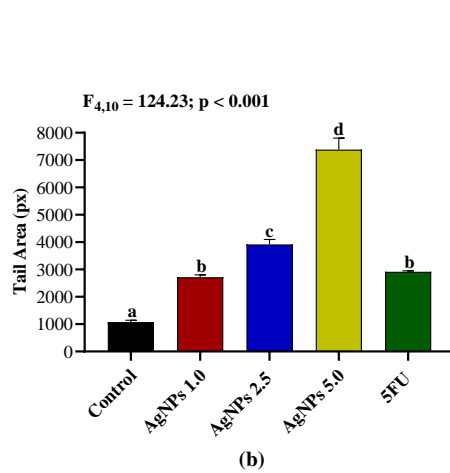


Figure 7.3: (a) Acridine orange/Ethidium bromide (AO/EtBr) dual staining of A549 cells after treatment with different doses of AgNPs for 24 h (yellow arrow shows the live cells, red arrow shows apoptotic cells with nuclear condensation, and blue arrow shows apoptotic cells with nuclear fragmentation). **(b)** Percentage of dead cells after treatment of A549 with biosynthesized AgNPs. Control: A549 cells without treatment; AgNPs 1.0, AgNPs 2.5 and AgNPs 5.0: A549 cells treated with 1.0, 2.5 and 5.0 µg/ml of AgNPs respectively; 5FU: A549 cells treated with 100 µg/ml of 5FU (positive control). Values are expressed as Mean ± SEM. Different letters indicate significant variation.



(a)



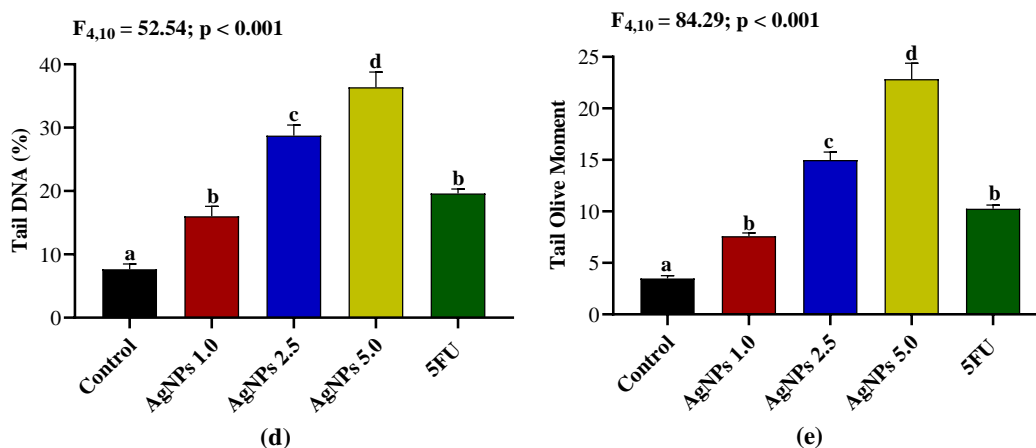


Figure 7.4: (a) Fluorescence images of Comets observed in control and A549 cells treated with different concentrations of AgNPs. (b - e) The extent of DNA damage expressed in terms of tail area, tail length, tail DNA and tail olive moment. Control: A549 cells without treatment; AgNPs 1.0, AgNPs 2.5 and AgNPs 5.0: A549 cells treated with 1.0, 2.5 and 5.0 $\mu\text{g/ml}$ of AgNPs respectively; 5FU: A549 cells treated with 100 $\mu\text{g/ml}$ of 5FU. Values are expressed as Mean \pm SEM. Different letters indicate significant variation.

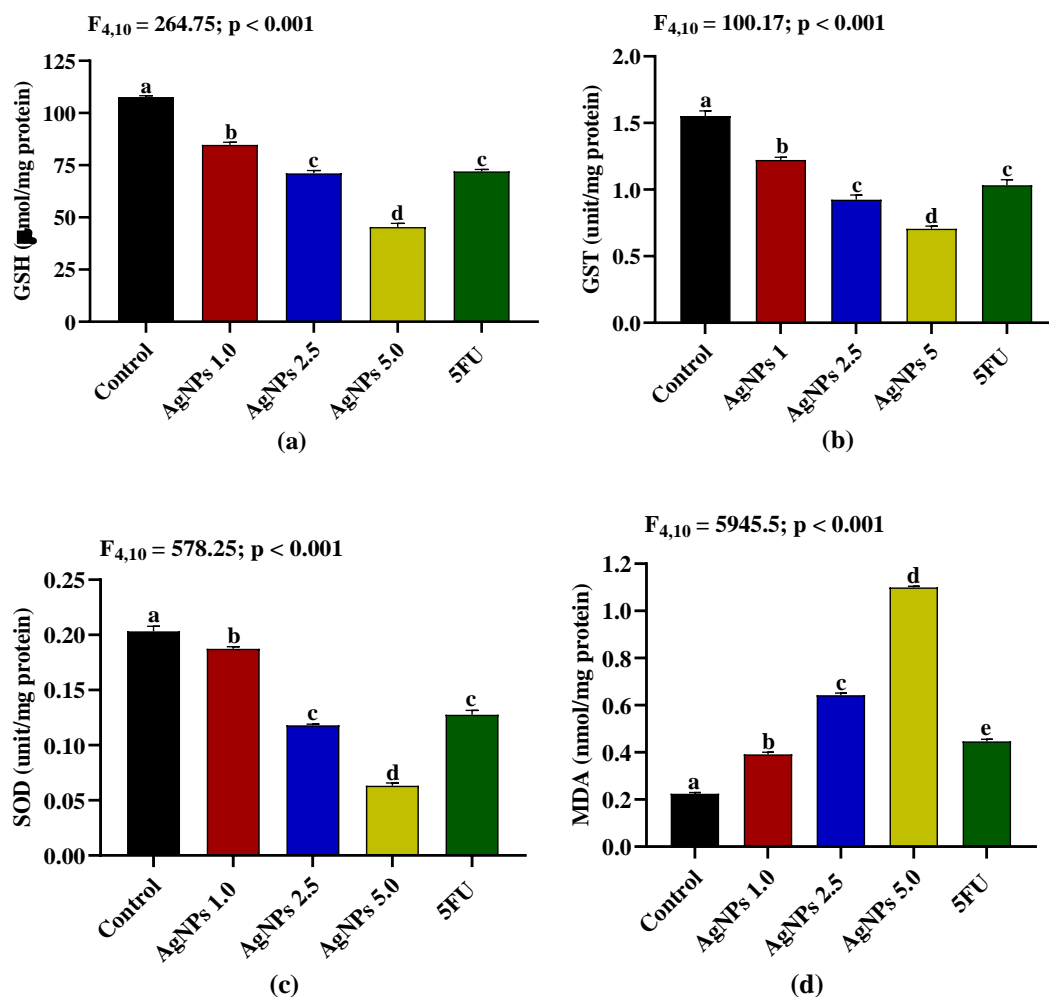
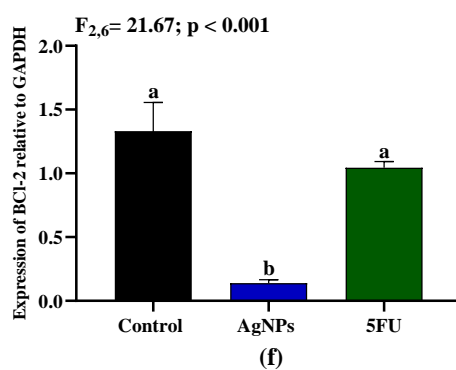
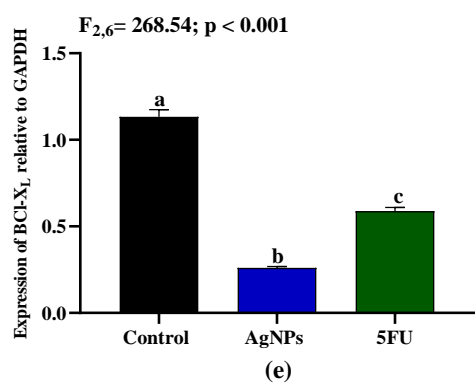
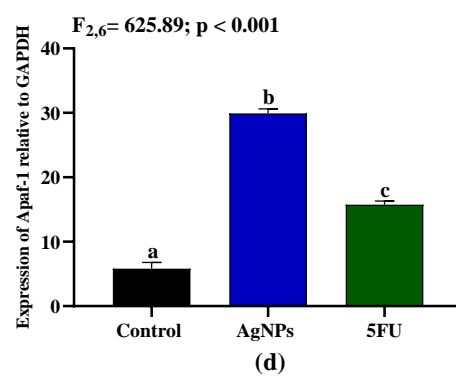
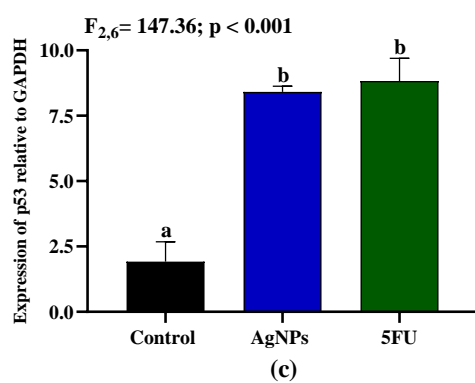
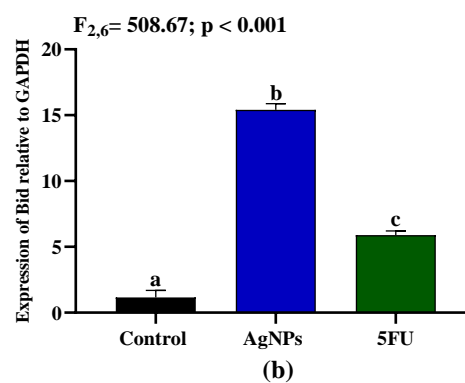
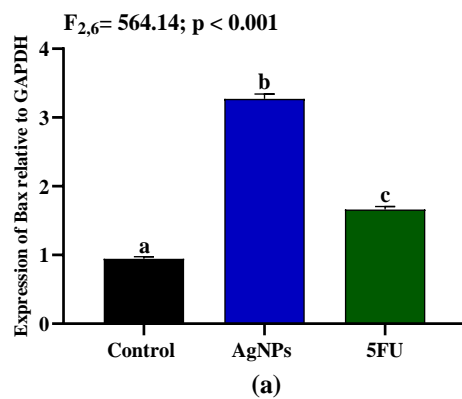


Figure 7.5: Effects of AgNPs on (a) glutathione (GSH) level; (b) glutathione-s-transferase (GST) activity; (c) superoxide dismutase (SOD) activity; and (d) lipid peroxidation (LPO) expressed in malondialdehyde (nmol/mg protein) in A549 cells after 24 h treatment. Control: A549 cells without treatment; AgNPs 1.0, AgNPs 2.5 and AgNPs 5.0: A549 cells treated with 1.0, 2.5 and 5.0 $\mu\text{g/ml}$ of AgNPs respectively; 5FU: A549 cells treated with 100 $\mu\text{g/ml}$ of 5FU. Values are expressed as Mean \pm SEM. Different letters indicate significant variation.



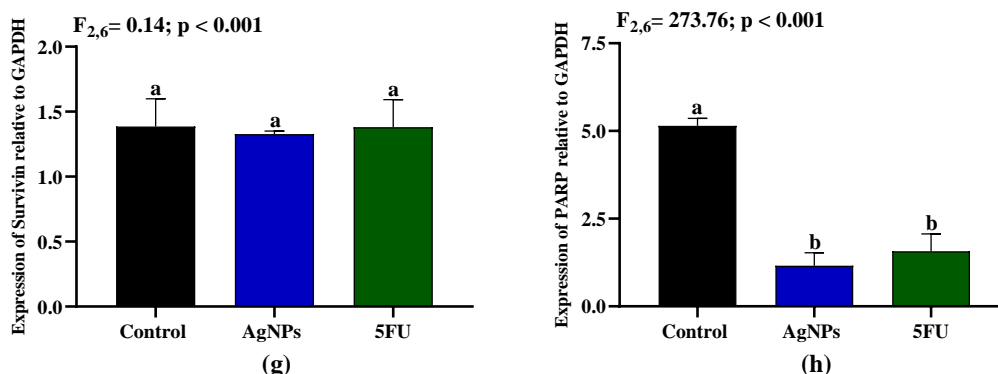


Figure 7.6: Effects of AgNPs on mRNA expression levels of (a) *Bax*; (b) *Bid*; (c) *p53*; (d) *Apaf-1*; (e) *BCl-X_L*; (f) *BCl-2*; (g) *Survivin* and (h) *PARP* in A549 cells after 24 h treatment. Control: A549 cells without treatment; AgNPs: A549 cells treated with 2.5 $\mu\text{g/ml}$ of AgNPs; 5FU: A549 cells treated with 100 $\mu\text{g/ml}$ of 5FU. Values are expressed as Mean \pm SEM. Different letters indicate significant variation.

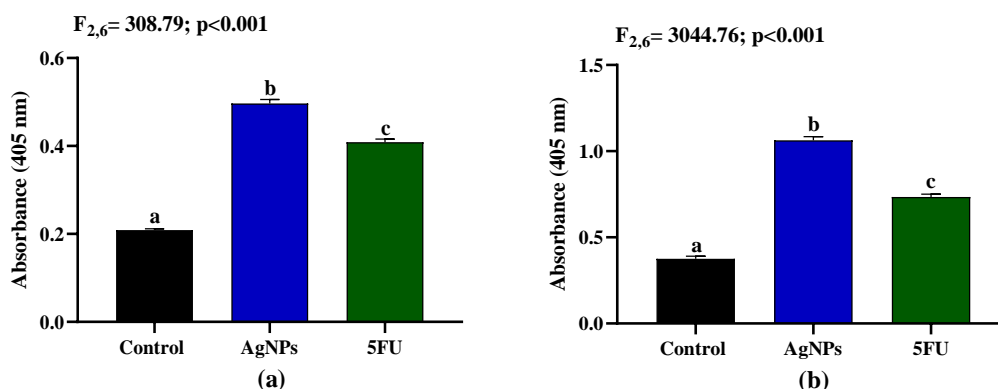


Figure 7.7: Effects of AgNPs on activities of (a) Caspase-3 and (b) Caspase-6 in A549 cells after 24 h treatment. Control: A549 cells without treatment; AgNPs: A549 cells treated with 2.5 $\mu\text{g/ml}$ of AgNPs; 5FU: A549 cells treated with 100 $\mu\text{g/ml}$ of 5FU. Values are expressed as Mean \pm SEM. Different letters indicate significant variation.

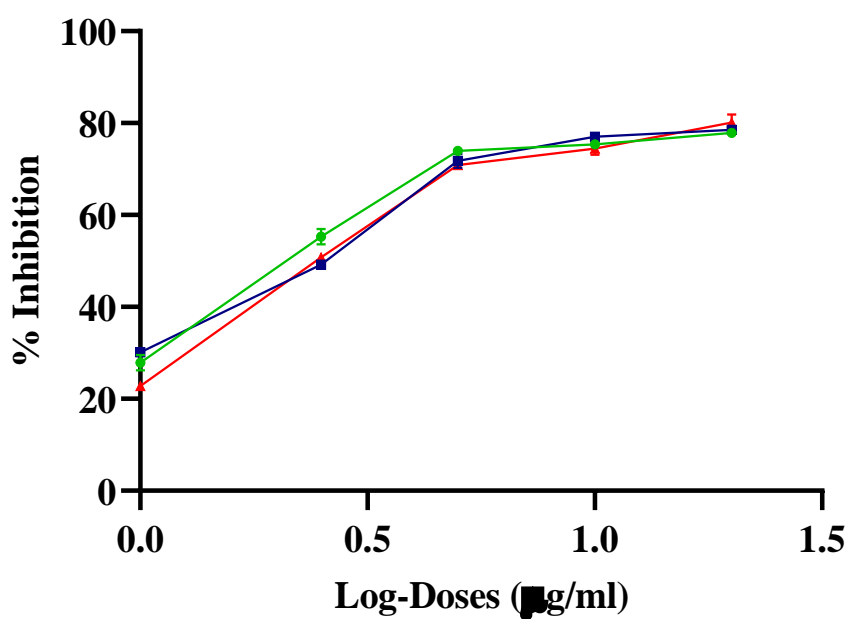


Figure 7.8: Plots of log-doses of various concentration of AgNPs synthesized using *A. Ciliata* in triplicate against inhibition (%) of A549 cells after 24 h treatment for the calculation of IC_{50} .

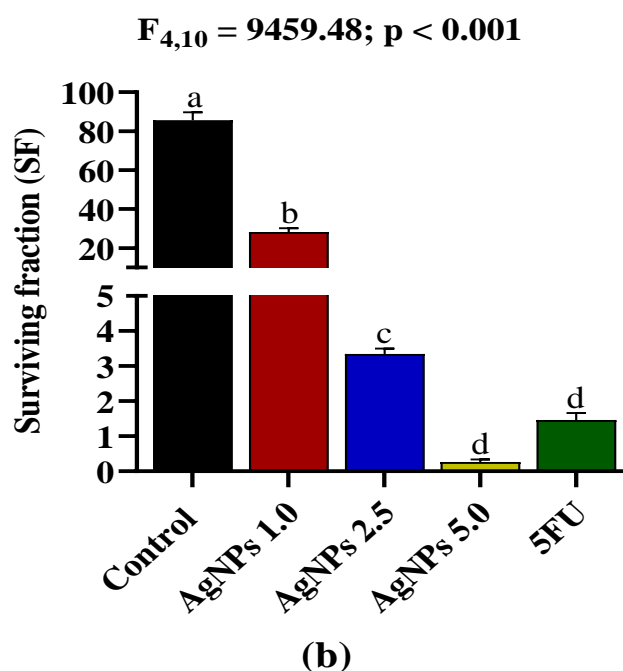
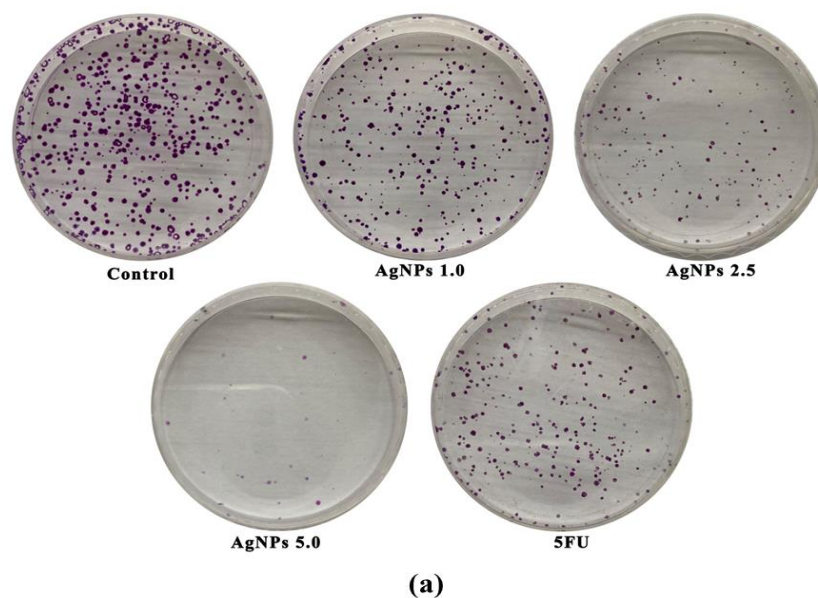


Figure 7.9: (a) Inhibition of colony formation of A549 cells mediated by AgNPs. (b) Effect of AgNPs on the reproductive viability of A549 cells, expressed as a surviving fraction (SF). Control: A549 cells without treatment; AgNPs 1.0, AgNPs 2.5 and AgNPs 5.0: A549 cells treated with 1.0, 2.5 and 5.0 $\mu\text{g/ml}$ of AgNPs respectively; 5FU: A549 cells treated with 100 $\mu\text{g/ml}$ of 5FU (positive control). Values are expressed as Mean \pm SEM. Different letters indicate significant variation.

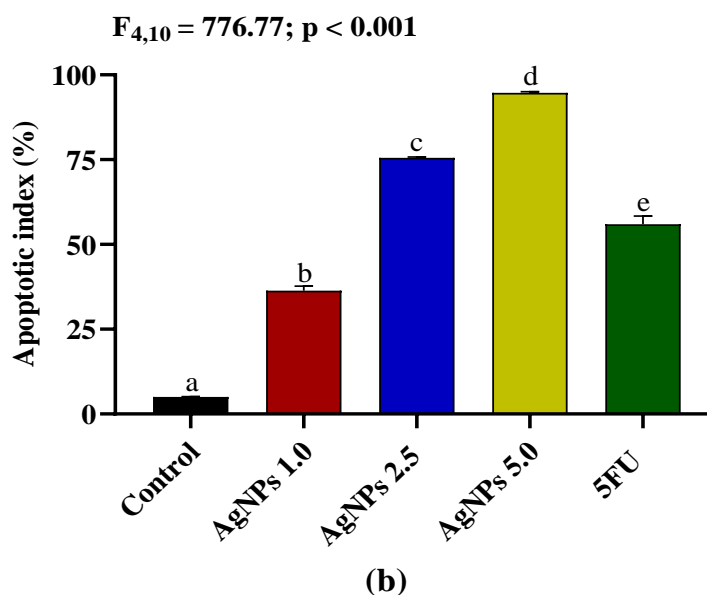
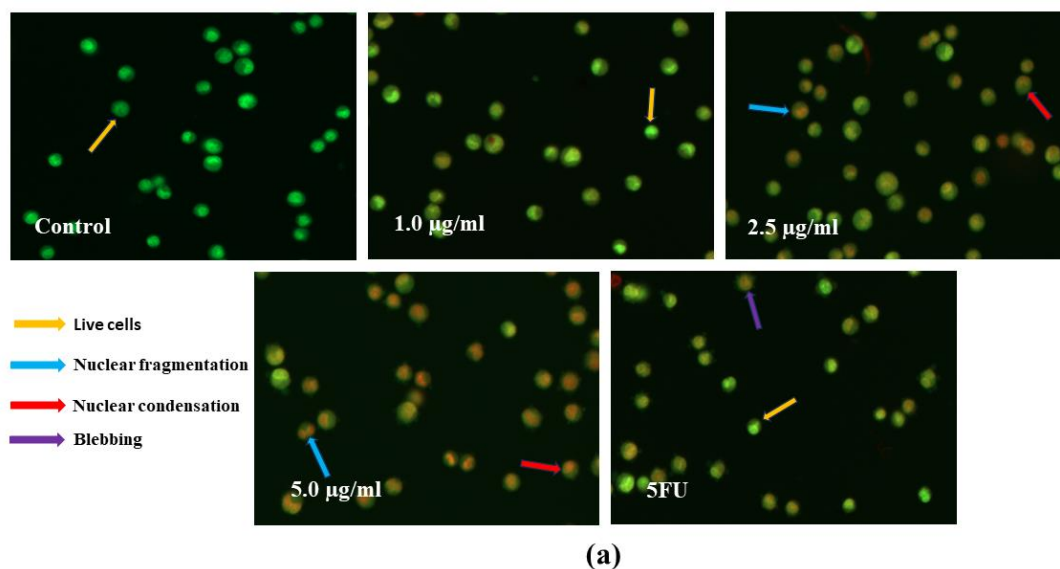
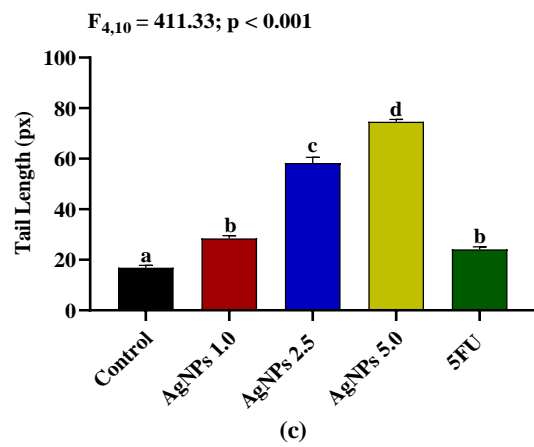
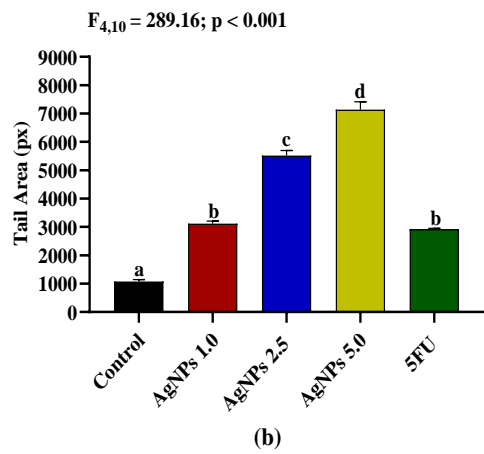
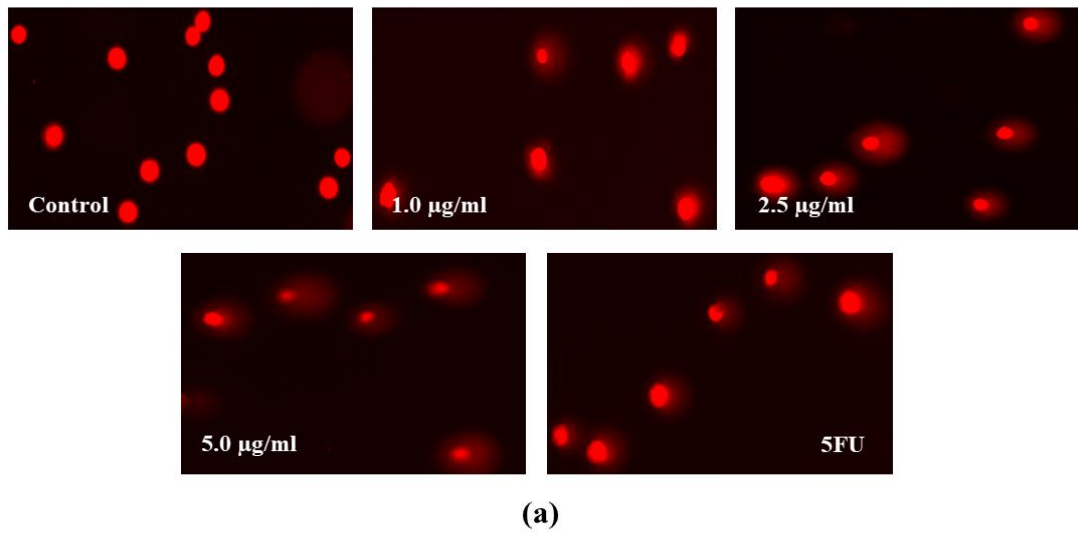


Figure 7.10: (a) Acridine orange/Ethidium bromide (AO/EtBr) dual staining of A549 cells after treatment with different doses of AgNPs for 24 h (yellow arrow shows the live cells, red arrow shows apoptotic cells with nuclear condensation, and blue arrow shows apoptotic cells with nuclear fragmentation). (b) Percentage of dead cells after treatment of A549 with biosynthesized AgNPs. Control: A549 cells without treatment; AgNPs 1.0, AgNPs 2.5 and AgNPs 5.0: A549 cells treated with 1.0, 2.5 and 5.0 µg/ml of AgNPs respectively; 5FU: A549 cells treated with 100 µg/ml of 5FU (positive control). Values are expressed as Mean \pm SEM. Different letters indicate significant variation.



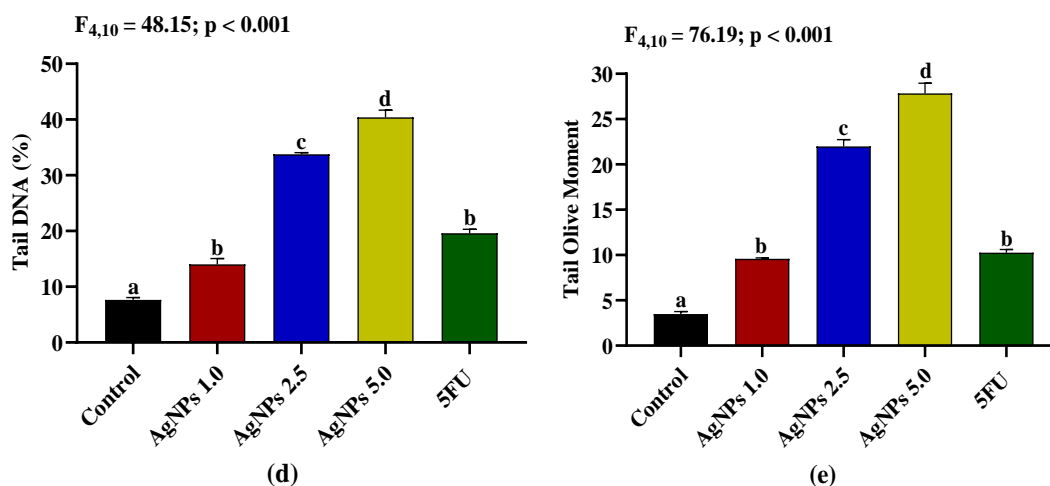


Figure 7.11: (a) Fluorescence images of Comets observed in control and A549 cells treated with different concentrations of AgNPs. **(b - e)** The extent of DNA damage expressed in terms of tail area, tail length, tail DNA and tail olive moment. Control: A549 cells without treatment; AgNPs 1.0, AgNPs 2.5 and AgNPs 5.0: A549 cells treated with 1.0, 2.5 and 5.0 $\mu\text{g/ml}$ of AgNPs respectively; 5FU: A549 cells treated with 100 $\mu\text{g/ml}$ of 5FU. Values are expressed as Mean \pm SEM. Different letters indicate significant variation.

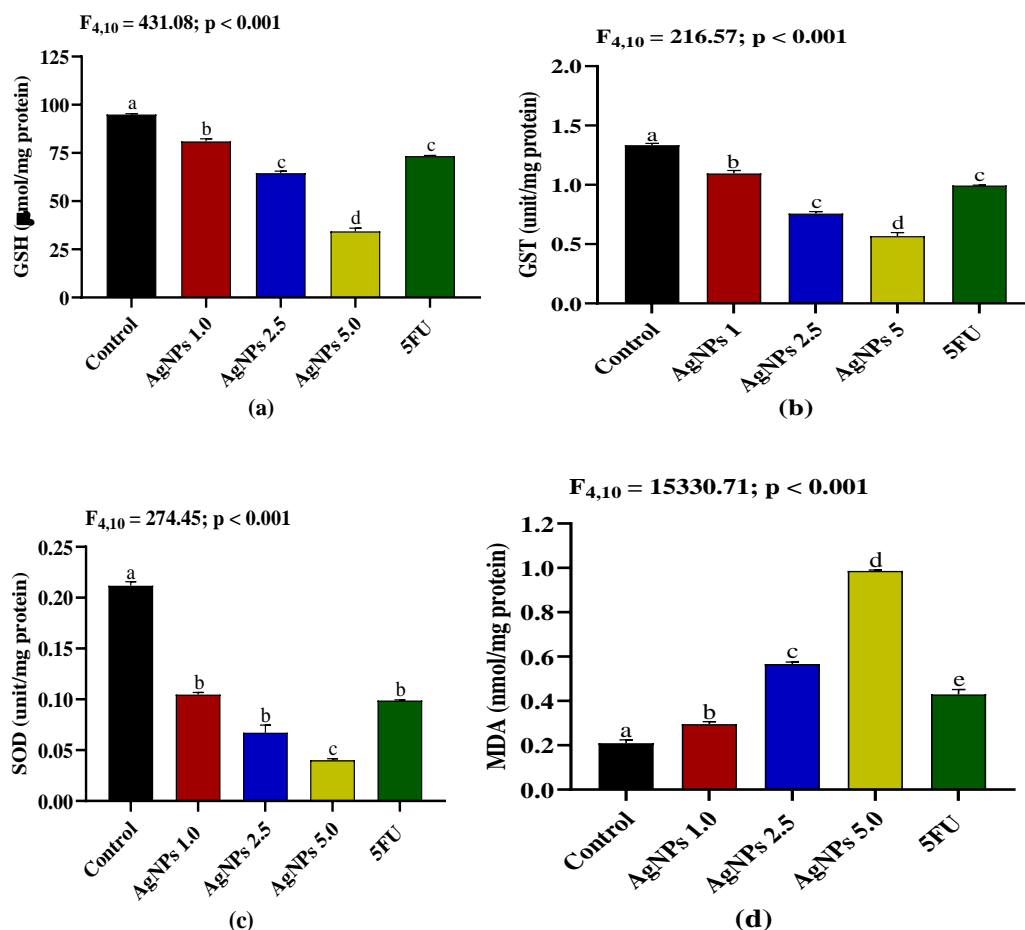
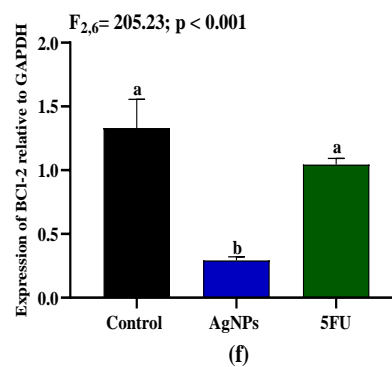
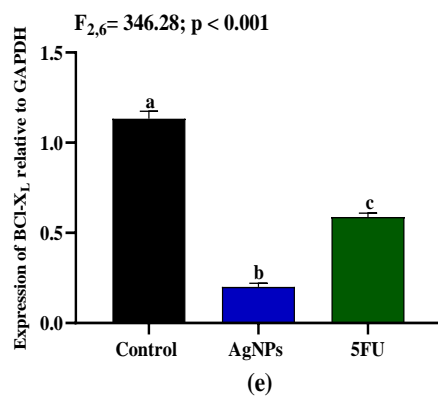
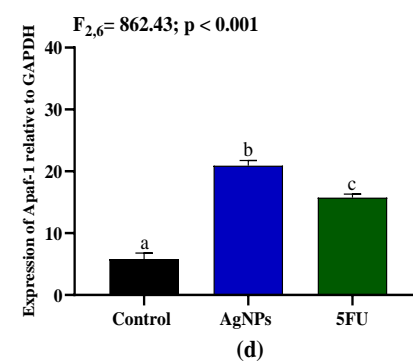
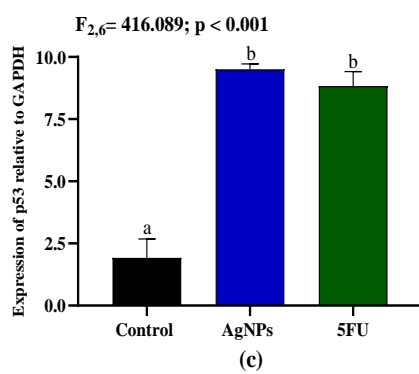
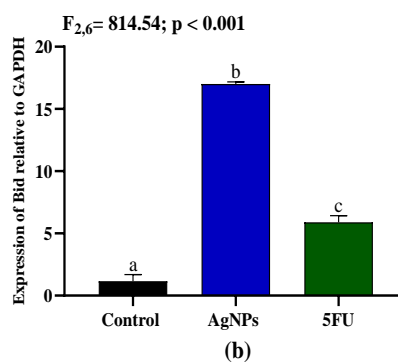
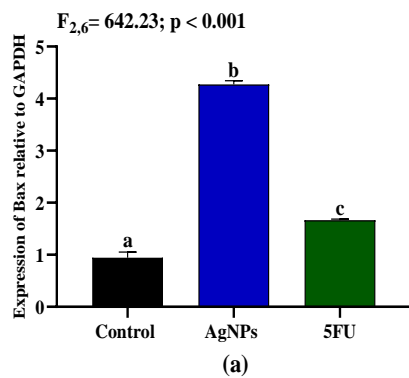


Figure 7.12: Effects of AgNPs on (a) glutathione (GSH) level; (b) glutathione-s-transferase (GST) activity; (c) superoxide dismutase (SOD) activity; and (d) lipid peroxidation (LPO) expressed in malondialdehyde (nmol/mg protein) in A549 cells after 24 h treatment. Control: A549 cells without treatment; AgNPs 1.0, AgNPs 2.5 and AgNPs 5.0: A549 cells treated with 1.0, 2.5 and 5.0 $\mu\text{g/ml}$ of AgNPs respectively; 5FU: A549 cells treated with 100 $\mu\text{g/ml}$ of 5FU. Values are expressed as Mean \pm SEM. Different letters indicate significant variation.



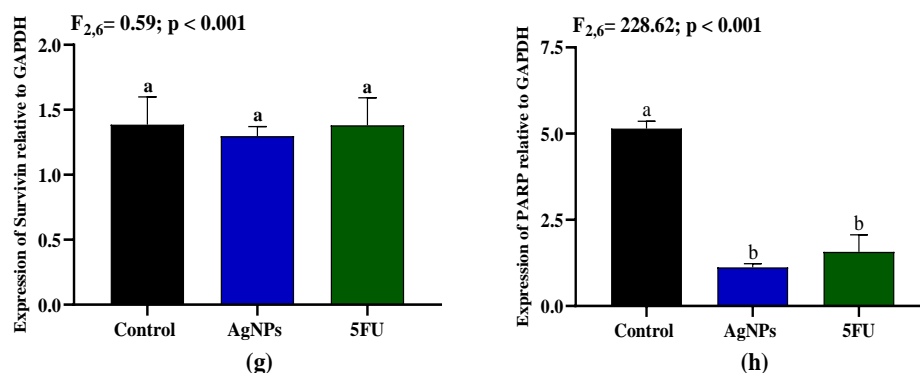


Figure 7.13: Effects of AgNPs on mRNA expression levels of (a) *Bax*; (b) *Bid*; (c) *p53*; (d) *Apaf-1*; (e) *Bcl-X_L*; (f) *Bcl-2*; (g) *Survivin* and (h) *PARP* in A549 cells after 24 h treatment. Control: A549 cells without treatment; AgNPs: A549 cells treated with 2.5 $\mu\text{g/ml}$ of AgNPs; 5FU: A549 cells treated with 100 $\mu\text{g/ml}$ of 5FU. Values are expressed as Mean \pm SEM. Different letters indicate significant variation.

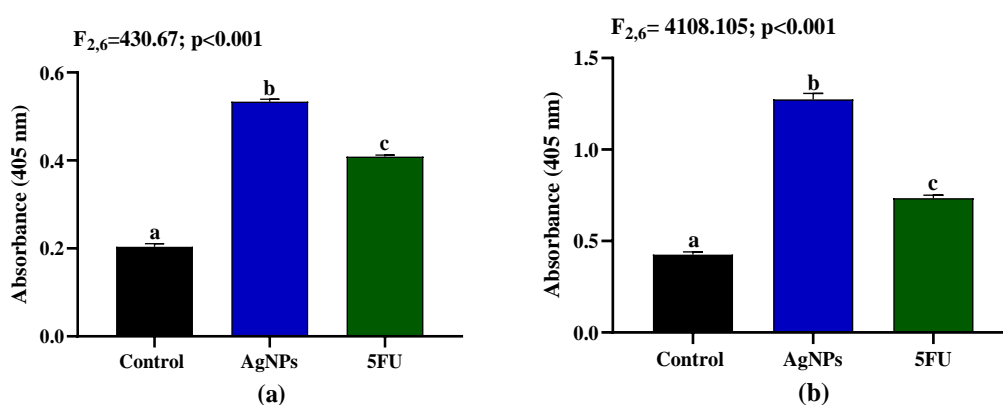


Figure 7.14: Effects of AgNPs on activities of (a) Caspase-3 and (b) Caspase-6 in A549 cells after 24 h treatment. Control: A549 cells without treatment; AgNPs: A549 cells treated with 2.5 $\mu\text{g/ml}$ of AgNPs; 5FU: A549 cells treated with 100 $\mu\text{g/ml}$ of 5FU. Values are expressed as Mean \pm SEM. Different letters indicate significant variation.

4. Discussion

Nanoparticles have the potential to enhance the efficacy of many drugs by enabling targeted delivery to certain cells. The therapeutic efficacy of nanoparticulated silver is based on its distinctive ability to induce apoptosis in mammalian cells. Despite variability in their physical and chemical characteristics, such as differences in size, shape, and capping material, their mechanism for causing cancer cell death is consistent and unalterable. AgNPs accumulate in endosomes after being taken up, mostly through endocytosis mechanisms, which are then targeted for fusion with lysosomes. The acidic environment of the lysosome causes a higher release of silver ions from the AgNPs. These reactive ions disrupt the balance of cellular homeostasis and, depending on the biological characteristics of the targeted cell, result in apoptotic cell death (Cameron *et al.*, 2018). This mechanism, also known as the "Trojan-horse" mechanism, implies that the cytotoxic effect of AgNPs manifests once the cells absorb them (Hsiao *et al.*, 2015). However, the most significant difference between AgNPs and traditional small molecular treatments is the "nano" characteristic of AgNPs, which eventually aids in mitigating the severity of adverse side effects. These nano-characteristics can passively or actively direct AgNPs to the tumor tissues, allowing them to accumulate in high concentrations. Passive accumulation occurs in tumor tissue due to neo-angiogenesis, altered endothelial layer, fenestrated vasculature, and impaired lymphatic drainage, allowing nano-sized materials to penetrate and accumulate within cancerous tissues. The enhanced permeability and retention (EPR) effect is a phenomenon that has been utilized in the nanomedicine field to facilitate the development of drugs (Kalyane *et al.*, 2019). Furthermore, it has been suggested that manipulating the shape, size, and capping compounds of nanoparticles can enhance their passive accumulation.

Researchers have proposed active targeting strategies as viable alternatives to passive targeting to enhance the cancer specificity of silver nanoparticles. Active targeting involves binding a cancer cell-specific moiety to nanoparticle surfaces, allowing nanomaterials to be taken up by the desired cells. In this regard, the application of silver nanoparticles as a coating material holds promise for recognising target cells and facilitating gene-targeted therapy. The toxicity of AgNPs on various

cell lines is mostly influenced by the uptake efficiency of intact nanoparticles rather than the sensitivity of cancer cells to Ag ions, emphasizing the harmful impacts of the released Ag ions within the cell (Fahrenholtz *et al.*, 2017).

The cytotoxic effect of aqueous silver nanoparticles synthesized from *Chaetomorpha linum* has been found to be potent against HCT-116 cancer cells, which is consistent with our findings (Acharya *et al.*, 2021). The synthesis of AgNPs employing plant extracts as reducing agents has garnered significant interest in nanomedicine due to the abundance of phytochemicals in plants, which can function as coating agents during the synthesis of nanoparticles. These methods of AgNPs synthesis also have the benefit of being environmentally benign; the process is easily accessible, affordable, relatively simple to carry out, and offers the potential for large-scale production (Ivanova *et al.*, 2018). The main features of the silver nanoparticles using plant extract includes reduced side effects and cytotoxicity at a relatively low concentration especially in cancer experimental models. Accelerated cell proliferation is one of the hallmarks of cancer. Thus, targeting the rapidly dividing cells seems most appropriate when searching for a novel anticancer agent.

The silver nanoparticle synthesized using *M. micrantha* and *A. ciliata* extract exhibit high antiproliferative activity against the lung cancer cells A549. Both AgNPs and leaves extract have antiproliferative activities, however this action is enhanced when the two are combined and appears to show synergistic effect. An important criterion in considering an effective anticancer agent is the induction of apoptosis. Morphological alterations indicate that AgNPs treatment induces cell death, such as apoptosis. The programmed cell death apoptosis is no doubt the preferred cell death mechanism for any cytotoxic agent. The biosynthesized AgNPs showed cytotoxic effects in A549 cells and triggers the apoptotic pathway. Upregulation of the pro-apoptotic genes and down regulation of the anti-apoptotic genes could imply that the biosynthesized AgNPs selectively target the apoptotic pathway. Whether the apoptotic pathway activated by the biosynthesized AgNPs is the intrinsic or extrinsic pathway needs more investigation, however, judging from our results, it is likely that the mitochondrial pathway is involved. This is because the balance of pro- and anti-apoptotic BCL-2 proteins can influence the susceptibility of cells to apoptotic stimuli. An over-abundance of pro-apoptotic BCL-2 proteins such as Bax at the mitochondrial

surface generates the permeability transition (PT) pore, resulting in the hierarchical release of pro-apoptotic proteins such as cytochrome c, Smac/Diablo, and apoptosis-inducing factor (AIF) and the subsequent activation of caspase-3 and caspase-6 (Bidian *et al.*, 2023). In our study, significant increase in caspase-3 and caspase-6 activities in A549 cells following AgNPs treatment strongly suggested that AgNPs-induced apoptosis was carried out via a caspase-dependent pathway. The silver ions released by AgNPs were primarily responsible for caspase-3 and caspase-6 activation and oxidative stress.

Many anticancer agents currently in the market viz. such as doxorubicin, paclitaxel, vinblastine and some that are currently undergoing clinical trials induced a reactive oxygen species (ROS)-dependent apoptosis. Similarly, treatment of cancer cells with the biosynthesized AgNPs triggered a ROS induced apoptotic pathway. Aside from inducing apoptosis through ROS-mediated DNA damage, AgNPs can also directly damage DNA structure by releasing Ag^0 and Ag^+ (Ishida *et al.*, 2017). This is evident from the fact that treatment of A549 cells with the biosynthesized AgNPs leads to increased ROS in the cell and decreased antioxidant activities. It was found that the effect of AgNPs on the antioxidant/oxidant status of A549 cells was substantially more effective than that of 5FU. Despite the fact that effective antioxidants are essential for maintaining redox homeostasis, elevated antioxidant levels have been linked to cancer progression and chemoresistance. For instance, it has been observed that cancer cells with high glutathione levels exhibit increased neoplastic transformation (Hayes *et al.*, 2020), drug resistance, and cancer therapy failure (Kennedy *et al.*, 2020). It has been found that certain human cancer cells exhibit resistance to therapeutic intervention due to elevated activities of GST and SOD (Gupta *et al.*, 2020). AgNPs induce the formation of ROS to disturb the structure of DNA, or they can directly interact with DNA, resulting in DNA mutations (Farah *et al.*, 2016). Elevated levels of ROS can cause damage to the DNA double helix in a concentration-dependent manner, which includes breaking single or double-stranded DNA, influencing base alterations, and DNA linkages (Nayak *et al.*, 2016; Hsin *et al.*, 2008). Cancer cells treated with AgNPs exhibit DNA methylation, errors in DNA base pairing, defects in DNA repair, and an increase in chromosomal aberrations (Barcinska *et al.*, 2018). Furthermore, AgNPs treatment also induced a significant elevation in lipid peroxidation levels, which could

be mediated by a reduction in antioxidant activity that leads to an accumulation of cellular ROS (Fenoglio *et al.*, 2008). The DNA damaging effects of AgNPs correspond well with the elevation of lipid peroxidation in A549 cells treated with AgNPs since malondialdehyde, the end product of LPO, can generate mutagenic adducts that result in DNA damage (Yui *et al.*, 2023). Redox imbalance is often the causative agent for apoptosis whereby too much ROS in the cells triggers the apoptotic pathway. Whether the biosynthesized AgNPs treatment by itself affects increased ROS production is not known, however, the increase in ROS due to AgNPs could be the result of inefficient antioxidant system caused by the treatment.

The results of our study indicate that cellular damage is initiated by AgNPs-induced oxidative stress, which impacts almost every signalling pathway in the cell. Therefore, it is likely that the activation of oxidative stress exclusively causes the signalling processes experienced after AgNPs treatments. Oxidative stress initiates lipid peroxidation, disrupts mitochondrial function, oxidizes amino acids in proteins, deactivates enzymes, and causes damage to DNA and RNA, which can potentially result in autophagy, apoptosis, and necrosis of cancer cells (Zhang *et al.*, 2016). Smaller sizes and higher concentrations of AgNPs demonstrate higher induction of ROS and greater cytotoxicity, and significantly increased ROS emerge from several cancer cells treated with AgNPs (Avalos *et al.*, 2014).

5. Conclusion

We report a reductive green synthesis of AgNPs using aqueous leaves extract of *M. micrantha* and *A. ciliata* against the deadly disease cancer. Importantly, our study demonstrates the cytotoxic effects of AgNPs on human lung adenocarcinoma A549 cells by targeting the apoptotic pathway which is the preferred cell death pathway for any novel drug candidate. The involvement of apoptotic pathway was shown by the upregulation of pro-apoptotic genes and down-regulation of anti-apoptotic genes as well as activation of caspases. The biosynthesized AgNPs also activates the apoptotic pathway via increasing the ROS levels and decreased antioxidant levels. Our study therefore highlights an important role of the biosynthesized MNP and ANP as a potential novel candidate for cancer therapy.

Consolidated summary

Nanotechnology and nanoparticles have been paving the way for scientific and technological advancement, providing revolutionary prospects in various disciplines. Silver nanoparticles (AgNPs) have gained significant attention in various fields due to their unique properties including appropriate electrical conductivity, chemical stability, catalytic and antimicrobial activities. The utilization of biological resources in green synthesis, in particular, provides a sustainable approach that reduces environmental impact yet retains the desired biological activity. Our study shows that *Mikania micrantha* and *Acmella ciliata* leaf extract are capable of green and eco-friendly production of silver nanoparticles, providing a simple, cost-effective, and efficient process. The formation of AgNPs was confirmed by a UV-Vis spectrum that revealed an absorption band at 459 nm (MNP) and 430 nm (ANP). The bioactive molecules of the leaf extract that functioned as a reducing and capping agent were verified by a shift in the absorption bands in FT-IR. The presence of elemental silver was indicated by EDS, and the XRD spectrum reveals sharp peaks that demonstrate the crystalline nature. SEM and TEM analysis confirmed the spherical morphology and size of AgNPs, respectively. The significance of each characterization technique in the synthesis of AgNPs is that it provides a comprehensive understanding of the properties, which subsequently functions as the foundation for the applications.

The standard method for synthesizing AgNPs is a biological technique that primarily involves using plant extracts to reduce silver ions and produce stable silver nanoparticles. When plant extracts are typically employed in the production of nanoparticles, the antioxidant activity of AgNPs is often compared to that of the plant extract alone. Nevertheless, nanoparticles consistently exhibit evidently greater results compared to the plant extract alone. The antioxidant activity of silver nanoparticles is typically influenced by the chemical composition of the extract, and these attributes generally improve as the concentration of AgNPs increases. The silver nanoparticles exhibit substantial scavenging activity when the extract contains a high concentration of flavonoids and phenolic compounds. Our findings suggest that biosynthesized AgNPs may interact with erythrocyte membrane lipids and protect against haemolysis

owing to their unique physio-chemical properties and high surface area to volume ratio.

The toxic side effects of doxorubicin restrict its multifarious application in cancer treatment. Consequently, it is imperative to mitigate the drug's long-term adverse effects in order to further enhance its therapeutic value. According to our study, the biosynthesized AgNPs from *A. ciliata* leaf extract provides outstanding protections against DOX-induced cardiotoxicity and hepatotoxicity in DLA-bearing mice, potentially via enhancing antioxidant activity and lowering lipid peroxidation. Co-administration of biosynthesized AgNPs also reduces the DOX-induced increase in the activities of various serum enzyme markers, confirming its antioxidant potential. Further research is needed to clarify the specific mechanism by which biosynthesized AgNPs protect against DOX-induced toxicity. Our study indicate that biosynthesized AgNPs may effectively counteract the toxic effects caused by DOX and offer a feasible option for enhancing the therapeutic efficacy of doxorubicin.

Silver nanoparticles as antimicrobial agents offer a potential solution to the rising issue of antimicrobial resistance, which poses a threat worldwide. AgNPs can be altered to obtain specificity and transport to certain targets while also meeting the necessary criteria for the effectiveness of novel antimicrobial technologies, such as antimicrobial performance, quick action, and low toxicity. The antifungal activity is likely significantly correlated with its reduced size and altered shape, which results in an increased surface area that enhances its antifungal activity. Evaluating the impact of AgNPs in biological environments, together with their interactions with other substances, can provide critical understanding for the development of cutting-edge technologies and nanomaterials that can efficiently prevent infections or specifically eliminate pathogenic microorganisms.

Metal nanoparticles, particularly silver nanoparticles, are an emergent new class that has significant potential in the field of cancer biology. Because of their cancer-specific targeting, reduced side effects, and substantial anti-cancer properties, nanoparticle therapies are appealing platforms for clinically applicable drug development. Our study illustrates the cytotoxic effects of AgNPs on human lung adenocarcinoma A549 cells by focusing on the apoptotic pathway, which is the preferred cell death pathway for any novel drug candidate. The involvement of

apoptotic pathway was shown by the upregulation of pro-apoptotic genes and down-regulation of anti-apoptotic genes as well as activation of caspases. The biosynthesized AgNPs also activates the apoptotic pathway via increasing the ROS levels and decreased antioxidant levels. Our findings highlight the significant role of biosynthesized MNP and ANP as a promising novel option for cancer treatment.

This research extensively investigates the synthesis, characterization, and biological uses of silver nanoparticles. The distinct physicochemical characteristics of AgNPs, such as their substantial surface area-to-volume ratio and variable size, have been shown to significantly enhance their biological interactions, namely in the fields of antioxidative, antimicrobial, and anticancer applications. Further research into AgNPs synthesized using extracts from *M. micrantha* and *A. ciliata* could bring a promising application in the fields in agriculture and medicine. Nevertheless, it is crucial to acknowledge the challenges related to the clinical application of AgNPs. Future studies should prioritize refining the synthesis methods to produce AgNPs with enhanced biocompatibility and targeted therapeutic action, opening the path for future advancements in nanotechnology.



Certificate

This is to certify that the project entitled “**Antioxidant mediated hepatoprotective and cardioprotective effects of Silver nanoparticles (AgNPs) against Doxorubicin induced toxicity in Dalton’s Lymphoma Ascites bearing mice**” has been approved by the IAEC having IAEC approval No. **MZU/IAEC/2022-23/03**.

Authorized by	Name	Signature	Date
Chairman:	Prof. G. Gurusubramanian		27/5/2022
Member Secretary:	Dr. Amit Kumar Trivedi		28/5/2022
Main Nominee of:	Dr. Gunjan Das		28/5/22
CPCSEA:			

References

- Abdel-Aziz, M. S., Shaheen, M. S., El-Nekeety, A. A., & Abdel-Wahhab, M. A. (2014). Antioxidant and antibacterial activity of silver nanoparticles biosynthesized using *Chenopodium murale* leaf extract. *Journal of Saudi Chemical Society*, 18(4), 356-363. <https://doi.org/10.1016/j.jscs.2013.09.011>.
- Abeyesiri, G. R. P. I., Dharmadasa, R. M., Abeysinghe, D. C., & Samarasinghe, K. (2013). Screening of phytochemical, physico-chemical and bioactivity of different parts of *Acmella oleraceae* Murr.(Asteraceae), a natural remedy for toothache. *Industrial crops and products*, 50, 852-856. <https://doi.org/10.1016/j.indcrop.2013.08.043>
- Acharya, D., Satapathy, S., Somu, P., Parida, U. K., & Mishra, G. (2021). Apoptotic effect and anticancer activity of biosynthesized silver nanoparticles from marine algae *Chaetomorpha linum* extract against human colon cancer cell HCT-116. *Biological Trace Element Research*, 199(5), 1812-1822. doi: 10.1007/s12011-020-02304-7.
- Adamson, I. Y. (1976). Pulmonary toxicity of bleomycin. *Environmental health perspectives*, 16, 119-125.
- Adeyemi, J. O., Oriola, A. O., Onwudiwe, D. C., & Oyedele, A. O. (2022). Plant Extracts Mediated Metal-Based Nanoparticles: Synthesis and Biological Applications. *Biomolecules*, 12(5), 627. <https://doi.org/10.3390/biom12050627>.
- Adjou, E. S., Kouton, S., Dahouenon-Ahoussi, E., Sohounhloue, C. K., & M. M. Soumanou, M. M. (2012). Antifungal activity of *Ocimum canum* essential oil against toxinogenic fungi isolated from peanut seeds in post-harvest in Benin. *International Research Journal of Biological Sciences*, 1(7), 20–26.
- Agarwal, H., Kumar, S. V., & Rajeshkumar, S. (2017). A review on green synthesis of zinc oxide nanoparticles – An eco-friendly approach. *Resource-Efficient*

- Technologies*, 3(4), 406-413. doi: <https://doi.org/10.1016/j.reffit.2017.03.002>.
- Agati, G., Azzarello, E., Pollastri, S., & Tattini, M. (2012). Flavonoids as antioxidants in plants: location and functional significance. *Plant science*, 196, 67-76. doi:10.1016/j.plantsci.2012.07.014
- Agnihotri, S., Mukherji, S., & Mukherji, S. (2013). Immobilized silver nanoparticles enhance contact killing and show highest efficacy: elucidation of the mechanism of bactericidal action of silver. *Nanoscale*, 5(16), 7328-7340. <https://doi.org/10.1039/C3NR00024A>.
- Ahmad, N., Bhatnagar, S., Ali, S. S., & Dutta, R. (2015). Phytofabrication of bioinduced silver nanoparticles for biomedical applications. *International journal of nanomedicine*, 45(2), 7019-7030.
- Ahmad, N., Sharma, S., Alam, M. K., Singh, V. N., Shamsi, S. F., Mehta, B. R., & Fatma, A. (2010). Rapid synthesis of silver nanoparticles using dried medicinal plant of basil. *Colloids and Surfaces B: Biointerfaces*, 81(1), 81-86. <https://doi.org/10.1016/j.colsurfb.2010.06.029>.
- Ahmed, A. M., Mohammed, A. T., Bastawy, S., Attalla, H. A., Yousef, A. A., Abdelrazek, M. S., ... & Ghareeb, A. (2019). Serum biomarkers for the early detection of the early-onset neonatal sepsis: a single-center prospective study. *Advances in Neonatal Care*, 19(5), E26-E32. <https://doi.org/10.1097/ANC.0000000000000631>.
- Ahmed, M. J., Murtaza, G., Rashid, F., & Iqbal, J. (2019). Eco-friendly green synthesis of silver nanoparticles and their potential applications as antioxidant and anticancer agents. *Drug development and industrial pharmacy*, 45(10), 1682-1694.

- Ahmed, S., & Ikram, S.A. (2015). Silver nanoparticles: One Pot Green Synthesis Using *Terminalia arjuna* Extract for Biological Application. *Journal of Nanomedicine & Nanotechnology*, 6, 1-6. doi:10.4172/2157-7439.1000309.
- Ahmed, S., Ahmad, M., Swami, B. L., & Ikram, S. (2016). A review on plants extract mediated synthesis of silver nanoparticles for antimicrobial applications: a green expertise. *Journal of advanced research*, 7(1), 17-28.
- Alexander J. W. (2009). History of the medical use of silver. *Surgical infections*, 10(3), 289–292. <https://doi.org/10.1089/sur.2008.9941>.
- Alghuthaymi, M. A., Abd-Elsalam, K. A., AboDalem, H. M., Ahmed, F. K., Ravichandran, M., Kalia, A., & Rai, M. (2022). *Trichoderma*: An Eco-Friendly Source of Nanomaterials for Sustainable Agroecosystems. *Journal of fungi (Basel, Switzerland)*, 8(4), 367. <https://doi.org/10.3390/jof8040367>.
- Ali, M. H., Azad, M. A. K., Khan, K. A., Rahman, M. O., Chakma, U., & Kumer, A. (2023). Analysis of Crystallographic Structures and Properties of Silver Nanoparticles Synthesized Using PKL Extract and Nanoscale Characterization Techniques. *ACS omega*, 8(31), 28133–28142. <https://doi.org/10.1021/acsomega.3c01261>.
- Alivisatos, P. (2004). The use of nanocrystals in biological detection. *Nature biotechnology*, 22(1), 47-52.
- Allafchian, A. R., Mirahmadi-Zare, S. Z., Jalali, S. A. H., Hashemi, S. S., & Vahabi, M. R. (2016). Green synthesis of silver nanoparticles using phlomis leaf extract and investigation of their antibacterial activity. *Journal of Nanostructure in Chemistry*, 6, 129-135. <https://doi.org/10.1007/s40097-016-0187-0>.
- Almatroudi A. (2020). Silver nanoparticles: synthesis, characterisation and biomedical applications. *Open life sciences*, 15(1), 819–839. <https://doi.org/10.1515/biol-2020-0094>.

- Al-Sheddi, E. S., Farshori, N. N., Al-Oqail, M. M., Al-Massarani, S. M., Saquib, Q., Wahab, R., Musarrat, J., Al-Khedhairi, A.A. & Siddiqui, M. A. (2018). Anticancer potential of green synthesized silver nanoparticles using extract of *Nepeta deflersiana* against human cervical cancer cells (HeLA). *Bioinorganic Chemistry and Applications*, 2018(1), 9390784. doi:10.1155/2018/9390784
- Altammar, K. A. (2023). A review on nanoparticles: characteristics, synthesis, applications, and challenges. *Frontiers in microbiology*, 14, 1155622. <https://doi.org/10.3389/fmicb.2023.1155622>
- Amaral, J. D., Xavier, J. M., Steer, C. J., & Rodrigues, C. M. (2010). The role of p53 in apoptosis. *Discovery medicine*, 9(45), 145-152.
- Anand, P., Kunnumakara, A. B., Sundaram, C., Harikumar, K. B., Tharakan, S. T., Lai, O. S., Sung B & Aggarwal, B. B. (2008). Cancer is a preventable disease that requires major lifestyle changes. *Pharmaceutical research*, 25(9), 2097-2116.
- Ankamwar, B., Damle, C., Ahmad, A., & Sastry, M. (2005). Biosynthesis of gold and silver nanoparticles using *Emblica officinalis* fruit extract, their phase transfer and transmetallation in an organic solution. *Journal of nanoscience and nanotechnology*, 5(10), 1665-1671.
- Ansari, M. A., Khan, H. M., Alzohairy, M. A., Jalal, M., Ali, S. G., Pal, R., & Musarrat, J. (2015). Green synthesis of Al₂O₃ nanoparticles and their bactericidal potential against clinical isolates of multi-drug resistant *Pseudomonas aeruginosa*. *World journal of microbiology & biotechnology*, 31(1), 153–164. <https://doi.org/10.1007/s11274-014-1757-2>.
- Antunes Filho, S., Dos Santos, M. S., Dos Santos, O. A. L., Backx, B. P., Soran, M. L., Opreș, O., Lung, I., Stegarescu, A., & Bououdina, M. (2023). Biosynthesis of nanoparticles using plant extracts and essential oils. *Molecules*, 28(7), 3060.

- Apak, R., Özyürek, M., Güçlü, K., & Çapanoğlu, E. (2016). Antioxidant activity/capacity measurement. 1. Classification, physicochemical principles, mechanisms, and electron transfer (ET)-based assays. *Journal of agricultural and food chemistry*, 64(5), 997-1027.
- Arokiyaraj, S., Arasu, M. V., Vincent, S., Prakash, N. U., Choi, S. H., Oh, Y. K., Choi, K.C & Kim, K. H. (2014). Rapid green synthesis of silver nanoparticles from *Chrysanthemum indicum* L and its antibacterial and cytotoxic effects: an in vitro study. *International Journal of Nanomedicine*, 379-388.
- Arokiyaraj, S., Saravanan, M., & Badathala, V. (2015). Green Synthesis of Silver Nanoparticles Using Aqueous Extract of *Taraxacum officinale* and its Antimicrobial Activity. *South Indian Journal of Biological Sciences*, 1, 115-118.
- Arumugam, A., Karthikeyan, C., Haja Hameed, A. S., Gopinath, K., Gowri, S., & Karthika, V. (2015). Synthesis of cerium oxide nanoparticles using *Gloriosa superba* L. leaf extract and their structural, optical and antibacterial properties. *Materials science & engineering. C, Materials for biological applications*, 49, 408–415.
- Aruoma, O. I., & Halliwell, B. (1987). Superoxide-dependent and ascorbate-dependent formation of hydroxyl radicals from hydrogen peroxide in the presence of iron. Are lactoferrin and transferrin promoters of hydroxyl-radical generation?. *Biochemical Journal*, 241(1), 273-278. <https://doi.org/10.1042/bj2410273>.
- Asha, A., Sivaranjani, T., Thirunavukkarasu, P., & Asha, S. (2016). Green synthesis of silver nanoparticle from different plants—a review. *International Journal of Pure & Applied Bioscience*, 4(2), 118-124.
- Ashikawa, K., Shishodia, S., Fokt, I., Priebe, W., & Aggarwal, B. B. (2004). Evidence that activation of nuclear factor- κ B is essential for the cytotoxic effects of doxorubicin and its analogues. *Biochemical pharmacology*, 67(2), 353-364.

- Ashokkumar, S., Ravi, S., Kathiravan, V., & Velmurugan, S. (2014). Rapid biological synthesis of silver nanoparticles using *Leucas martinicensis* leaf extract for catalytic and antibacterial activity. *Environmental Science and Pollution Research*, 21, 11439-11446.
- Atiyeh, B. S., Costagliola, M., Hayek, S. N., & Dibo, S. A. (2007). Effect of silver on burn wound infection control and healing: review of the literature. *burns*, 33(2), 139-148.
- Austin, L. A., Mackey, M. A., Dreaden, E. C., & El-Sayed, M. A. (2014). The optical, photothermal, and facile surface chemical properties of gold and silver nanoparticles in biodiagnostics, therapy, and drug delivery. *Archives of toxicology*, 88, 1391-1417.
- Auyeung, A., Casillas-Santana, M. A., Martinez-Castanon, G. A., Slavin, Y. N., Zhao, W., Asnis, J., Häfeli, U.O. & Bach, H. (2017). Effective control of molds using a combination of nanoparticles. *PLoS One*, 12(1), e0169940.
- Avalos, A., Haza, A. I., Mateo, D., & Morales, P. (2014). Cytotoxicity and ROS production of manufactured silver nanoparticles of different sizes in hepatoma and leukemia cells. *Journal of applied toxicology*, 34(4), 413-423.
- Avilés, A., Arévila, N., Díaz Maqueo, J. C., & Nambo, M. J. (1993). Late cardiac toxicity of doxorubicin, epirubicin, and mitoxantrone therapy for Hodgkin's disease in adults. *Leukemia & lymphoma*, 11(3-4), 275-279.
- Awwad, A. M., Salem, N. M., & Abdeen, A. O. (2013). Green synthesis of silver nanoparticles using carob leaf extract and its antibacterial activity. *International journal of Industrial chemistry*, 4, 1-6.
<http://www.industchem.com/content/4/1/29>
- Awwad, A.M., Salem, N.M., Ibrahim, Q.M., & Abdeen, A.O. (2015). Phytochemical fabrication and characterization of silver/ silver chloride nanoparticles using *Albizia julibrissin* flowers extract. *Advanced Materials Letters*, 6, 726-730.

- Ayyub, P., Chandra, R., Taneja, P., Sharma, A. K., & Pinto, R. (2001). Synthesis of nanocrystalline material by sputtering and laser ablation at low temperatures. *Applied Physics A*, 73, 67-73.
- Azeez, L., Lateef, A., & Adebisi, S. A. (2017). Silver nanoparticles (AgNPs) biosynthesized using pod extract of *Cola nitida* enhances antioxidant activity and phytochemical composition of *Amaranthus caudatus* Linn. *Applied Nanoscience*, 7, 59-66.
- Bachur, N. R., Gordon, S. L., Gee, M. V., & Kon, H. (1979). NADPH cytochrome P-450 reductase activation of quinone anticancer agents to free radicals. *Proceedings of the National Academy of Sciences*, 76(2), 954-957. <https://doi.org/10.1073/pnas.76.2.954>.
- Badmus, J. A., Oyemomi, S. A., Fatoki, J. O., Yekeen, T. A., Adedosu, O. T., Adegbola, P. I., Azeez, M.A., Adebayo, E.A. & Lateef, A. (2022). Anti-haemolytic and cytogenotoxic potential of aqueous leaf extract of *Annona muricata* (L.) and its bio-fabricated silver nanoparticles. *Caryologia*, 75(1), 3-13. doi: 10.36253/caryologia-1353
- Badmus, S. O., Amusa, H. K., Oyehan, T. A., & Saleh, T. A. (2021). Environmental risks and toxicity of surfactants: overview of analysis, assessment, and remediation techniques. *Environmental Science and Pollution Research*, 28(44), 62085–62104. <https://doi.org/10.1007/s11356-021-16483-w>.
- Banala, R. R., Nagati, V. B., & Karnati, P. R. (2015). Green synthesis and characterization of Carica papaya leaf extract coated silver nanoparticles through X-ray diffraction, electron microscopy and evaluation of bactericidal properties. *Saudi journal of biological sciences*, 22(5), 637–644. <https://doi.org/10.1016/j.sjbs.2015.01.007>.
- Bar, H., Bhui, D. K., Sahoo, G. P., Sarkar, P., Pyne, S., & Misra, A. (2009). Green synthesis of silver nanoparticles using seed extract of *Jatropha*

- curcas. *Colloids and Surfaces A: Physicochemical and Engineering Aspects*, 348(1-3), 212-216. doi:10.1016/j.colsurfa.2009.07.021.
- Barcińska, E., Wierzbicka, J., Zauszkiewicz-Pawlak, A., Jacewicz, D., Dabrowska, A., & Inkielewicz-Stepniak, I. (2018). Role of Oxidative and Nitro-Oxidative Damage in Silver Nanoparticles Cytotoxic Effect against Human Pancreatic Ductal Adenocarcinoma Cells. *Oxidative Medicine and Cellular Longevity*, 2018(1), 8251961.
- Bardaweel, S. K., Gul, M., Alzweiri, M., Ishaqat, A., ALSalamat, H. A., & Bashatwah, R. M. (2018). Reactive Oxygen Species: The Dual Role in Physiological and Pathological Conditions of the Human Body. *The Eurasian journal of medicine*, 50(3), 193–201. <https://doi.org/10.5152/eurasianjmed.2018.17397>
- Basu, S., Maji, P., & Ganguly, J. (2016). Rapid green synthesis of silver nanoparticles by aqueous extract of seeds of *Nyctanthes arbor-tristis*. *Applied Nanoscience*, 6, 1-5.
- Bayda, S., Adeel, M., Tuccinardi, T., Cordani, M., & Rizzolio, F. (2019). The History of Nanoscience and Nanotechnology: From Chemical-Physical Applications to Nanomedicine. *Molecules (Basel, Switzerland)*, 25(1), 112. <https://doi.org/10.3390/molecules25010112>
- Beach, J. A., Nary, L. J., Hirakawa, Y., Holland, E., Hovanessian, R., & Medh, R. D. (2011). E4BP4 facilitates glucocorticoid-evoked apoptosis of human leukemic CEM cells via upregulation of Bim. *Journal of Molecular Signaling*, 6(1), 1-13.
- Bedlovičová, Z., Strapáč, I., Baláž, M., & Salayová, A. (2020). A Brief Overview on Antioxidant Activity Determination of Silver Nanoparticles. *Molecules (Basel, Switzerland)*, 25(14), 3191. <https://doi.org/10.3390/molecules25143191>.
- Beutler, E. (1984). In red cell metabolism. *A manual of biochemical methods*.

- Bhakya, S., Muthukrishnan, S., Sukumaran, M., & Muthukumar, M. (2016). Biogenic synthesis of silver nanoparticles and their antioxidant and antibacterial activity. *Applied Nanoscience*, 6, 755-766. <https://doi.org/10.1007/s13204-015-0473-z>.
- Bhatte, K. D., Deshmukh, K. M., Patil, Y. P., Sawant, D. N., Fujita, S. I., Arai, M., & Bhanage, B. M. (2012). Synthesis of powdered silver nanoparticles using hydrogen in aqueous medium. *Particuology*, 10(1), 140-143.
- Bhaumik, J., Thakur, N. S., Aili, P. K., Ghanghoriya, A., Mittal, A. K., & Banerjee, U. C. (2015). Bioinspired nanotheranostic agents: synthesis, surface functionalization, and antioxidant potential. *ACS Biomaterials Science & Engineering*, 1(6), 382-392.
- Bhutto, A. A., Kalay, Ş., Sherazi, S. T. H., & Culha, M. (2018). Quantitative structure–activity relationship between antioxidant capacity of phenolic compounds and the plasmonic properties of silver nanoparticles. *Talanta*, 189, 174-181.
- Bidian, C., Filip, G. A., David, L., Moldovan, B., Olteanu, D., Clichici, S., Olănescu-Vaida-Voevod, M.C., Leostean, C., Macavei, S., Muntean, D.M. & Baldea, I. (2023). Green synthesized gold and silver nanoparticles increased oxidative stress and induced cell death in colorectal adenocarcinoma cells. *Nanomaterials*, 13(7), 1251. doi:10.3390/nano13071251.
- Bindhu, M. R., & Umadevi, M. (2013). Synthesis of monodispersed silver nanoparticles using *Hibiscus cannabinus* leaf extract and its antimicrobial activity. *Spectrochimica Acta Part A: Molecular and Biomolecular Spectroscopy*, 101, 184-190.
- Bindhu, M. R., & Umadevi, M. (2015). Antibacterial and catalytic activities of green synthesized silver nanoparticles. *Spectrochimica acta part A: molecular and biomolecular spectroscopy*, 135, 373-378.

- Biswas, A., Vanlalveni, C., Adhikari, P. P., Lalfakzuala, R., & Rokhum, L. (2018). Green biosynthesis, characterisation and antimicrobial activities of silver nanoparticles using fruit extract of *Solanum viarum*. *IET nanobiotechnology*, 12(7), 933-938. doi: 10.1049/iet-nbt.2018.0050.
- Blecher, K., Nasir, A., & Friedman, A. (2011). The growing role of nanotechnology in combating infectious disease. *Virulence*, 2(5), 395-401.
- Boisselier, E., & Astruc, D. (2009). Gold nanoparticles in nanomedicine: preparations, imaging, diagnostics, therapies and toxicity. *Chemical society reviews*, 38(6), 1759-1782.
- Borchert, H., Shevchenko, E. V., Robert, A., Mekis, I., Kornowski, A., Grübel, G., & Weller, H. (2005). Determination of nanocrystal sizes: a comparison of TEM, SAXS, and XRD studies of highly monodisperse CoPt₃ particles. *Langmuir*, 21(5), 1931-1936.
- Borchmann, P., Hübel, K., Schnell, R., & Engert, A. (1997). Idarubicin: a brief overview on pharmacology and clinical use. *International journal of clinical pharmacology and therapeutics*, 35(2), 80-83.
- Box, V. G. (2007). The intercalation of DNA double helices with doxorubicin and nagalomycin. *Journal of Molecular Graphics and Modelling*, 26(1), 14-19.
- Bradford, M. M. (1976). A rapid and sensitive method for the quantitation of microgram quantities of protein utilizing the principle of protein-dye binding. *Analytical biochemistry*, 72(1-2), 248-254. <https://doi.org/10.1006/abio.1976.9999>.
- Breslow, N. E., Ou, S. S., Beckwith, J. B., Haase, G. M., Kalapurakal, J. A., Ritchey, M. L., Shamberger, R.C., Thomas, P.R., D'Angio, G.J. & Green, D. M. (2004). Doxorubicin for favorable histology, stage II–III Wilms tumor: results from the National Wilms Tumor Studies. *Cancer*, 101(5), 1072-1080.
- Brodusch, N., Brahimi, S. V., Barbosa De Melo, E., Song, J., Yue, S., Piché, N., & Gauvin, R. (2021). Scanning Electron Microscopy versus Transmission

- Electron Microscopy for Material Characterization: A Comparative Study on High-Strength Steels. *Scanning*, 2021(1), 5511618. <https://doi.org/10.1155/2021/5511618>
- Brown, A. N., Smith, K., Samuels, T. A., Lu, J., Obare, S. O., & Scott, M. E. (2012). Nanoparticles functionalized with ampicillin destroy multiple-antibiotic-resistant isolates of *Pseudomonas aeruginosa* and *Enterobacter aerogenes* and methicillin-resistant *Staphylococcus aureus*. *Applied and environmental microbiology*, 78(8), 2768-2774.
- Brown, G. C., & Borutaite, V. (2001). Nitric oxide, mitochondria, and cell death. *IUBMB life*, 52(3-5), 189-195. <https://doi.org/10.1080/15216540152845993>.
- Bruna, T., Maldonado-Bravo, F., Jara, P., & Caro, N. (2021). Silver Nanoparticles and Their Antibacterial Applications. *International journal of molecular sciences*, 22(13), 7202. <https://doi.org/10.3390/ijms22137202>.
- Buege, J. A., & Aust, S. D. (1978). Microsomal lipid peroxidation. In *Methods in enzymology*, 52, 302-310). Academic press.
- Bunghez, I. R., Barbinta Patrascu, M. E., Badea, N. M., Doncea, S. M., Popescu, A., & Ion, R. M. (2012). Antioxidant silver nanoparticles green synthesized using ornamental plants. *Journal of optoelectronics and advanced materials*, 14(11), 1016.
- Burda, C., Chen, X., Narayanan, R., & El-Sayed, M. A. (2005). Chemistry and properties of nanocrystals of different shapes. *Chemical reviews*, 105(4), 1025-1102.
- Cameron, S. J., Hosseinian, F., & Willmore, W. G. (2018). A Current Overview of the Biological and Cellular Effects of Nanosilver. *International journal of molecular sciences*, 19(7), 2030. <https://doi.org/10.3390/ijms19072030>.
- Cardoso, S., Santos, R. X., Carvalho, C., Correia, S., Pereira, G. C., Pereira, S. S.,

- Oliveira, P.J., Santos, M.S., Proença, T. & Moreira, P. I. (2008). Doxorubicin increases the susceptibility of brain mitochondria to Ca^{2+} -induced permeability transition and oxidative damage. *Free Radical Biology and Medicine*, 45(10), 1395-1402.
- Carlson, C. (2006). *In vitro toxicity assessment of silver nanoparticles in rat alveolar macrophages* (Master's thesis, Wright State University).
- Carvalho, C., Santos, R. X., Cardoso, S., Correia, S., Oliveira, P. J., Santos, M. S., & Moreira, P. I. (2009). Doxorubicin: the good, the bad and the ugly effect. *Current medicinal chemistry*, 16(25), 3267-3285. <https://doi.org/10.2174/092986709788803312>.
- Castellano, J. J., Shafii, S. M., Ko, F., Donate, G., Wright, T. E., Mannari, R. J., Payne, W.G., Smith, D.J. & Robson, M. C. (2007). Comparative evaluation of silver-containing antimicrobial dressings and drugs. *International wound journal*, 4(2), 114-122.
- Caswell, K. K., Bender, C. M., & Murphy, C. J. (2003). Seedless, surfactantless wet chemical synthesis of silver nanowires. *Nano Letters*, 3(5), 667-669.
- Cataleya, C. (2006) In vitro toxicity assessment of silver nanoparticles in rat alveolar macrophages., Master thesis, Wright state University, USA, 1-75.
- Chaloupka, K., Malam, Y., & Seifalian, A. M. (2010). Nanosilver as a new generation of nanoparticle in biomedical applications. *Trends in Biotechnology*, 28(11), 580–588. doi:10.1016/j.tibtech.2010.07.006.
- Chanda A., & Mohanta D. Nanotechnology-a potent pharmacological tool (2016). *International Journal of Research in Advent Technology*, 4 (3), 6-16.
- Chang, S. T., Wu, J. H., Wang, S. Y., Kang, P. L., Yang, N. S., & Shyur, L. F. (2001). Antioxidant activity of extracts from *Acacia confusa* bark and heartwood. *Journal of Agricultural and Food chemistry*, 49(7), 3420-3424.

- Chang, X., Wang, X., Li, J., Shang, M., Niu, S., Zhang, W., ... & Xue, Y. (2021). Silver nanoparticles induced cytotoxicity in HT22 cells through autophagy and apoptosis via PI3K/AKT/mTOR signaling pathway. *Ecotoxicology and Environmental Safety*, 208, 111696. doi:10.1016/j.ecoenv.2020.111696.
- Chaudhuri, J., Basu, U., Zarrin, A., Yan, C., Franco, S., Perlot, T., T., Vuong, B., Wang, J., Phan, R.T., Datta, A. & Manis, J. (2007). Evolution of the immunoglobulin heavy chain class switch recombination mechanism. *Advances in immunology*, 94, 157-214. [https://doi.org/10.1016/S0065-2776\(06\)94006-1](https://doi.org/10.1016/S0065-2776(06)94006-1).
- Chen, Y. L., Tuan, H. Y., Tien, C. W., Lo, W. H., Liang, H. C., & Hu, Y. C. (2009). Augmented biosynthesis of cadmium sulfide nanoparticles by genetically engineered *Escherichia coli*. *Biotechnology progress*, 25(5), 1260-1266. <https://doi.org/10.1002/btpr.199>.
- Cheng, G., Dai, M., Ahmed, S., Hao, H., Wang, X., & Yuan, Z. (2016). Antimicrobial drugs in fighting against antimicrobial resistance. *Frontiers in Microbiology*, 7, 470. <https://doi.org/10.3389/fmicb.2016.00470>.
- Chikdu D., Pal P., Gujar A., Deshemukh R., Kate S. Green synthesis and characterization of silver nanoparticles using *Aloe barbadensis* and its antibacterial activity. *Journal of Global Bioscience*, 4 (7), 2015, 2713-2719. 11.
- Christian, P., Von der Kammer, F., Baalousha, M., & Hofmann, T. (2008). Nanoparticles: structure, properties, preparation and behaviour in environmental media. *Ecotoxicology*, 17, 326-343.
- Chung, I. M., Park, I., Seung-Hyun, K., Thiruvengadam, M., & Rajakumar, G. (2016). Plant-mediated synthesis of silver nanoparticles: their characteristic properties and therapeutic applications. *Nanoscale research letters*, 11, 1-14.
- Chung, I. M., Park, I., Seung-Hyun, K., Thiruvengadam, M., & Rajakumar, G. (2016). Plant-Mediated Synthesis of Silver Nanoparticles: Their Characteristic Properties and Therapeutic Applications. *Nanoscale research letters*, 11(1), 40. <https://doi.org/10.1186/s11671-016-1257-4>.

- Costantini, P., Chernyak, B. V., Petronilli, V., & Bernardi, P. (1996). Modulation of the Mitochondrial Permeability Transition Pore by Pyridine Nucleotides and Dithiol Oxidation at Two Separate Sites (*). *Journal of Biological Chemistry*, 271(12), 6746-6751.
- Coyle, J. T., & Puttfarcken, P. (1993). Oxidative stress, glutamate, and neurodegenerative disorders. *Science*, 262(5134), 689-695.
- Cutts, S. M., Parsons, P. G., Sturm, R. A., & Phillips, D. R. (1996). Adriamycin-induced DNA adducts inhibit the DNA interactions of transcription factors and RNA polymerase. *Journal of Biological Chemistry*, 271(10), 5422-5429.
- Dahoumane, S. A., Mechouet, M., Wijesekera, K., Filipe, C. D. M., Sicard, C., Bazylnski, D. A., Clayton, J. (2017). Algae-mediated biosynthesis of inorganic nanomaterials as a promising route in nanobiotechnology – a review". The Royal Society of Chemistry, 19(3),552-887. <https://doi.org/10.1039/C6GC02346K>.
- Dahoumane, S.A., Yéprémian, C., Djédiat, C., Couté, A., Fiévet, F., Coradin, T., & Brayner, R. (2016). Improvement of kinetics, yield, and colloidal stability of biogenic gold nanoparticles using living cells of *Euglena gracilis* microalga. *Journal of Nanoparticle Research*, 18, 1-12. <https://doi.org/10.1007/s11051-016-3378-1>.
- Dai, J., & Bruening, M. L. (2002). Catalytic nanoparticles formed by reduction of metal ions in multilayered polyelectrolyte films. *Nano Letters*, 2(5), 497-501.
- Dakal, T. C., Kumar, A., Majumdar, R. S., & Yadav, V. (2016). Mechanistic basis of antimicrobial actions of silver nanoparticles. *Frontiers in microbiology*, 7, 1831.
- Danesi, R., Fogli, S., Gennari, A., Conte, P., & Del Tacca, M. (2002). Pharmacokinetic-pharmacodynamic relationships of the anthracycline anticancer drugs. *Clinical pharmacokinetics*, 41, 431-444.

- Daniel, M. C., & Astruc, D. (2004). Gold nanoparticles: assembly, supramolecular chemistry, quantum-size-related properties, and applications toward biology, catalysis, and nanotechnology. *Chemical reviews*, 104(1), 293–346. <https://doi.org/10.1021/cr030698>.
- Das, G., Patra, J. K., Basavegowda, N., Vishnuprasad, C. N., & Shin, H. S. (2019). Comparative study on antidiabetic, cytotoxicity, antioxidant and antibacterial properties of biosynthesized silver nanoparticles using outer peels of two varieties of Ipomoea batatas (L.) Lam. *International Journal of Nanomedicine*, 4741-4754.
- Dawadi, S., Katuwal, S., Gupta, A., Lamichhane, U., Thapa, R., Jaisi, S., Lamichhane, G., Bhattarai, D.P & Parajuli, N. (2021). Current research on silver nanoparticles: synthesis, characterization, and applications. *Journal of nanomaterials*, 2021(1), 6687290. <https://doi.org/10.1155/2021/6687290>.
- de Brito, F. A. E., de Freitas, A. P. P., & Nascimento, M. S. (2022). Multidrug-Resistant Biofilms (MDR): Main Mechanisms of Tolerance and Resistance in the Food Supply Chain. *Pathogens (Basel, Switzerland)*, 11(12), 1416. <https://doi.org/10.3390/pathogens11121416>.
- Dela Paz, M., Goodwin, P. H., Raymundo, A. K., Ardales, E. Y., Vera Cruz, C. M. (2006). Phylogenetic analysis based on ITS sequences and conditions affecting the type of conidial germination of Bipolaris oryzae. *Plant Pathology*, 55(8), 756–765.
- Della Torre, P., Imondi, A. R., Bernardi, C., Podestà, A., Moneta, D., Riflettuto, M., & Mazué, G. (1999). Cardioprotection by dexrazoxane in rats treated with doxorubicin and paclitaxel. *Cancer chemotherapy and pharmacology*, 44, 138-142. <https://doi.org/10.1007/s002800050958>.
- Docea, A. O., Calina, D., Buga, A. M., Zlatian, O., Paoliello, M. M. B., Mogosanu, G. D., G.D., Streba, C.T., Popescu, E.L., Stoica, A.E., Bîrcă, A.C., Vasile, B.Ş., & Mogoanta, L. (2020). The effect of silver nanoparticles on antioxidant/pro-

- oxidant balance in a murine model. *International Journal of Molecular Sciences*, 21(4), 1233.
- Dong, L. M., Jia, X. C., Luo, Q. W., Zhang, Q., Luo, B., Liu, W. B., Zhang, X., Xu, Q.L. & Tan, J. W. (2017). Phenolics from *Mikania micrantha* and their antioxidant activity. *Molecules*, 22(7), 1140. <https://doi.org/10.3390/molecules22071140>.
- Dong, Z. Y., Narsing Rao, M. P., Xiao, M., Wang, H. F., Hozzein, W. N., Chen, W., & Li, W. J. (2017). Antibacterial Activity of Silver Nanoparticles against *Staphylococcus warneri* Synthesized Using Endophytic Bacteria by Photo-irradiation. *Frontiers in microbiology*, 8, 1090. <https://doi.org/10.3389/fmicb.2017.01090>
- Dou, X., Zhang, Y., Sun, N., Wu, Y., & Li, L. (2014). The anti-tumor activity of *Mikania micrantha* aqueous extract in vitro and in vivo. *Cytotechnology*, 66, 107-117. doi: 10.1007/s10616-013-9543-9.
- Drake, J. A., Mooney, H. A., Castri, F. D., Groves, R. H., Kruger, F. J., Williamson, M. (1989). *Biological Invasions: A Global Perspective*. *Biometrics*, 47(1), 352. doi:10.2307/2532533.
- Du, L., Suo, S., Wang, G., Jia, H., Liu, K. J., Zhao, B., & Liu, Y. (2013). Mechanism and cellular kinetic studies of the enhancement of antioxidant activity by using surface-functionalized gold nanoparticles. *Chemistry—A European Journal*, 19(4), 1281-1287.
- Dubey, S., Maity, S., Singh, M., Saraf, S. A., & Saha, S. (2013). Phytochemistry, pharmacology and toxicology of *Spilanthes acmella*: a review. *Advances in Pharmacological and Pharmaceutical Sciences*, 2013(1), 423750. <https://doi.org/10.1155/2013/423750>.
- Durán, N., Marcato, P. D., Conti, R. D., Alves, O. L., Costa, F., & Brocchi, M. (2010). Potential use of silver nanoparticles on pathogenic bacteria, their toxicity and

- possible mechanisms of action. *Journal of the Brazilian Chemical Society*, 21, 949-959.
- Dwivedi, A. D., & Gopal, K. (2010). Biosynthesis of silver and gold nanoparticles using *Chenopodium album* leaf extract. *Colloids and Surfaces A: Physicochemical and Engineering Aspects*, 369(1-3), 27-33. <https://doi.org/10.1016/j.colsurfa.2010.07.020>.
- Ebrahimzadeh, M. A., Nabavi, S. F., & Nabavi, S. M. (2009). Antioxidant activities of methanol extract of *Sambucus ebulus* L. flower. *Pakistan journal of biological sciences: PJBS*, 12(5), 447-450.
- Eder, A. R., & Arriaga, E. A. (2006). Capillary electrophoresis monitors enhancement in subcellular reactive oxygen species production upon treatment with doxorubicin. *Chemical research in toxicology*, 19(9), 1151-1159.
- Edison, T. N. J. I., Atchudan, R., Kamal, C., & Lee, Y. R. (2016). *Caulerpa racemosa*: a marine green alga for eco-friendly synthesis of silver nanoparticles and its catalytic degradation of methylene blue. *Bioprocess and Biosystems Engineering*, 39, 1401-1408. <https://doi.org/10.1007/s00449-016-1616-7>.
- Elberry, A. A., Abdel-Naim, A. B., Abdel-Sattar, E. A., Nagy, A. A., Mosli, H. A., Mohamadin, A. M., & Ashour, O. M. (2010). Cranberry (*Vaccinium macrocarpon*) protects against doxorubicin-induced cardiotoxicity in rats. *Food and chemical toxicology*, 48(5), 1178-1184. <https://doi.org/10.1016/j.fct.2010.02.008>.
- Elemike, E. E., Fayemi, O. E., Ekennia, A. C., Onwudiwe, D. C., & Ebenso, E. E. (2017). Silver nanoparticles mediated by *Costus afer* leaf extract: synthesis, antibacterial, antioxidant and electrochemical properties. *Molecules*, 22(5), 701.
- Ellis, M. B. (1965). Dematiaceous Hyphomycetes. Commonwealth Mycological Institute, Kew. *Mycological Papers*, 103(29), 1-46.

- El-Rafie, H. M., El-Rafie, M., & Zahran, M. K. (2013). Green synthesis of silver nanoparticles using polysaccharides extracted from marine macro algae. *Carbohydrate polymers*, 96(2), 403-410. <https://doi.org/10.1016/j.carbpol.2013.03.071>.
- Elshikh, M., Ahmed, S., Funston, S., Dunlop, P., McGaw, M., Marchant, R., & Banat, I. M. (2016). Resazurin-based 96-well plate microdilution method for the determination of minimum inhibitory concentration of biosurfactants. *Biotechnology letters*, 38(6), 1015–1019. <https://doi.org/10.1007/s10529-016-2079-2>.
- Ewer, M. S., & Ewer, S. M. (2010). Cardiotoxicity of anticancer treatments: what the cardiologist needs to know. *Nature Reviews Cardiology*, 7(10), 564-575.
- Fageria, L., Pareek, V., Dilip, R. V., Bhargava, A., Pasha, S. S., Laskar, I. R., ... & Panwar, J. (2017). Biosynthesized protein-capped silver nanoparticles induce ROS-dependent proapoptotic signals and prosurvival autophagy in cancer cells. *ACS omega*, 2(4), 1489-1504. doi: 10.1021/acsomega.7b00045.
- Fahn, S., & Cohen, G. (1992). The oxidant stress hypothesis in Parkinson's disease: evidence supporting it. *Annals of neurology*, 32(6), 804-812.
- Fahrenholtz, C. D., Swanner, J., Ramirez-Perez, M., & Singh, R. N. (2017). Heterogeneous responses of ovarian cancer cells to silver nanoparticles as a single agent and in combination with cisplatin. *Journal of Nanomaterials*, 2017(1), 5107485. <https://doi.org/10.1155/2017/5107485>.
- Farah, M. A., Ali, M. A., Chen, S. M., Li, Y., Al-Hemaid, F. M., Abou-Tarboush, F. M., Al-Anazi, K.M & Lee, J. (2016). Silver nanoparticles synthesized from *Adenium obesum* leaf extract induced DNA damage, apoptosis and autophagy via generation of reactive oxygen species. *Colloids and Surfaces B: Biointerfaces*, 141, 158-169.

- Farooq, U., Ahmad, T., Khan, A., Sarwar, R., Shafiq, J., Raza, Y., Ahmed, A., Ullah, S., Ur Rehman, N., & Al-Harrasi, A. (2019). Rifampicin conjugated silver nanoparticles: a new arena for development of antibiofilm potential against methicillin resistant *Staphylococcus aureus* and *Klebsiella pneumoniae*. *International journal of nanomedicine*, 14, 3983–3993. <https://doi.org/10.2147/IJN.S198194>
- Fatima, F., Verma, S. R., Pathak, N., & Bajpai, P. (2016). Extracellular mycosynthesis of silver nanoparticles and their microbicidal activity. *Journal of global antimicrobial resistance*, 7, 88-92.
- Fendler, J. H., & Meldrum, F. C. (1995). The colloid chemical approach to nanostructured materials. *Advanced Materials*, 7(7), 607-632.
- Feng, Q. L., Wu, J., Chen, G. Q., Cui, F. Z., Kim, T. N., & Kim, J. O. (2000). A mechanistic study of the antibacterial effect of silver ions on *Escherichia coli* and *Staphylococcus aureus*. *Journal of biomedical materials research*, 52(4), 662-668.
- Fenoglio, I., Corazzari, I., Francia, C., Bodoardo, S., & Fubini, B. (2008). The oxidation of glutathione by cobalt/tungsten carbide contributes to hard metal-induced oxidative stress. *Free radical research*, 42(8), 437-745. <https://doi.org/10.1080/10715760802350904>.
- Firuzi, O., Miri, R., Tavakkoli, M., & Saso, L. (2011). Antioxidant therapy: current status and future prospects. *Current medicinal chemistry*, 18(25), 3871-3888. doi:10.2174/092986711803414368.
- Fissan, H., Ristig, S., Kaminski, H., Asbach, C., & Epple, M. (2014). Comparison of different characterization methods for nanoparticle dispersions before and after aerosolization. *Analytical Methods*, 6(18), 7324-7334.
- Flieger, J., Flieger, W., Baj, J., & Maciejewski, R. (2021). Antioxidants: Classification, natural sources, activity/capacity measurements, and usefulness for the

- synthesis of nanoparticles. *Materials*, 14(15), 4135. <https://doi.org/10.3390/ma14154135>.
- Fraiser, L. H., Kanekal, S., & Kehrer, J. P. (1991). Cyclophosphamide toxicity: characterising and avoiding the problem. *Drugs*, 42, 781-795.
- Franco-Molina, M. A., Mendoza-Gamboa, E., Sierra-Rivera, C. A., Gómez-Flores, R. A., Zapata-Benavides, P., Castillo-Tello, P., Alcocer-González, J.M., Miranda-Hernández, D.F., Tamez-Guerra, R.S. & Rodríguez-Padilla, C. (2010). Antitumor activity of colloidal silver on MCF-7 human breast cancer cells. *Journal of Experimental & Clinical Cancer Research*, 29, 1-7.
- Franken, N. A., Rodermond, H. M., Stap, J., Haveman, J., & Van Bree, C. (2006). Clonogenic assay of cells in vitro. *Nature protocols*, 1(5), 2315-2319. <https://doi.org/10.1038/nprot.2006.339>.
- Fried, R. (1975). Enzymatic and non-enzymatic assay of superoxide dismutase. *Biochimie*, 57(5), 657-660. [https://doi.org/10.1016/S0300-9084\(75\)80147-7](https://doi.org/10.1016/S0300-9084(75)80147-7).
- Galluzzi, L., Brunet, M., Puig, P. E., Didelot, C., & Kroemer, G. (2006). Mechanisms of cytochrome c release from mitochondria. *Cell Death & Differentiation*, 13(9).
- Gao, X., Cui, Y., Levenson, R. M., Chung, L. W., & Nie, S. (2004). In vivo cancer targeting and imaging with semiconductor quantum dots. *Nature biotechnology*, 22(8), 969-976.
- Gaschler, M. M., & Stockwell, B. R. (2017). Lipid peroxidation in cell death. *Biochemical and biophysical research communications*, 482(3), 419-425. <https://doi.org/10.1016/j.bbrc.2016.10.086>.
- Gavade, N. L., Kadam, A. N., Suwarnkar, M. B., Ghodake, V. P., & Garadkar, K. M. (2015). Biogenic synthesis of multi-applicative silver nanoparticles by using *Ziziphus Jujuba* leaf extract. *Spectrochimica Acta Part A: Molecular and*

- Biomolecular Spectroscopy*, 136, 953-960.
<https://doi.org/10.1016/j.saa.2014.09.118>
- Gavarkar, S. P., Adnaik, S. R., Mohite, K. S., & Magdum, S. C. (2015). Green synthesis and antimicrobial activity of silver nanoparticles of *Cucumismelo* extract. *International Journal of Universal Pharma Bio sciences*, 3(4), 392-396.
- Gavas, S., Quazi, S., & Karpiński, T. M. (2021). Nanoparticles for Cancer Therapy: Current Progress and Challenges. *Nanoscale research letters*, 16(1), 173.
<https://doi.org/10.1186/s11671-021-03628-6>
- Ge, L., Li, Q., Wang, M., Ouyang, J., Li, X., & Xing, M. M. (2014). Nanosilver particles in medical applications: synthesis, performance, and toxicity. *International journal of nanomedicine*, 9, 2399–2407.
<https://doi.org/10.2147/IJN.S55015>.
- Gericke, M., & Pinches, A. (2006). Microbial production of gold nanoparticles. *Gold bulletin*, 39(1), 22-28. <https://doi.org/10.1007/BF03215529>.
- Gill, R. K., Arora, S., & Thukral, A. K. (2015). Evaluation of protective effects (antioxidant and antimutagenic) of methanol extract of seeds of *Chlorophytum borivillianum* Sant. et Fernand. *Journal of Pharmacognosy and Phytochemistry*, 3(5), 167-172.
- Gilman, J. C. (1957). A manual of soil fungi. The Iowa State Univ. Press. Ames, Iowa, *Soil Science*, 84(2), 183.
- Giri, P. K., Bhattacharyya, S., Singh, D. K., Kesavamoorthy, R., Panigrahi, B. K., & Nair, K. G. M. (2007). Correlation between microstructure and optical properties of ZnO nanoparticles synthesized by ball milling. *Journal of Applied Physics*, 102(9).
- Gonzalez, L., Loza, R. J., Han, K. Y., Sunoqrot, S., Cunningham, C., Purta, P., Drake, J., Jain, S., Hong, S. & Chang, J. H. (2013). Nanotechnology in corneal

- neovascularization therapy—a review. *Journal of ocular pharmacology and therapeutics*, 29(2), 124-134.
- Gopinath, K., Karthika, V., Gowri, S., [Senthilkumar](#), V., [Kumaresan](#), S., & [Arumugam](#), A. (2014). Antibacterial activity of ruthenium nanoparticles synthesized using *Gloriosa superba* L. leaf extract. *Journal of Nanostructure in Chemistry*, 4, 83. <https://doi.org/10.1007/s40097-014-0083-4>.
- Gopinath, V., & Velusamy, P. (2013). Extracellular biosynthesis of silver nanoparticles using *Bacillus* sp. GP-23 and evaluation of their antifungal activity towards *Fusarium oxysporum*. *Spectrochimica acta. Part A, Molecular and biomolecular spectroscopy*, 106, 170–174. <https://doi.org/10.1016/j.saa.2012.12.087>
- Gou, Y., Zhou, R., Ye, X., Gao, S., & Li, X. (2015). Highly efficient *in vitro* biosynthesis of silver nanoparticles using *Lysinibacillus sphaericus* MR-1 and their characterization. *Science and Technology of Advanced Materials*, 16(1) 1-8. <https://doi.org/10.1088/1468-6996/16/1/015004>.
- Grätzel, M. (2001). Photoelectrochemical cells. *nature*, 414(6861), 338-344.
- Guilger, M., Pasquoto-Stigliani, T., Bilesky-Jose, N., Grillo, R., Abhilash, P. C., Fraceto, L. F., & Lima, R. D. (2017). Biogenic silver nanoparticles based on *Trichoderma harzianum*: synthesis, characterization, toxicity evaluation and biological activity. *Scientific reports*, 7(1), 44421.
- Gupta, N., Verma, K., Nalla, S., Kulshreshtha, A., Lall, R., & Prasad, S. (2020). Free radicals as a double-edged sword: The cancer preventive and therapeutic roles of *Curcumin*. *Molecules*, 25(22), 5390. <https://doi.org/10.3390/molecules25225390>.
- Gurunathan, S., Han, J. W., Eppakayala, V., Jeyaraj, M., & Kim, J. H. (2013). Cytotoxicity of biologically synthesized silver nanoparticles in MDA-MB-

- 231 human breast cancer cells. *BioMed research international*, 2013(1), 535796. doi:10.1155/2013/535796
- Hackenberg, S., Scherzed, A., Kessler, M., Hummel, S., Technau, A., Froelich, K., Ginzkey, C., Koehler, C., Hagen, R., & Kleinsasser, N. (2011). Silver nanoparticles: evaluation of DNA damage, toxicity and functional impairment in human mesenchymal stem cells. *Toxicology letters*, 201(1), 27–33. <https://doi.org/10.1016/j.toxlet.2010.12.001>
- Hahn, M. (2014). The rising threat of fungicide resistance in plant pathogenic fungi: Botrytis as a case study. *Journal of chemical biology*, 7, 133-141.
- Halliwell, B., & Gutteridge, J. M. (2015). Oxygen: boon yet bane—introducing oxygen toxicity and reactive species. *Free radicals in biology and medicine*, 1-29. <https://doi.org/10.1093/acprof:oso/9780198717478.003.0001>
- Hamouda, R. A., Hussein, M. H., Abo-Elmagd, R. A., & Bawazir, S. S. (2019). Synthesis and biological characterization of silver nanoparticles derived from the cyanobacterium *Oscillatoria limnetica*. *Scientific reports*, 9(1), 13071.
- Hamouda, R. A., Qarabai, F. A. K., Shahabuddin, F. S., Al-Shaikh, T. M., & Makharita, R. R. (2023). Antibacterial Activity of Ulva/Nanocellulose and Ulva/Ag/Cellulose Nanocomposites and Both Blended with Fluoride against Bacteria Causing Dental Decay. *Polymers*, 15(4), 1047. <https://doi.org/10.3390/polym15041047>.
- Hashem, A. H., Saied, E., Amin, B. H., Alotibi, F. O., Al-Askar, A. A., Arishi, A. A., Elkady, F.M. & Elbahnasawy, M. A. (2022). Antifungal activity of biosynthesized silver nanoparticles (AgNPs) against *aspergillus* causing aspergillosis: Ultrastructure Study. *Journal of Functional Biomaterials*, 13(4), 242. <https://doi.org/10.3390/jfb13040242>.
- Hass, D. T., & Barnstable, C. J. (2021). Uncoupling proteins in the mitochondrial defense against oxidative stress. *Progress in retinal and eye research*, 83, 100941. <https://doi.org/10.1016/j.preteyeres.2021.100941>.

- Hayes, J. D., Dinkova-Kostova, A. T., & Tew, K. D. (2020). Oxidative stress in cancer. *Cancer cell*, 38(2), 167-197. doi:10.1016/j.ccell.2020.06.001
- Hojjat, S. S., & Hojjat, H. (2016). Effects of silver nanoparticle exposure on germination of Lentil. *Int. J. Farm. Allied Sci*, 5(3), 248-252.
- Holder, C. F., & Schaak, R. E. (2019). Tutorial on powder X-ray diffraction for characterizing nanoscale materials. *Acs Nano*, 13(7), 7359-7365. DOI: 10.1021/acsnano.9b05157.
- Hollstein, M., Alexandrov, L. B., Wild, C. P., Ardin, M., & Zavadil, J. (2017). Base changes in tumor DNA have the power to reveal the causes and evolution of cancer. *Oncogene*, 36(2), 158-167.
- Holohan, C., Van Schaeybroeck, S., Longley, D. B., & Johnston, P. G. (2013). Cancer drug resistance: an evolving paradigm. *Nature reviews. Cancer*, 13(10), 714–726. <https://doi.org/10.1038/nrc3599>.
- Homan, K. A., Souza, M., Truby, R., Luke, G. P., Green, C., Vreeland, E., & Emelianov, S. (2012). Silver nanoplate contrast agents for in vivo molecular photoacoustic imaging. *ACS nano*, 6(1), 641-650.
- Hsiao, I. L., Hsieh, Y. K., Wang, C. F., Chen, I. C., & Huang, Y. J. (2015). Trojan-horse mechanism in the cellular uptake of silver nanoparticles verified by direct intra- and extracellular silver speciation analysis. *Environmental science & technology*, 49(6), 3813-3821. <https://doi.org/10.1021/es504705p>.
- Hsin, Y. H., Chen, C. F., Huang, S., Shih, T. S., Lai, P. S., & Chueh, P. J. (2008). The apoptotic effect of nanosilver is mediated by a ROS-and JNK-dependent mechanism involving the mitochondrial pathway in NIH3T3 cells. *Toxicology letters*, 179(3), 130-139.
- Hsueh, Y. H., Lin, K. S., Ke, W. J., Hsieh, C. T., Chiang, C. L., Tzou, D. Y., & Liu, S. T. (2015). The antimicrobial properties of silver nanoparticles in *Bacillus subtilis* are mediated by released Ag⁺ ions. *PloS one*, 10(12), e0144306.

- Huang, J., Li, Q., Sun, D., Lu, Y., Su, Y., Yang, X., Wang, H., Wang, Y., Shao, W., He, N., Hong, J. & Chen, C. (2007). Biosynthesis of silver and gold nanoparticles by novel sundried *Cinnamomum camphora* leaf. *Nanotechnology*, 18(10), 105104. <https://doi.org/10.1088/0957-4484/18/10/105104>.
- Hudzicki, J. (2009). Kirby-Bauer disk diffusion susceptibility test protocol. *American society for microbiology*, 15(1), 1-23.
- Huebner, C., Roggelin, M., & Flessa, S. (2016). Economic burden of multidrug-resistant bacteria in nursing homes in Germany: a cost analysis based on empirical data. *BMJ open*, 6(2), e008458.
- Husain, S., Nandi, A., Simnani, F. Z., Saha, U., Ghosh, A., Sinha, A., Sahay, A., Samal, S. K., Panda, P. K., & Verma, S. K. (2023). Emerging Trends in Advanced Translational Applications of Silver Nanoparticles: A Progressing Dawn of Nanotechnology. *Journal of Functional Biomaterials*, 14(1), 47. <https://doi.org/10.3390/jfb14010047>.
- Husen, A., & Siddiqi, K. S. (2014). Plants and microbes assisted selenium nanoparticles: characterization and application. *Journal of nanobiotechnology*, 12, 1-10.
- Ibrahim, Haytham M.M. (2015). Green synthesis and characterization of silver nanoparticles using banana peel extract and their antimicrobial activity against representative microorganisms. *Journal of Radiation Research and Applied Sciences*, 8(3), 265–275. doi:10.1016/j.jrras.2015.01.007.
- Im, S. H., Lee, Y. T., Wiley, B., & Xia, Y. (2005). Large-scale synthesis of silver nanocubes: the role of hcl in promoting cube perfection and monodispersity. *Angewandte Chemie International Edition*, 44(14), 2154-2157.
- Ioele, G., Chieffallo, M., Occhiuzzi, M. A., De Luca, M., Garofalo, A., Ragno, G., & Grande, F. (2022). Anticancer Drugs: Recent Strategies to Improve Stability Profile, Pharmacokinetic and Pharmacodynamic

- Properties. *Molecules*, 27(17), 5436.
<https://doi.org/10.3390/molecules27175436>.
- Iravani, S. (2011). Green synthesis of metal nanoparticles using plants. *Green chemistry*, 13(10), 2638-2650. <https://doi.org/10.1039/c1gc15386b>.
- Iravani, S., Korbekandi, H., Mirmohammadi, S. V., & Zolfaghari, B. (2014). Synthesis of silver nanoparticles: chemical, physical and biological methods. *Research in pharmaceutical sciences*, 9(6), 385-406.
- Ishida, T. (2017). Anticancer activities of silver ions in cancer and tumor cells and DNA damages by Ag⁺-DNA base-pairs reactions. *MedCrave Online Journal of Tumor Research*, 1(1), 8-16. <https://medcraveonline.com/MOJTR/MOJTR-01-00003.pdf>.
- Ivanova, N., Gugleva, V., Dobрева, M., Pehlivanov, I., Stefanov, S., & Andonova, V. (2018). *Silver nanoparticles as multi-functional drug delivery systems* (pp. 71-92). London, UK: IntechOpen. <http://dx.doi.org/10.5772/intechopen.80238>.
- Ivask, A., ElBadawy, A., Kaweeteerawat, C., Boren, D., Fischer, H., Ji, Z., Chang, C.H., Liu, R., Tolaymat, T., Telesca, D. & Godwin, H. A. (2014). Toxicity mechanisms in *Escherichia coli* vary for silver nanoparticles and differ from ionic silver. *ACS nano*, 8(1), 374-386.
- Ivask, A., Kurvet, I., Kasemets, K., Blinova, I., Aruoja, V., Suppi, S., Vija, H., Kärkinen, A., Titma, T., Heinlaan, M. and Visnapuu, M. & Kahru, A. (2014). Size-dependent toxicity of silver nanoparticles to bacteria, yeast, algae, crustaceans and mammalian cells in vitro. *PloS one*, 9(7), e102108.
- Jain, D., Daima, H. K., Kachhwaha, S., & Kothari, S. L. (2009). Synthesis of plant-mediated silver nanoparticles using papaya fruit extract and evaluation of their anti-microbial activities. *Digest journal of nanomaterials and biostructures*, 4(3), 557-563.

- Janani, B., Syed, A., Raju, L. L., Bahkali, A. H., Al-Rashed, S., Elgorban, A. M., ... & Khan, S. S. (2022). Designing intimate porous Al₂O₃ decorated 2D CdO nano-heterojunction as enhanced white light driven photocatalyst and antibacterial agent. *Journal of Alloys and Compounds*, 896, 162807.
- Jansen, R. K. 1985. The systematics of *Acmella* (Asteraceae–Heliantheae). *Systematic Botany Monographs*, 8, 1–115.
- Jayalakshmi, Y. A., & Yogamoorthi, A. (2014). Green synthesis of copper oxide nanoparticles using aqueous extract of flowers of *Cassia alata* and particles characterization. *International Journal of Nanomaterials and Biostructures*, 4, 66–71.
- Jha, A. K., Prasad, K., Kumar, V., & Prasad, K. (2009). Biosynthesis of silver nanoparticles using *Eclipta* leaf. *Biotechnology progress*, 25(5), 1476-1479. <https://doi.org/10.1002/btpr.233>.
- Jini, D., & Sharmila, S. (2019). Green synthesis of silver nanoparticles from allium *Cepa* and its in vitro antidiabetic activity. *Materials Today: Proceedings*, 22, 432–438.
- Jo, Y. K., Cromwell, W., Jeong, H. K., Thorkelson, J., Roh, J. H., & Shin, D. B. (2015). Use of silver nanoparticles for managing *Gibberella fujikuroi* on rice seedlings. *Crop Protection*, 74, 65-69.
- Jomova, K., Raptova, R., Alomar, S. Y., Alwasel, S. H., Nepovimova, E., Kuca, K., & Valko, M. (2023). Reactive oxygen species, toxicity, oxidative stress, and antioxidants: chronic diseases and aging. *Archives of toxicology*, 97(10), 2499–2574. <https://doi.org/10.1007/s00204-023-03562-9>.
- Joseph, T. M., Kar Mahapatra, D., Esmaeili, A., Piszczyk, Ł., Hasanin, M. S., Kattali, M., Haponiuk, J., & Thomas, S. (2023). Nanoparticles: Taking a Unique Position in Medicine. *Nanomaterials*, (Basel, Switzerland), 13(3), 574. <https://doi.org/10.3390/nano13030574>.

- Joudeh, N., & Linke, D. (2022). Nanoparticle classification, physicochemical properties, characterization, and applications: a comprehensive review for biologists. *Journal of Nanobiotechnology*, 20(1), 262. <https://doi.org/10.1186/s12951-022-01477-8>
- Jyoti, K., Baunthiyal, M., Singh, A., 2016. Characterization of silver nanoparticles synthesized using *Urtica dioica* Linn. leaves and their synergistic effects with antibiotics. *Journal of Radiation Research and Applied Sciences*, 9, 217–227. <https://doi.org/10.1016/j.jrras.2015.10.002>.
- Kadir, H. A., Zakaria, M. B., Kechil, A. A., & Azirun, M. D. (1989). Toxicity and electrophysiological effects of *Spilanthes amella* Murr. extracts on *Periplaneta americana* L. *Pesticide Science*, 25(4), 329-335. <https://doi.org/10.1002/ps.2780250402>.
- Kalyanasundaram, G. T., Doble, M., & Gummadi, S. N. (2012). Production and downstream processing of (1→ 3)-β-D-glucan from mutant strain of *Agrobacterium* sp. ATCC 31750. *AMB Express*, 2, 1-10. <https://doi.org/10.1186/2191-0855-2-31>.
- Kalyane, D., Raval, N., Maheshwari, R., Tambe, V., Kalia, K., & Tekade, R. K. (2019). Employment of enhanced permeability and retention effect (EPR): Nanoparticle-based precision tools for targeting of therapeutic and diagnostic agent in cancer. *Materials science & engineering. C, Materials for biological applications*, 98, 1252–1276. <https://doi.org/10.1016/j.msec.2019.01.066>.
- Kampmann, Y., De Clerck, E., Kohn, S., Patchala, D. K., Langerock, R., & Kreyenschmidt, J. (2008). Study on the antimicrobial effect of silver-containing inner liners in refrigerators. *Journal of Applied Microbiology*, 104(6), 1808-1814.
- Kannan, R. R. R., Arumugam, R., Ramya, D., Manivannan, K., & Anantharaman, P. (2013). Green synthesis of silver nanoparticles using marine macroalga

- Chaetomorpha linum*. *Applied Nanoscience*, 3, 229-233.
<https://doi.org/10.1007/s13204-012-0125-5>.
- Karthika R., & Sevarkodiyone S. P. (2015). Synthesis and characterization of silver nanoparticles using aqueous extract goat faecal pellets. *International journal of current science and research*, 1(1), 1-7.
- Kasibhatla, S., Amarante-Mendes, G. P., Finucane, D., Brunner, T., Bossy-Wetzel, E., & Green, D. R. (2006). Acridine orange/ethidium bromide (AO/EB) staining to detect apoptosis. *Cold Spring Harbor Protocols*, 34(3), 4493.
- Kassem, A., Abbas, L., Coutinho, O., Opara, S., Najaf, H., Kasperek, D., Pokhrel, K., Li, X., & Tiquia-Arashiro, S. (2023). Applications of Fourier Transform-Infrared spectroscopy in microbial cell biology and environmental microbiology: advances, challenges, and future perspectives. *Frontiers in microbiology*, 14, 1304081. <https://doi.org/10.3389/fmicb.2023.1304081>.
- Katsuki, H., & Komarneni, S. (2003). Nano-and micro-meter sized silver metal powders by microwave-polyol process. *Journal of the Japan Society of Powder and Powder Metallurgy*, 50(10), 745-750.
- Kaur, K., Ahmed, B., Singh, J., Rawat, M., Kaur, G., AlKahtani, M., Alhomaidi, E.A. & Lee, J. (2022). *Bryonia laciniosa* Linn mediated green synthesized Au NPs for catalytic and antimicrobial applications. *Journal of King Saud University-Science*, 34(4), 102022.
- Keat, C. L., Aziz, A., Eid, A. M., & Elmarzughi, N. A. (2015). Biosynthesis of nanoparticles and silver nanoparticles. *Bioresources and Bioprocessing*, 2, 1-11.
- Kędziora, A., Speruda, M., Krzyżewska, E., Rybka, J., Łukowiak, A., & Bugła-Płoskońska, G. (2018). Similarities and differences between silver ions and silver in nanoforms as antibacterial agents. *International journal of molecular sciences*, 19(2), 444.

- Kennedy, L., Sandhu, J. K., Harper, M. E., & Cuperlovic-Culf, M. (2020). Role of glutathione in cancer: from mechanisms to therapies. *Biomolecules*, 10(10), 1429. <https://doi.org/10.3390/biom10101429>.
- Kesharwani, J., Yoon, K. Y., Hwang, J., & Rai, M. (2009). Phytofabrication of silver nanoparticles by leaf extract of *Datura metel*: hypothetical mechanism involved in synthesis. *Journal of Bionanoscience*, 3(1), 39-44.
- Khan, I., Saeed, K., & Khan, I. (2019). Nanoparticles: Properties, applications and toxicities. *Arabian journal of chemistry*, 12(7), 908-931. doi:10.1016/j.arabjc.2017.05.011
- Khan, M., Al-Marri, A. H., Khan, M., Shaik, M. R., Mohri, N., Adil, S. F., Kuniyil, M., Alkhathlan, H.Z., Al-Warthan, A., Tremel, W., Tahir, M.N. & Siddiqui, M. R. H. (2015). Green approach for the effective reduction of graphene oxide using *Salvadora persica* L. root (Miswak) extract. *Nanoscale research letters*, 10, 1-9. <https://doi.org/10.1186/s11671-015-0987-z>.
- Khan, R. A., Khan, M. R., Sahreen, S., & Ahmed, M. (2012). Evaluation of phenolic contents and antioxidant activity of various solvent extracts of *Sonchus asper* (L.) Hill. *Chemistry Central Journal*, 6, 1-7. <https://doi.org/10.1186/1752-153X-6-12>.
- Kharissova, O. V., Dias, H. R., Kharisov, B. I., Pérez, B. O., & Pérez, V. M. J. (2013). The greener synthesis of nanoparticles. *Trends in biotechnology*, 31(4), 240-248. <https://doi.org/10.1016/j.tibtech.2013.01.003>.
- Khodashenas, B., Ghorbani, H. R. (2019). Synthesis of silver nanoparticles with different shapes, *Arabian Journal of Chemistry*, 12(8), 1823-1838. <https://doi.org/10.1016/j.arabjc.2014.12.014>.
- Kim, Y. T., Kim, K., Han, J. H., & Kimmel, R. M. (2008). Antimicrobial active packaging for food. *Smart Packaging Technologies for Fast Moving Consumer Goods*, 99-110. <http://dx.doi.org/10.1002/9780470753699.ch6>.

- Kitching, M., Ramani, M., & Marsili, E. (2015). Fungal biosynthesis of gold nanoparticles: mechanism and scale up. *Microbial biotechnology*, 8(6), 904–917. <https://doi.org/10.1111/1751-7915.12151>.
- Kitimu, S. R., Kirira, P., Abdille, A. A., Sokei, J., Ochwang'i, D., Mwitari, P., Makanya, A & Maina, N. (2022). Anti-angiogenic and anti-metastatic effects of biogenic silver nanoparticles synthesized using *Azadirachta indica*. *Advances in Bioscience and Biotechnology*, 13(04), 188-206.
- Klaunig, J. E., Xu, Y., Isenberg, J. S., Bachowski, S., Kolaja, K. L., Jiang, J., Stevenson, D.E & Walborg Jr, E. F. (1998). The role of oxidative stress in chemical carcinogenesis. *Environmental health perspectives*, 106(suppl 1), 289-295. <https://doi.org/10.1289/ehp.98106s1289>.
- Kłębowski, B., Depciuch, J., Parlińska-Wojtan, M., & Baran, J. (2018). Applications of Noble Metal-Based Nanoparticles in Medicine. *International journal of molecular sciences*, 19(12), 4031. <https://doi.org/10.3390/ijms19124031>.
- Klefenz, H. (2004). Nanobiotechnology: from molecules to systems. *Engineering in life sciences*, 4(3), 211-218.
- Knoll, B., & Keilmann, F. (1999). Near-field probing of vibrational absorption for chemical microscopy. *nature*, 399(6732), 134-137.
- Kora, A. J., Sashidhar, R. B., & Arunachalam, J. (2010). Gum kondagogu (*Cochlospermum gossypium*): A template for the green synthesis and stabilization of silver nanoparticles with antibacterial application. *Carbohydrate Polymers*, 82(3), 670-679. <https://doi.org/10.1016/j.carbpol.2010.05.034>.
- Kouvaris, P., Delimitis, A., Zaspalis, V., Papadopoulos, D., Tsiapas, S. A., & Michailidis, N. (2012). Green synthesis and characterization of silver nanoparticles produced using *Arbutus unedo* leaf extract. *Materials Letters*, 76, 18-20. doi:10.1016/j.matlet.2012.02.025.

- Kovacic, P., Pozos, R. S., Somanathan, R., Shangari, R., & O'Brien, P. J. (2005). Mechanism of mitochondrial uncouplers, inhibitors, and toxins: Focus on electron transfer, free radicals, and structure-activity relationships. *Current Medicinal Chemistry*, 12, 22601–22623. <https://doi.org/10.2174/092986705774370646>
- Kovács, D., Igaz, N., Gopisetty, M. K., & Kiricsi, M. (2022). Cancer therapy by silver nanoparticles: fiction or reality? *International journal of molecular sciences*, 23(2), 839. <https://doi.org/10.3390/ijms23020839>.
- Krishnamoorthy, K., Veerapandian, M., Zhang, L. H., Yun, K., & Kim, S. J. (2012). Antibacterial efficiency of graphene nanosheets against pathogenic bacteria via lipid peroxidation. *The journal of physical chemistry C*, 116(32), 17280-17287.
- Krithiga, J., & Briget, M. M. (2015). Synthesis of AgNPs of *Momordica charantia* leaf extract, characterization and antimicrobial activity. *Pharmaceutica Analytica Acta*, 6(10), 1-7.
- Krutyakov, Y. A., Kudrinskiy, A. A., Olenin, A. Y., & Lisichkin, G. V. (2008). Synthesis and properties of silver nanoparticles: advances and prospects. *Russian Chemical Reviews*, 77(3), 233.
- Kulkarni, N., & Muddapur, U. (2014). Biosynthesis of metal nanoparticles: a review. *Journal of Nanotechnology*, 2014(1), 510246.
- Kumar, H., Bhardwaj, K., Kuča, K., Kalia, A., Nepovimova, E., Verma, R., & Kumar, D. (2020). Flower-based green synthesis of metallic nanoparticles: Applications beyond fragrance. *Nanomaterials*, 10(4), 766.
- Kumar, N., & Goel, N. (2019). Phenolic acids: Natural versatile molecules with promising therapeutic applications. *Biotechnology reports*, 24, e00370. <https://doi.org/10.1016/j.btre.2019.e00370>

- Kumar, P., Senthamilselvi, S., Lakshmipraba, A., Premkumar, K., Muthukumaran, R., Visvanathan, P., Ganeshkumar, R.S. & Govindaraju, M. (2012). Efficacy of bio-synthesized silver nanoparticles using *Acanthophora spicifera* to encumber biofilm formation. *Digest Journal of Nanomaterials and Biostructures*, 7(2), 511-522.
- Kumar, V. S., Nagaraja, B. M., Shashikala, V., Padmasri, A. H., Madhavendra, S. S., Raju, B. D., & Rao, K. R. (2004). Highly efficient Ag/C catalyst prepared by electro-chemical deposition method in controlling microorganisms in water. *Journal of Molecular Catalysis A: Chemical*, 223(1-2), 313-319.
- Kumar, V., & Yadav, S. K. (2009). Plant-mediated synthesis of silver and gold nanoparticles and their applications. *Journal of Chemical Technology & Biotechnology: International Research in Process, Environmental & Clean Technology*, 84(2), 151-157.
- Lagnika, L., Amoussa, A. M. O., Adjileye, R. A., Laleye, A., & Sanni, A. (2016). Antimicrobial, antioxidant, toxicity and phytochemical assessment of extracts from *Acmella uliginosa*, a leafy-vegetable consumed in Bénin, West Africa. *BMC Complementary and Alternative Medicine*, 16, 1-11. <https://doi.org/10.1186/s12906-016-1014-3>
- Lai, W., Wang, Q., Li, L., Hu, Z., Chen, J., & Fang, Q. (2017). Interaction of gold and silver nanoparticles with human plasma: Analysis of protein corona reveals specific binding patterns. *Colloids and Surfaces B: Biointerfaces*, 152, 317-325.
- Lalmuansangi, C., Zosangzuali, M., Lalremruati, M., Tochwawng, L., & Siama, Z. (2022). Evaluation of the protective effects of *Ganoderma applanatum* against doxorubicin-induced toxicity in Dalton's Lymphoma Ascites (DLA) bearing mice. *Drug and Chemical Toxicology*, 45(3), 1243-1253. <https://doi.org/10.1080/01480545.2020.1812630>.

- Latif, H., Ghareib, M., & Tahon, M. (2017). Phytosynthesis of silver nanoparticles using leaf extracts from *Ocimum basilicum* and *Mangifira indica* and their effect on some biochemical attributes of *Triticum aestivum*. *Gesunde Pflanzen*, 69(1).
- Lav R. Khot, L. R., Sankaran, S., Maja, J. M., Ehsani, R., & Schuster, E. W. (2012). Applications of nanomaterials in agricultural production and crop protection: A review. *Crop Protection*, 35, 64-70. <https://doi.org/10.1016/j.cropro.2012.01.007>.
- Le Ouay, B., & Stellacci, F. (2015). Antibacterial activity of silver nanoparticles: A surface science insight. *Nano today*, 10(3), 339-354.
- Ledentsov, N. N., Grundmann, M., Kirstaedter, N., Schmidt, O., Heitz, R., Böhrer, J., J., Bimberg, D., Ustinov, V.M., Shchukin, V.A., Egorov, A.Y., Zhukov, A.E. & Heydenreich, J. (1996). Ordered arrays of quantum dots: Formation, electronic spectra, relaxation phenomena, lasing. *Solid-State Electronics*, 40(1-8), 785-798.
- Leong, L. P., & Shui, G. (2002). An investigation of antioxidant capacity of fruits in Singapore markets. *Food chemistry*, 76(1), 69-75.
- Li, J., Rong, K., Zhao, H., Li, F., Lu, Z., Chen, R., 2013. Highly selective antibacterial activities of silver nanoparticles against *Bacillus subtilis*. *Journal of Nanoscience Nanotechnology*, 13, 6806–6813.
- Li, R., Jia, Z., & Trush, M. A. (2016). Defining ROS in Biology and Medicine. *Reactive oxygen species*, 1(1), 9–21. <https://doi.org/10.20455/ros.2016.803>
- Li, S., Shen, Y., Xie, A., Yu, X., Qiu, L., Zhang, L., & Zhang, Q. (2007). Green synthesis of silver nanoparticles using *Capsicum annuum* L. extract. *Green Chemistry*, 9(8), 852-858. <https://doi.org/10.1039/b615357g>.

- Li, X., Xu, H., Chen, Z. S., & Chen, G. (2011). Biosynthesis of nanoparticles by microorganisms and their applications. *Journal of nanomaterials*, 2011(1), 270974. <https://doi.org/10.1155/2011/270974>.
- Liao, W.M., Lai, W.T. Li, P.W., Kuo, M.T., Chen, P. S. & Tsai, M. J. 5th IEEE Conference on Nanotechnology, 2005, 2, pp. 549–552. 14
- Lim, Z. Z. J., Li, J. E. J., Ng, C. T., Yung, L. Y. L., & Bay, B. H. (2011). Gold nanoparticles in cancer therapy. *Acta Pharmacologica Sinica*, 32(8), 983-990.
- Lima, R., Feitosa, L. O., Ballottin, D., Marcato, P. D., Tasic, L., & Durán, N. (2013). Cytotoxicity and genotoxicity of biogenic silver nanoparticles. In *Journal of Physics: Conference Series*, 429(1), 012020. IOP Publishing. doi:10.1088/1742-6596/429/1/012020.
- Limongi, T., Tirinato, L., Pagliari, F., Giugni, A., Allione, M., Perozziello, G., Candeloro, P., Fabrizio, E. D. (2017). Fabrication and Applications of Micro/Nanostructured Devices for Tissue Engineering. *Nano-Micro Letters*. 9, 1 <https://doi.org/10.1007/s40820-016-0103-7>.
- Lin, P. C., Lin, S., Wang, P. C., & Sridhar, R. (2014). Techniques for physicochemical characterization of nanomaterials. *Biotechnology advances*, 32(4), 711-726.
- Littler, H. M., Chambers, L. R., & Knowlton, K. F. (2017). Animal agriculture as a contributor to the global challenge of antibiotic resistance. *CABI Reviews*, (2017), 1-9..
- Livak, K. J., & Schmittgen, T. D. (2001). Analysis of relative gene expression data using real-time quantitative PCR and the 2^{(-Delta Delta C(T))} Method. *Methods (San Diego, Calif.)*, 25(4), 402–408. <https://doi.org/10.1006/meth.2001.1262>.
- López-Miranda, J. L., Vázquez, M., Fletes, N., Esparza, R., & Rosas, G. (2016). Biosynthesis of silver nanoparticles using a *Tamarix gallica* leaf extract and

- their antibacterial activity. *Materials Letters*, 176, 285-289. doi:10.1016/j.matlet.2016.04.126
- Loutfy, S. A., Al-Ansary, N. A., Abdel-Ghani, N. T., Hamed, A. R., Mohamed, M. B., Craik, J. D., Eldin, T.A., Abdellah, A.M., Hussein, Y., Hasanin, M.T. & Elbehairi, S. E. (2015). Anti-proliferative activities of metallic nanoparticles in an in vitro breast cancer model. *Asian Pacific Journal of Cancer Prevention*, 16(14), 6039-6046.
- Lowry, O. H., Rosebrough, N. J., Farr, A. L., & Randall, R. J. (1951). Protein measurement with the Folin phenol reagent. *The Journal of Biological Chemistry*, 193(1), 265-275. [https://doi.org/10.1016/s0021-9258\(19\)52451-6](https://doi.org/10.1016/s0021-9258(19)52451-6).
- Lu, Z., Rong, K., Li, J., Yang, H., & Chen, R. (2013). Size-dependent antibacterial activities of silver nanoparticles against oral anaerobic pathogenic bacteria. *Journal of Materials Science: Materials in Medicine*, 24, 1465-1471.
- Luepke, K. H., Suda, K. J., Boucher, H., Russo, R. L., Bonney, M. W., Hunt, T. D., & Mohr, J. F., 3rd (2017). Past, Present, and Future of Antibacterial Economics: Increasing Bacterial Resistance, Limited Antibiotic Pipeline, and Societal Implications. *Pharmacotherapy*, 37(1), 71–84. <https://doi.org/10.1002/phar.1868>.
- M. Doble, and A. K. Kruthiventi. (2007). *Green Chemistry and Engineering* Elsevier: Academic Press.1-26.
- M. Okuda, Y. Kobayashi, K. Suzuki, K. Sonoda, T. Kondoh, A. Wagawa, A. Kondo & Yoshimura, H. (2005). Self-organized inorganic nanoparticle arrays on protein lattices. *Nano letters*, 5(5), 991-993.
- Macdonald, J. S. (1999). Toxicity of 5-fluorouracil. *Oncology (Williston Park, NY)*, 13(73), 33-34.

- Madigan, M. T., Martinko, J. M., & Parker, J. (1997). *Brock biology of microorganisms* (Vol. 11). Upper Saddle River, NJ: Prentice Hall.
- Malatesta M. (2021). Transmission Electron Microscopy as a Powerful Tool to Investigate the Interaction of Nanoparticles with Subcellular Structures. *International journal of molecular sciences*, 22(23), 12789. <https://doi.org/10.3390/ijms222312789>
- Malathi, S., Prabhu, P., Nishanthi, R., Suresh, B.R., Sriraman, S.N., Palani, P. (2014). Highly potential antifungal activity of quantum-sized silver nanoparticles against *Candida albicans*. *Applied Biochemistry and Biotechnology*, 173, 55–66.
- Malik, P., Shankar, R., Malik, V., Sharma, N., & Mukherjee, T. K. (2014). Green chemistry based benign routes for nanoparticle synthesis. *Journal of Nanoparticles*, 2014(1), 302429. <https://doi.org/10.1155/2014/302429>.
- Malik, S., Muhammad, K., & Waheed, Y. (2023). Nanotechnology: A Revolution in Modern Industry. *Molecules (Basel, Switzerland)*, 28(2), 661. <https://doi.org/10.3390/molecules28020661>.
- Mallmann, E. J. J., Cunha, F. A., Castro, B. N., Maciel, A. M., Menezes, E. A., & Fechine, P. B. A. (2015). Antifungal activity of silver nanoparticles obtained by green synthesis. *Revista do instituto de Medicina Tropical de sao Paulo*, 57(2), 165-167.
- Mandal, F. B. (2011). The management of alien species in India. *International Journal of Biodiversity and Conservation*, 3(9), 467-473.
- Manzoor, M., Khan, A. H. A., Ullah, R., Khan, M. Z., & Ahmad, I. (2016). Environmental epidemiology of cancer in South Asian population: risk assessment against exposure to polycyclic aromatic hydrocarbons and volatile organic compounds. *Arabian Journal for Science and Engineering*, 41, 2031-2043.

- Mao, X., Seidlitz, E., Truant, R., Hitt, M., & Ghosh, H. P. (2004). Re-expression of TSLC1 in a non-small-cell lung cancer cell line induces apoptosis and inhibits tumor growth. *Oncogene*, 23(33), 5632-5642.
- Marambio-Jones, C., & Hoek, E. M. (2010). A review of the antibacterial effects of silver nanomaterials and potential implications for human health and the environment. *Journal of nanoparticle research*, 12, 1531-1551. <https://doi.org/10.1007/s11051-010-9900-y>.
- Marchiol, L. (2012). Synthesis of metal nanoparticles in living plants. *Italian Journal of Agronomy*, 7(3), 279. <http://dx.doi.org/10.4081/ija.2012.e37>.
- Masarovičová, E., & Král'ová, K. (2012). Plant-heavy metal interaction: phytoremediation, biofortification and nanoparticles. *Advances in selected plant physiology aspects. InTech, Rijeka*, 75-102.
- Mashwani, Z. U. R., Khan, T., Khan, M. A., & Nadhman, A. (2015). Synthesis in plants and plant extracts of silver nanoparticles with potent antimicrobial properties: current status and future prospects. *Applied microbiology and biotechnology*, 99, 9923-9934.
- Mathew, L., Chandrasekaran, N., & Mukherjee, A. (2010). Biomimetic synthesis of nanoparticles: science, technology & applicability. *Biomimetics learning from nature*. <https://doi.org/10.5772/8776>.
- Mathew, P. P., Thankachen, N., & Abraham, E. (2016). Green synthesis and applications of silver nanoparticles. *European Journal of Pharmaceutical and Medical Research*, 3(5), 233-240.
- Matras, E., Gorczyca, A., Przemieniecki, S. W., & Oćwieja, M. (2022). Surface properties-dependent antifungal activity of silver nanoparticles. *Scientific reports*, 12(1), 18046. <https://doi.org/10.1038/s41598-022-22659-2>.

- Matsumura, Y., Yoshikata, K., Kunisaki, S. I., & Tsuchido, T. (2003). Mode of bactericidal action of silver zeolite and its comparison with that of silver nitrate. *Applied and environmental microbiology*, 69(7), 4278-4281.
- Matussin, S., Harunsani, M. H., Tan, A. L., & Khan, M. M. (2020). Plant-extract-mediated SnO₂ nanoparticles: synthesis and applications. *ACS Sustainable Chemistry & Engineering*, 8(8), 3040-3054.
- Medintz, I. L., Mattoussi, H., & Clapp, A. R. (2008). Potential clinical applications of quantum dots. *International journal of nanomedicine*, 3(2), 151–167. <https://doi.org/10.2147/ijn.s614>.
- Meena, P. R. H., Singh, A. P., & Tejavath, K. K. (2020). Biosynthesis of Silver Nanoparticles using *Cucumis prophetarum* aqueous leaf extract and their antibacterial and antiproliferative activity against cancer cell lines. *ACS omega*, 5(10), 5520–5528. <https://doi.org/10.1021/acsomega.0c00155>.
- Mei, N., Zhang, Y., Chen, Y., Guo, X., Ding, W., Ali, S. F., Biris, A.S., Rice, P., Moore, M.M. & Chen, T. (2012). Silver nanoparticle-induced mutations and oxidative stress in mouse lymphoma cells. *Environmental and molecular mutagenesis*, 53(6), 409-419.
- Meva, F. E. A., Ntomba, A. A., Kedi, P. B. E., Tchoumbi, E., Schmitz, A., Schmolke, L., Klopotoski, M., Moll, B., Kökcam-Demir, Ü., Mpondo, E.A.M., Lehman, L.G. & Janiak, C. (2019). Silver and palladium nanoparticles produced using a plant extract as reducing agent, stabilized with an ionic liquid: sizing by X-ray powder diffraction and dynamic light scattering. *Journal of Materials Research and Technology*, 8(2), 1991-2000.
- Mikhailova E. O. (2021). Gold Nanoparticles: Biosynthesis and Potential of Biomedical Application. *Journal of functional biomaterials*, 12(4), 70. <https://doi.org/10.3390/jfb12040070>.
- Miller, C. N., Newall, N., Kapp, S. E., Lewin, G., Karimi, L., Carville, K., Gliddon, T. & Santamaria, N. M. (2010). A randomized-controlled trial comparing

- cadexomer iodine and nanocrystalline silver on the healing of leg ulcers. *Wound repair and regeneration*, 18(4), 359-367.
- Minai, L., Yeheskely-Hayon, D., & Yelin, D. (2013). High levels of reactive oxygen species in gold nanoparticle-targeted cancer cells following femtosecond pulse irradiation. *Scientific reports*, 3(1), 2146.
- Mishra, R. K., Zachariah, A. K., & Thomas, S. (2017). Energy-dispersive X-ray spectroscopy techniques for nanomaterial. In *Microscopy methods in nanomaterials characterization* (pp. 383-405). Elsevier. doi:10.1016/B978-0-323-46141-2.00012-2.
- Mittal, A. K., Chisti, Y., & Banerjee, U. C. (2013). Synthesis of metallic nanoparticles using plant extracts. *Biotechnology advances*, 31(2), 346–356. <https://doi.org/10.1016/j.biotechadv.2013.01.003>.
- Mohammadlou, M., Maghsoudi, H., & Jafarizadeh-Malmiri, H. J. I. F. R. J. (2016). A review on green silver nanoparticles based on plants: Synthesis, potential applications and eco-friendly approach. *International Food Research Journal*, 23(2), 446.
- Mohan, M., Kamble, S., Gadhi, P., & Kasture, S. (2010). Protective effect of Solanum torvum on doxorubicin-induced nephrotoxicity in rats. *Food and chemical toxicology*, 48(1), 436-440. <https://doi.org/10.1016/j.fct.2009.10.042>.
- Mohanpuria, P., Rana, N. K., & Yadav, S. K. (2008). Biosynthesis of nanoparticles: technological concepts and future applications. *Journal of nanoparticle research*, 10, 507-517.
- Mohanty, S., Mishra, S., Jena, P., Jacob, B., Sarkar, B., & Sonawane, A. (2012). An investigation on the antibacterial, cytotoxic, and antibiofilm efficacy of starch-stabilized silver nanoparticles. *Nanomedicine: Nanotechnology, Biology and Medicine*, 8(6), 916-924.

- Moosa, A., Ridha, A. M., & Allawi, M. H. (2015). Green synthesis of silver nanoparticles using spent tea leaves extract with atomic force microscopy. *International Journal of Current Engineering and Technology*, 5(5), 3233-3241.
- More, P. R., Pandit, S., Filippis, A., Franci, G., Mijakovic, I., & Galdiero, M. (2023). Silver Nanoparticles: Bactericidal and Mechanistic Approach against Drug Resistant Pathogens. *Microorganisms*, 11(2), 369. <https://doi.org/10.3390/microorganisms11020369>.
- Moron, M. S., Depierre, J. W., & Mannervik, B. (1979). Levels of glutathione, glutathione reductase and glutathione S-transferase activities in rat lung and liver. *Biochimica et biophysica acta (BBA)-general subjects*, 582(1), 67-78. [https://doi.org/10.1016/0304-4165\(79\)90289-7](https://doi.org/10.1016/0304-4165(79)90289-7).
- Mosmann, T. (1983). Rapid colorimetric assay for cellular growth and survival: application to proliferation and cytotoxicity assays. *Journal of immunological methods*, 65(1-2), 55-63.
- Mourdikoudis, S., Pallares, R. M., & Thanh, N. T. (2018). Characterization techniques for nanoparticles: comparison and complementarity upon studying nanoparticle properties. *Nanoscale*, 10(27), 12871-12934.
- Mude, N., Ingle, A., Gade, A., & Rai, M. (2009). Synthesis of silver nanoparticles using callus extract of *Carica papaya*—a first report. *Journal of Plant Biochemistry and Biotechnology*, 18, 83-86. <https://doi.org/10.1007/BF03263300>.
- Muhamad, M., Ab. Rahim, N., Wan Omar, W. A., & Nik Mohamed Kamal, N. N. S. (2022). Cytotoxicity and Genotoxicity of Biogenic Silver Nanoparticles in A549 and BEAS-2B Cell Lines. *Bioinorganic Chemistry and Applications*, 2022(1), 8546079.
- Mukherjee, S., & Patra, C. R. (2016). Therapeutic application of anti-angiogenic nanomaterials in cancers. *Nanoscale*, 8(25), 12444-12470.

- Mukherjee, S., Chowdhury, D., Kotcherlakota, R., Patra, S., Vinothkumar, B., Bhadra, M. P., Sreedhar, B. & Patra, C. R. (2014). Potential theranostics application of bio-synthesized silver nanoparticles (4-in-1 system). *Theranostics*, 4(3), 316.
- Mukherjee, S., Dasari, M., Priyamvada, S., Kotcherlakota, R., Bollu, V. S., & Patra, C. R. (2015). A green chemistry approach for the synthesis of gold nanoconjugates that induce the inhibition of cancer cell proliferation through induction of oxidative stress and their in vivo toxicity study. *Journal of Materials Chemistry B*, 3(18), 3820-3830.
- Mukherjee, S., Sushma, V., Patra, S., Barui, A. K., Bhadra, M. P., Sreedhar, B., & Patra, C. R. (2012). Green chemistry approach for the synthesis and stabilization of biocompatible gold nanoparticles and their potential applications in cancer therapy. *Nanotechnology*, 23(45), 455103.
- Mukunthan, K. S., & Balaji, S. (2012). Cashew apple juice (*Anacardium occidentale* L.) speeds up the synthesis of silver nanoparticles. *International Journal of Green Nanotechnology*, 4(2), 71-79. <https://doi.org/10.1080/19430892.2012.676900>.
- Mulvaney, P. (1996). Surface plasmon spectroscopy of nanosized metal particles. *Langmuir*, 12(3), 788-800.
- Munger, M. A., Radwanski, P., Hadlock, G. C., Stoddard, G., Shaaban, A., Falconer, J., Grainger, D.W. & Deering-Rice, C. E. (2014). In vivo human time-exposure study of orally dosed commercial silver nanoparticles. *Nanomedicine: Nanotechnology, Biology and Medicine*, 10(1), 1-9.
- Murray, C. B., Sun, S., Doyle, H., & Betley, T. (2001). Monodisperse 3d transition-metal (Co, Ni, Fe) nanoparticles and their assembly into nanoparticle superlattices. *Mrs Bulletin*, 26(12), 985-991.

- Mussin, J., & Giusiano, G. (2022). Biogenic silver nanoparticles as antifungal agents. *Frontiers in chemistry*, 10, 1023542. <https://doi.org/10.3389/fchem.2022.1023542>.
- Muthukrishnan, S., Bhakya, S., Kumar, T. S., & Rao, M. V. (2015). Biosynthesis, characterization and antibacterial effect of plant-mediated silver nanoparticles using *Ceropegia thwaitesii*—An endemic species. *Industrial crops and products*, 63, 119-124. <https://doi.org/10.1016/j.indcrop.2014.10.022>.
- Nakkala, J. R., Mata, R., Gupta, A. K., Sadras, S. R. (2014). Biological activities of green silver nanoparticles synthesized with Acorous calamus rhizome extract. *European Journal of Medicinal Chemistry*. 85, 784–794. <http://dx.doi.org/10.1016/j.ejmech.2014.08.024>.
- Narayanan, K. B., & Sakthivel, N. (2011). Synthesis and characterization of nano-gold composite using *Cylindrocladium floridanum* and its heterogeneous catalysis in the degradation of 4-nitrophenol. *Journal of hazardous materials*, 189(1-2), 519-525. <https://doi.org/10.1016/j.jhazmat.2011.02.069>.
- Nasrollahi, A., Pourshamsian, K. H., & Mansourkiaee, P. (2011). Antifungal activity of silver nanoparticles on some of fungi. *International Journal of Nano Dimension*, 1, 233–239.
- Natsuki, J., Natsuki, T., & Hashimoto, Y. (2015). A review of silver nanoparticles: synthesis methods, properties and applications. *International Journal of Materials Science and Applications*, 4(5), 325-332.
- Nayak, D., Kumari, M., Rajachandar, S., Ashe, S., Thathapudi, N. C., & Nayak, B. (2016). Biofilm impeding AgNPs target skin carcinoma by inducing mitochondrial membrane depolarization mediated through ROS production. *ACS applied materials & interfaces*, 8(42), 28538-28553.
- Nayak, S. K., Maharana, M., Jagat, S., Khatoon, A., & Satapathy, K. B. (2017). Anti-bacterial potential and qualitative phytochemical analysis of an invasive alien

- plant *Mikania micrantha* kunth found in Dhenkanal district of Odisha, India. *International Journal of Pharmaceutical Sciences Review and Research*, 42, 32-35.
- Nieman, G. W., Weertman, J. R., & Siegel, R. W. (1991). Mechanical behavior of nanocrystalline Cu and Pd. *Journal of Materials Research*, 6, 1012-1027.
- Nisha H. M., Tamileaswari R., Jesurani S. S. (2015). Comparative analyses of antimicrobial activity of silver nanoparticles from pomegranate seed, peel, and leaves. *International Journal of Engineering Research and Science & Technology*, 4 (7), 733-743. 13.
- Nowack, B., Krug, H. F., & Height, M. (2011). 120 years of nanosilver history: implications for policy makers. *Environmental Science & Technology*, 45(4), 1177-1183. doi: 10.1021/es103316q.
- Nyilasi, I., Kocsubé, S., Krizsán, K., Galgóczy, L., Pesti, M., Papp, T., & Vágvölgyi, C. (2010). In vitro synergistic interactions of the effects of various statins and azoles against some clinically important fungi. *FEMS microbiology letters*, 307(2), 175-184.
- Oberdörster, G., Oberdörster, E., & Oberdörster, J. (2005). Nanotoxicology: an emerging discipline evolving from studies of ultrafine particles. *Environmental health perspectives*, 113(7), 823-839.
- Ojha, S., Al Taei, H., Goyal, S., Mahajan, U. B., Patil, C. R., Arya, D. S., & Rajesh, M. (2016). Cardioprotective potentials of plant-derived small molecules against doxorubicin associated cardiotoxicity. *Oxidative medicine and cellular longevity*, 2016(1), 5724973. <https://doi.org/10.1155/2016/5724973>.
- Okuyama, K., & Lenggoro, I. W. (2003). Preparation of nanoparticles via spray route. *Chemical engineering science*, 58(3-6), 537-547.
- Oliveira, P. J., Santos, M. S., & Wallace, K. B. (2006). Doxorubicin-induced thiol-dependent alteration of cardiac mitochondrial permeability transition and

- respiration. *Biochemistry (Moscow)*, 71, 194-199.
- Ortega, F. G., Fernández-Baldo, M. A., Fernandez, J. G., Serrano, M. J., Sanz, M. I., Diaz-Mochon, J. J., Lorente J.A. & Raba, J. (2015). Study of antitumor activity in breast cell lines using silver nanoparticles produced by yeast. *International journal of nanomedicine*, 2021-2031.
- Osman, A. I., Zhang, Y., Farghali, M., Rashwan, A. K., Eltaweil, A. S., Abd El-Monaem, E. M., Mohamed, I.M., Badr, M.M., Ihara, I., Rooney, D.W. & Yap, P. S. (2024). Synthesis of green nanoparticles for energy, biomedical, environmental, agricultural, and food applications: A review. *Environmental Chemistry Letters*, 22(2), 841-887. <https://doi.org/10.1007/s10311-023-01682-3>
- Otunola, G. A., & Afolayan, A. J. (2018). In vitro antibacterial, antioxidant and toxicity profile of silver nanoparticles green-synthesized and characterized from aqueous extract of a spice blend formulation. *Biotechnology & Biotechnological Equipment*, 32(3), 724-733.
- Oyaizu, M. (1986). Studies on products of browning reaction antioxidative activities of products of browning reaction prepared from glucosamine. *The Japanese journal of nutrition and dietetics*, 44(6), 307-315. <https://doi.org/10.5264/eiyogakuzashi.44.307>.
- Pandey, S., Mewada, A., Thakur, M., Shah, R., Oza, G., & Sharon, M. (2013). Biogenic gold nanoparticles as fotillas to fire berberine hydrochloride using folic acid as molecular road map. *Materials Science and Engineering: C*, 33(7), 3716-3722. Kharissova, O. V., Dias, H. R., Kharisov, B. I., Pérez, B. O., & Pérez, V. M. J. (2013). The greener synthesis of nanoparticles. *Trends in biotechnology*, 31(4), 240-248.
- Pandit, R. (2015). Green synthesis of silver nanoparticles from seed extract of *Brassica nigra* and its antibacterial activity. *Nusantara Bioscience*, 7(1).

- Panigrahi, S., Kundu, S., Ghosh, S., Nath, S., & Pal, T. (2004). General method of synthesis for metal nanoparticles. *Journal of nanoparticle Research*, 6(4), 411-414. <https://doi.org/10.1007/s11051-004-6575-2>.
- Panja, S., Chaudhuri, I., Khanra, K., & Bhattacharyya, N. (2016). Biological application of green silver nanoparticle synthesized from leaf extract of *Rauvolfia serpentina* Benth. *Asian Pacific Journal of Tropical Disease*, 6(7), 549-556.
- Panneerselvam, C., Ponarulselvam, S., & Murugan, K. (2011). Potential anti-plasmodial activity of synthesized silver nanoparticle using *Andrographis paniculata* Nees (Acanthaceae). *Arch Appl Sci Res*, 3(6), 208-217.
- Panyal, N. R., Peña-Méndez, E., & Havel, J. (2008). Silver or silver nanoparticles: a hazardous threat to the environment and human health? *Journal of Applied Biomedicine*, 6, 117–129.
- Paramelle, D., Sadovoy, A., Gorelik, S., Free, P., Hobley, J., & Fernig, D. G. (2014). A rapid method to estimate the concentration of citrate capped silver nanoparticles from UV-visible light spectra. *Analyst*, 139(19), 4855-4861.
- Parveen, M., Ahmad, F., Malla, A. M., & Azaz, S. (2016). Microwave-assisted green synthesis of silver nanoparticles from *Fraxinus excelsior* leaf extract and its antioxidant assay. *Applied Nanoscience*, 6, 267-276. doi:10.1007/s13204-015-0433-7.
- Patel, V., Berthold, D., Puranik, P., & Gantar, M. (2015). Screening of cyanobacteria and microalgae for their ability to synthesize silver nanoparticles with antibacterial activity. *Biotechnology Reports*, 5, 112-119. <https://doi.org/10.1016/j.btre.2014.12.001>.
- Patra, C. R., & Barui, A. K. (2013). Nanoflowers: a future therapy for cardiac and ischemic disease? *Nanomedicine*, 8(11), 1735-1738.

- Patra, C. R., Mukherjee, S., & Kotcherlakota, R. (2014). Biosynthesized silver nanoparticles: a step forward for cancer theranostics?. *Nanomedicine*, 9(10), 1445-1448.
- Patra, S., Mukherjee, S., Barui, A. K., Ganguly, A., Sreedhar, B., & Patra, C. R. (2015). Green synthesis, characterization of gold and silver nanoparticles and their potential application for cancer therapeutics. *Materials Science and Engineering: C*, 53, 298-309.
- Paul, N. S., & Yadav, R. P. (2015). Biosynthesis of silver nanoparticles using plant seeds and their antimicrobial activity. *Asian Journal of Biomedical and Pharmaceutical Sciences*, 5(45), 26.
- Paulraj, J., Govindarajan, R., & Palpu, P. (2013). The genus *Spilanthes* ethnopharmacology, phytochemistry, and pharmacological properties: a review. *Advances in Pharmacological and Pharmaceutical Sciences*, 2013(1), 510298. <http://dx.doi.org/10.1155/2013/510298>
- Phatak, R. S., & Hendre, A. S. (2015). Sunlight induced green synthesis of silver nanoparticles using sundried leaves extract of *Kalanchoe pinnata* and evaluation of its photocatalytic potential. *Der Pharmacia Lettre*, 7(5), 313-324.
- Pilleron, S., Sarfati, D., Janssen-Heijnen, M., Vignat, J., Ferlay, J., Bray, F., & Soerjomataram, I. (2019). Global cancer incidence in older adults, 2012 and 2035: a population-based study. *International journal of cancer*, 144(1), 49-58.
- Prabhakar, U., Maeda, H., Jain, R. K., Sevic-Muraca, E. M., Zamboni, W., Farokhzad, O. C., Barry S.T., Gabizon A., Grodzinski P., & Blakey, D. C. (2013). Challenges and key considerations of the enhanced permeability and retention effect for nanomedicine drug delivery in oncology. *Cancer Research*, 73(8), 2412-2417. doi: 10.1158/0008-5472.

- Priya, A. M., Selvan, R. K., Senthilkumar, B., Satheeshkumar, M. K., & Sanjeeviraja, C. (2011). Synthesis and characterization of CdWO₄ nanocrystals. *Ceramics International*, 37(7), 2485-2488.
- Priya, J. F., Vimala, R. J., Bama, S. R., & Lavanya, M. (2016). Green synthesis of silver nanoparticles using aqueous extract of *Ficus racemosa* bark and its antimicrobial activity. *World Journal of Pharmaceutical Sciences*, 5(5), 753-765.
- Pyšek, P., Hulme, P. E., Simberloff, D., Bacher, S., Blackburn, T. M., Carlton, J. T., Dawson, W., Essl, F., Foxcroft, L. C., Genovesi, P., Jeschke, J. M., Kühn, I., Liebhold, A. M., Mandrak, N. E., Meyerson, L. A., Pauchard, A., Pergl, J., Roy, H. E., Seebens, H., van Kleunen, M., & Richardson, D. M. (2020). Scientists' warning on invasive alien species. *Biological reviews of the Cambridge Philosophical Society*, 95(6), 1511–1534. <https://doi.org/10.1111/brv.12627>.
- Qing, R., Hao, S., Smorodina, E., Jin, D., Zalevsky, A., & Zhang, S. (2022). Protein Design: From the Aspect of Water Solubility and Stability. *Chemical reviews*, 122(18), 14085–14179. <https://doi.org/10.1021/acs.chemrev.1c00757>.
- Qing, Y. A., Cheng, L., Li, R., Liu, G., Zhang, Y., Tang, X., Wang, J., Liu, H. & Qin, Y. (2018). Potential antibacterial mechanism of silver nanoparticles and the optimization of orthopedic implants by advanced modification technologies. *International journal of nanomedicine*, 3311-3327.
- Quinteros, M. A., Aristizábal, V. C., Dalmaso, P. R., Paraje, M. G., & Páez, P. L. (2016). Oxidative stress generation of silver nanoparticles in three bacterial genera and its relationship with the antimicrobial activity. *Toxicology in vitro*, 36, 216-223.
- Quinteros, M. A., Cano Aristizábal, V., Dalmaso, P. R., Paraje, M. G., & Páez, P. L. (2016). Oxidative stress generation of silver nanoparticles in three bacterial genera and its relationship with the antimicrobial activity. *Toxicology in vitro*

- : an international journal published in association with BIBRA, 36, 216–223.
<https://doi.org/10.1016/j.tiv.2016.08.007>.
- Radhakrishnan, V. S., Reddy Mudiam, M. K., Kumar, M., Dwivedi, S. P., Singh, S. P., & Prasad, T. (2018). Silver nanoparticles induced alterations in multiple cellular targets, which are critical for drug susceptibilities and pathogenicity in fungal pathogen (*Candida albicans*). *International journal of nanomedicine*, 2647-2663.
- Rahim, R. A., Jayusman, P. A., Muhammad, N., Mohamed, N., Lim, V., Ahmad, N. H., Mohamad, S., Abdul Hamid, Z. A., Ahmad, F., Mokhtar, N., Shuid, A. N., & Mohamed, I. N. (2021). Potential Antioxidant and Anti-Inflammatory Effects of *Spilanthes acmella* and Its Health Beneficial Effects: A Review. *International journal of environmental research and public health*, 18(7), 3532. <https://doi.org/10.3390/ijerph18073532>.
- Rai, P. K., & Singh, J. S. (2020). Invasive alien plant species: Their impact on environment, ecosystem services and human health. *Ecological indicators*, 111, 106020. <https://doi.org/10.1016/j.ecolind.2019.106020>.
- Rai, R. N., Reddi, R. S. B., & Rai, U. S. (2013). Developments and future directions of phase diagram, physicochemical and optical studies of binary organic complexes. *Progress in crystal growth and characterization of materials*, 59(2), 73-111. doi:10.1016/j.pcrysgrow.2013.04.001.
- Raj, S., Trivedi, R., & Soni, V. (2021). Biogenic synthesis of silver nanoparticles, characterization and their applications—a review. *Surfaces*, 5(1), 67-90. <https://doi.org/10.3390/surfaces5010003>
- Rajesh, W. R., Jaya, R. L., Niranjan, S. K., Vijay, D. M., & Sahebrao, B. K. (2009). Phytosynthesis of silver nanoparticle using *Gliricidia sepium* (Jacq.). *Current Nanoscience*, 5(1), 117-122.

- Rajoriya, P., Misra P., Singh, V. K., Shukla, P. K., & Ramteke, P. W. (2017). Green synthesis of silver nanoparticles. *Biotech Today: An International Journal of Biological Sciences*, 7(1), 7-20.
- Ramamurthy, C. H., Padma, M., Mareeswaran, R., Suyavaran, A., Kumar, M. S., Premkumar, K., & Thirunavukkarasu, C. (2013). The extra cellular synthesis of gold and silver nanoparticles and their free radical scavenging and antibacterial properties. *Colloids and Surfaces B: Biointerfaces*, 102, 808-815.
- Rammohan, M., & Balakrishnan, K. (2011). Rapid Synthesis and Characterization of Silver Nano Particles by Novel *Pseudomonas sp.*” ram bt-1”. *J.ournal of Ecobiotechnology*, 3(1), 24-28.
- Rani, P., Ahmed, B., Singh, J., Kaur, J., Rawat, M., Kaur, N., ... & Lee, J. (2022). Silver nanostructures prepared via novel green approach as an effective platform for biological and environmental applications. *Saudi journal of biological sciences*, 29(6), 103296.
- Rao, P. V., Nallappan, D., Madhavi, K., Rahman, S., Jun Wei, L., & Gan, S. H. (2016). Phytochemicals and biogenic metallic nanoparticles as anticancer agents. *Oxidative medicine and cellular longevity*, 2016(1), 3685671.
- Rashid, S., Ali, N., Nafees, S., Ahmad, S. T., Arjumand, W., Hasan, S. K., & Sultana, S. (2013). Alleviation of doxorubicin-induced nephrotoxicity and hepatotoxicity by chrysin in Wistar rats. *Toxicology mechanisms and methods*, 23(5), 337-345. <https://doi.org/10.3109/15376516.2012.759306>.
- Ratan, Z. A., Haidere, M. F., Nurunnabi, M., Shahriar, S. M., Ahammad, A. J. S., Shim, Y. Y., Reaney, M. J. T., & Cho, J. Y. (2020). Green Chemistry Synthesis of Silver Nanoparticles and Their Potential Anticancer Effects. *Cancers*, 12(4), 855. <https://doi.org/10.3390/cancers12040855>

- Rath, M., Panda, S. S., & Dhal, N. K. (2014). Synthesis of silver nano particles from plant extract and its application in cancer treatment: a review. *International Journal of Plant, Animal and Environmental Sciences*, 4(3), 137-45.
- Ravichandran, M. C., Fink, S., Clarke, M. N., Hofer, F. C., & Campbell, C. S. (2018). Genetic interactions between specific chromosome copy number alterations dictate complex aneuploidy patterns. *Genes & development*, 32(23-24), 1485–1498. <https://doi.org/10.1101/gad.319400.118>.
- Raza, M. A., Kanwal, Z., Rauf, A., Sabri, A. N., Riaz, S., & Naseem, S. (2016). Size- and shape-dependent antibacterial studies of silver nanoparticles synthesized by wet chemical routes. *Nanomaterials*, 6(4), 74.
- Razavi, M., Salahinejad, E., Fahmy, M., Yazdimamaghani, M., Vashae, D., & Tayebi, L. (2015). Green chemical and biological synthesis of nanoparticles and their biomedical applications. *Green processes for nanotechnology: From inorganic to bioinspired nanomaterials*, 207-235.
- Re, R., Pellegrini, N., Proteggente, A., Pannala, A., Yang, M., & Rice-Evans, C. (1999). Antioxidant activity applying an improved ABTS radical cation decolorization assay. *Free radical biology and medicine*, 26(9-10), 1231-1237. [https://doi.org/10.1016/s0891-5849\(98\)00315-3](https://doi.org/10.1016/s0891-5849(98)00315-3).
- Roca, I., Akova, M., Baquero, F., Carlet, J., Cavaleri, M., Coenen, S., Cohen, J., Findlay, D., Gyssens, I., Heuer, O. E., Kahlmeter, G., Kruse, H., Laxminarayan, R., Liébana, E., López-Cerero, L., MacGowan, A., Martins, M., Rodríguez-Baño, J., Rolain, J. M., Segovia, C., Vila, J. (2015). The global threat of antimicrobial resistance: science for intervention. *New microbes and new infections*, 6(5), 22–29. <https://doi.org/10.1016/j.nmni.2015.02.007>.
- Rónavári, A., Igaz, N., Adamecz, D. I., Szerencsés, B., Molnar, C., Kónya, Z., Pfeiffer, I., Kiricsi, M. (2021). Green Silver and Gold Nanoparticles: Biological Synthesis Approaches and Potentials for Biomedical Applications. *Molecules*, 26(4), 844. <https://doi.org/10.3390/molecules26040844>.

- Rondanelli, M., Fossari, F., Vecchio, V., Braschi, V., Riva, A., Allegrini, P., Petrangolini, G., Iannello, G., Faliva, M.A., Peroni, G., Nichetti, M., & Perna, S. (2020). *Acmella oleracea* for pain management. *Fitoterapia*, 140, 104419. <https://doi.org/10.1016/j.ftote.2019.104419>.
- Roy, A., Sharma, A., Yadav, S., Jule, L. T., & Krishnaraj, R. (2021). Nanomaterials for Remediation of Environmental Pollutants. *Bioinorganic chemistry and applications*, 2021, 1764647. <https://doi.org/10.1155/2021/1764647>.
- Rudayni, H. A., Rabie, A. M., Aladwani, M., Alneghery, L. M., Abu-Taweel, G. M., Al Zoubi, W., ... & Bellucci, S. (2023). Biological activities of sargassum algae mediated ZnO and Co doped ZnO nanoparticles as enhanced antioxidant and anti-diabetic agents. *Molecules*, 28(9), 3692. <https://doi.org/10.3390/molecules28093692>.
- Salata, O. V. (2004). Applications of nanoparticles in biology and medicine. *Journal of nanobiotechnology*, 2, 1-6.
- Sandhu, Z. A., Raza, M. A., Alqurashi, A., Sajid, S., Ashraf, S., Imtiaz, K., Aman, F., Alessa, A. H., Shamsi, M. B., & Latif, M. (2024). Advances in the Optimization of Fe Nanoparticles: Unlocking Antifungal Properties for Biomedical Applications. *Pharmaceutics*, 16(5), 645. <https://doi.org/10.3390/pharmaceutics16050645>.
- Sangaonkar, G. M., & Pawar, K. D. (2018). Garcinia indica mediated biogenic synthesis of silver nanoparticles with antibacterial and antioxidant activities. *Colloids and surfaces B: Biointerfaces*, 164, 210–217. <https://doi.org/10.1016/j.colsurfb.2018.01.044>
- Sangomla, S., Saifi, M. A., Khurana, A., & Godugu, C. (2018). Nanoceria ameliorates doxorubicin induced cardiotoxicity: Possible mitigation via reduction of oxidative stress and inflammation. *Journal of Trace Elements in Medicine and Biology*, 47, 53-62. <https://doi.org/10.1016/j.jtemb.2018.01.016>.

- Santana de Freitas-Blanco, V., Franz-Montan, M., Groppo, F. C., de Carvalho, J. E., Figueira, G. M., Serpe, L., ... & Ferreira Rodrigues, R. A. (2016). Development and evaluation of a novel mucoadhesive film containing *Acmella oleracea* extract for oral mucosa topical anesthesia. *PLoS One*, 11(9), e0162850. <https://doi.org/https://doi.org/10.1371/journal.pone.0162850>.
- Saranyaadevi, K., Subha, V., Ravindran, R. E., & Renganathan, S. A. H. A. D. E. V. A. N. (2014). Green synthesis and characterization of silver nanoparticle using leaf extract of *Capparis zeylanica*. *Asian Journal of Pharmaceutical and Clinical Research*, 7(2), 44-48.
- Savary, S., Ficke, A., Aubertot, J. N., & Hollier, C. (2012). Crop losses due to diseases and their implications for global food production losses and food security. *Food security*, 4(4), 519-537.
- Schabath, M. B., & Cote, M. L. (2019). Cancer progress and priorities: lung cancer. *Cancer epidemiology, biomarkers & prevention*, 28(10), 1563-1579. <https://doi.org/10.1158/1055-9965.EPI-19-0221>.
- Sengupta, S., Eavarone, D., Capila, I., Zhao, G., Watson, N., Kiziltepe, T., & Sasisekharan, R. (2005). Temporal targeting of tumor cells and neovasculature with a nanoscale delivery system. *Nature*, 436(7050), 568-572.
- Seong, M., & Lee, D. G. (2017). Silver nanoparticles against *Salmonella enterica* serotype typhimurium: role of inner membrane dysfunction. *Current microbiology*, 74, 661-670.
- Sereemasapun, A., Hongpitich, P., Rojanathan, R., Maneewatta, P., Ekgasit, S., & Warisnoich, W. (2008). Inhibition of human cytochrome P450 enzymes by metallic nanoparticles: a preliminary to nanogenomics. *International Journal of Pharmacology*, 4(6), 492-495.

- Shahid, M., Ahmed, B., & Khan, M. S. (2018). Evaluation of microbiological management strategy of herbicide toxicity to greengram plants. *Biocatalysis and agricultural biotechnology*, 14, 96-108.
- Shahid, M., Ahmed, B., Zaidi, A., & Khan, M. S. (2018). Toxicity of fungicides to *Pisum sativum*: a study of oxidative damage, growth suppression, cellular death and morpho-anatomical changes. *RSC advances*, 8(67), 38483-38498.
- Shahzadi, I., Aziz Shah, S. M., Shah, M. M., Ismail, T., Fatima, N., Siddique, M., ... & Ayaz, A. (2022). Antioxidant, cytotoxic, and antimicrobial potential of silver nanoparticles synthesized using *Tradescantia pallida* extract. *Frontiers in Bioengineering and Biotechnology*, 10, 907551. doi:10.3389/fbioe.2022.907551.
- Shalaby, T. I., Mahmoud, O. A., El Batouti, G. A., & Ibrahim, E. E. (2015). Green synthesis of silver nanoparticles: synthesis, characterization and antibacterial activity. *Nanoscience Nanotechnology*, 5(2), 23-29.
- Shankar, S. S., Rai, A., Ahmad, A., & Sastry, M. (2004). Rapid synthesis of Au, Ag, and bimetallic Au core–Ag shell nanoparticles using Neem (*Azadirachta indica*) leaf broth. *Journal of colloid and interface science*, 275(2), 496-502.
- Shanker, U., Jassal, V., Rani, M., & Kaith, B. S. (2016). Towards green synthesis of nanoparticles: from bio-assisted sources to benign solvents. A review. *International Journal of environmental analytical chemistry*, 96(9), 801-835.
- Shanmugasundaram, T., Radhakrishnan, M., Gopikrishnan, V., Pazhanimurugan, R., & Balagurunathan, R. (2013). A study of the bactericidal, anti-biofouling, cytotoxic and antioxidant properties of actinobacterially synthesized silver nanoparticles. *Colloids and Surfaces B: Biointerfaces*, 111, 680-687.
- Sharma, R., Karunambigai, A., Gupta, S., & Arumugam, N. (2022). Evaluation of biologically active secondary metabolites isolated from the toothache plant

- Acmella ciliata* (Asteraceae). *Advances in Traditional Medicine*, 22(4), 713-722. <https://doi.org/10.1007/s13596-021-00584-5>
- Sharma, V. K., & Zboril, R. (2017). Silver nanoparticles in natural environment: formation, fate, and toxicity. In *Bioactivity of Engineered Nanoparticles*, 239-258.
- Sharma, V. K., Yngard, R. A., & Lin, Y. (2009). Silver nanoparticles: green synthesis and their antimicrobial activities. *Advances in colloid and interface science*, 145(1-2), 83-96.
- Sharma, V., Boonen, J., Chauhan, N. S., Thakur, M., De Spiegeleer, B., & Dixit, V. K. (2011). *Spilanthes acmella* ethanolic flower extract: LC–MS alkylamide profiling and its effects on sexual behavior in male rats. *Phytomedicine*, 18(13), 1161-1169. <https://doi.org/10.1016/j.phymed.2011.06.001>
- Sheam, M., Haque, Z., & Nain, Z. (2020). Towards the antimicrobial, therapeutic and invasive properties of *Mikania micrantha* Knuth: a brief overview. *Journal of Advanced Biotechnology and Experimental Therapeutics*, 3(2), 92-101. <https://doi.org/10.5455/jabet.2020.d112>.
- Shi, X., Qiao, Z., Pradhan, P., Liu, P., Assoufid, L., Kim, K. J., & Shvyd'ko, Y. (2023). At-wavelength characterization of X-ray wavefronts in Bragg diffraction from crystals. *Journal of synchrotron radiation*, 30(Pt 6), 1100–1107. <https://doi.org/10.1107/S1600577523007531>.
- Shinwari, Z. K., & Khan, A. A. (2003). Medicinal and other useful plants of District Swat, Pakistan. *Al-Aziz Communications*, 97–98.
- Shinwari, Z. K., Rehman, M., Watanabe, T., & Yoshikawa, Y. (2006). Medicinal and aromatic plants of Pakistan. *Kohat University of Science and Technology, Kohat, Pakistan*, 492.

- Shiraishi, Y., & Toshima, N. (1999). Colloidal silver catalysts for oxidation of ethylene. *Journal of molecular catalysis A: Chemical*, 141(1-3), 187-192.
- Shivakumar, P., Rani, M. U., Reddy, A. G., & Anjaneyulu, Y. (2012). A study on the toxic effects of doxorubicin on the histology of certain organs. *Toxicology international*, 19(3), 241. <https://doi.org/10.4103/0971-6580.103656>.
- Shriniwas, P. P., & Subhash, T. K. (2017). Antioxidant, antibacterial and cytotoxic potential of silver nanoparticles synthesized using terpenes rich extract of *Lantana camara* L. leaves. *Biochem. Biophys. Rep*, 10, 76-81. <https://doi.org/10.1016/j.bbrep.2017.03.002>.
- Siddiqi, K. S., & Husen, A. (2016). Fabrication of metal nanoparticles from fungi and metal salts: scope and application. *Nanoscale research letters*, 11, 1-15.
- Siegel, R. L., Miller, K. D., & Jemal, A. (2015). Cancer statistics, 2015. *CA: a cancer journal for clinicians*, 65(1), 5–29. <https://doi.org/10.3322/caac.21254>.
- Silva, L. P., Silveira, A. P., Bonatto, C. C., Reis, I. G., & Milreu, P. V. (2017). Silver nanoparticles as antimicrobial agents: Past, present, and future. In *Nanostructures for antimicrobial therapy* (pp. 577-596). Elsevier.
- Silveira, N., Saar, J., Santos, A. D. C., Barison, A., Sandjo, L. P., Kaiser, M., ... & Biavatti, M. W. (2016). A new alkamide with an endoperoxide structure from *Acmella ciliata* (Asteraceae) and its in vitro antiplasmodial activity. *Molecules*, 21(6), 765. <https://doi.org/10.3390/molecules21060765>.
- Singh, J., Dutta, T., Kim, K. H., Rawat, M., Samddar, P., & Kumar, P. (2018). ‘Green’ synthesis of metals and their oxide nanoparticles: applications for environmental remediation. *Journal of nanobiotechnology*, 16, 84. <https://doi.org/10.1186/s12951-018-0408-4>.
- Singh, N. P., McCoy, M. T., Tice, R. R., & Schneider, E. L. (1988). A simple technique for quantitation of low levels of DNA damage in individual cells. *Experimental cell research*, 175(1), 184-191.

- Singh, N., & Rajini, P. S. (2008). Antioxidant-mediated protective effect of potato peel extract in erythrocytes against oxidative damage. *Chemico-biological interactions*, 173(2), 97-104. <https://doi.org/10.1016/j.cbi.2008.03.008>
- Singh, P., Kim, Y. J., Singh, H., Wang, C., Hwang, K. H., Farh, M. E. A., & Yang, D. C. (2015). Biosynthesis, characterization, and antimicrobial applications of silver nanoparticles. *International journal of nanomedicine*, 2567-2577.
- Singh, P., Kim, Y. J., Zhang, D., & Yang, D. C. (2016). Biological synthesis of nanoparticles from plants and microorganisms. *Trends in biotechnology*, 34(7), 588-599.
- Singh, S., Verma, S. K., & Singh, S. K. (2020). In vitro investigation of anti-cancer potential of *Spilanthes acmella*. *Journal of Pharmaceutical Sciences and Research*, 12(1), 124-128.
- Smith, D. M., Simon, J. K., & Baker Jr, J. R. (2013). Applications of nanotechnology for immunology. *Nature Reviews Immunology*, 13(8), 592-605.
- Sood, R., & Chopra, D. S. (2018). Metal–plant frameworks in nanotechnology: an overview. *Phytomedicine*, 50, 48-156. <https://doi.org/10.1016/j.phymed.2017.08.025>.
- Soumya, R., Sajeev, T.V. Introduction of *Lantana camara* L. and *Chromolaena odorata* (L.) King and Robins to India and their spread to Kerala: political ecology perspective. *Tropical Ecology*, 61, 387–399 (2020). <https://doi.org/10.1007/s42965-020-00095-5>.
- Stadtman E. R. (1992). Protein oxidation and aging. *Science (New York, N.Y.)*, 257(5074), 1220–1224. <https://doi.org/10.1126/science.1355616>.
- Stensberg, M. C., Wei, Q., McLamore, E. S., Porterfield, D. M., Wei, A., & Sepúlveda, M. S. (2011). Toxicological studies on silver nanoparticles: challenges and opportunities in assessment, monitoring and imaging. *Nanomedicine*, 6(5), 879-898.

- SudhaLakshmi G.Y. (2011). Green synthesis of silver nanoparticles from *Cleome Viscosa* : Synthesis and antimicrobial activity. *International conference on Bioscience , Biochemistry and Bioinformatics*, 5, 334 – 337.
- Sundara, Rao, W. V. B., & Sinha, M. K. (1963). Phosphate dissolving microorganisms in the soil and rhizosphere. *The Indian Journal of Agricultural Science*, 33(6), 272– 278.
- Sylvestre, J. P., Poulin, S., Kabashin, A. V., Sacher, E., Meunier, M., & Luong, J. H. (2004). Surface chemistry of gold nanoparticles produced by laser ablation in aqueous media. *The Journal of Physical Chemistry B*, 108(43), 16864-16869. <https://doi.org/10.1021/jp047134>.
- Takemura, G., & Fujiwara, H. (2007). Doxorubicin-induced cardiomyopathy: from the cardiotoxic mechanisms to management. *Progress in cardiovascular diseases*, 49(5), 330-352.
- Talib, W. H., Alsayed, A. R., Barakat, M., Abu-Taha, M. I., & Mahmod, A. I. (2021). Targeting drug chemo-resistance in cancer using natural products. *Biomedicines*, 9(10), 1353. <https://doi.org/10.3390/biomedicines9101353>
- Tang, S., & Zheng, J. (2018). Antibacterial Activity of Silver Nanoparticles: Structural Effects. *Advanced healthcare materials*, 7(13), e1701503. <https://doi.org/10.1002/adhm.201701503>.
- Tao, A., Kim, F., Hess, C., Goldberger, J., He, R., Sun, Y., Xia, Y. & Yang, P. (2003). Langmuir– Blodgett silver nanowire monolayers for molecular sensing using surface-enhanced Raman spectroscopy. *Nano letters*, 3(9), 1229-1233.
- Tessier, P. M., Velev, O. D., Kalambur, A. T., Lenhoff, A. M., Rabolt, J. F., & Kaler, E. W. (2001). Structured metallic films for optical and spectroscopic applications via colloidal crystal templating. *Advanced Materials*, 13(6), 396-400.

- Thakkar, K. N., Mhatre, S. S., & Parikh, R. Y. (2010). Biological synthesis of metallic nanoparticles. *Nanomedicine: nanotechnology, biology and medicine*, 6(2), 257-262.
- Thanh, N. T., Maclean, N., & Mahiddine, S. (2014). Mechanisms of nucleation and growth of nanoparticles in solution. *Chemical reviews*, 114(15), 7610-7630. DOI: 10.1021/cr400544s
- Thatyana, M., Dube, N. P., Kemboi, D., Manicum, A. E., Mokgalaka-Fleischmann, N. S., & Tembu, J. V. (2023). Advances in Phytonanotechnology: A Plant-Mediated Green Synthesis of Metal Nanoparticles Using *Phyllanthus* Plant Extracts and Their Antimicrobial and Anticancer Applications. *Nanomaterials (Basel, Switzerland)*, 13(19), 2616. <https://doi.org/10.3390/nano13192616>.
- Theivasanthi, T., & Alagar, M. (2011). Nano sized copper particles by electrolytic synthesis and characterizations. *International Journal of Physical Sciences*, 6(15), 3662-3671.
- Tsang, W. P., Chau, S. P., Kong, S. K., Fung, K. P., & Kwok, T. T. (2003). Reactive oxygen species mediate doxorubicin induced p53-independent apoptosis. *Life sciences*, 73(16), 2047-2058.
- Uetrecht, J. (2010). *Handbook of Experimental Pharmacology: Preface*, 196. <https://doi.org/10.1007/978-3-642-00663-0>.
- Vaiserman, A., Koliada, A., Zayachkivska, A., & Lushchak, O. (2020). Nanodelivery of natural antioxidants: an anti-aging perspective. *Frontiers in bioengineering and biotechnology*, 7, 447.
- Velayutham, K., Rahuman, A. A., Rajakumar, G., Roopan, S. M., Elango, G., Kamaraj, C., Marimuthu, S., Santhoshkumar, T., Iyappan, M. & Siva, C. (2013). Larvicidal activity of green synthesized silver nanoparticles using

- bark aqueous extract of *Ficus racemosa* against *Culex quinquefasciatus* and *Culex gelidus*. *Asian Pacific Journal of Tropical Medicine*, 6(2), 95-101.
- Velayutham, M., Villamena, F. A., Fishbein, J. C., & Zweier, J. L. (2005). Cancer chemopreventive oltipraz generates superoxide anion radical. *Archives of biochemistry and biophysics*, 435(1), 83-88.
- Velmurugan, P., Sivakumar, S., Young-Chae, S., Seong-Ho, J., Pyoung-In, Y., Jeong-Min, S., & Sung-Chul, H. (2015). Synthesis and characterization comparison of peanut shell extract silver nanoparticles with commercial silver nanoparticles and their antifungal activity. *Journal of Industrial and Engineering Chemistry*, 31, 51-54.
- Venugopal, K., Rather, H. A., Rajagopal, K., Shanthi, M. P., Sheriff, K., Illiyas, M., Rather, R.A., Manikandan, E., Uvarajan, S., Bhaskar, M. & Maaza, M. (2017). Synthesis of silver nanoparticles (Ag NPs) for anticancer activities (MCF 7 breast and A549 lung cell lines) of the crude extract of *Syzygium aromaticum*. *Journal of Photochemistry and Photobiology B: Biology*, 167, 282-289.
- Verma K. D., Hasan H. S., Banik M. R. (2015). Swift green synthesis of silver nanoparticles using aqueous extract of *Tamarindus indica* leaves and evaluation of its antimicrobial potential. *International Journal of Innovative Research in Science, Engineering and Technology*, 4(11), 11182- 11190.
- Vijayaraghavan, K., & Ashokkumar, T. (2017). Plant-mediated biosynthesis of metallic nanoparticles: A review of literature, factors affecting synthesis, characterization techniques and applications. *Journal of environmental chemical engineering*, 5(5), 4866-4883.
<https://doi.org/10.1016/j.jece.2017.09.026>
- Vijayaram, S., Razafindralambo, H., Sun, Y. Z., Vasantharaj, S., Ghafarifarsani, H., Hoseinifar, S. H., & Raeeszadeh, M. (2024). Applications of green

- synthesized metal nanoparticles—a review. *Biological Trace Element Research*, 202(1), 360-386. <https://doi.org/10.1007/s12011-023-03645-9>
- Vijilvani, C., Bindhu, M. R., Frincy, F. C., AlSalhi, M. S., Sabitha, S., Saravanakumar, K., Devanesan, S., Umadevi, M., Aljaafreh, M. J., & Atif, M. (2020). Antimicrobial and catalytic activities of biosynthesized gold, silver and palladium nanoparticles from *Solanum nigurum* leaves. *Journal of photochemistry and photobiology B: Biology*, 202, 111713. <https://doi.org/10.1016/j.jphotobiol.2019.111713>
- Wadhvani, S. A., Shedbalkar, U. U., Singh, R., & Chopade, B. A. (2016). Biogenic selenium nanoparticles: current status and future prospects. *Applied microbiology and biotechnology*, 100, 2555-2566.
- Wang Y, & Herron N. (1991). Nanometer-sized semiconductor clusters: materials synthesis, quantum size effects, and photophysical properties. *The Journal of Physical Chemistry*, 95, 525–532. <https://doi.org/10.1021/j100155a009>.
- Wang, H., Xu, L., Zhang, Z., Lin, J., Huang, X. (2018). First Report of *Curvularia pseudobrachyspora* Causing Leaf Spots in *Areca catechu* in China. *Plant Disease*, 103(5), 150.
- Wang, L., Xu, H., Gu, L., Han, T. T., Wang, S., & Meng, F. B. (2016). Bioinspired synthesis, characterization and antibacterial activity of plant-mediated silver nanoparticles using purple sweet potato root extract. *Materials Technology*, 31(8), 437-442.
- White, T. J., Bruns, T., Lee, S., & Taylor, J. (1990). Amplification and direct sequencing of fungal ribosomal RNA genes for phylogenetics. Academic Press, San Diego, 315–322.
- Widatalla, H. A., Yassin, L. F., Alrasheid, A. A., Ahmed, S. A. R., Widdatallah, M. O., Eltilib, S. H., & Mohamed, A. A. (2022). Green synthesis of silver nanoparticles using green tea leaf extract, characterization and evaluation of

- antimicrobial activity. *Nanoscale Advances*, 4(3), 911-915. doi:10.1039/d1na00509j.
- Williams, D. B., Carter, C. B., Williams, D. B., & Carter, C. B. (1996). *The transmission electron microscope* (pp. 3-17). Springer Us.
- Wongsawatkul, O., Prachayasittikul, S., Isarankura-Na-Ayudhya, C., Satayavivad, J., Ruchirawat, S., & Prachayasittikul, V. (2008). Vasorelaxant and antioxidant activities of *Spilanthes acmella* Murr. *International journal of molecular sciences*, 9(12), 2724-2744. <https://doi.org/10.3390/ijms9122724>.
- World Health Organization. 10 Facts on Antimicrobial Resistance. Available online: http://www.who.int/features/factfiles/antimicrobial_resistance/en/ (accessed on 10 June 2018).
- Wypij, M., Jędrzejewski, T., Trzcińska-Wencel, J., Ostrowski, M., Rai, M., & Golińska, P. (2021). Green Synthesized Silver Nanoparticles: Antibacterial and Anticancer Activities, Biocompatibility, and Analyses of Surface-Attached Proteins. *Frontiers in microbiology*, 12, 632505. <https://doi.org/10.3389/fmicb.2021.632505>.
- Xu, L., Wang, Y. Y., Huang, J., Chen, C. Y., Wang, Z. X., & Xie, H. (2020). Silver nanoparticles: Synthesis, medical applications and biosafety. *Theranostics*, 10(20), 8996–9031. <https://doi.org/10.7150/thno.45413>
- Yacamán, M. J., Ascencio, J. A., Liu, H. B., & Gardea-Torresdey, J. (2001). Structure shape and stability of nanometric sized particles. *Journal of Vacuum Science & Technology B: Microelectronics and Nanometer Structures Processing, Measurement, and Phenomena*, 19(4), 1091-1103.
- Yin, M., Xu, X., Han, H., Dai, J., Sun, R., Yang, L., & Wang, Y. (2022). Preparation of triangular silver nanoparticles and their biological effects in the treatment of ovarian cancer. *Journal of Ovarian Research*, 15(1), 121.

- Yoon, J. W., Sasaki, T., & Koshizaki, N. (2003). Pressure-controlled preparation of nanocrystalline complex oxides using pulsed-laser ablation at room temperature. *Applied Physics A*, 76, 641-643.
- Yoosaf, K., Ipe, B. I., Suresh, C. H., & Thomas, K. G. (2007). In situ synthesis of metal nanoparticles and selective naked-eye detection of lead ions from aqueous media. *The Journal of Physical Chemistry C*, 111(34), 12839-12847. <https://doi.org/10.1021/jp073923q>.
- Yuan, Y. G., Zhang, S., Hwang, J. Y., & Kong, I. K. (2018). Silver nanoparticles potentiates cytotoxicity and apoptotic potential of camptothecin in human cervical cancer cells. *Oxidative medicine and cellular longevity*, 2018(1), 6121328.
- Yugandhar, P., Haribabu, R., & Savithramma, N. (2015). Synthesis, characterization and antimicrobial properties of green-synthesized silver nanoparticles from stem bark extract of *Syzygium alternifolium*. *3 Biotech*, 5(6), 1031–1039. <https://doi.org/10.1007/s13205-015-0307-4>
- Yui, K., Imataka, G., & Shiohama, T. (2023). Lipid peroxidation via regulating the metabolism of docosahexaenoic acid and arachidonic acid in autistic behavioral symptoms. *Current Issues in Molecular Biology*, 45(11), 9149-9164. doi:10.3390/cimb45110574.
- Yurkov, A. M., Kemler, M., & Begerow, D. (2011). Species accumulation curves and incidence-based species richness estimators to appraise the diversity of cultivable yeasts from beech forest soils. *PLoS One*, 6(8), e23671. <https://doi.org/10.1371/journal.pone.0023671>.
- Zahed, F. M., Hatamluyi, B., Lorestani, F., & Es'haghi, Z. (2018). Silver nanoparticles decorated polyaniline nanocomposite based electrochemical sensor for the determination of anticancer drug 5-fluorouracil. *Journal of Pharmaceutical and Biomedical Analysis*, 161, 12-19.

- Zargar, M., Hamid, A. A., Bakar, F. A., Shamsudin, M. N., Shameli, K., Jahanshiri, F., & Farahani, F. (2011). Green synthesis and antibacterial effect of silver nanoparticles using *Vitex negundo* L. *Molecules*, 16(8), 6667-6676.
- Zelzer, M., & Ulijn, R. V. (2010). Next-generation peptide nanomaterials: molecular networks, interfaces and supramolecular functionality. *Chemical Society reviews*, 39(9), 3351–3357. <https://doi.org/10.1039/c0cs00035c>.
- Zhang, D., Zhao, Y. X., Gao, Y. J., Gao, F. P., Fan, Y. S., Li, X. J., & Wang, H. (2013). Anti-bacterial and in vivo tumor treatment by reactive oxygen species generated by magnetic nanoparticles. *Journal of Materials Chemistry B*, 1(38), 5100-5107. <https://doi.org/10.1039/C3TB20907E>.
- Zhang, X. F., Liu, Z. G., Shen, W., & Gurunathan, S. (2016). Silver Nanoparticles: Synthesis, Characterization, Properties, Applications, and Therapeutic Approaches. *International journal of molecular sciences*, 17(9), 1534. <https://doi.org/10.3390/ijms17091534>.
- Zhao, H. X., Zhang, H. S., & Yang, S. F. (2014). Phenolic compounds and its antioxidant activities in ethanolic extracts from seven cultivars of Chinese jujube. *Food Science and Human Wellness*, 3(3-4), 183-190. <https://doi.org/10.1016/j.fshw.2014.12.005>.

Abbreviations

NPs	Nanoparticles
AgNPs	Silver nanoparticles
MNP	<i>Mikania micrantha</i> silver nanoparticles
ANP	<i>Acmella ciliata</i> silver nanoparticles
MMAE	<i>M. micrantha</i> leaf extract
ACAE	<i>Acmella ciliata</i> leaf extract
AgNO ₃	Silver nitrate
FT-IR	Fourier transform infrared spectroscopy
SEM	Scanning electron microscopy
EDS	Energy dispersive spectroscopy
TEM	Transmission electron microscopy
XRD	X-ray diffraction
EDS	Energy dispersive spectroscopy
SPR	Surface plasmon resonance
FCC	Face-centered cubic
ROS	Reactive Oxygen Species
DPPH	1,1-diphenyl 2-picrylhydrazyl
ABTS	2,2'-azino-bis- (3-ethylbenzothiazoline-6-sulfonic acid)
AST	Aspartate amino-transferase
ALT	Alanine amino-transferase

LDH	Lactate dehydrogenase
GSH	Glutathione
GST	Glutathione-s-transferase
SOD	Superoxide dismutase
LPO	Lipid peroxidation
MIC	Minimum Inhibitory Concentration
MBC	Minimum Bactericidal concentration
MHA	Mueller–Hinton agar
PDA	Potato Dextrose Agar
CBZ	Carbendazim
DOX	Doxorubicin
5FU	5-Fluorouracil
µg	Microgram
mg	Milligram
g	Gram
kg	Kilogram
µl	Microliter
ml	Milliliter
s	Second
min	Minute
h	Hour
µmol	Micromole
nmol	Nanomole
mM	Millimole
M	Moles

nm	Nanometer
cm	Centimeter
mm ³	Cubic millimeter
OD	Optical Density
ANOVA	One-way analysis of variance
SEM	Standard error of mean
IC ₅₀	Inhibitory concentration
PBS	Phosphate buffered saline
DLA	Dalton's Lymphoma Ascites
NIH	National Institutes of Health
OECD	Organisation for Economic Co-operation and Development
i.p	Intraperitoneal
b. wt.	Bodyweight
DNA	Deoxyribonucleic acid
cDNA	Complementary DNA
RNA	Ribonucleic acid
mRNA	Messenger RNA
PCR	Polymerase Chain Reaction
qRT-PCR	Quantitative Real Time-PCR
RT	Real time
GAPDH	Glyceraldehyde-3-Phosphate Dehydrogenase
P53	Tumor Protein p53
BCl-2	B-cell lymphoma 2

BCl-X _L	B-cell lymphoma extra large
Bax	BCL2 Associated X, Apoptosis Regulator
Apaf-1	Apoptotic protease activating factor 1
PARP	Poly [ADP-ribose] polymerase
Bid	BH3 interacting-domain death agonist,
MDA	Malondialdehyde

BIO DATA**Name** : F. Lalsangpuii**Father's Name** : F. Challawma**Date of Birth** : 29.10.1993**Nationality** : Indian**Religion** : Christian**Contact** : 8575690058**Email ID** : sangpuiifanai29@gmail.com**Permanent address:** H/No. CV-1, Near Thuamluaia field, Lunglei, Lunglei District-796701, Mizoram**Address for correspondence:** Senhri Women Hostel, Mizoram University, Tanhril-796004, Aizawl, Mizoram**Educational Qualifications**

Exam passed	Year	Board/University	Subject	Division	Percentage
HSLC	2009	Mizoram Board of School Education	General	Distinction	78.8 %
HSSLC	2011	Mizoram Board of School Education	Science	Second	55.2 %
B. Sc	2014	Mizoram University	Botany	First	78.17 %
M.Sc	2016	Mizoram University	Botany	Distinction	81.4 %

List of publications

1. **Lalsangpuui, F.**, Rokhum, S. L., Nghakliana, F., V L Ruatpuia, J., Tochhawng, L., Trivedi, A. K., Lalfakzuala, R., & Siama, Z. (2024). *Mikania micrantha* silver nanoparticles exhibit anticancer activities against human lung adenocarcinoma via caspase-mediated apoptotic cell death. *Artificial cells, nanomedicine, and biotechnology*, 52(1), 186–200.
2. **Lalsangpuui, F.**, Rokhum, S. L., Nghakliana, F., Fakawmi, L., Ruatpuia, J. V. L., Laltlanmawii, E., Lalfakzuala, R., & Siama, Z. (2022). Green Synthesis of Silver Nanoparticles Using *Spilanthus acmella* Leaf Extract and its Antioxidant-Mediated Ameliorative Activity against Doxorubicin-Induced Toxicity in Dalton's Lymphoma Ascites (DLA)-Bearing Mice. *ACS omega*, 7(48), 44346–44359.
3. Ruatpuia, J. V. L. , Halder, G , Michael Vanlalchhandama, M., **Lalsangpuui F**, Boddula, R., Al-Qahtani, N., Niju, S., Mathimani, T., Rokhum, S. L., (2024) *Jatropha curcas* oil a potential feedstock for biodiesel production: A critical review. *Fuel* 370, 131829.
4. Lalfakawmi, **Lalsangpuui, F.**, Tochhawng, L., Lalzarzovi, S. T., Lalnuntluanga, P., Siama, Z. (2023) Synergistic Antioxidative Potential of Cosmosiin and Vanillic Acid in vitro and ex vivo. *Indian Journal of Science and Technology*, 16, 48-56.
5. Zosangzuali, M., **Lalsangpuui, F.**, Lalmuansangi, C., Tochhawng, L., Trivedi, A. K., Kumar, N. S., Siama, Z. (2023) Methanolic Extract of *Mallotus roxburghianus* Muell. Exhibit Anti-Cancer Activity against Dalton's Lymphoma Ascites (DLA) bearing Mice via Alterations of Apoptotic Genes Expression and Redox-Homeostasis. *Indian Journal of Science and Technology*. 16, 75-88.

Conferences/seminars/workshops attended

1. Mizoram Science Congress 2018 (MAS, MISTIC, STAM & BIOCONe) held at Pachhunga University College during 4-5 October, 2018.
2. One day National Workshop on IPR and Plant Protection with special references to NE India, jointly organized by Department of Botany, Mizoram University and Department of Horticulture, Government of Mizoram.
3. International Conferences of Recent Advances in Animal Sciences (ICRAAS) National conference on Microbes in Health, Agriculture & Environment organized by Department of Biotechnology, School of Life Science, Mizoram University, during 20 & 21 June, 2019.
4. One Day Awareness on Invasive Alien Plant in Himalayas: Status, Ecological Impact and Management (Mizoram & Tripura Chapter), organized by Botanical Survey of India in collaboration with Department of Botany, Mizoram university, on 26 April, 2019.
5. Workshop on Statistical and Computing Methods for Life-Science Data Analysis (BAU, ISI Kolkata, Department of Botany, Mizoram University)
6. National seminar on Biodiversity, Conservation, Utilization and Commercialization of medicinal and Aromatic Plant on 8 February, 2024, organized by the Department of Botany, Mizoram University.
7. Two days “Skill development program on Organic farming for Farmers and Entrepreneurs of North-East Hilly (NEH) region, India” jointly organized by ICAR-National Bureau of Agriculturally Important microorganism (NBAIM) and Department of Botany, School of Life Sciences, Mizoram University, during 27 & 28 march, 2024.

Papers presented

International:

1. **Green Synthesis of Silver Nanoparticles using *Spilanthes acmella* (L.) Aqueous Leaf Extract and their Antimicrobial Activity**, in the 2nd Annual Convention of North East (India) Academy of Science and Technology (NEAST) & International Seminar on Recent Advances in Science and Technology (IRSRAST) during 16th–18th November 2020.
2. **Green synthesis of silver nanoparticles using *Mikania micrantha* aqueous leaf extract and their antimicrobial activity**, International Conference on Biotechnology for Environment & Health (ICBEH), organized by School of Bio Sciences and Technology, Vellore Institute of Technology along with Association of Biotechnology and Pharmacy, from November 25 - 27, 2021.

National:

1. **Green synthesis of silver nanoparticles using *Spilanthes acmella* leaf extract and its antioxidant mediated ameliorative activity against doxorubicin-induced toxicity in Dalton's lymphoma ascites (DLA) bearing mice**, at the National Conference on Recent Advances in Plant Biology with Special References to North-East, India, organized by the Department of Botany, School of Life Sciences, Mizoram University, from April 20-21, 2023.

PARTICULARS OF THE CANDIDATE

NAME OF THE CANDIDATE	: F. Lalsangpuui
DEGREE	: Doctor of Philosophy
DEPARTMENT	: Botany
TITLE OF THE THESIS	: Green synthesis of silver nanoparticles using invasive alien plant species and evaluation of their anti-oxidative, anti-microbial and anti-cancer activities
DATE OF ADMISSION	: 04.09.2018

APPROVAL OF RESEARCH PROPOSAL

1. D.R.C.	: 02.05.2019
2. B.O.S.	: 03.05.2019
3. SCHOOL BOARD	: 17.05.2019
MZU REGISTRATION No.	: 1101 of 2011
Ph. D REGISTRATION No. & DATE	: MZU/Ph.D./1273 of 04.09.2018
EXTENSION	: NA

(Prof. F. LALNUNMAWIA)

Head

Department of Botany

ABSTRACT

GREEN SYNTHESIS OF SILVER NANOPARTICLES USING INVASIVE ALIEN PLANT SPECIES AND EVALUATION OF THEIR ANTI-OXIDATIVE, ANTI-MICROBIAL AND ANTI- CANCER ACTIVITIES

**AN ABSTRACT SUBMITTED IN PARTIAL FULFILLMENT OF
THE REQUIREMENTS FOR THE DEGREE OF DOCTOR OF
PHILOSOPHY**

F. LALSANGPUII

MZU REGN NO: 1101 of 2011

Ph. D REGN NO: MZU/Ph.D./1273 of 04.09.2018



**DEPARTMENT OF BOTANY
SCHOOL OF LIFE SCIENCES
AUGUST 2024**

ABSTRACT

GREEN SYNTHESIS OF SILVER NANOPARTICLES USING INVASIVE ALIEN
PLANT SPECIES AND EVALUATION OF THEIR ANTI-OXIDATIVE, ANTI-
MICROBIAL AND ANTI-CANCER ACTIVITIES

BY

F. LALSANGPUII

MZU REGN NO: 1101 of 2011

Ph. D REGN NO: MZU/Ph.D./1273 of 04.09.2018

Name of supervisor: Prof. R. LALFAKZUALA

Joint supervisor: Dr. SAMUEL LALTHAZUALA ROKHUM

Submitted

In partial fulfillment of the requirement of the degree of Doctor of Philosophy in
Botany of Mizoram University, Aizawl

Abstract

Silver nanoparticles (AgNPs) have emerged as a prominent nanomaterial in the biomedical and agriculture sectors owing to their unique physicochemical properties. In the realm of nanotechnology, it is imperative to establish reliable and environment-friendly approaches to the production of nanoparticles (NPs), as the conventional methods are expensive, harmful, and detrimental to the environment. To facilitate overcoming these issues, biological sources such as plants, bacteria, fungi, and biopolymers have been utilized to produce AgNPs, which can serve as both reducing and capping agents. This study focuses on the research on plant-assisted synthesis of AgNPs, an emerging area in nanotechnology, and their biological applications. Silver nanoparticles, usually with sizes less than 100 nm and consisting of 20–15,000 silver atoms, exhibit unique physical, chemical, and biological characteristics in comparison to their larger precursor materials. AgNPs have distinct physical and optical characteristics, along with tailored biochemical functionality achieved by controlling their size and shape. These features render them highly potential for various applications, including as antimicrobial agents, anticancer therapy, drug delivery carriers, anti-diabetic agents, wound healing, and biosensors. Although AgNPs have therapeutic benefits, it is crucial to prioritize gaining a deeper understanding of their mechanisms in order to expand their potential applications in nanomedicine, including diagnostics, therapeutics, and pharmaceuticals.

This thesis is broadly divided into seven chapters. Chapter 1 provides a general introduction, while chapter 2 focuses on reviewing the literature. Chapter 3 describes the synthesis and characterization of silver nanoparticles using *Mikania micrantha* and *Acmella ciliata* leaf extract. Chapter 4 provides a detailed account of the free radical scavenging activities of silver nanoparticles derived from *Mikania micrantha* and *Acmella ciliata* (*in vitro* and *ex vivo*). The chemical composition of the extract typically influences the antioxidant effects of silver nanoparticles, and these attributes generally enhance as the concentration of AgNPs increases. Chapter 5 describes the antioxidant-mediated ameliorative of *Acmella ciliata* silver nanoparticles activity against doxorubicin-induced toxicity in Dalton's Lymphoma Ascites (DLA) bearing

mice. This study found that biosynthesized AgNPs from *A. ciliata* leaf extract offers outstanding protections against cardiotoxicity and hepatotoxicity caused by DOX in DLA-bearing mice possibly by elevating the activities of antioxidants and reduction of lipid peroxidation. Chapter 6 gives an in-depth investigation of the antimicrobial activity exhibited by *Mikania micrantha* and *Acmella ciliata* silver nanoparticles. Our findings validate the concept that silver nanoparticles are appropriate for developing novel microbiocidal agents. Chapter 7 describes the cytotoxicity and anti-cancer activities of silver nanoparticles synthesized from *Mikania micrantha* and *Acmella ciliata* leaf extract against type-II human lung adenocarcinoma (A549) cells. Our study demonstrates the cytotoxic effects of AgNPs on human lung adenocarcinoma A549 cells by targeting the apoptotic pathway, which is the preferred cell death pathway for any novel drug candidate.

Chapter 3. Synthesis and characterization of silver nanoparticles using *Mikania micrantha* and *Acmella ciliata* leaf extract.

Nanotechnology associated with metal nanoparticles emerges as a rapidly growing field in the realm of science and technology, principally in biomedical sciences due to its unique optical catalytic, electronic, magnetic and thermal characteristics. The utilization of biological sources for silver nanoparticles (AgNPs) synthesis suggests a simple, environmentally friendly, and alternative approach to traditional chemical synthesis methods. Plant extracts are more effective for nanoparticles synthesis than other biological methods because they eliminate the complex cell culture process and allow for large-scale AgNPs production. Despite its invasive nature, *Mikania micrantha* and *Acmella ciliata* serves as an accumulation for a multitude of compounds that possess therapeutic potential. This study describes the synthesis of AgNPs using aqueous leaf extract of *Mikania micrantha* and *Acmella ciliata*. Different analytical techniques were employed to evaluate the characteristics of nanoparticles. AgNPs were synthesized through the reaction of silver nitrate (AgNO_3) solution with the leaf extract of these two invasive plants, which served as a reducing agent as well as stabilizing agent. The formation of AgNPs was first confirmed by visual observation. UV-vis spectroscopy reveals the surface plasmon resonating property of AgNPs. Fourier Transform Infra-Red Spectroscopy (FT-IR) spectrum analysis was used to investigate the possible functional groups involved in the synthesis of AgNPs.

The crystalline metallic AgNPs was examined by X-ray diffraction analysis (XRD). Transmission Electron Microscopy (TEM) and Scanning Electron Microscopy (SEM) were employed to study the morphology of biosynthesized AgNPs. The synthesis of AgNPs was confirmed using UV-Vis spectrum that exhibited an absorption band at 459 nm in *Mikania micrantha* silver nanoparticles (MNP) and 430 nm in *Acmella ciliata* silver nanoparticles (ANP), respectively. The bioactive compounds of leaves extract that functioned as reducing and capping agents were confirmed by a shift in the absorption bands in FT-IR. SEM and TEM studies validated the spherical shape and size of AgNPs. The average size of the MNP and ANP is 23.9 nm and 6.702 nm, respectively. Energy dispersive spectroscopy (EDS) analysis revealed the presence of elemental silver in the biosynthesized AgNPs. The crystalline nature of the biosynthesized AgNPs was confirmed by the XRD analysis.

Chapter 4. Free radical scavenging activities of *Mikania micrantha* silver nanoparticles (MNP) and *Acmella ciliata* silver nanoparticles (ANP) (*in-vitro* and *ex-vivo*).

The overproduction of free radicals and reactive oxygen species (ROS) in living organisms due to metabolic activity can result in oxidative damage to biomolecules including lipids, proteins, and DNA, which can lead to various diseases, including cancer. Antioxidants mitigate oxidative stress by neutralizing the detrimental impact of ROS, indicating their potential efficacy in oxidative stress-related diseases. This study aims to evaluate the antioxidative potential, ferric reducing power, and free radical scavenging activity of AgNPs synthesized using aqueous leaf extracts of *Mikania micrantha* and *Acmella ciliata* under both in vitro and ex vivo conditions. DPPH (1,1-diphenyl-2-picrylhydrazyl), $O_2^{\bullet-}$ (superoxide anions), and ABTS (2, 2'-azino-bis-3-ethylbenzothiazoline-6-sulfonic acid) scavenging activities of various concentration of MNP and ANP were determined in a cell-free system using standard protocols. Different concentration of AgNPs inhibited the generation of DPPH, $O_2^{\bullet-}$ and ABTS radicals in a concentration-dependent manner. The scavenging activities of MNP against DPPH (IC_{50} : 4.90 ± 0.31 $\mu\text{g/ml}$), $ABTS^{\bullet+}$ (IC_{50} : 16.27 ± 0.62 $\mu\text{g/ml}$) and $O_2^{\bullet-}$ (IC_{50} : 13.33 ± 0.38 $\mu\text{g/ml}$) were found to be significantly higher than *M. Micrantha* extract (IC_{50} : 991.86 ± 11.30 $\mu\text{g/ml}$ for DPPH; 1256.67 ± 9.53 $\mu\text{g/ml}$ for

ABTS^{•+}; 2713.67 ± 89.99 $\mu\text{g/ml}$ for $\text{O}_2^{\bullet-}$). Similarly, the scavenging activities of ANP against DPPH (IC_{50} : 3.85 ± 0.04 $\mu\text{g/mL}$), ABTS^{•+} (IC_{50} : 14.62 ± 0.10 $\mu\text{g/mL}$) and $\text{O}_2^{\bullet-}$ (IC_{50} : 16.13 ± 0.11 $\mu\text{g/mL}$) were found to be significantly higher than *A. ciliata* extract (IC_{50} : 474.0 ± 8.80 $\mu\text{g/mL}$ for DPPH; 1409.33 ± 17.8 $\mu\text{g/mL}$ for ABTS^{•+}; 6156.33 ± 15.23 $\mu\text{g/mL}$ for $\text{O}_2^{\bullet-}$). The ability of AgNPs to convert ferric (Fe^{3+}) into ferrous (Fe^{2+}) was used to determine their reducing power and the reducing activity of AgNPs increased in a dose-dependent manner. The biosynthesized AgNPs also showed significant inhibitory activities against erythrocyte hemolysis and lipid peroxidation in the liver homogenate. The anti-haemolytic activity of MNP and ANP were 61.7 % and 64.07 %, respectively. The ANP was found to possess higher inhibitory activity against lipid peroxidation with 84.2 % inhibition than MNP (79.9 %). Our study shows that AgNPs have a significant ability to scavenge free radicals and act as antioxidants, suggesting their potential application in biological therapy.

Chapter 5. Antioxidant-mediated ameliorative of *Acmella ciliata* silver nanoparticles activity against doxorubicin-induced toxicity in Dalton's Lymphoma Ascites (DLA) bearing mice.

Doxorubicin (DOX) is a widely used chemotherapeutic drug for the treatment of several forms of cancer, such as leukaemia, lymphomas, and solid tumors. The cumulative dose-dependent effect of doxorubicin, leading to organ toxicity such as cardiotoxicity and hepatotoxicity, has diminished its therapeutic efficacy, thereby restricting its prolonged administration in chemotherapy. Hence, the adverse effects of doxorubicin in cancer therapy are widely recognized. To compensate for the reduction in antioxidant levels caused by DOX treatment, the administration of external antioxidants could be an effective strategy for preventing DOX-induced toxicity. This study demonstrated that biosynthesized silver nanoparticles offer protection against cardio- and hepatotoxicity induced by DOX in Dalton's Lymphoma Ascites (DLA) bearing mice. Treatment of Dalton's Lymphoma Ascites (DLA) mice with 20 mg/kg of DOX significantly increased the activities of serum toxicity markers including aspartate amino-transferase (AST), alanine amino-transferase (ALT) and lactate dehydrogenase (LDH). However, compared to DOX alone treatment, the co-administration of DOX and AgNPs reduced AST, ALT, and LDH activities. DOX

alone treatment reduced glutathione (GSH) contents and decreased the activities of glutathione-s-transferase (GST) and superoxide dismutase (SOD) in DLA mice. However, co-administration of AgNPs to DOX-treated DLA mice increased GSH content, and the activities of GST and SOD. Administration of AgNPs provides protection against DOX-induced cellular lipid peroxidation, potentially suppressing lipid peroxidation chain reactions within the cytoplasm. Our results thus suggest that the protective role of AgNPs in DOX-induced toxicity could be an attribute of the antioxidant properties conferred by the high phenolic and flavonoid contents as well as their unique physio-chemical characteristics.

Chapter 6. Anti-microbial activity of *Mikania micrantha* and *Acmella ciliata* silver nanoparticles.

The emergence and dissemination of drug-resistant pathogens that have developed novel resistance mechanisms have rendered antimicrobial resistance a significant concern in the successful detection and management of infectious diseases. As a result, the development of a novel potent antimicrobial agent is imperative given the growing concern about multidrug-resistant pathogens. Silver nanoparticles (AgNPs) are widely recognized for their strong antibacterial activity against a range of pathogens, including bacteria, viruses, and fungi, owing to their small size and large surface area. This study aims to assess the antibacterial activity of green-synthesised AgNPs against pathogenic bacteria using the disk diffusion method, minimum inhibitory concentration (MIC), and minimum bactericidal concentration test (MBC). Further, the potency and efficacy of AgNPs against rice pathogens were evaluated. AgNPs showed significant antibacterial activity as indicated by the formation of inhibition zone. The antibacterial activity of AgNPs at a concentration of 10 µg/ml was comparable to that of standard antibiotics. A lower minimum inhibitory concentration (MIC) for tested bacterial strains indicates higher inhibition activity and the results show that the MBC was 2-fold higher than the MIC. Morphological and molecular characterization was performed to identify the fungal isolate. The synthesized silver nanoparticles exhibited prominent antifungal activity against fungal pathogen, *Curvularia pseudobrachyspora*. The biosynthesized silver nanoparticles exhibit a notable inhibitory effect on the growth of *Curvularia pseudobrachyspora* colonies and

exerted destructive effects on mycelial morphology, which became expanded and distorted. The gradual increase in AgNPs resulted in an increasingly significant inhibition of mycelia growth, indicating a consistent pattern of biomass reduction. Therefore, silver nanoparticles can be utilized as an effective fungistatic agent to aid in the reduction or substitution of chemical pesticides. Our study showed that the biosynthesized AgNPs exhibited exceptional antimicrobial efficacy at very low concentrations, suggesting their potential use as an innovative nanoproduct in biomedical and agricultural fields.

7. Cytotoxicity and anti-cancer activities of *Mikania micrantha* and *Acmella ciliata* silver nanoparticles against type-II human lung adenocarcinoma (A549) cells.

Cancer has emerged as the leading cause of death globally, with lung cancer accounting for the majority of cancer-related death. The lack of early detection, non-specific systemic medication distribution, lipophilic chemistry, and high first-pass metabolism of chemotherapeutic drugs limit cancer treatment and prognosis. Due to their cancer-specific targeting, reduced adverse reactions, and substantial anti-cancer properties, nanoparticles serve as potential candidates for future therapeutics. Metal nanoparticles, particularly silver nanoparticles, are an emergent new class that has significant potential in the field of cancer biology. The purpose of this study was to evaluate the cytotoxic and anti-cancer properties of silver nanoparticles (AgNPs) on A549 cells, a type of human lung adenocarcinoma. AgNPs were assessed for their cytotoxicity using the MTT assay, and their effect on the reproductive viability of A549 cells was determined using the clonogenic assay. The specific type of cell death and the accompanying morphological alterations caused by AgNPs were confirmed by using AO/EB dual staining methods. The genotoxic effect and the antioxidant/oxidant status were assessed via comet and biochemical assays, respectively. The enzymatic activity of caspase 3/6 and the levels of expression of pro-apoptotic and anti-apoptotic genes were assessed in A549 cells that were treated with AgNPs for 24 h. AgNPs effectively induced cytotoxicity and prevented A549 cell colony formation in a dose-dependent manner. Treatment of A549 cells with AgNPs also increased DNA damage, which was coupled with elevated lipid peroxidation and

decreased antioxidant enzymes such as glutathione (GSH), glutathione-s-transferase (GST), and superoxide dismutase (SOD). Following AgNPs treatment, the mRNA expression levels of the pro-apoptotic genes as well as the activities of caspases were significantly elevated in A549 cells while the expression levels of anti-apoptotic genes were downregulated. Our study demonstrates the potential of the synthesized AgNPs for cancer therapy possibly targeting the apoptotic pathway.